H. Shibuya

ISSN 0385-2520

Rock Magnetism and Paleogeophysics

volume 10

1983

DELP PUBLICATION No. 1

Edited by Rock Magnetism and Paleogeophysics Research Group

Published by the Japanese National Committee for the Dynamics and Evolution of the Lithosphere Project (DELP)

ま え が き

本書は岩石磁気学・古地球物理学研究グループの1983年度の年次研究レポートであり，「国際リソスフェア探査開発計画 (DELP)」の成果報告書第1号として刊行されるものである。

岩石磁気学・古地球物理学研究グループでは，以前から Annual Report の形で英文の報文集を刊行してきた。(Annual Progress Report of the Rock Magnetism (Paleogeophysics) Research Group in Japan, 1963–1968. Rock Magnetism and Paleogeophysics, 1973–) これらの報文集は図書館などからの寄贈要請も多く，諸外国の関連分野の研究者によってかなり広く活用されている。このような経過から，この報告書も全て英文によって編集された。日本国内の研究者の方々にはいく分御迷惑をおかけすることになるが，事情を御理解いただきたいと思う。

岩石磁気学・古地球物理学研究グループは，昭和60年度からの実施が予定されているDELP計画において，課題5「日本列島の構造発達」の部門で大きな寄与ができるよう準備を進めている。今年はこの準備の一環として，7月26－28日に箱根において「アクリーション・テクトニクス」を中心とする研究会を開催した。この内容は本書viページ以下に収録してあり，また本書中にも多くの関連する論文がおさめられている（Deformation and Tectonic Movements of Japanese Islands および Tectonics in Circum-Pacific Areaの項参照）。我々は，こうした研究を発展させて，プレートの衝突・沈み込みに伴う集積・付加過程が，日本列島の形成や発達の歴史においてどのような重要性を持っていたか，またそれらは他の地学現象（日本海の形成，造山運動など）とどのような関連があるのかを明らかにしていきたいと考えている。

本書の刊行および研究会の開催は文部省科学研究費補助金総合研究 (B)「リソスフェア探査開発計画の推進」（代表者：秋本俊一，東大物性研）によった。ここに記して感謝の意を表する。

1983年12月

岩石磁気学・古地球物理学研究グループ

PREFACE

This volume is an annual progress report of the Rock Magnetism and Paleogeophysics Research Group in Japan for the year 1983. As the previous reports were so, this volume contains a collection of summaries, extended abstracts or brief notes of the research works carried out in our group this year. Many of the reports contain materials which may undergo a significant revision or may be updated as the research activity continues. In this respect, the readers are warned to regard them as tentative, and also requested to refer from a complete paper if such is published as a final result.

The articles are gruoped into five categories: (1) methods and apparatuses, (2) paleomagnetism of sedimentary cores, (3) deformation and tectonic movements of Japanese islands, (4) tectonics in the Circum-Pacific area, and (5) miscellaneous. The large number of articles in groups (3) and (4) reflects the present trend in research interest of our group; the formation and evolution of the Japanese islands and other tectonic problems attract more and more people as the central objective of research in paleomagnetism. This is in accord with the planned Japanese Lithosphere Project (dubbed DELP, for Dynamics and Evolution of the Lithosphere Project), which is expected to start soon and to become one of the central themes in earth sciences in Japan for the coming years.

The publication of this volume was made possible by a grant-in-aid from Ministry of Education, Science and Culture awarded to Prof. S. Akimoto, Chairman of the DELP Committee, for "Promotion of the Dynamics and Evolution of the Lithosphere Project". We thank Prof. Akimoto for his kind offer of publication.

Tokyo
December 1983

Masaru Kono

Editor
Rock Magnetism and Paleogeophysics
Research Group in Japan

TABLE OF CONTENTS

DEFORMATION AND TECTONIC MOVEMENTS OF JAPANESE ISLANDS

TECTONICS IN CIRCUM-PACIFIC AREA

MISCELLANEOUS STUDIES

ROCK MAGNETISM AND PALEOGEOPHYSICS SYMPOSIUM 15

The fifteenth Rock Magnetism and Paleogeophysics Symposium was held on 26-28 July, 1983 at Gora, Fuji and Hakone National Park. The main theme of the symposium was "ACCRETION TECTONICS" and several speakers (asterisks below) were invited to summarize current status in researches. In addition to the presentation of papers listed below, a half-day excursion was conducted in Quaternary Hakone volcanoes with a guidance by Osamu Oshima, Tokyo University.

26 July Evening

1. S. Yoshida (Kyoto Univ.)
   Rotational movement of ferromagnetic minerals in dilute sediments

2. H. Sakai and K. Hirooka (Toyama Univ.)
   Paleomagnetism of Atotsugawa trench site

3. T. Tagami (Kyoto Univ.)
   History of activity of Median Tectonic Line by means of fission track method

27 July Morning

4. E. Kikawa and H. Kinoshita (Chiba Univ.)
   Quaternary tilting of Western Izu and Oshima island from paleomagnetic data

5. M. Koyama (Tokyo Univ.)
   Stratigraphy and paleomagnetism of Izu Peninsula: present status and problems for the future researches

6. Y. Saito* (National Science Museum)
   Fossils and paleoreconstruction

7. M. Kimura* (Kagawa Univ.)
   Collision tectonics in Hokkaido

27 July Afternoon

8. K. Kimura (Japan Petroleum Agency)
   Ridge subduction in northern Honshu island

9. A. Taira* (Kochi Univ.)
   Plate tectonic evolution of eastern Asia

10. T. Seno* (Building Reserch Institute)
    Plate motion in Early Tertiary

11. K. Kobayashi (Tokyo Univ.)
A peculier event which took place in the northern part of the Philippine sea plate

12. T. Yokoyama (Doshisha Univ.), K. Hirooka(Toyama Univ.) and S. Nishimura (Kyoto Univ.)
On the rotation of Sumatra island in Quaternary

13. T. Nishitani (Akita Univ.) and Leg 92 On-Board Scientists
Inclination measurements on basalts from IPOD, Leg 92

28 July Morning

14. H. Sakai, S. Maruyama and K. Hirooka (Toyama Univ.)
Paleomagnetism of Kurosegawa allochtone and Sawadani seamount

15. K. Hirooka* (Toyama Univ.)
Tectonic movements of Japanese islands as seen from paleomagnetic data

16. T. Tosha* (Tokyo Univ.)
Present status of paleomagnetic study of northwestern Japan

17. Y. Fujiwara and Y. Morinaga (Hokkaido Univ.)
Paleomagnetism of Paleozoic and Mesozoic of northern Japan

18. M. Torii, A. Hayashida, Y. Otofuji and S. Sasajima (Kyoto Univ.)
Rotation of southwestern Japan

19. S. Uchiyama, K. Hirooka, T. Date and H. Kanai (Toyama Univ.)
Paleomagnetism of Mesozoic rocks in the Inner Belt of southwestern Japan

28 July Afternoon

20. T. Matsuda* (Tokyo Univ.)
Evolution of Fossa Magna

21. N. Niitsuma (Shizuoka Univ.)
Tectonics and paleomagnetism of southern Fossa Magna area

22. K. Tokieda, H. Ito (Shimane Univ.) and K. Suwa (Nagoya Univ.)
Paleomagnetism of Mahe island, Seychelles

23. K. Heki (Tokyo Univ.)
Paleomagnetic confirmation of Bolivian orocline

A RING-CORE FLUXGATE FOR SPINNER MAGNETOMETER

Masaru KONO[1], Masahiko KOYANAGI[1] and Susumu KOKUBUN[2]

1 Department of Applied Physics, Tokyo Institute of Technology, Ookayama 2-12-1, Meguro-ku, Tokyo 152, Japan
2 Geophysics Research Laboratory, University of Tokyo, Hongo 7-3-1, Bunkyo-ku, Tokyo 113, Japan

1. Introduction

Fluxgate magnetometer is an instrument to measure magnetic fields by utilizing the nonlinear transfer characteristics of ferromagnetic core material (e.g., Primdahl, 1970). Although fluxgates ceased to belong to the class of the "most sensitve" magnetic detectors since the advent of cryogenic magnetometers (Goree and Fuller, 1976), they continue to be an essential part of many magnetometer systems because of their high reliability, relative simplicity, ruggedness and economy. They are employed in various systems for rock magnetism and paleomagnetism such as the spinner magnetometers commercially available from Schonstedt and from Digico. One of the merits of fluxgates as sensors is their ability to cover a very wide dynamic range. A whole spectrum of magnetization in rocks ranging from very strong ones in basalts to very weak ones in sediments or metamorphics can be measured by a single instrument without any special attachments.

A recent innovation in fluxgate technology is the introduction of ring-core geometry by which the loss is minimized and a high sensitivity is achieved due to flux closure. (e.g., Gordon and Brown, 1972). Ring-core magnetometers of 6-81 Mo-Permalloy with high sensitivity and stability were developed by Gordon et al.(1968) and Acuna (1974) for exploration of planetary magnetic fields by space probes. Perhaps the state of art in fluxgate magnetometers is that achieved by the Magsat vector magnetometers (Acuna et al., 1978). The Magsat spacecraft successfully measured vector components of the earth's magnetic field with an estimated accuracy of 3 nT by three orthogonal ring-core sensors (Langel et al. 1982). The design of Magsat magnetometers contain novel ideas for making both the stability and the sensitivity very high under severe environments.

In developing a new fluxgate magnetometer, we have closely followed their ideas in the basic design of sensor geometry and electronic circuitry, and added some of our own to achieve characteristics favorable for sensors in a newly developed spinner magnetometer system using multiple frequency components and variable rotational speeds (Kono et al., 1981). The frequency responce of the new magnetometer was examined in detail and found to be satisfactory in the frequency range of 0 to 200 Hz. As the stability and sensitivity of this magnetometer is quite high, it may be useful not only as a sensor for spinner magnetometer but also as a detector for magnetic signals having frequencies between 0 and about 200 Hz such as is observed in magnetic induction studies.

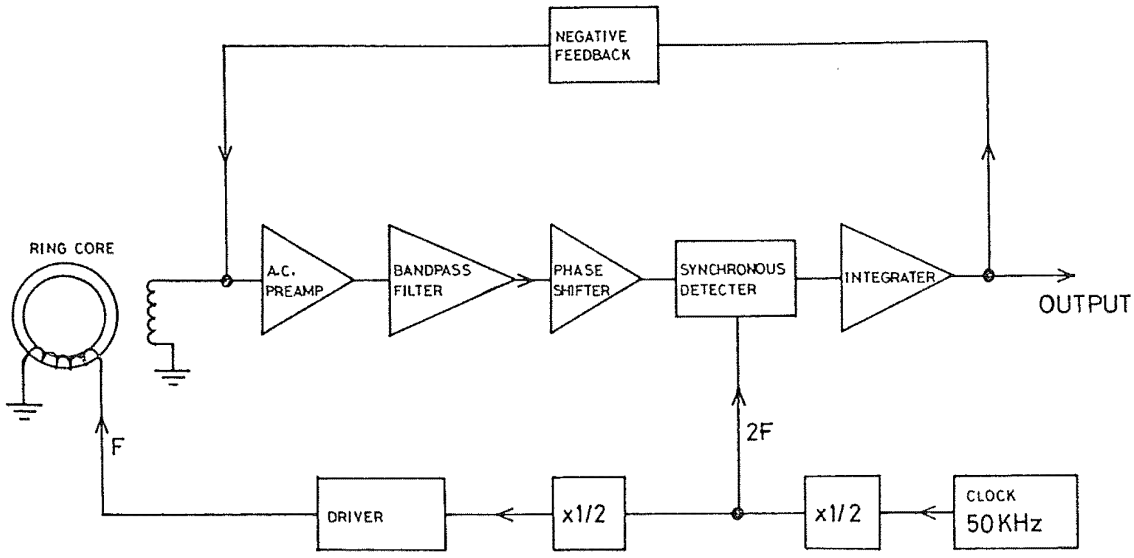

Fig. 1 Schematic block diagram of the ring-core magnetometer.

2. Electronic Circuits

Fig. 1 shows a schematic block diagram of the magnetometer electronics. The sensor used is a 6-81 Mo-Permalloy wound around a 25 mm diameter bobbin, available from Tohoku Kinzoku Kogyo, Ltd. A phenol-coated copper wire 0.26 mm diameter was wound about 250 times to produce a toroidal drive coil. The drive circuit is composed of a crystal-controled time base supplying 50 kHz square waves, two stages of flip-flops producing a drive signal (f = 12.5 kHz) and a refernce frequency for synchronous detector (2f = 25 kHz), a buffer, and a pair of complementary power transistors (Fig. 1). The output current from the transistors is supplied to the drive coil through a highly efficient "capacitive discharge" circuit (Acuna, 1974), supplying a peak current of 0.6 A, which is enough to produce a magnetic field of 2.3 mT, or about 50 times higher than the coercivity of the ring-core, and yet the average power required is only about 0.3 W. The low power consumption may be useful in such studies as magnetic induction, where a portable system is required.

A pickup/feedback coil is wound on a square frame made of a glass-epoxy resin. The input signal is processed by an A.C. preamplifier, filters to reduce f and 3f frequency components, a buffer, a phase shifter, and a synchronous detector (Fig. 1). The input stage is a low-offset, low-noise operational amplifier with a gain of about 25 dB, broadly centered at 25 kHz. For the filtering of drive frequency noise, two stages of identical active band-pass filters tuned at 25 kHz (Q = 8.4) were used to reduce 12.5 kHz noise as well as amplify the signal by a further 10 dB. The voltage gain of the buffer stage can be set as required, but is presently about 12 dB. The output from the phase shifter is synchronously amplified with a reference signal (2f) from the drive circuit. The low frequency portion of the signals are, in effect, completely returned to the pickup/feedback coil through the feedback loop (Fig. 1). The over-all sensitivity is

set at about 10 mV/nT, although a higher value can easily be obtained.

The most crucial part of the circuit is the integrator in the synchronous detector and the feedback amplifier. We followed the design of Acuna et al. (1978) for feedback circuit, while our integrator circuit is of somewhat simplified version. The system response to signals can essentially be represented by a transfer function

$$G(s) = \frac{d}{(c_1 c_2 R_1 R_2 d/KA)s^2 + (c_2 d(R_1+R_2)/KA)s + 1}$$

where A is the amplifier gain (266 in our case), K is the sensor sensitivity (0.2 mV/nT), and d is the overall sensitivity (10 mV/nT). In the ideal case, the system behaves exactly as a Butterworth low-pass filter with a cut-off frequency of 500 Hz.

The actual transfer function of the present magnetometer is shown in Fig. 2, which was obtained by spectrum analyser using as the input a magnetic field of a few nanoteslas produced by a white noise. The response in Fig. 2 is somewhat different from the one calculated by the ideal relation. This is mainly due to the fact that the operational amplifiers are asumed to be ideal in deriving eq. (1). The most non-linear elements in the circuit are the band-pass filters (Fig. 1) which have a high Q of 8.4 and are limiting the frequency response of the system. Although a slight increase appears in the amplitude spectrum near the corner frequency (Fig. 2), the response is sufficiently flat

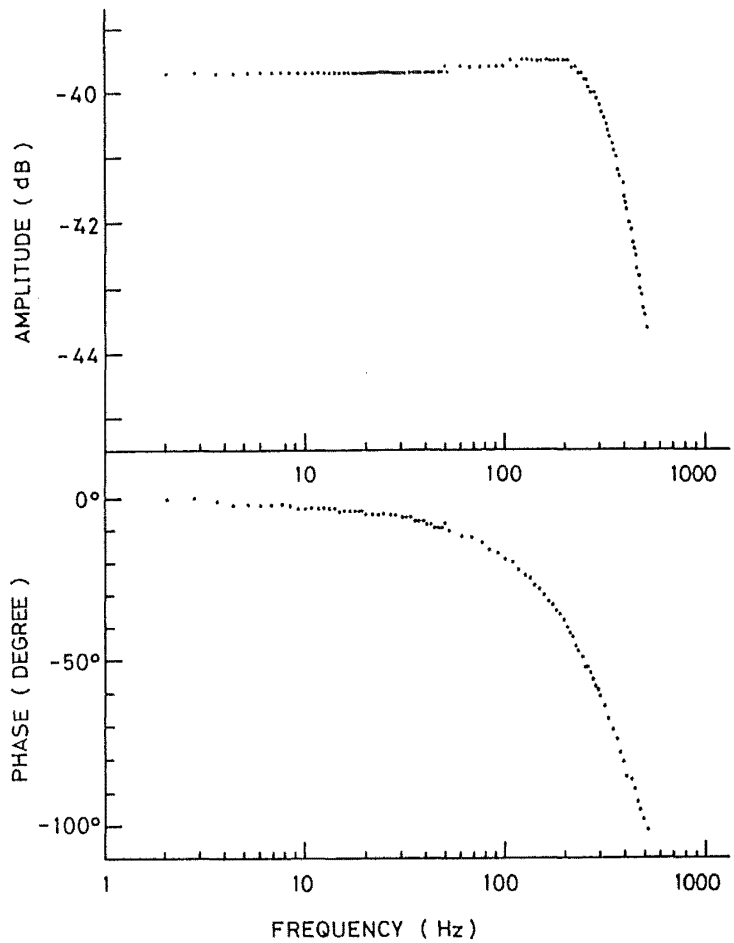

Fig. 2 Transfer function of the actual system. A slight peak at 50 Hz is the noise from A.C. power line.

to about 200 Hz, and the cut-off frequency of about 450 Hz was obtained. The small peaks in both amplitude and phase at 50 Hz show the effect of the noise due to A.C. mains. The performance of this system is quite satisfactory as a sensor for spinner magnetometers.

3. Sensitivity and Stability

The feedback loop is composed of a constant-current supply amplifier after the design of Acuna et al. (1978). We can set the gain of the system by selecting a proper value for the current limiting registor. Currently the gain is set at about 10 mV/nT. This value was selected to obtain as large a dynamic range as possible when used in a spinner magnetometer. If the distance between the sample and the sensor is 60 mm, say, a field of 1000 nT corresponds to a magnetic moment of 2×10^{-3} Am^2 (or 2 emu), which is about the largest value expected of a standard-sized sample (core with a diameter of 25 mm and a length of 23 mm) of exceptionally strongly magnetized basalt. Since the noise level of this ring-core is about 0.03 nT, the weakest magnetization measurable without any signal enhancement is 6×10^{-8} Am^2 (6×10^{-5} emu). As a 10 to 100 enhancement of signal to noise ratio can be achieved by numerical filtering using stacking and FFT techniques (Kono et al., 1981), the magnetometer can measure effectively all the magnetizations in natural rocks except the weakest ones.

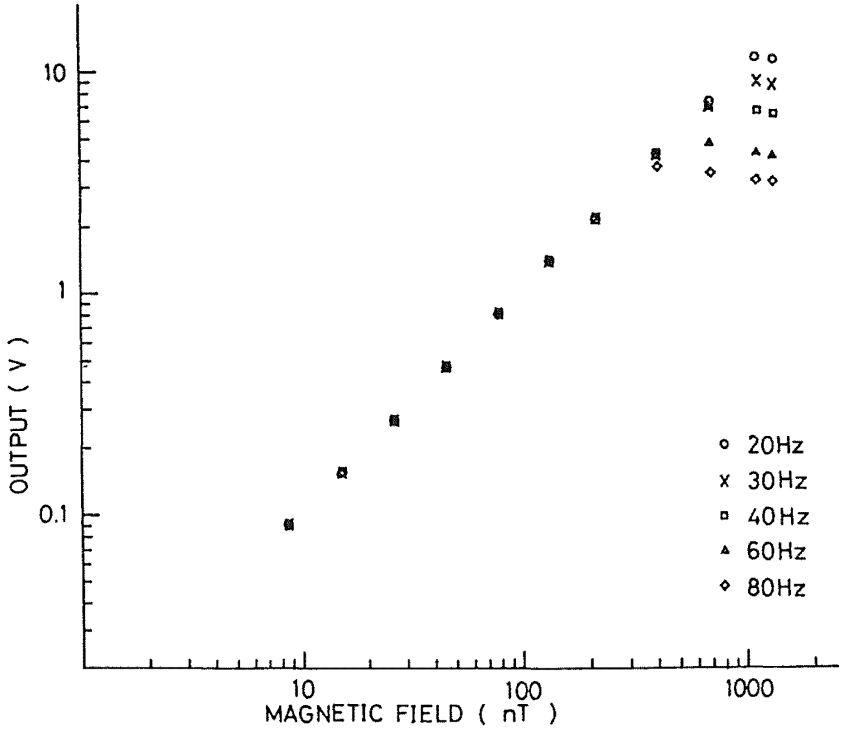

Fig. 3 Sensitivity at various magnetic fields and frequencies. Sensitivity at 20 Hz is constant in the whole range. The point at highest field indicates the saturation of the amplifier.

Fig. 3 shows the magnetometer output voltages for various

field strengths and frequencies. In the frequency range shown, the gain is practically constant for fields less than 300 nT. At higher fields, saturation effect is observed for high frequency signals, so that large-amplitude signals may be reproduced without distortion in a frequency range 0-20 Hz. The gain is also constant in a temperature range of practical interest (Fig. 4). Although we did not pay much attension to the temperature stability problem as was done by Acuna et al. (1978), the actual gain is constant within 10^{-3} for temperatures between $-4^{o}C$ and $62^{o}C$, which is more than enough in spinner magnetometers.

4. Discussion and Conclusions

The transfer characteristics of a typical, commercially available "high sensitive" fluxgate sensor is shown in Fig. 4 for comparison. The gain is ten times less than ours and yet the frequency response is much poorer. Because of such behaviors, fluxgates were conventionally thought as inappropriate for signals faster than a few Hz. The present results show that they may be employed for large amplitude signals (<1000 nT) at least to 20 Hz, and to 100 Hz or more if the amplitude of signals is smaller than 100 nT. A slight improvement of frequency response to large-amplitude signals was observed when notch filters were used instead of bandpass filters.

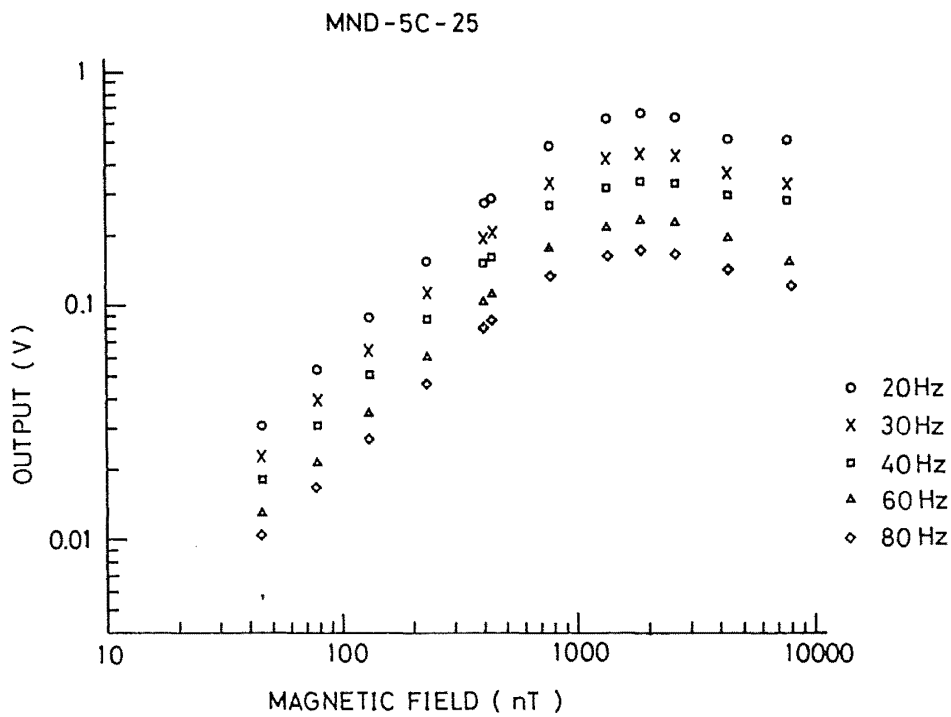

Fig. 4 Sensitivity of a commercially available fluxgate magnetometer at various frequencies.

One important aspect of the present magnetometer is its

phase response. The overall characteristics is Butterworth with a cut-off at 450 Hz (Fig. 2), but a closer examination of phase between 0 and 200 Hz shows that the delay angle is proportional to the frequency with a gradient of 0.192 degree/Hz. Therefore, the shape of the input signal is faithfully reproduced in the output with a constant time delay (0.192/360 = 533 microseconds) even when multiple frequency components exist. This property is ideal for use in the advanced spinner magnetometer of Kono et al. (1981). In this magnetometer, samples are rotated around two axes simultaneously in a field-free space and 64 or 128 measurements of magnetic signals are carried out in one revolution. The obtained wave form is ideally a sum of three signals with frequencies of f, 3f/4, and 11f/4, where f is the frequency of revolution around the vertical axis, corresponding to three orthogonal components of the magnetic dipole. If a delay circuit of proper time constant (533 microseconds in the present case) is inserted, there is no need to carry out cumbersome compensations for different frequency components for signals of 200 Hz or less. This property also enables us to rotate the sample at different speed, either to speed up the measurements of ordinary samples or to slow down in order not to destroy fragile samples.

We can conclude that a satisfactory sensor for weak fields was produced. The transfer function of this system (Fig. 2) is very flat to about 60 Hz, and a better tuning will perhaps extend this range at least to 100 Hz. Such a magnetometer with high sensitivity and good frequency response may also find use in problems other than rock magnetism and paleomagnetism.

The frequency response of the present system is limited not only by the time constant of the integrator but also by the band width of active filters (Fig. 1). The present ones have a very high Q and that makes the signal band width narrower. The use of notch filters is a partial solution for high frequency measurements, though we did not observe a substantial improvement in a circuit with notch filters.

References

Acuna, M.H.(1974) IEEE Trans. Mag., MAG-10, 519.

Acuna, M.H., C.D. Scearce, J.B. Seek and J. Scheifele (1978) NASA Tech. Memo. 79656, 20p.

Gordon, D.I. and R.E. Brown (1978) IEEE Trans. Mag., MAG-8, 76.

Gordon, D.I., R.H. Lundsten, R.A. Chiarodo and H. Helms, Jr. (1968) IEEE Trans. Mag., MAG-4, 397.

Goree, W.S. and M. Fuller (1976) Rev. Geophys. Space Phys., 14, 591.

Kono, M., Y. Hamano, T. Nishitani and T. Tosha (1981) Geophys. J. Roy. Astron. Soc., 67, 217.

Langel, R., G. Ousley, J. Berbert, J. Murphy and M. Settle (1982) Geophys. Res. Lett., 9, 243.

Primdahl, F. (1970) IEEE Trans. Mag., MAG-6, 376.

(Submitted to J. Geomag. Geoelectr.)

BLEACHING OF ESR SIGNALS FROM PLANKTONIC FORAMINIFERA

Takaharu SATO

Department of Physics, Faculty of Engineering Science,
Osaka University, Toyonaka, Japan

In the last decade electron spin resonance (ESR) technique has been used as a useful tool for dating Quaternal materials (Ikeya, 1975; Ikeya and Miki, 1980; Sato, 1982). There have been some studies of the effects of light on thermoluminescence (TL) reported in the literature (Wintle and Huntley, 1979; 1980), but there is very little quantitative data on the effects of light on ESR signals (Sato, 1983). I report here on bleaching of ESR signals from planktonic foraminifera associated with the defects produced by natural and/or artificial radiation.

ESR spectra of planktonic foraminifera of diameter 0.250 - 0.503 mm from KH 73-4-7 (2° 41' N, 164° 50' E) 430 cm were measured with an JES-ME2X ESR-spectrometer at room temperature. Approximately 20 identical samples of 150 mg in weight were prepared for this study. Artificial irradiation from a ^{60}Co source (dose rate of 10 krad per hour) was performed at the Radiation Institute of Science and Industrial Research, Osaka University.

The reduction in ESR intensity caused by some tungsten lamp exposures given to foraminifera is shown in Fig. 1-a. It can be seen that the intensity of the predominant signal (B) at g=2.004 is rapidly reduced with the increase in exposure time. A signal (C) at g=2.003 is also weakened. The intensity of a signal (A) at g=2.005 is reduced much more slowly and a signal (D) at g=2.001 shows no significant change.

Bleaching experiments have also performed on the samples which an artificial gamma dose had been given. Figure 1-b shows the results for additional gamma dose of 220 krad. The rates of

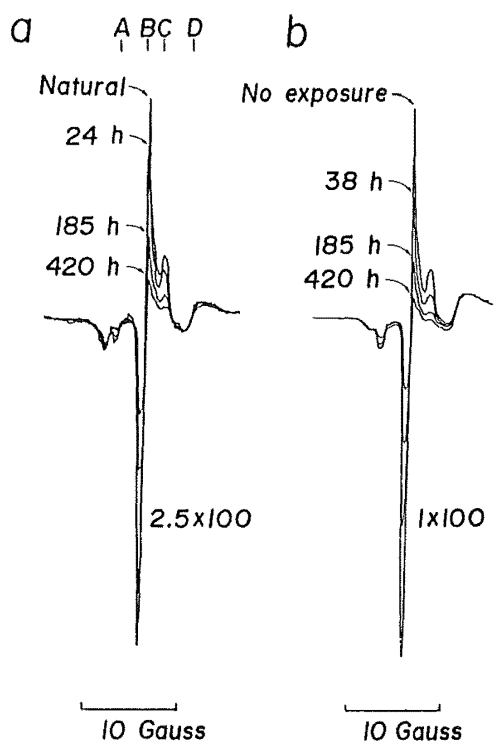

Fig. 1 ESR spectrum of foraminifera after various exposures to a 100 W tungsten lamp 7 cm above the samples. (a) Natural samples, (b) as (a) but after additional gamma doses of 220 krad.

intensity of the ESR signal (B) before bleaching by tungsten lamp exposures to those of the signal (B) after bleaching for various exposure times are shown in Fig. 2. The abcissa is plotted on a logarithmic scale for convenience. To minimize errors due to changes in instrument sensitivity and differences in sample weight, the signal intensity was measured relative to the intensity of Mn^{2+} signals. It can be seen in Fig. 2 that the exposure times required to halve the ESR signal are about 50 hours for the irradiated samples and about 100 hours for the natural samples. The intensity of the signal from the irradiated sample, which was about 2.5 times as great as that from the natural sample, before a light exposure reduced to be nearly equal intensity to that from the natural samples after a 420 hours exposure. This may be attributed to the existence of components which are insensitive to light in the natural signal as Wintle and Huntley (1980) reported in their work on TL dating of oceanic silt.

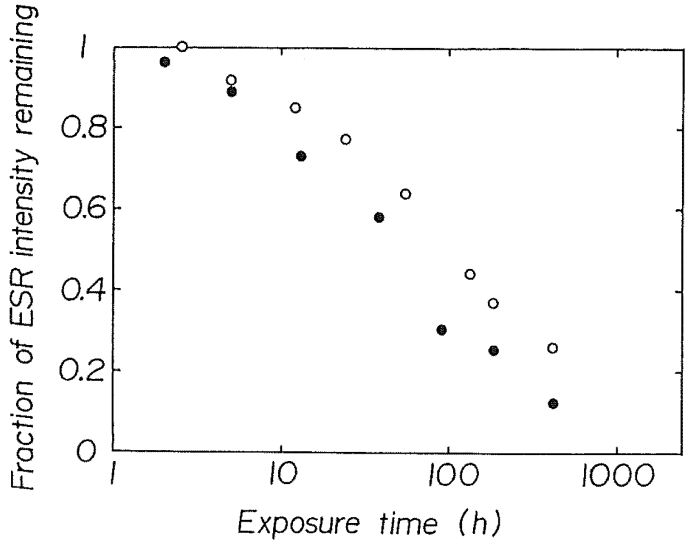

Fig. 2 The fraction of the ESR intensity remaining after a tungsten lamp exposure against exposure time. The experiments were performed on the natural samples (open circles) and samples given additional gamma doses of 220 krad (solid circles).

The effects of sunlight were also tested for the natural samples. Similar changes in the ESR signals were observed. The ESR intensity reduced by approximately 40 % after exposure to November afternoon sunlight for only 1 hour.

It can be concluded that the ESR signals are sensitive to light and precautions for light are required for sample preparation and storaging. More detailed studies of the insensitive components will also be necessary.

References

Ikeya, M. (1975) Nature, 255, 48.
Ikeya, M. and T. Miki (1980) Science, 207, 977.
Sato, T. (1982) Nature, 300, 518.
Sato, T. (1983) Nature, 305, 162.
Wintle, A. G. and D. J. Huntley (1979) Nature, 279, 710.
Wintle, A. G. and D. J. Huntley (1980) Can. J. Earth Sci. 17, 348.

ANALYSIS OF THE THELLIERS' METHOD OF PALEOINTENSITY DETERMINATION
1. ESTIMATION OF STATISTICAL ERRORS

Masaru KONO and Hidefumi TANAKA

Department of Applied Physics, Tokyo Institute of Technology
Ookayama 2-12-1, Meguro-ku, Tokyo 152, Japan

1. Introduction

Among the various types of natural remanent magnetization (NRM) carried by rocks, thermoremanent magnetization (TRM) is the most suitable for paleointensity experiments. Many experimental methods for determining paleointensity have been proposed, but the Thelliers' method (Thellier and Thellier, 1959) is currently regarded as the most reliable of all the methods using TRM (e.g., Coe and Grommé, 1973; Kono, 1978). The Thelliers' method is based on the following properties of TRM or partial TRM (PTRM); (1) the blocking temperature is the same as the unblocking temperture, (2) a PTRM is independent of other PTRMs so that the additivity of PTRM holds, and (3) the PTRM is proportional to the magnitude of the ambient magnetic field, if the magnitude of the field is not very large.

When all the above conditions are satisfied, a sample in which the original NRM is of TRM origin and which is heated to a temperature T lower than the Curie point (T_C) and cooled to the room temperature in the presence of a laboratory magnetic field F_L will have a remanence which is a sum of the partially demagnetized NRM and a newly acquired PTRM (Fig. 1)

$$J_+(T) = Y(T) + X(T) \tag{1}$$

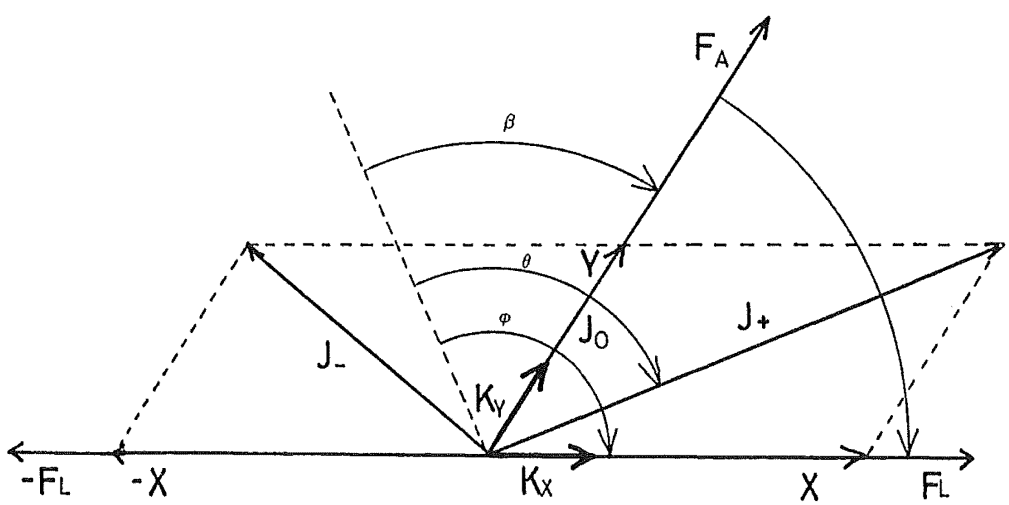

Figure 1. Definition of the various vectors and angles. The angles θ, ϕ, β are measured from some arbitrary fixed reference direction shown by a dashed line.

The NRM and TRM components Y and X can be expressed as

$$Y(T) = F_A \int_T^1 p(T)dT \tag{2}$$

and

$$X(T) = F_L \int_0^T p(T)dT \tag{3}$$

where F_A is the ancient field in which the sample acquied the NRM (as a ^{A}TRM), and p(T) is the blocking temperature spectrum satisfying the relation

$$\int_0^1 p(T)dT = 1, \qquad p(T) \geq 0, \qquad 0 \leq T \leq 1 \tag{4}$$

Note that the temperature is non-dimensionalized and that the magnetic field and the remanence have the same units in this treatment. Samples are heated to successively higher temperatures T_i to obtain the pairs X_i and Y_i at various temperatures until the Curie point is exceeded ($T_N \geq 1$). In an ideal case where blocking spectrum is unchanged before and after the heating, we can eliminate T from equations (2) and (3) and obtain a linear relation

$$Y = a + bX \tag{5}$$

where

$$a = Y(0) \qquad \text{.... original NRM}$$

$$b = -F_A/F_L \tag{6}$$

In this report, we examine statistical errors in the estimation of paleointensities, and derive the range of uncertainties in the paleointensity data. The problem is treated only mathematically; we assume that we know the temperature interval in which all the assumptions are satisfied and try to estimate the slope of linear relation and its uncertainty.

A previous treatment of errors in the determination of paleointensities was given by Coe et al., (1978), in which they proposed to use York's (1966) method of least squares fitting to determine F_A and its error. This is a correct approach, but instead of deriving the actual forms, Coe et al. (1978) assumed some simple forms for the variances of X and Y. We show that their assumptions are quite erroneous. We shall obtain valid expressions for variances in three versions of the Thelliers' method currently in use, and compare the performance of the different versions from the viewpoint of errors.

2. Errors in Experimental Data Points

The data obtained by experiments of the Thelliers' method are the coordinate pairs (X_1, Y_1), (X_2, Y_2), ..., (X_N, Y_N), corresponding to N different temperatures. In this data set, both of the X and Y coordinates contain errors. Methods of least squares fitting of straight lines to such data sets are given by

York (1966) and Williamson (1968). In these methods, the weights for data points are needed and are calculated by

$$W_i = 1/(s_{yi}^2 + b^2 s_{xi}^2), \quad i = 1,\ldots,N \tag{7}$$

where s_{xi}^2 and s_{yi}^2 are the variances in X and Y coordinates at the i-th data point. Coe et al. (1978) assumed that at every temperature $s_{xi}^2 = (F_L s)^2$ and $s_{yi}^2 = (F_A s)^2$, where s is a constant, but this assumption is not reasonable.

When the magnetic properties of a sample is unchanged by heating, deviations in the data are caused by (1) error in the temperature (dT), (2) errors in the laboratory field magnitude (dF_L) and its direction ($d\phi$), and (3) errors in the measurement of intensity (dJ) and direction ($d\theta$) of remanence. These error sources can be regarded as independent of each other, and so averages of their products may be set to zero in the following analysis. The total vector error in J_+ (eq. 1) can therefore be written, to the first order, as

$$dJ_+(T) = (F_L - F_A)\, p(T)dT + (k_x dF_L + F_L \hat{k}_x d\phi)\, {}_0^T\, p(T)dT + k_j dJ + J_+ \hat{k}_j d\theta \tag{8}$$

where k_x and k_j are unit vectors in the direction of F_L (X axis) and J_+, while $\hat{k}_x$ and $\hat{k}_j$ are unit vectors <u>perpendicular</u> to the direction of F_L and J_+, respectively. The last two terms represent the effect of measurement errors which are present even when experiments are perfectly done. The variance s_+^2 of J_+ can be obtained by taking the average of the squared value of (8)

$$s_+^2(T) = (F_A^2 + F_L^2 - 2F_A F_L \cos\alpha)\, p^2(T) s_T^2 + X^2(s_f^2 + s_\phi^2) + (X^2 + Y^2 + 2XY\cos\alpha)(s_j^2 + s_\theta^2) \tag{9}$$

where α is the angle between F_A and F_L (Fig. 1), and s_T, s_f, s_ϕ, s_j, and s_θ are normalized standard errors in temperature, in intensity and direction of the laboratory field, and in intensity and direction of the measurement of remanences, respectively. The variances in the measurements of J_- or J_0 (Fig. 1) can similarly be obtained:

$$s_-^2(T) = (F_A^2 + F_L^2 + 2F_A F_L \cos\alpha)\, p^2(T) s_T^2 + X^2(s_f^2 + s_\phi^2) + (X^2 + Y^2 - 2XY\cos\alpha)(s_j^2 + s_\theta^2) \tag{10}$$

$$s_0^2(T) = F_A^2\, p^2(T) s_T^2 + X^2 s_f^2 + Y^2(s_j^2 + s_\theta^2) \tag{11}$$

The second term in (11) expresses the effect of the residual field in "nonmagnetic" space.

3. Errors in Various Methods

There are three versions of the Thelliers' method currently in use. In the original method (Thellier and Thellier, 1959), samples are heated twice to the same temperature but with

different settings so that the field applied to the sample during heatings are in opposite directions as seen from the coordinate attached to the sample (F_L and $-F_L$ in Fig. 1). In this method, X and Y are obtained by halving the vector difference and sum of J_+ and J_-. If $C = |A + B|$ and errors in A and B are unrelated, it follows that $s_C^2 = s_A^2 + s_B^2$. Therefore, in the original method

$$s_x^2 = s_y^2 = \frac{1}{2}(F_A^2 + F_L^2)\, p^2(T)\, s_T^2 + \frac{1}{2} X^2 (s_f^2 + s_\phi^2) + \frac{1}{2}(X^2 + Y^2)(s_j^2 + s_\theta^2) \qquad (12)$$

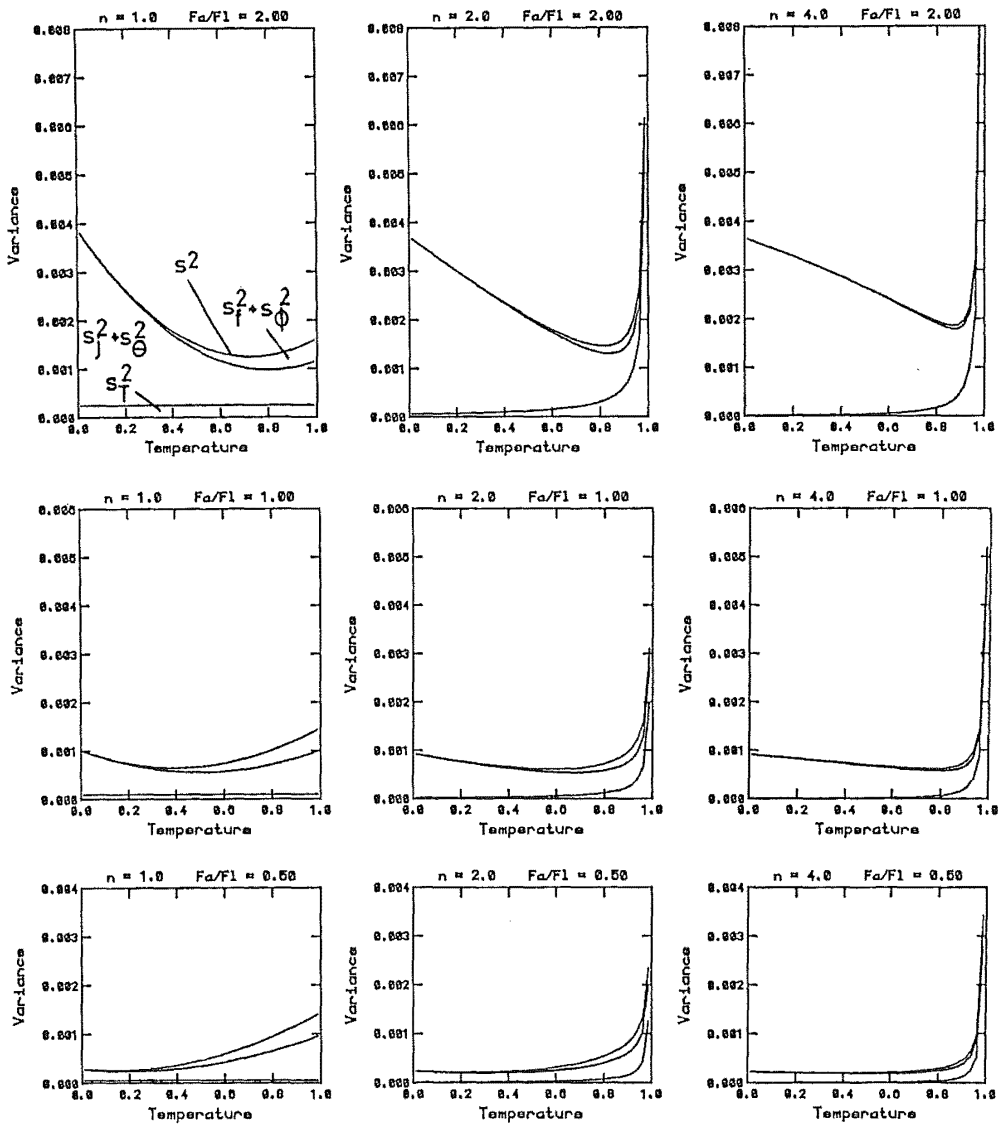

Figure 2. Contributions from various sources of error to the variances of X (TRM component) and Y (NRM component) in the original method of Thellier and Thellier (1959).

This equation shows that the variances in X and Y coordinates are the same but varies with temperature.

To evaluate relative importance of various error sources, we assume that the blocking spectrum may be represented by

$$p(T) = (1/n)\ (1 - T)^{(1/n)-1} \tag{13}$$

which satisfies the condition (4). The parameter n in (13) indicates the degree of concentration of the blocking spectrum near the Curie temperature (T = 1). The variance s^2 (= s_x^2 = s_y^2) can then be caluculated as

$$\begin{aligned} s^2 = & \frac{1}{2}\ (F_A^2 + F_L^2)\ [\frac{1}{n}\ (1 - T)^{(1/n)-1}]^2\ s_T^2 \\ & + \frac{1}{2}\ F_A^2\ (1 - T)^{2/n}\ (s_j^2 + s_\theta^2) \\ & + \frac{1}{2}\ F_L^2\ [1 - (1 - T)^{1/n}]^2\ (s_f^2 + s_\phi^2 + s_j^2 + s_\theta^2) \end{aligned} \tag{14}$$

Fig. 2 shows the relative contributions from various sources to the variance s^2 for the cases n = 1, 2, and 4. The parameters used in the calculation are typical or somewhat conservative estimates of errors in actual paleomagnetic experiments, so that the obtained variance is on the safer side. From Fig. 2 it is clear that the variance s^2 is heavily dependent on the temperature. The most important contribution to s^2 is by s_θ^2 and by s_j^2 (errors in measurements), but the effect of s_ϕ^2 becomes also important at high temperatures. It is to be noted that, even if there is no chemical changes due to heating, the data close to the Curie point may contain large errors and deviate much from the ideal linear line.

In the version of the Thelliers' method proposed by Coe (1967), samples are heated first in nonmagnetic field and then in F_L, so that the coordinates are obtained as $X = |J_+ - J_0|$ and $Y = |J_0|$. In this case

$$\begin{aligned} s_x^2 = & (2F_A^2 + F_L^2 - 2F_AF_L \cos\alpha)\ p^2(T)\ s_T^2 \\ & + X^2\ (2s_f^2 + s_\phi^2) + (X^2 + 2Y^2 + 2XY \cos\alpha)(s_j^2 + s_\theta^2) \\ s_y^2 = & F_A^2\ p^2(T)\ s_T^2 + X^2 s_f^2 + Y^2\ (s_j^2 + s_\theta^2) \end{aligned} \tag{15}$$

Comparing equation (15) with equation (14), it can be seen that in Coe's method s_x is always larger than that of the original method and s_y is always smaller.

In the single heating method of Kono and Ueno (1977), the direction of NRM is assumed to be known and F_L is always applied perpendicular to the NRM direction in heating experiments. X and Y are therefore perpendicular to each other and can be determined from a single measurement of remanence with the assumption of the fixed directions of NRM (Y) and TRM (X). Writing unit vectors in X and Y directions as k_x and k_y and those perpendicular to them as k_x and k_y, respectively, the NRM and TRM components can be calculated by $X = J_+ k_x$ and by $Y = J_+ k_y$. As the vector representation of X is $X = k_x(J_+ k_x)$, the vector errors contributing to the measurement of X are

$$dX = k_x(k_x dJ_+) + X\hat{k}_x d\phi + Y\hat{k}_y d\beta \qquad (16)$$

where the second and third terms are errors due to the assumption of known TRM direction and that of constant NRM direction, respectively. Using eq. (8) for dJ_+ with the condition that F_L and F_A are orthogonal, the above relation can be reduced to

$$dX = F_L p(T)dT + X(dF_L/F_L) + X(dJ/J_+) + J_+\hat{k}_j k_x d\theta + Yk_x\hat{k}_y d\beta \qquad (17)$$

Noting that the expectations of $|\hat{k}_j k_x|^2$ and $|k_x\hat{k}_y|^2$ are $Y^2/2J_+^2$ and 1/2, respectively, we obtain

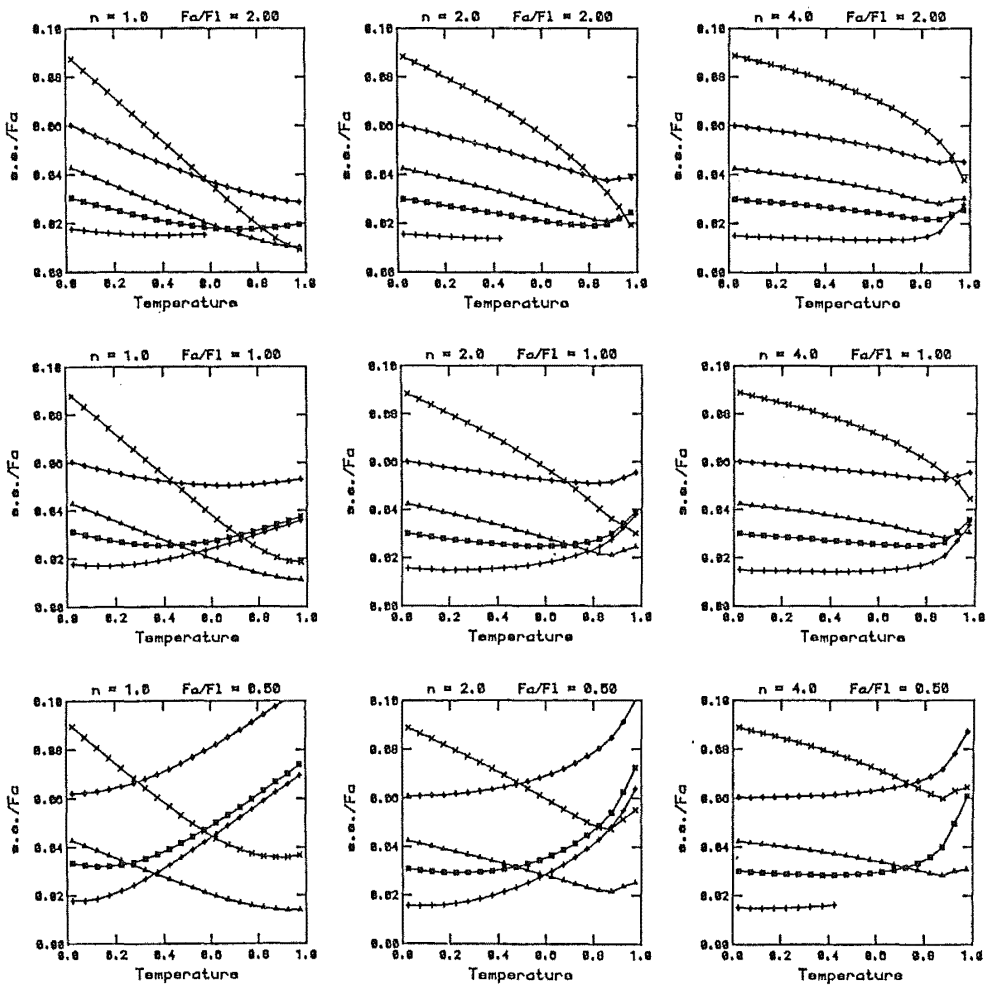

Figure 3. Comparison of errors in three versions of the Thelliers' method. Squares: s_x^2 and s_y^2 in the original method of Thellier and Thellier (1959). Diamonds and triangles: s_x^2 and s_y^2 in the method of Coe (1967). Crosses and plus signs: s_x^2 and s_y^2 in the single heating method of Kono and Ueno (1977).

$$s_x^2 = F_L^2 p^2(T) s_T^2 + X^2(s_f^2 + s_j^2) + \frac{1}{2} Y^2(s_\theta^2 + s_\beta^2) \qquad (18)$$

and similarly

$$s_y^2 = F_A^2 p^2(T) s_T^2 + X^2(s_\phi^2 + s_\theta^2) \qquad (19)$$

Fig. 3 compares the standard errors s_x and s_y for three versions of the Thellier's method using the same parameters. It is seen from this figure that when n is large errors are quite significant near the Curie point in every method. As expected, the single heating method gives larger errors compared to other methods, but the difference is not so big and it may be concluded that the loss of high reliability is well compensated by the reduced number of heatings. Another interesting thing is that the original method is superior to the Coe version in the sense that the errors in both coordinates are well balanced. s_y in Coe version is small, but the large s_x values compared to the original method makes many data points rather useless.

5. Conclusions

We have estimated variances in the X and Y coordinates (TRM and NRM components) of the results of the Thelliers' method of paleointensity determination. It was shown that they depend heavily on temperature, and the error is very large near the Curie point especially when the PTRM spectrum is concentrated at higher temperatures. In these variances, measurement errors dominate in the low temperature range, but the effects of errors in laboratory field setting and in temperature become significant and cannot be neglected at high temperatures. Errors are shown to become very large if the intensity ratio F_A/F_L (= $|b|$) is much different from unity.

Among the three versions of the Thelliers' method currently in use, the original version (Thellier and Thellier, 1959) was found the most superior. Heating in a nonmagnetic field (Coe, 1967) does not contribute much to a better performance; variances in both coordinates become unbalanced in such methods. The single heating method (Kono and Ueno, 1977) was found to be the most inferior in reliability. But its performance is tolerable as the number of heatings is roughly halved in this method.

References

Coe, R.S. (1967) J. Geophys. Res., 72, 3247.
Coe, R.S. and C.S. Grommé (1973) J. Geomag. Geoelectr., 25, 415.
Coe, R.S., C.S. Grommé and E.A. Mankinen (1978) J. Geophys. Res., 83, 1740.
Kono, M. (1978) Geophys. J. Roy. Astr. Soc., 54, 241.
Kono, M. and N. Ueno (1977) Phys. Earth Planet. Inter., 13, 305.
Thellier, E. and O. Thellier (1959) Ann. Géophys., 15, 285.
Williamson, J.H. (1968) Canad. J. Phys., 46, 1845.
York, D. (1966) Canad. J. Phys., 44, 1079.

(Submitted to J. Geomag. Geoelectr.)

ANALYSIS OF THE THELLIERS' METHOD OF PALEOINTENSITY DETERMINATION 2. APPLICABILITY TO HIGH AND LOW MAGNETIC FIELDS

Hidefumi TANAKA and Masaru KONO

Department of Applied Physics, Tokyo Institute of Technology, Ookayama 2-12-1, Meguro-ku, Tokyo 152, Japan

1. Introduction

One of the most reliable method to determine the paleointensity is that proposed by Thellier and Thellier (1959). There are many reports of basic studies concerning the various aspects of the Thelliers' method (e.g., Coe and Grommé, 1973). Adequate attention has not been paid, however, to the question of the range of field intensity values to which the Thelliers' method is applicable. We report some experimental results pertaining to this problem in this note.

Statistical analyses of paleointensity data for the last 5 or 10 million years indicate a normal distribution of the virtual geomagnetic dipole moments (VDM) with a standard deviation of about 35 percent of the mean (Kono, 1971; McFadden and McElhinny, 1982). This places some constraint on the models of the geomagnetic field. However, it is necessary to show that experimental paleointensity methods are really applicable to high and low fields much different from 50 uT. If the range of applicability of the method is limited while experimental errors are large and random, we may obtain a normal distribution of paleointensities regardless of the true nature of the geomagnetic variation. It is worthwhile, therefore, to test if there exist some practical limits in the range of paleointensity values for which the Thelliers' method may be used.

Thermoremanent magnetization (TRM) was given to natural samples in inducing magnetic fields of 2-1000 uT. These samples were subjected to the Thelliers' method and the experimentally determined intensity values were compared with the known magnitudes of the magnetic fields. It was also demonstrated how the accuracy of data varies with the change in ancient field magnitude and experimental procedures.

2. Samples and Experimental Procedures

Samples used were taken from Kotaki pyroclastic flow of Mt. Asama in the central part of Honshu Island, with a radiocarbon age of about 2200 years B.P. The rock type is augite-hypersthene andesite, and thermomagnetic analysis shows a Curie point of about 520°C, indicating that the main ferromagnetic mineral is a Ti-poor titanomagnetite produced by high temperature oxidation (Kono, 1978).

The NRM in this rock is very stable and paleointensity experiments carried out by different methods and in different atmospheres always gave successful and consistent results (Kono, 1978; Tanaka, 1980), showing that the magnetic properties do not

significantly change by heat treatment. Kotaki pyroclastic flow has already been used for checking the validity of the Thelliers' method performed on different apparatuses (Tanaka, 1980), and for evaluating Shaw's (1974) method of paleointensity determination (Kono, 1978).

All the heatings were done in air. Experimental method follows that of Coe (1967). For heating, a movable electric furnace placed in a three-layer permalloy shield was used. The heating and cooling rates within this furnace were about 1000°C/hr and 500°C/hr, respectively. The reproducibility of temperature is better than 5°C. The residual field in the nonmagnetic space is about 100 nT. The errors in the laboratory field setting is also about 100 nT. The remanences were measured by a Schonstedt SSM-1A spinner magnetometer. Experimental results were analyzed by the method proposed in an accompanying paper (Kono and Tanaka, 1983).

3. Experiment 1 (Ordinary Thelliers' Method)

Nine samples were prepared for which TRMs were given in laboratory magnetic fields of widely different intensities of 2 to 1000 uT. They were subjected to the Thelliers' method with a laboratory magnetic field of 50 uT, to simulate the ordinary situation when the ambient field is utilized for inducing TRM. The results were analyzed by the Arai diagrams , i.e., NRM-TRM diagrams (Arai, 1963; Nagata et al., 1963). Although the ratio of the "NRM" to TRM differ widely among the present samples, satisfactorily linear relations were obtained from all the resuls as demonstrated in Fig. 1. Some of the samples gave points deviated from the linear lines at high temperatures. Possible reasons for this behavior will be discussed below.

Fig. 2a shows the NRM-TRM diagrams for an extremely small intensity with a 10 times exaggeration of the vertical scale. It is rather surprising that the Thelliers' method gave a nearly correct value of 2.3 ± 0.4 uT when the actual value was 2 uT, in spite of the 25 times difference in TRM-inducing fields. However, the close agreement may be just a coincidence since the sample for 5 uT intensity shows a larger error.

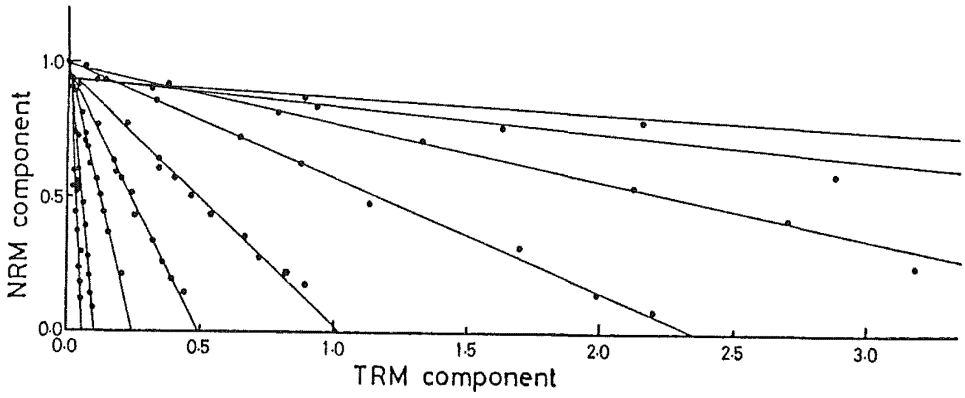

Figure 1. Arai diagrams of the results of all the ordinary Thelliers' experiments plotted at a same scale.

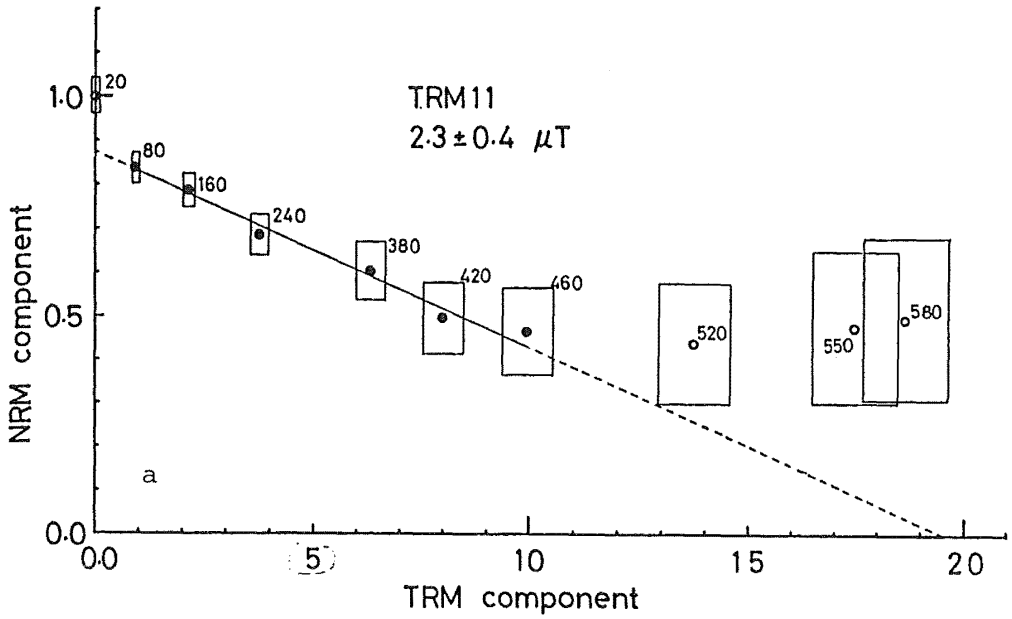

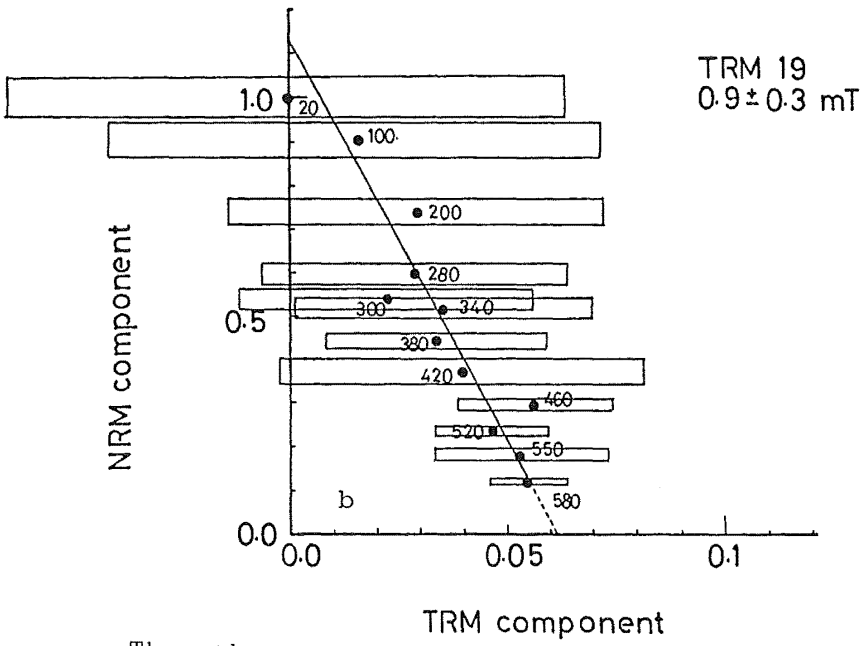

Figure 2. Results for an extremely small magnetic field of 2 uT (a) and extremely large field of 1000 uT (b). The experiment was performed with a laboratory field of 50 uT.

The other extreme case of very large inensity is illustrated in Fig. 2b in which a linear relation is marginally recognized between the NRM and the TRM, although the points are scattered in this diagram and especially the errors in horizontal coordinates are quite large. The slope of the linear relation for this sample obtained by least squares analysis is somewhat lower than the ideal value of 20. This perhaps reflects the large errors in data as well as the fact that the proportionality between the magnetic field and TRM no longer holds at 1 mT. In passing, we might note that even this result (TRM19, F_0 = 1000 uT) can be

regarded as satisfactorily linear if no horizontal exaggeration was applied (cf., Fig. 1). The impression of nonlinearity for Fig. 2b is partly due to exaggeration and partly due to large error boxes.

4. Experiment 2 (Use of Matched Laboratory Fields)

In this case, the Thelliers' experiment was performed with an inducing magnetic field of exactly the same magnitude as the original one in which the specimen acquired TRM. Four specimens having TRM which was given in magnetic fields of 2, 20, 200 and 1000 uT were examined by this procedure. All the samples gave better results when compared to the outcome of experiment 1. Fig. 3a shows the case of extremely small intensity. A sharp decrease in the NRM component at the step of 100°C indicates the removal of the viscous component of remanence which is conspicuous only in this sample because of the small magnitude of the TRM. After rejecting this and other four points at highest temperatures a very good intensity estimate of 2.1 ± 0.3 uT was obtained by the method of Kono and Tanaka (1983).

The case of extremely large intensity

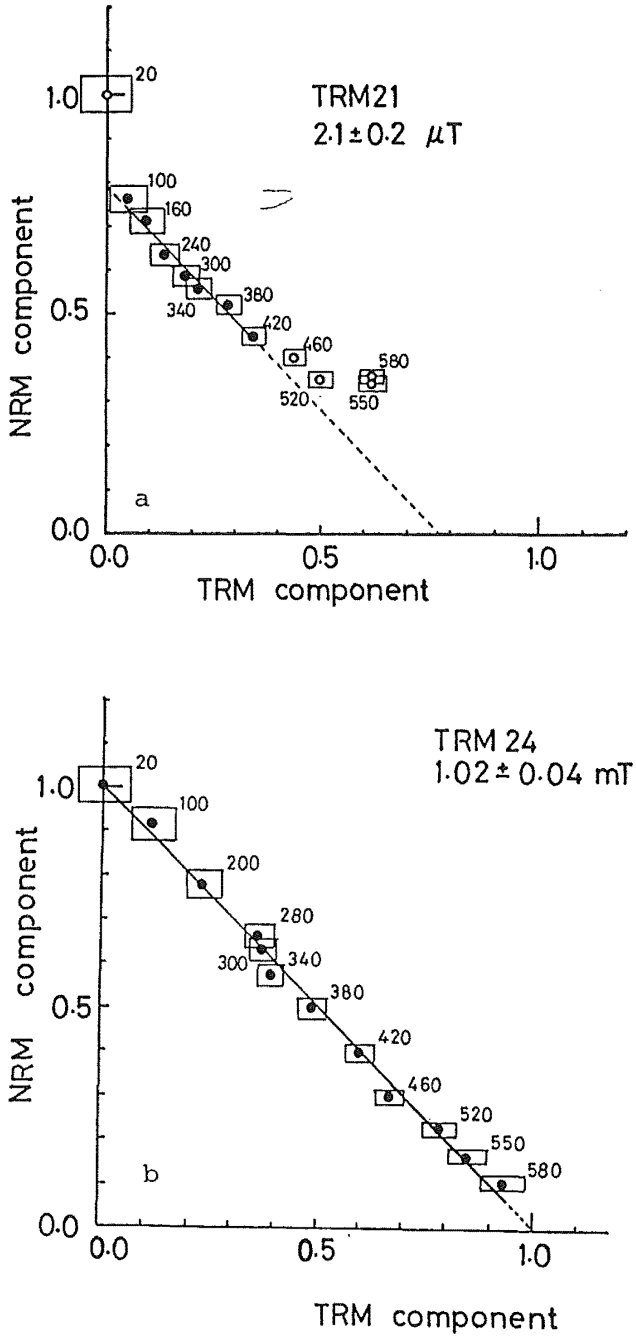

Figure 3. Results for extremely values of magnetic fields of 2 and 1000 uT. Matched laboratory fields were used in this series of experiment.

is shown in Fig. 3b. This sample was given a TRM in a magnetic field of 1000 uT, and the Thelliers' experiment was performed with an inducing magnetic field of 1000 uT. This result is more satisfactory than that of Fig. 2b, where inducing magnetic field is one-twentieth of the original field. Fig. 3b shows that even after the proportionality between the TRM and the magnetic field breaks down, the additivity of partial TRMs continues to hold to higher fields. Fig. 3 point out the importance of selecting an appropriate magnetic field in the Thelliers' method. With a choice of matched field value, the error may be reduced to a considerable extent and the reliability of data is enhanced.

5. Discussion

Fig. 4 shows the ratio of intensity F determined by the paleointensity experiment to the original intensity F_0. In this figure, solid circles represent those by the ordinary Thelliers' method (experiment 1) and open circles represent results from the matched-field experiments (experiment 2). It is remarkable that the Thelliers' method can successfully be applied to a very wide range of paleointensities. In the case of experiment 1 in which an inducing field of 50 uT was used, intensity values between 10 and 500 uT were obtained with errors less than 10 percent. For the 1000 uT TRM, a somewhat smaller value of 909 uT was obtained indicating the breakdown of the proportionality of the TRM to the magnetic field. However, the NRM-TRM relation is sufficiently

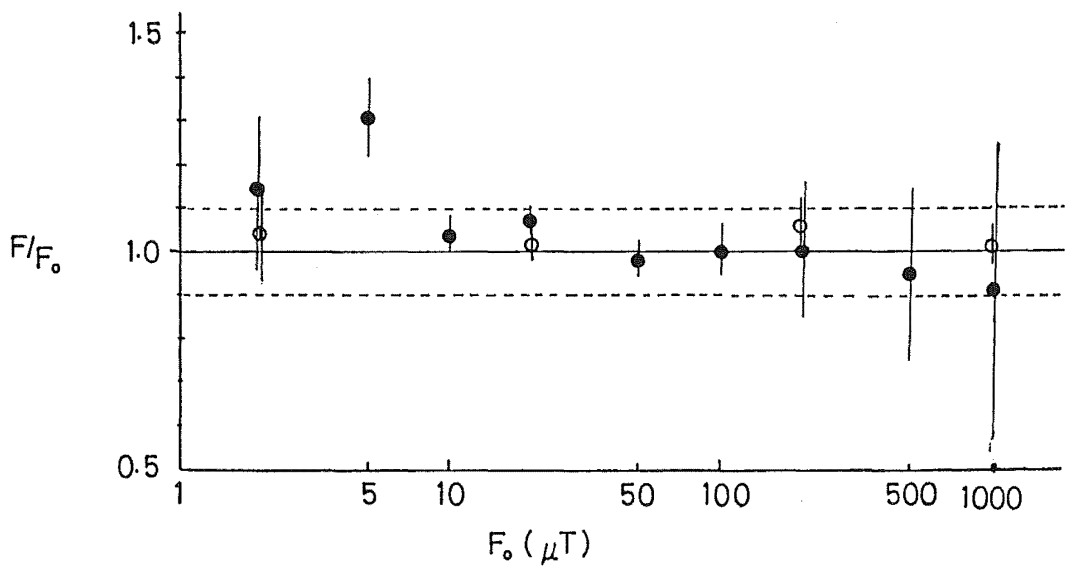

Figure 4. F/F_0 ratios for various values of F_0. Solid circles from experiment 1 and open circles from experiment 2. Error bars were calculated by the method of Kono and Tanaka (1983), using the least squares algorthm of Williamson (1968). Horizontal lines indicate ideal value and $\pm$ 10 percent error level.

linear even in this sample (Fig. 2b). Thus the additivity of partial TRMs still holds at this field. For very small intensities, the use of 50 uT field induces a large error in NRM-TRM diagram (Fig. 2a) and consequently the obtained field intensities may be much different from the true value. Such is the case for the 5 uT sample. For both the very small and large fields, errors will be much reduced if inducing field magnitude is matched to, that is close to, the paleointensity value. The use of matched laboratory fields for critical samples is therefore strongly recommended.

Kono (1971) showed that paleointensities as expressed by virtual geomagnetic dipole moment exhibit a normal distribution for both normal and reversed polarities in the last 10 m.y. Recently, McFadden and McElhinny (1982) confirmed Kono's finding on a much increased data set for the last 5 m.y., but they suggested a normal distribution truncated at very small dipole intensity. The difference between the two studies may be due to the data selection; Kono used all the data available while McFadden and McElhinny omitted data corresponding to geomagnetic reversal or excursion periods.

The present results show that the absence of very small paleointenities may partly be explained by experimental errors for F/F_0 ratios much different from unity. Since all the paleointensity experiments reported to date were done with laboratory fields of 30-60 uT, and since the data for small paleointensities are scarce, it is possible that large experimental errors have obscured such data and resulted in a seemingly truncated distribution.

The errors attached to the ratios F/F_0 shown in Fig. 6 were obtained from the standerd error (s_b) of the slope of the NRM-TRM relation in the NRM-TRM diagram (see Kono and Tanaka, 1983). Errors are larger at larger F/F_0 ratios than at smaller F/F_0 because contamination of the TRM components by misalignment of the NRM component occurrs at all temperatures (see Fig. 2b). On the other hand, as the effect of magnetic field setting error is relatively small in comparison with that of measurement errors in angles (Kono and Tanaka, 1983), low temperature points for small F/F_0 do not contain large errors (see Fig. 2a).

4. Conclusions

We have demonstrated the applicability of the Thelliers' method to a very wide range of paleointensity values (10 to 500 uT if 10 % error is permissible) by experiments using natural rock samples which acquired TRM in laboratory fields of various magnitudes. The field range can even be extended by the use of a matched laboratory field. Our results suggest that, if the magnitude of laboratory field is properly selected, we can determine paleointensities of the geomagnetic field for three orders of magnitude (1 to 1000 uT). As the errors become very large if F/F_0 is much different from unity, the use of matched laboratory fields may be sometimes mandatory. From these results, we can conclude that the intensity fluctuations shown by the presently available paleointensity data are real features of the geomagnetic field variation. The absence of very small

paleointensities, however, may, in part, be caused by large errors inherent in experiments with F/F_0 ratios much different from unity.

References

Arai, Y. (1963) M.Sc. Thesis, Univ. of Tokyo.

Coe, R.S. (1967) J. Geomag. Geoelectr., 19, 157.

Coe, R.S. and C. S. Grommé (1973) J. Geomag. Geoelectr., 25, 415.

Kono, M. (1971) Earth Planet. Sci. Lett., 11, 10.

Kono, M. (1978) Geophys. J. Roy. Astr. Soc., 54, 241.

Kono, M. and H. Tanaka (1983) J. Geomag. Geoelectr., submitted.

McFadden, P. L. and M. W. McElhinny (1982) J. Geomag. Geoelectr., 34, 163.

Nagata, T., Y. Arai, and K. Momose (1963) J. Geophys. Res., 68, 5277.

Shaw, J. (1974) Geophys. J. Roy. Astr. Soc., 39, 133.

Tanaka, H. (1980) J. Geomag. Geoelectr., 32, 171.

Thellier, E. and O. Thellier (1959) Ann. Géophys., 15, 285.

Williamson, J. H. (1968) Canad. J. Phys., 46, 1845-1847, 1968.

(Submitted to J. Geomag. Geoelectr.)

SECULAR VARIATION OF GEOMAGNETIC INCLINATION SINCE 9,000 YR B.P. IN JAPAN RECORDED BY SEDIMENTS IN LAKE KASUMIGAURA

Toshitsugu YAMAZAKI, Masato JOSHIMA and Yoshiki SAITO

Marine Geology Dept., Geological Survey of Japan,
1-1-3 Higashi, Yatabe, Ibaraki, 305, Japan

Introduction

This report presents reliable records of secular variation of geomagnetic inclination in central Japan since 9,000 yr B.P. recorded by sediments in Lake Kasumigaura. So far as recent 2,000 years, the secular variation curve in Southwest Japan has already been constructed by archaeomagnetic investigations (Hirooka, 1972; Sibuya, 1980), but as the period of before 2,000 yr B.P. insufficient data have been able to be available for drawing reliable secular variation curve.

Lake Kasumigaura is the second largest lake in area in Japan. Its water depth is only 4 to 5 m now. Holocene sediments of maximum thickness of about 50 m, however, have filled up this lake. Most of them are marine in origin. These rapidly and continuously deposited fine grained sediments were suitable for obtaining continuous palaeomagnetic records of sufficient resolution to study geomagnetic secular variations.

Sampling and Measurement

Two cores, KB1 and KB2 in Fig. 1, were bored down to about 25 m and 40 m, respectively, under the lake bottom by modified LIVINGSTONE Piston Sampler (Aoki and Mizuno, 1970) with core-catcher. Undisturbed continuous core samples were obtained. These sediments are composed of silt and clay except for lowermost several meters where sands and gravels occupy. Rates of core-recovery in silts or clays exceeded 95%. The Sampler was drawn up each 2 m digging, and the absolute orientations of each core are not known, so horizontal component of the remanence changes relatively between each 2 m core. Specimens for palaeomagnetic measurements were taken in succession except for the part of the core catcher of about 10 cm in length by small plastic cubic case of 2.5 cm in length of one side. Total numbers of the specimens were 900 (KB1) and 1,400 (KB2). Natural remanent magnetization of all specimens

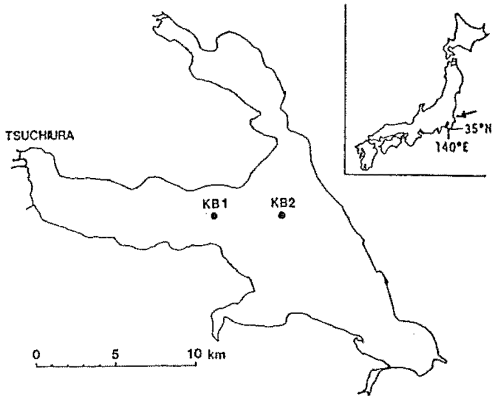

Fig. 1 Location of coring sites.

were measured on a cryogenic rock magnetometer (SCT Model 113). The specimens selected as pilots at intervals of several meters were demagnetized stepwise by alternating field (AF). For silt and clay, unstable components were removed by peak field of less than 50 Oe. Typical examples are shown in Fig. 2. The changes in direction between each demagnetizaton level above 50 Oe were 2° to 3°, and showed no systematic trend. Remaining all specimens were cleaned by peak field of 50 to 100 Oe. The samples of sand and gravel from lowermost several meters were, however, rejected because of their larger directional changes in stepwise AF demagnetization.

Too large changes in declination with depth for secular variations were revealed except for uppermost few meters where the sediments were very soft. Furthermore, the orientation of the rotation (clockwise or anticlockwise) changed between each 2 m core. Judging from these results, it may be concluded that these changes do not represent true secular variations of declination, and they are probably due to the sampler's rotation during its penetration. Only inclination data are treated in following discussion.

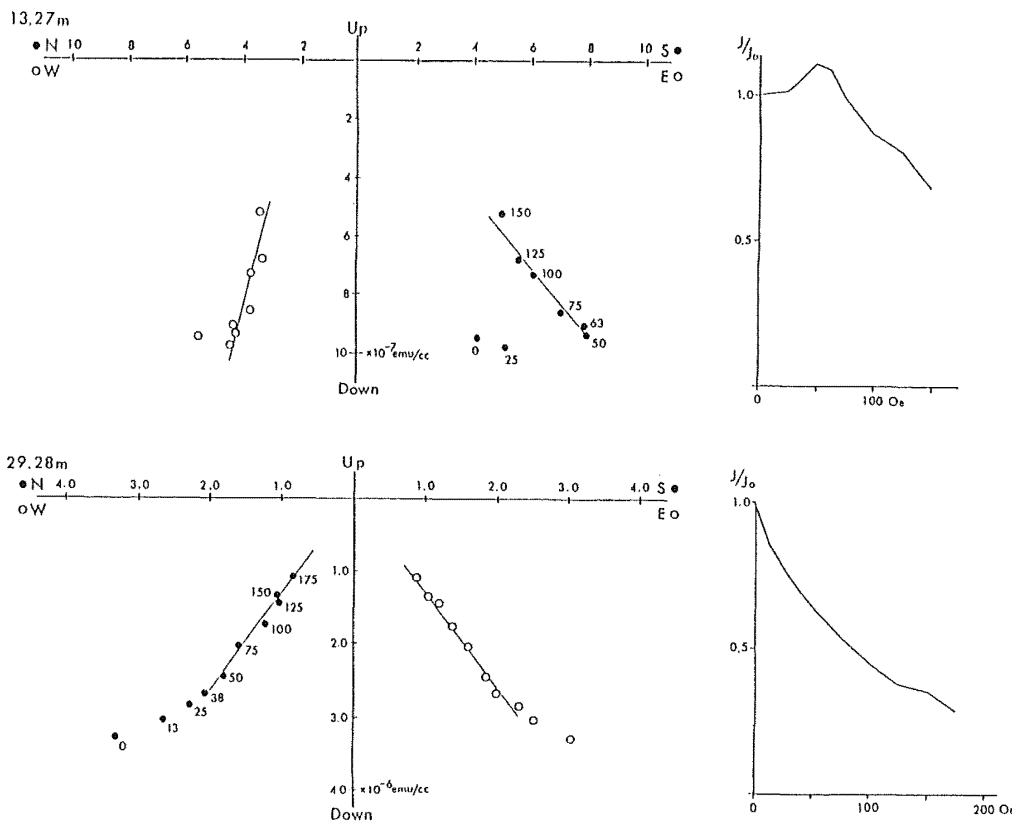

Fig. 2 Typical data of the stepwise alternating field demagnetization. Demagnetization steps are indicated by the value of the peak field in Oe.

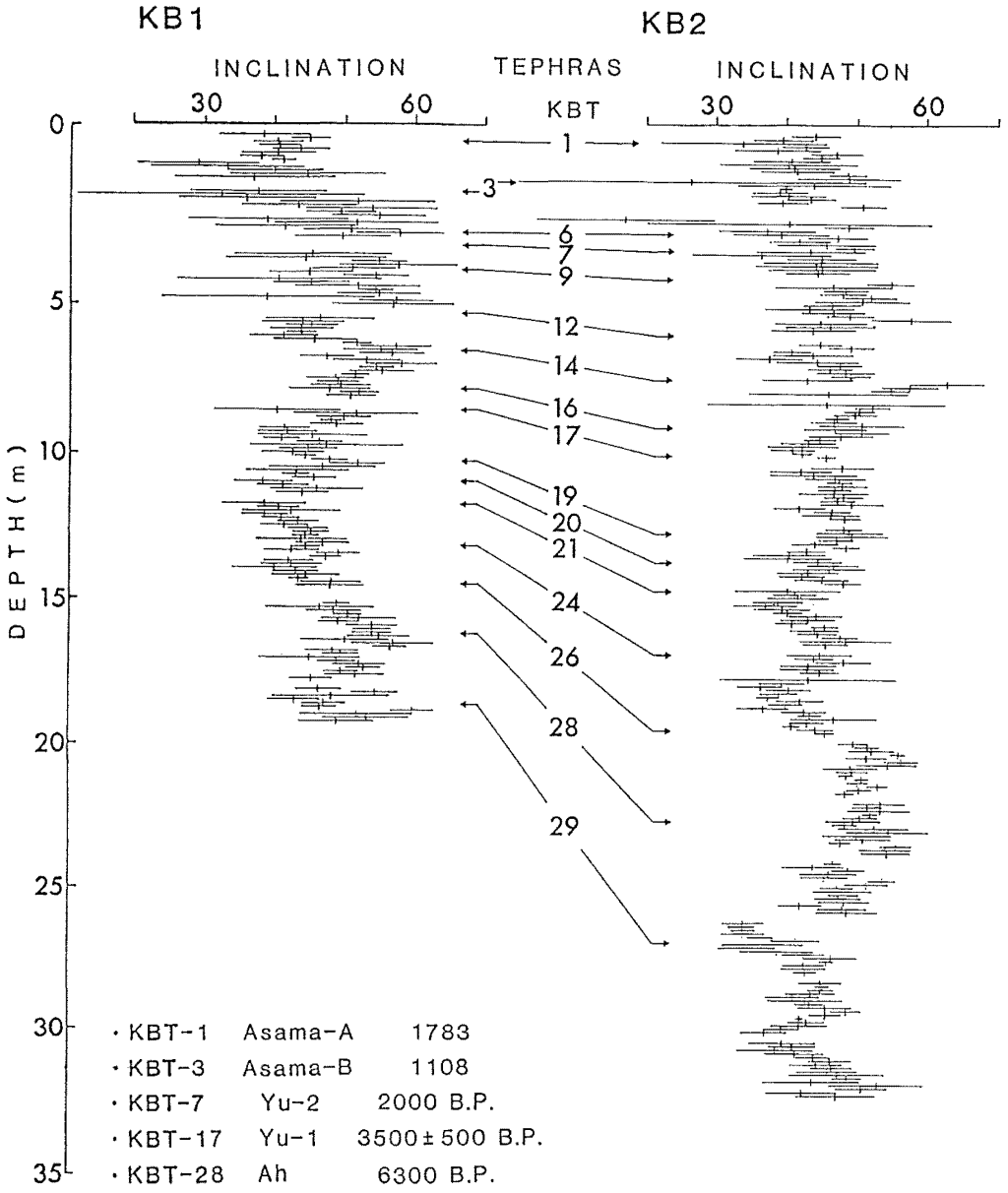

Fig. 3 Inclination records and the correlation of the two cores by tephras (KB1-KB29). Cross and horizontal bar represent the mean and the standard deviation of each five specimens in vertical succession. Marker-tephras are summerized on the bottom of this figure.

Results and Discussion

Inclination records of the two sites are presented in Fig. 3. The mean (cross) and the standard deviation (horizontal bar) of each five specimens in vertical succession are indicated. In Lake Kasumigaura, the sedimentation rate is so great that it takes only about 40 years (the mean of KB 2) to accumulate for five specimens (about 13 cm). We can regard these five specimens as taken from the "same horizon" because changes of the geomagnetic field in such a short period are considered to be able to be ignored. As illustrated in Fig. 3 the inclination data treated in this manner show fairly good convergence except the uppermost few meters, especially those of KB 1, where the intensity of the remanence was the weakest (order of 10^{-7} emu/cc).

The sediments in Lake Kasumigaura intercalate many thin (1 to 10 mm in thickness) volcanic ash layers (Tephras KBT 1 to KBT 29 in Fig. 3). Two cores, KB 1 and KB 2, were precisely correlated by these tephras. As shown in Fig. 3, this correlation revealed that the variations of the inclination with time in the two cores closely agreed between each other even on the detailed fluctuations. This fact much improved the reliability of the secular variations of the inclination in this report. Some tephras among them, furthermore, are correlative with those of other areas in Japan the ages of which have already been known. KBT 28 was identified by Dr. F.Arai as the Akahoya ash (Ah) (6300 yr B.P.; Machida and Arai, 1978) which is one of the widespread marker-tephras in Japan. KBT 7 and KBT17 are the Yufune scorias (Yu) which are maker-tephras in the Kanto district of Japan.

Fig. 4 shows the relation between the inclination and the age about KB 2 of which the quality of the inclination data seems to be higher than that of KB 1. The ages used are as follows;

KBT 7	(Yu-2)	2,000 yr B.P.
kBT17	(Yu-1)	3,800 yr B.P.
KBT28	(Ah)	6,300 yr B.P.

We adopt at present the value of 9,000 yr B.P. as the age of the bottom of the core, but in the near future more precise age will become clear because the age of the peats derived from the base of the cores are now in measurements by the carbon-14 method. Constant sedimentation rates among these ages were assumed.

The particular features of the secular variation of the inclination in central Japan shown in Fig. 4 are as follows;

(1) An episode of steep inclination had lasted from 7,000 to 6,000 yr B.P., and a period from 6,000 to 4,000 yr B.P. is characterized by the fluctuations of small amplitude and short wavelength. The existing data compiled by Hirooka and Tokieda (1979) are consistent with the above mentioned features.

(2) The characteristic shapes of the rounded inclination maxima and the pointed minima, which were pointed out by Creer (1983) by the data from Lake Superior, Lac de joux, and the Black Sea, are also recognizable.

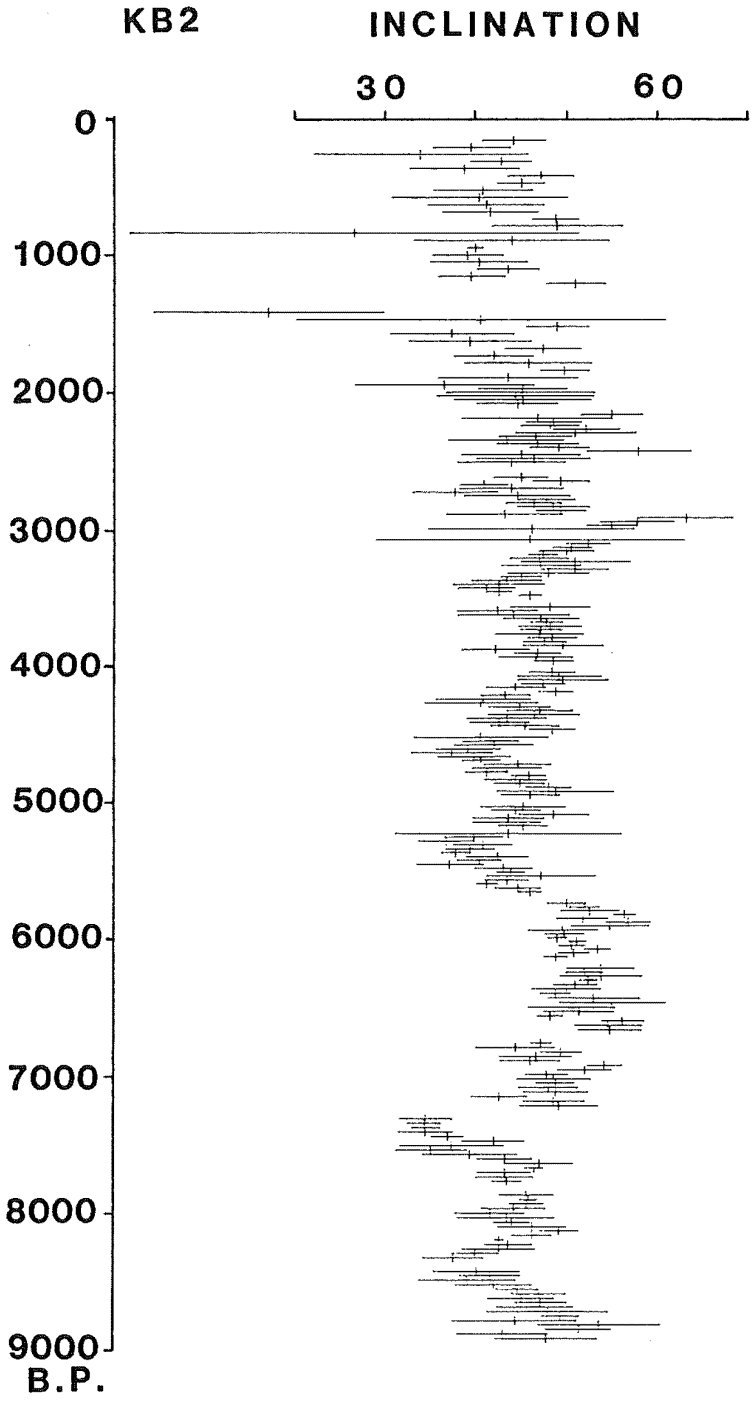

Fig. 4 Secular variation of the geomagnetic inclination recorded by the boring-core KB2.

References

Aoki, I. and A. Mizuno (1970) J. Geol. Soc. Japan., 76, 519-523. (In Japanese with English Abstract)
Creer, K. M. (1983) Nature, 304, 695-699.
Hirooka, K. (1971) Mem. Fac. Sci. Kyoto Univ., Ser. Geol. Mineral., 38, 167-207.
Hirooka, K. and K. Tokieda (1979) Rock Mag. Paleogeophys., 6, 18-24.
Machida, H. and F. Arai (1978) The Quaternary Res., 17, 143-163. (In Japanese with English Abstract)
Shibuya, H. (1980) Master Thesis of Osaka Univ.

INTERNAL CONSISTENCY OF PALEOMAGNETIC RECORDS IN SEDIMENTS

Masayuki HYODO*, Satomi ONISHI** and Katsumi YASKAWA**

* Cryogenic center, Kobe University, Nada, Kobe 657
** Department of Earth Sciences, Faculty of Science, Kobe University, Nada, Kobe 657

1. Introduction

A number of core samples of sediment have been collected from lake and oceanic bottoms to investigate past environments of the earth. Several kinds of coring technique were invented to the purpose of each study. Using a wide-diameter corer is one of them. A giant core sample of sediment taken by the corer provides us an extended study on the informations recorded, since a statistical analysis of data is possible within the same age horizon. The most profitable matter of using these sediments in paleomagnetic studies is to be able to obtain a scatter of magnetization direction in each depth. We collected a core sample of sediment with a wide-diameter from Osaka Bay, Japan. Statistical treatment was made on remanent directions after measurement of magnetizations of several specimens in each depth. We discuss a suggestive relation between directional dispersion and intensity from the sediment.

2. Sampling and measurement

A core sample of sediment 20 cm in diameter was taken at latitude 34.6° S, longitide 135.3°E in a water depth of 16 m. Fore specimens in average were collected at intervals of 3.8 cm along depth over 155 horizons. Magnetizations were measured using a SQUID magnetometer with sensitivity of 10^{-8} emu. Although the core length was 7.1 m, the uppermost section of 1.1 m was so loose that specimens for measurement of remanence could not be taken. All data on natural remanent magnetization (NRM) are shown in Fig.1. It has been recognized that the curves upper 3 m of declination and inclination are consistent with those from archeomagnetism (Hyodo & Yaskawa, 1980). Two characteristic features are noted in the variation curves of magnetization. One is that the remanent intensity has a remarkable drop around 4.5 m, where there is a large fluctuation of direction. Another is that there is a common periodicity of a dominant wavelength in declination, inclination and intensity.

3. Directional dispersion and intensity

Dispersion of magnetization direction is often expressed by precission parameter K. Fig.2.b shows precission parameter from magnetizations of specimens in each depth of the sediment, on a log scale. It shows a periodic change like the declination, inclination and intensity curves. What brings magnetization direction scattering ? Some causes can be inferred. (a) The scattering is produced systematically in conformity with a process of remanence acquisition. (b) A sediment undergoes some disturbance which may be naturally broken out or added artificially during all procedures of paleomagnetic study. (c) Dispersion reflects a physical property of a sediment. We differentiate the variation curve of remanence azimuth in order to find a clue to the present problem. Fig.2.a shows the derivative of azimuth $|dA/dz|$, the angle moving in a unit depth, calculated with mean directions in each horizon. And then we calculate cross correlation coefficient between K and $|dA/dz|$. The result, shown in

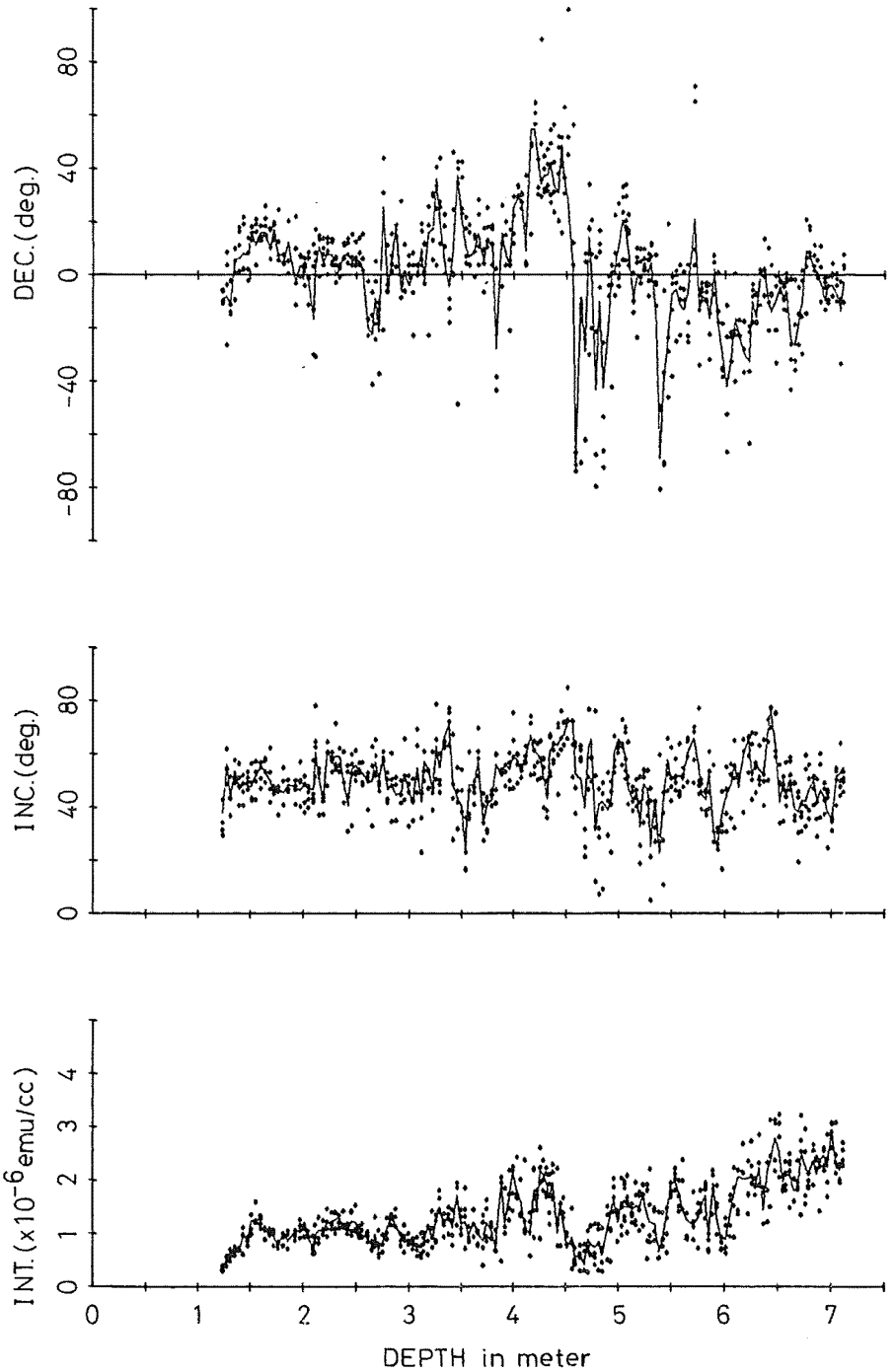

Fig.1 All data points and mean values in each depth (true lines) of NRM.

Fig.3.a, represents a strong negative correlation. The dispersion becomes wide where the magnetization direction changes steeply. This mutual relation is recognized not partly but throughout the length. This fact would suggest that the dispersion of remanent direction is produced in a process of magnetization and it is regarded as one of informations on the geomagnetic field. The sediment looks homogeneous from its color, grain size, and so on.

There is another interesting relation. Remanent intensity changes in accordance with dispersion of direction. Fig.2.c shows the NRM intensity normalized with saturation isothermal remanent magnetization (SIRM). Although the SIRM is used to remove the effect of change in quantity of magnetic minerals, it exactly shows a few slight fluctuations only. It suggests that the sediment is quite homogeneous with respect to magnetic minerals, too. Strong possitive correlation was calculated between the dispersion K and the intensity (Fig.3.b). It means that the intensity drops where the direction scatters.

We also test whether the remenent intensity varies being dependent on inclination. Cross correlation coefficient is calculated among them (Fig.3.c). According to the result, they do not show any correlativity when the lag is zero, but the correlation coefficient increases along negative axis suddenly around the lag = 10. This matter suggests that the remanent intensity does not directly depend on the inclination but has negative correlation with derivative of the inclination. It further shows that the magnetic signals in the sediment have a strong periodicity and a quarter of its dominant wavelength is ten intervals, which equals 38 cm.

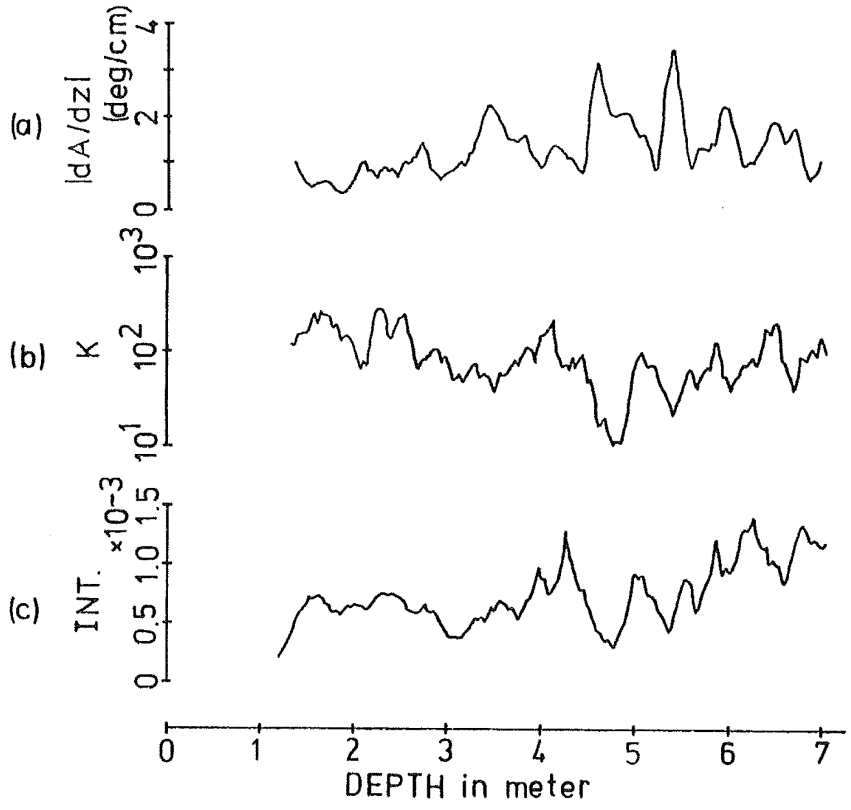

Fig.2 Three consistent variation curves. (a) Angle moving in a unit depth. (b) Precission parameter from remanences of fore specimens in each depth. (c) Remanent intensity of NRM normelized by SIRM. Each curve is smoothed by an operation of 5-points running mean.

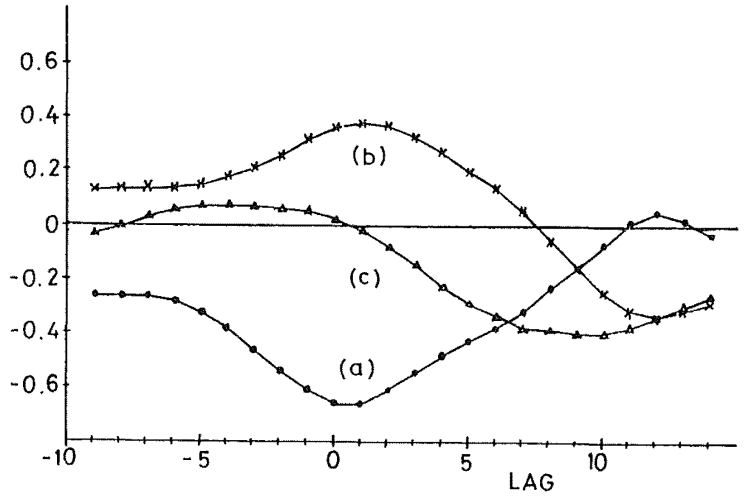

Fig.3 Cross correlation coefficients. (a) Precission parameter K / Derivative of azimuth |dA/dz|. (b) Precission parameter K / Intensity. (c) Intensity / Inclination.

4. Discussion and conclusion

Paleomagnetic data preserved in the sediment show that magnetization scatters in direction and drops in intensity where azimuth of the magnetization steeply changes along depth. This fact suggests that fixing of magnetic particles in a horizon occurs not simultaneously but gradually over some time span or some depth. It means that a sediment integrates the geomagnetic field variation in magnetizing.

With respect to remanent intensity, we can infer as follows. A sediment acquires remanence with low intensity in a field steeply changing in azimuth. Two interpretations can be made for this fact. (a) Field intensity actually decreases as the azimuth of the field becomes unstable. (b) Integration of a changing field in acquiring remanence results in irregular alignment of magnetic particles' axes and then cancellation of magnetic moments produces an intensity drop even when the field intensity is constant. It is in fact hard to consider that intensity of the earth's field changes correctly following the fine directional change as shown by the data from the magnetization of the sediment. Therefore only the component explained by (b) appears to take an important role in intensity. But the remanent intensity changes with too large amplitude to be interpreted by only the effect of integration. Some non-linear reducing factor, for example by extreme dispersion in particle alignment, should be added to the effect. Anyway, remanent intensity of sediments seems to depend mostly on the derivative of the azimuthal change of field.

The consistent change of directional dispersion and intensity throughout the length indicates that the remanence has been acquired through a uniform mechanism. This matter leads to the possibility of deducing a secular variation of the geomagnetic field from magnetization of sediments. Then the consistency of dispersion and intensity is used as an indicator of internal consistency of magnetic records in a sediment.

Reference

Hyodo, M. and K. Yaskawa (1980) J. Geomag. Geoelectr., 32, 581.

PALEOMAGNETIC MEASUREMENTS OF DEEP DRILLING CORE SAMPLES FROM LAKE BIWA

Masayuki TORII, Hidetoshi SHIBUYA, Akira HAYASHIDA *, Ikuo KATSURA, Shoji YOSHIDA, Takahiro TAGAMI, Yo-ichiro OTOFUJI **, Yukiko MAEDA *** and Sadao SASAJIMA

Department of Geology and Mineralogy, Faculty of Science, Kyoto University, Kyoto 606, Japan

In 1982 and 1983, drilling and coring achieved a total sub-bottom penetration of 1422.5 m at the central part of Lake Biwa by Institute of Paleolimnology and Paleoenvironment on Lake Biwa, Kyoto University. Paleomagnetic measurements have been conducted on over 5000 unconsolidated samples from sub-bottom depth of between 10 and 805 m. Vertically oriented cubic samples of 8 cc volume were taken from a half of split core approximately every 5 to 15 cm, exclusive to clay, silt and very fine sand. NRM measurements were carried out with a cryogenic magnetometer (ScT C-112) almost coeval with the coring operation in order to prevent drying and chemical alteration of unconsolidated sediment samples. Intensity of NRM was ranging from 10^{-5} to 10^{-8} cgs emu/cc except for volcanic ash layers. Several pilot samples from every section (1 m - 3 m) were subjected to a stepwise alternating field demagnetization up to 400 - 1000 Oe in peak field. Some of pilot samples were tested by a thermal method of demagnetization up to 600°C especially for the deeper part of the entire core. The other samples were finally demagnetized by the alternating field method at 150 or 200 Oe.

In respect to the samples from deeper sections of the core, a relatively stable secondary component was dominant, and could be erased out only by the thermal demagnetization at about 300 C as shown in Fig. 1. Alternating field demagnetization was not effective to eliminate the secondary component which might be a chemical overprint. It was practically difficult to carry out thermal treatment of a number of soft sediments, so the thermal demagnetization was restricted only for a few pilot samples from each core section.

The other problem is a distortion of the soft sediment core, which might be caused by a rotary drilling procedure adopted in this project. It is unescapable for soft sediments to be suffered from deformation in the case of drilling by a rotary (Prell et al., 1982). Fig. 2 shows typical examples of the magnetic directions scattered within a continuous core. The pattern of the declination change shown in Fig. 2a suggests that the core was twisted through the drilling operation. It was clearly observed, on one hand, that the core of Fig. 2b was broken into slices of several centimeters thick, so that the scatter of the declination is suggested due to separate rotation

---

present address:
* Dept. Earth Sci., Doshisha Univ., Kyoto 602, Japan
** Dept. Earth Sci., Kobe Univ., Kobe 657, Japan
*** JAPEX Geosci. Inst., Tokyo 107, Japan

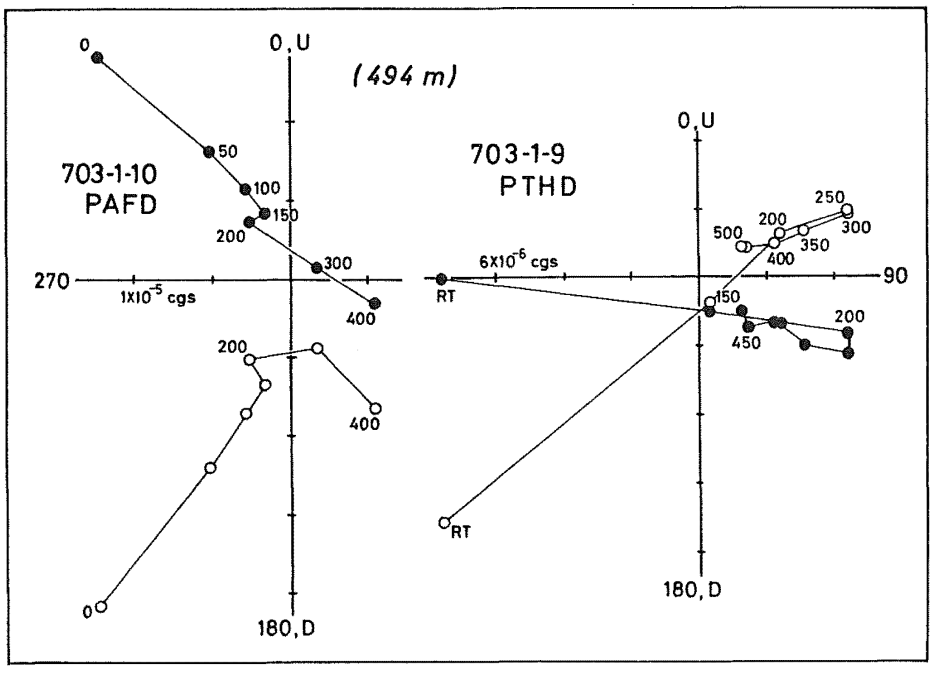

Fig. 1 Typical vector end-point diagrams of progressive alternating field and thermal demagnetization of samples from 494 m. Solid and open circles are projection of vector end-points on horizontal and 90-270 vertical planes, respectively. Numbers adjacent to symbols are peak alternating field in Oe and demagnetization temperature in °C.

of each segment. It should be noted that the core distortion affect not only on declination but also on inclination; differential rotation of two sliced segments of a uniformly magnetized core gives deeper inclination than the original value. Fig. 3 shows inclination change of the vector sum caused by relative angular displacement of each magnetic vector, taking the original inclination as a parameter. Dipping error of inclination caused by the separate rotation is observable as an erratic flip of remanent vectors into high inclination zone show in Fig. 2 (b).

Based on the results of thermal demagnetization experiment of samples from undeformed sections, the entire magnetic polarity log is shown to consist of two magnetozones: the upper normal polarity zone and the lower reversed polarity zone (Fig. 4). Because the uppermost part of the core corresponds to the recent sediments of Lake Biwa, the upper magnetozone (5 m - 450 m) can be correlated to the Brunhes normal polarity epoch. The lower half (450 m - 805 m) is, hence, correlated to the Matuyama reversed polarity epoch. A short normal polarity interval from 605 m to 638 m is acceptable as a record of the Jaramillo normal event. These correlations seem to be in good agreement with the result of tephrostratigraphic correlation of the core to the land sections around Lake Biwa (Yokoyama and Takemura, 1983). If we simply extrapolate the present result of paleomagnetic correlation, the basal part of unconsolidated sediments, which is supposed the

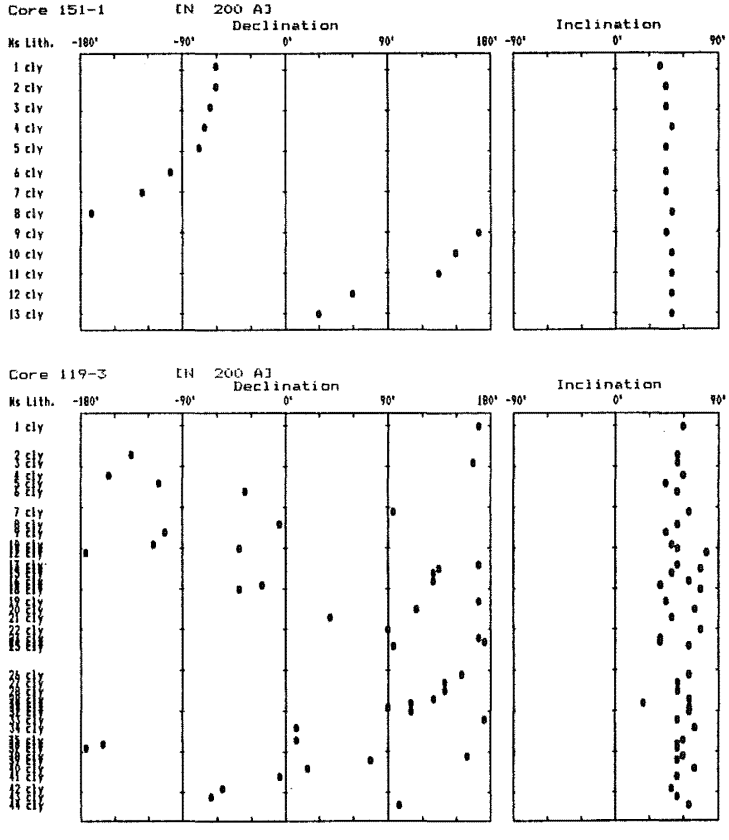

Fig. 2 Typical example of magnetic directions in the upper part of the core. (a) twisted core (plastic deformation). (b) sliced core (differentially rotated segments).

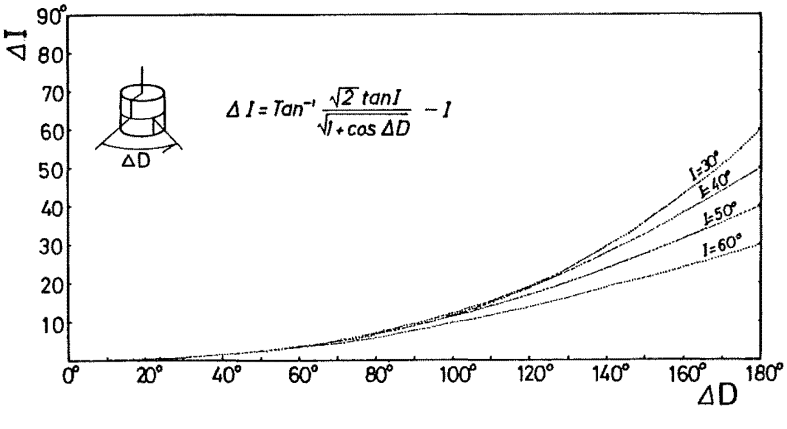

Fig. 3. Dipping of magnetic vector (ΔI) due to differential rotation (ΔD) of two sliced blocks. The calculation was made for four inclinations of the blocks (I).

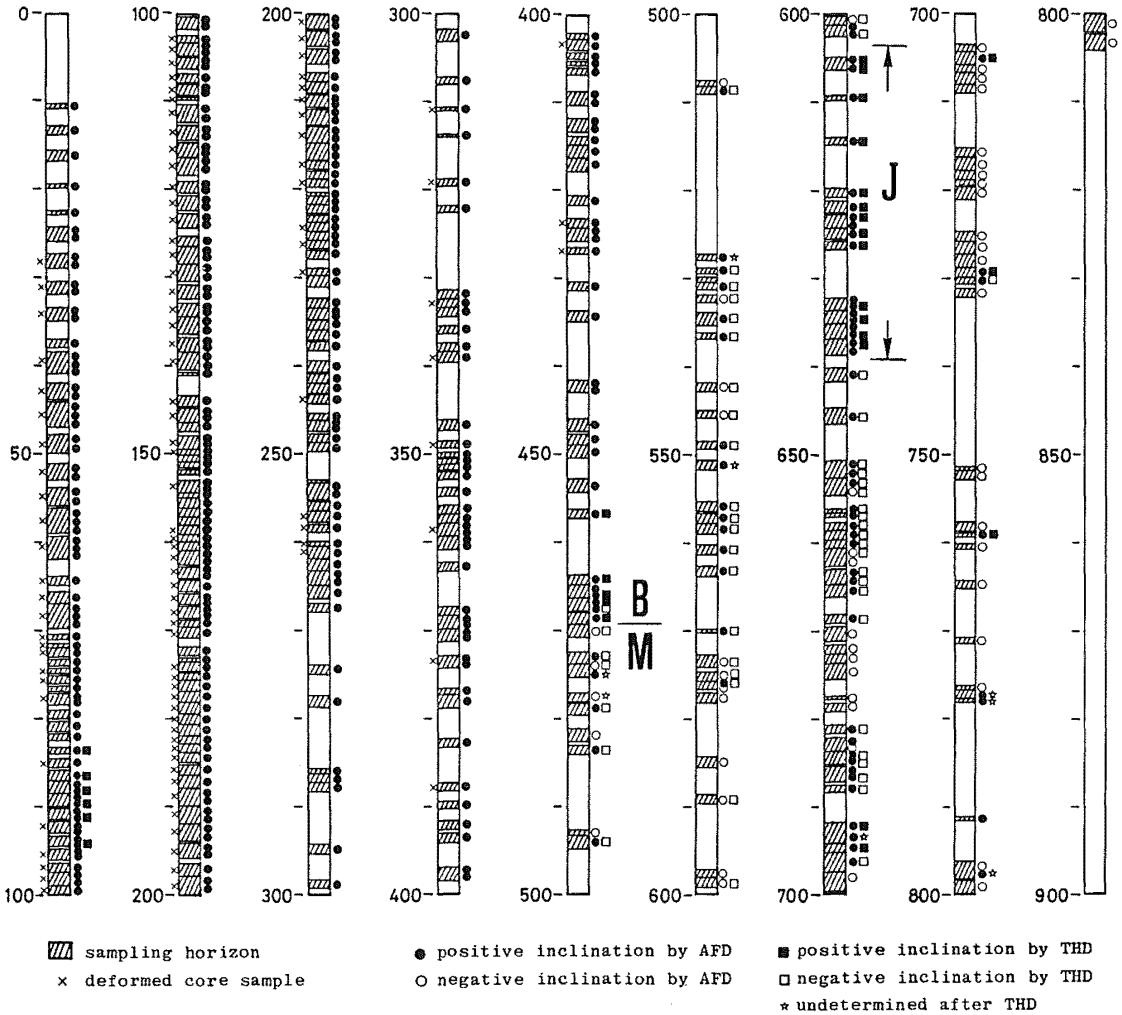

Fig. 4. Summary of paleomagnetic results. B/M shows horizon of the Brunhes/Matuyama polarity epoch boundary. J denotes the Jaramillo normal polarity event.

oldest lake sediments of the present Lake Biwa basin, is postulated to be 1.3 Ma in age. We could not find out any short reversed polarity intervals correlative to the Blake, Biwa I or Biwa II event, which were recorded in the 200 m core sediments recovered from almost the same location in 1971 (Kawai et al., 1972). It is rather difficult to point out reasons for the absence of reversed polarity zones in the upper normal zone. One of the most likely causes is an effect of deformation of the core mentioned above, which might act to remagnetize the loose sediments of the upper part without any visual texture of deformation.

References:

Kawai,N., K.Yaskawa, T.Nakajima, M.Torii and S.Horie (1972) Proc. Japan Acad., **48**, 186.

Prell,W.L., J.V.Gardner et al. (1982) Init. Repts. DSDP, **68**, U.S. Govt. Printing Office, Washington.

Yokoyama,T. and K.Takemura (1983) IPPCCE Newsletter, 3, 21.

(to be submitted to J. Geomag. Geoelectr.)

DOUBLE JARAMILLO EVENT IN THE CORE P171 RECOVERED FROM THE CENTRAL PACIFIC BASIN NEAR THE EQUATOR

Masato JOSHIMA

Geological Survey of Japan, Higashi 1-1-3,
Yatabe-machi, Tsukuba-gun, Ibaragi 305

1. Introduction

Many cores were obtained from the Central Pacific Basin near equator by the research vessel Hakurei-maru during the geological survey cruise GH80-1. They were sampled by a piston corer of 8m length barrel, and their positions were set on the transect lines from Wake to Tahiti.

The specimen for magnetic measurement was sampled from the cutting plane of the core which was split to the half. Chrolide vynil cubic case with the size of 2.3 * 2.3 * 2.0 cm was pushed in the surface vertically and then pulled out sucsessively. All these specimen were packed in larger chroride vynil case and sealed with vynil tape for avoiding dehydration, and brought back to our laboratory for measurement of remanent magnetization. And their preliminary results were already reported in our cruise report (Joshima 1982).

Lithorogy and sumarizud results of magnetic measurement of these cores was shown in Fig.1 (Nakao et.al.1982).

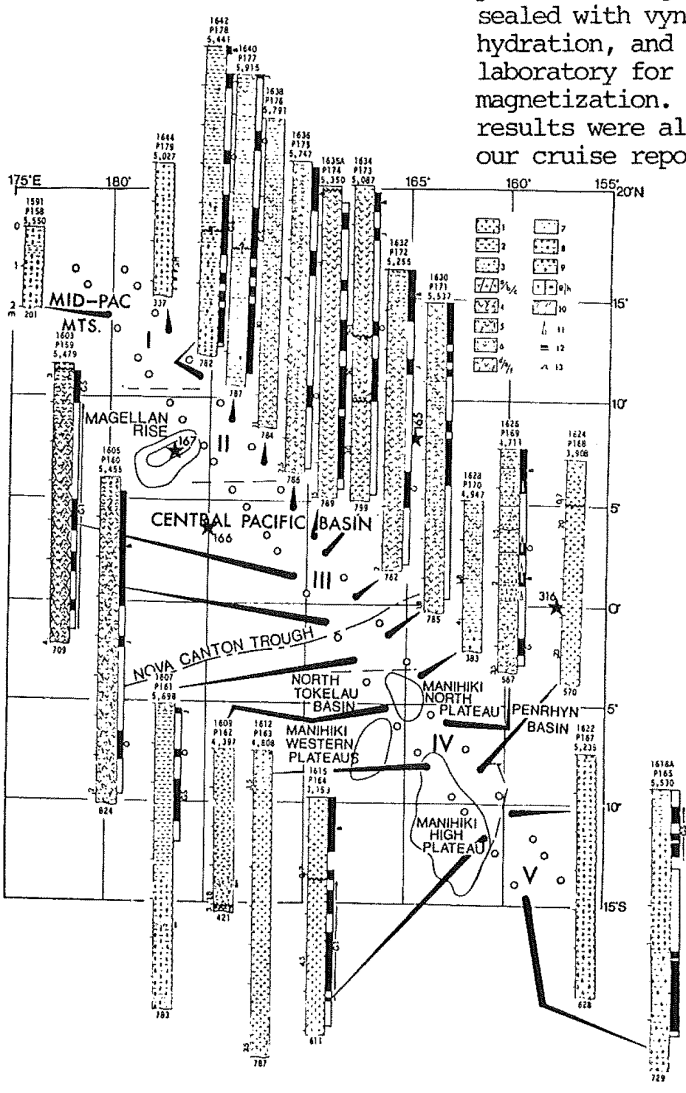

Fig.1 Lithology and magnetic stratigraphy of cores obtained in GH801. Explanations for legend: 1, calcareous ooze; 2, calcareous mud or clay; 3, calcareous fossils rich clay; 4, siliceous ooze; 5, siliceous mud or clay; 6, siliceous fossils rich clay; 7, pelagic clay; 8, zeolitic mud or clay; 9, zeolitic rich clay; 10, consolidated rocks.

Among these cores P171 showed pecurier results in the pattern of magnetic stratigraphy, it showed apparent two Jaramillo event. The results reported in cruise report are shown in Fig.2, and another results remeasured later on the specimen which were sampled again in another half of the core are shown in Fig.3.

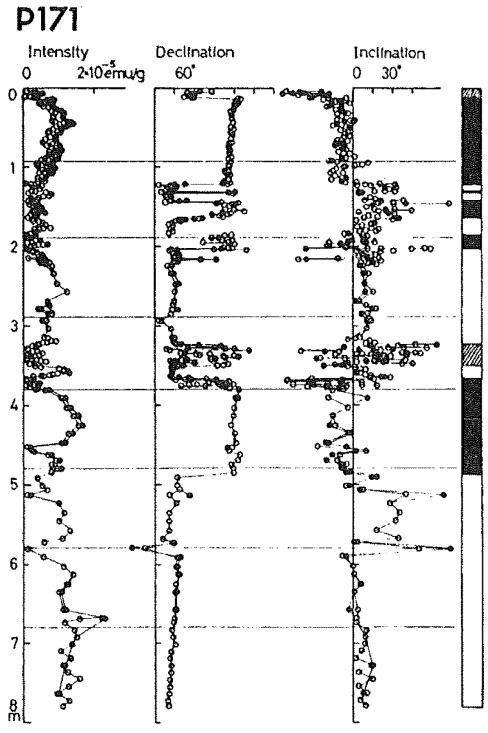

Fig.2 Preliminary results of remanent magnetization measurement of P171 long case of 22.5 cm length.

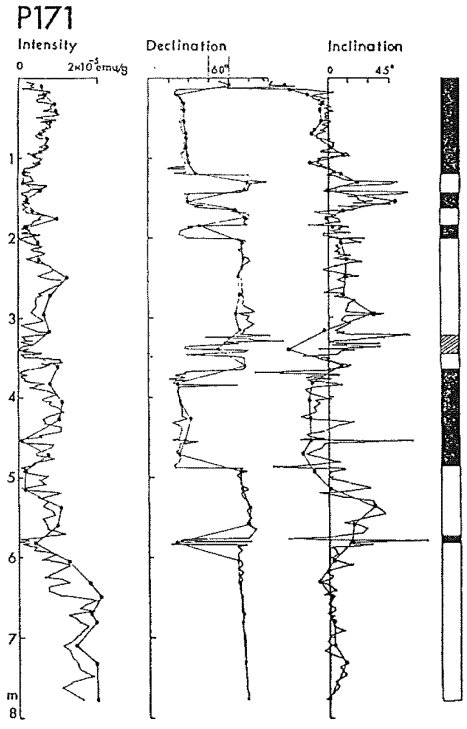

Fig.3 Remeasured results of another half of P171 using using cubic cases with the size of 2.3 * 2.3 * 2.0 cm.

Time interval between the two measurement was about two year but their results showed very good coinsidence. They showed normally magnetized part of 1 m's length at their top part and two short eventlike normally magnetized parts in the lower reversally magnetized parts. The detail of the apparant two Jaramillo events in core P171 was reported below.

2. Microfossiles

Takayanagi et. al. (1982) have shown the data on the radiolalia and foraminifera of these cores and the top part of P171 was detrmined to be Buccinosphaera invaginata zone and their age ranges from now to 200 thousand year. And the bottom part was determined to be Pterocanium prismatium zone and their age is set between 1.5 amd 2.7 Ma, but upper limit of the bottom age was not clearly determined. The central part of the core, 1.5 m, 3.5 m and 5.5 m, was restricted to be Amphirhopalum praeypsilon zone and their age is between 0.9 and 0.4 Ma, but lower limit of their age was not defined clearly.

Nishimura have shown that Mesocena qudlanqla of Silicoflagellata appears much around the part of Jaramillo event and its age lied in the range between 1.4 and 0.6 Ma according to Jousé (1973), but the magnetostratigraphic data of the cores measured by Yamazaki supplied from the Central Pacific Basin near equator in GH81-4 showed that the range of its age seems to be shorter than that and be settled in the range between 1.2 and 0.8 Ma, then it doesn't reach to Brunhes epoch.

3. History of sedimentation

The results of microfossil, Mesocena quadrangula Haeckel of silicoflagellata which appeared in the depth of the core between 0.9 and 1.5 m and the results of remanent magnetization revealed that the upper short normally magnetized eventlike part is not put in the range of the microfossile. Furthermore the bottom part is shown to belong to Pterocanium primatium zone by Takayanagi et. al. (1982), so the normally magnetized part between 3.7 and 4.9 m is identified to be Olduvai event, then the assumption of the linearity of accumulation rate of lower part of the core needs that the short eventlike normally magnetized part at 5.8 m is identified to be Reunion event. The sedimentation curve with time is shown in Fig. 4 summarized with together magnetic stratigraphy and two kind of microfossile's data.

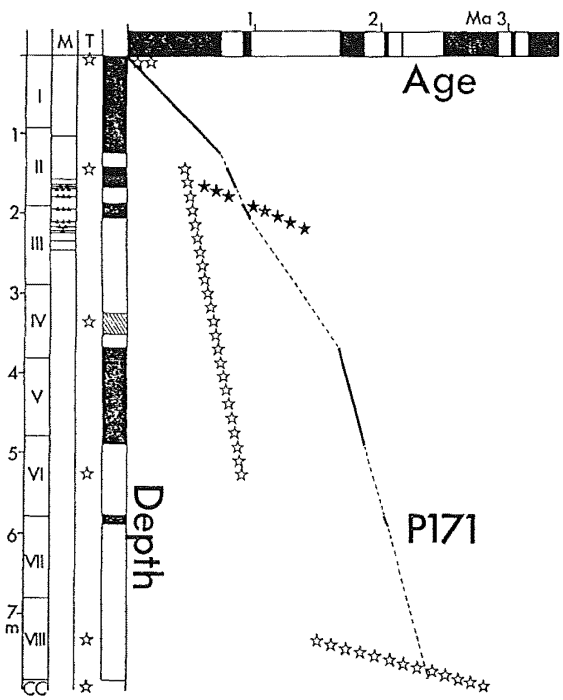

Fig.4 Sedimentation curve of P171 with age is shown withtogether micro fossil's data. Open star mark represents the data of Takayanagi et. al. and its sampling position in the core is marked in left column. Closed star mark is for silicoglagellata and their sampling position is marked by bar in left column and dot marks represent their abundance: ***; abundant, **; common, *; few, --; rare.

4. Discussion

Other short events or excurtions around Jaramillo event have reported by Maenaka (1983), Niitsuma (1979), and others, their magnetostratigraphic pattern of vertical sections showed many short normally magnetized part around Jaramillo event, although they didn't coincidence each other (Fig.5).

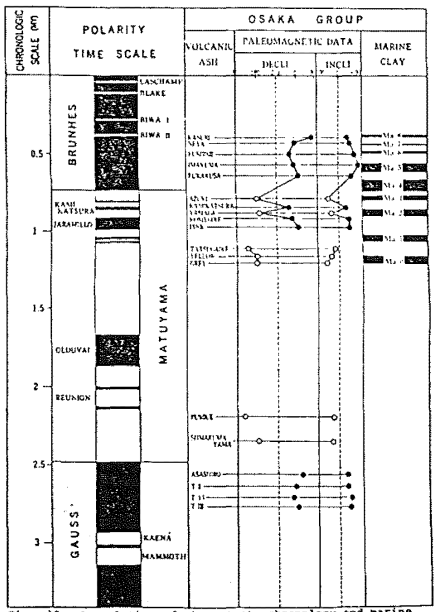

Maenaka (1983)

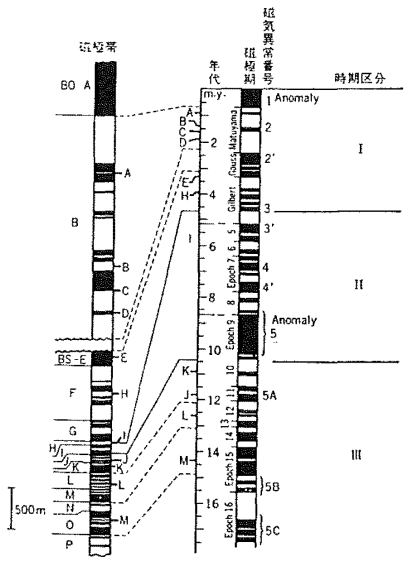

Niituma (1979)

Fig. 5 Examples of short events around Jaramillo event reported in some vertical sections.

The upper short normally magnetized part of P171 may be corresponded to these short events. There is a discontinuity at the depth of 1.7 m which coincidence with the lower limit of the upper short normally magnetized part and the color of the part was a little brighter than the lower part of the discontinuity, although upper limit of the brighter part is not clear and it changed upward gradually to the same color with the lower part. So the upper mormally magnetized part might have depositted faster than the part around and been magnetized in some one of shorter unnamed normal events after Jaramillo event.

REFERENCES

Joshima, M., (1982) Geological Survey of Japan Cruise Report, No.18, p.276-287.
Jousé, A. P. and Mukkinà, (1973) Oceanology, vol.13, no.3, p.386-394.
Maenaka, ., (1983) Memoirs of Hanazono University, no.14, p.1-65.
Niituma, ., (1979) Kagaku, vol.49, no.1, p.36-43.
Nishimura, A., to be published in G.S.J. Cruise Rept..
Takayanagi, Y. et. al., (1982) G.S.J. Cruise Rept., no.18, p.238-263.
Yamazaki, T., to be published in G.S.J. Cruise Rept..

POSSIBILLITY OF RECONSTRUCTION OF THE PAST GEOMAGNETIC FIELD FROM HOMOGENEOUS SEDIMENTS

Masayuki HYODO

Cryogenic Center, Kobe University,
Nada, Kobe 657, Japan

1. Introduction

Natural remanent magnetizations (NRM) of lake and shallow water sediments have been measured to investigate geomagnetic secular variations. Many cores of deep-sea sediment have also provided long-period changes of the earth's field. In these studies natural sediments have been often used as good memory storage of the past geomagnetic field because they are preferable to igneous rocks and archeomagnetic samples owing to the chronological continuity of sediments. The essential assumption in these treatments is that the sediment faithfully preserves the change of geomagnetic field, which should be experimentally tested.

Irving (1957) has discussed with the post depositional detrital remanent magnetization (PDRM) model that the magnetization of natural sediments is acquired accurately in alignment with a direction of an ambient field without any inclination error. The model was confirmed experimentally with both synthetic and natural sediments (Irving & Major, 1963; Kent, 1973). We also have some observed data from lake sediments which support the PDRM model. Two cores of sediment from lake St. Croix have the same magnetic records of high degree of correspondence in the magnetization directions (Lunt et al, 1976). Similar curves of directional changes in remanence have been observed in many cores from several lakes in Britain (Turner & Thompson, 1981), although they show somewhat lower degrees of correspondence than that of lake St. Croix. Moreover, the observed paleo-inclinations are close to the values calculated at the site with a central dipole field. These facts suggest that sediments acquire the remanences controled by the ambient field and could carry the same record of magnetization when they meet some conditions.

We cannot easily conclude that a PDRM points to the true direction of a past geomagnetic field even if several sediment columns bear the same records of changes in remanent magnetization. Each record may have undergone the same deformation to deviate from the true field direction. Another question is that there has been no observation of the same records of magnetization in sediments whose past depositional environments differ largely, in particular, accumulation rates are extremely different. The author discusses modification of a geomagnetic field variation recorded in a continuous sample of sediment on the basis of the experimental results on the mechanism of remanence acquisition.

2. Description of PDRM

Magnetic grains in a sediment are free to rotate in the water-filled voids of matrices even after deposition and are aligned along the external magnetic field. As the voids are gradually reduced by the weight of the overlying sedimentary column, the grains become hard to move and eventually cease to rotate, leaving the magnetization directions parallel to the ambient field. The fixing of a magnetic grain is attained by a balance of two opposing forces ; a magnetic torque and a mechanical resistance. The magnetic torque is expressed by a vector product of the magnetic moment of the particle and the external field. The mechanical resistance is caused

by viscosity of the surrounding fluid and a friction with void wall. The particle is fixed when the resistant force predominates the magnetic torque. Yaskawa (1974) postulated only an increase of viscosity due to compaction as a factor determining the depth of fixing of magnetic grains. Otofuji and Sasajima (1981) demonstrated that a magnetic particle rotation does not occur steadily but in a halting fashion and that the rotation is dominantly controled by a maximum friction with matrices grains but not by the viscosity.

Three characteristic features of depositional detrital remanent magnetization (DRM) have been revealed from many experimental results. The first is that most of the remanences of sediments are ascribed to PDRM components. Second, in a uniform field the magnetization acquired in each depth decreases as depth goes down. The change appears to represent an exponential decrease with depth. Hamano (1980) discussed on a red clay that the magnetization acquisition starts from the depth of 15 cm, half of the total remanence being acquired at 80 cm depth, and is completed at 2.5 m. The third is that the partial PDRM acquired in some compaction range has an additive property (Otofuji & Sasajima, 1981). If a partial magnetization acquired in a uniform field over the depth range from d_0 to d_1 ($d_0 < d_1$) is denoted by $M_{d_0}^{d_1}$, partial magnetizations $M_{d_0}^{d_1}$, $M_{d_1}^{d_2}$ and $M_{d_0}^{d_2}$ have the following relation;

$$M_{d_0}^{d_2} = M_{d_0}^{d_1} + M_{d_1}^{d_2} \quad (d_0 < d_1 < d_2)$$

This law was realized even when the field direction was reversed or the field strength was changed during the compaction process. This fact leads to a possibility that the magnetization of sediment can be represented by a supperposition of components acquired in different ages.

3. A linear system model

Let's consider a thin sediment sheet produced for unit time width in a long core with unit cross section. It contains magnetic grains of various sizes with different intensities. The sediment sheet is subjected to a gradual compaction after deposition and then the void volume formed by relatively large grains, in which smaller magnetic particles can rotate to align along the ambient field, is reduced with time. The following increases in viscosity of fluid and in friction with void wall cause blocking of magnetic particles. The magnetic particles do not cease to rotate simultaneously, but they are partially fixed in various stages of different degrees of compaction. The resultant magnetization of the sediment is sum of the magnetic moments of particles gradually fixed. To express the change of the partial fixing quantitatively, we define a function $r(t)$; the amount of magnetic moment blocked at t in a unit sediment sheet. The $r(t)$ can approximately be expressed by an exponential function according to Hamano's experiment, i.e.

$$r(t) = C\, e^{-At} \qquad (1)$$

$$r(t) = 0 \quad (t < t_0) \qquad (1.1)$$

$$\int_{t_0}^{\infty} r(t)\, dt = 1 \qquad (1.2)$$

$$\int_{t_1}^{\infty} r(t)\, dt = 0.5 \qquad (1.3)$$

$$\int_{t_2}^{\infty} r(t)\, dt \fallingdotseq 0 \qquad (1.4)$$

where coefficients A and C are constants, t_0, t_1 and t_2 ($t_0 < t_1 < t_2$) represent times of onset of magnetization, completion in the fixing of a half magnetic moments and end of the moment fixing. The integral value of $r(t)$ is normalized by m_0, amount of the total magnetic moment to be fixed in a uniform field of intensity f_0. Eq.1 is shown in Fig.1, being integrated. The dotted line represents the experimental result in which the end of moment fixing was confirmed. There is a small discrepancy below 1.5 m between the curves from experiment and approximated by an exponential, however, its contribution to the total remanence is expected small.

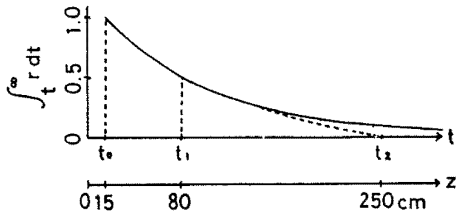

Fig.1 Moment fixing function. The true line shows an exponencial curve. The dotted line shows a curve from experiment.

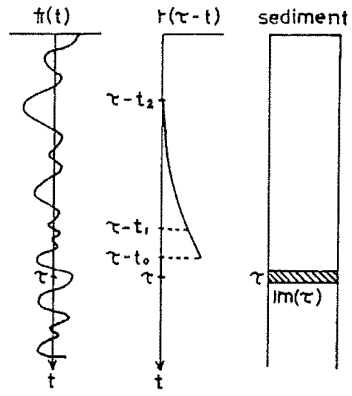

Fig.2 A schematic view of the present model. The $\mathbf{f}(t)$ shows a secular variation of geomagnetic field vector. The $r(\tau-t)$ represents a moment fixing function. The shaded area shows the unit sediment sheet of age τ.

Assuming that the axis of magnetic moment fixed at t is aligned in parallel with the geomagnetic field and each moment is additive, the magnetization of a unit sediment sheet of age τ, which has been exposed to a geomagnetic field variation $\mathbf{f}(t)$ from τ years ago through present, can be expressed as follows:

$$\mathbf{m}(\tau) = \int_0^\tau \mathbf{f}(t)\ r(\tau-t)\ dt \qquad (t_2 < \tau) \tag{2}$$

where $\mathbf{m}(\tau)$ is the magnetization and t shows the age axis which has its origin in the sediment/water interface and increases downward. The schematic view of Eq.2 is illustrated in Fig.2. The curve of $\mathbf{f}(t)$ on the left shows the geomagnetic field vector corresponds to the age of each horizon in the sediment column. Since the unit sediment sheet of age τ, expressed by a shaded portion in Fig.2, acquires remanent magnetization through a duration from t_0 to t_2 after deposition, namely, from $t=\tau-t_0$ to $t=\tau-t_2$, the moment fixing function r(t) is given as drawn in Fig.2.

This model implies that the magnetization of a sediment can be calculated by a convolution integral of a magnetic field variation $\mathbf{f}(t)$ and the moment fixing function r(t). And then it suggests two important features of magnetization acquired in a magnetic field always changing. One is that the direction of magnetization does not coincide with that of the external field unless $\mathbf{f}(t)$ is unchangeable in direction or r(t) is the Dirac's δ-function. The other is that the magnetization intensity is shown by a product of the component proportional to the field intensity and the component of intensity reduction caused by the cancellation due to the superposition of magnetic moments aligned in various directions. The latter component results from the integral of the directional change of field.

4. Effect of moment fixing function r(t)

Considering the four associated conditions of Eq.1, the integral limits of Eq.2 can be extented as:

$$\mathbf{m}(\tau) = \int_{-\infty}^{\infty} \mathbf{fe}(t)\ r(\tau-t)\ dt \tag{3}$$

where $\mathbf{fe}(t)=m_0/f_0 \cdot \mathbf{f}(t)$. Since Eq.3 is a convolution integral, it can be described by spectra using the Fourier transform as:

$$\mathbf{M}(\omega) = \mathbf{Fe}(\omega)\ R(\omega) \tag{4}$$

where $\mathbf{M}(\omega)$, $\mathbf{Fe}(\omega)$ and $R(\omega)$ are spectra of $\mathbf{m}(t)$, $\mathbf{fe}(t)$ and r(t),

respectively. Eq. 4 shows that the spectrum of magnetization $\mathbb{M}(\omega)$ can easily be calculated only by multiplying $\mathbb{F}e(\omega)$ by $R(\omega)$, whereas in the space domain the magnetization $m(t)$ is obtained by filtering $fe(t)$ with a filter $r(t)$. The $R(\omega)$ provides us detailed properties of the filter.

If we put $t_0=0$ since $t_0 \ll t_1$, Eq.1 becomes as:

$$r(t) = A\, e^{-At} \quad (A = \ln 0.5/T_{1/2}) \qquad (5)$$

where $T_{1/2}$ is a period for the fixing of a half magnetic moment. Thus the moment fixing function $r(t)$ can be determined by only $T_{1/2}$, i.e. only the condition (1.3) is enough for the determination of $r(t)$.

Since $r(t)=0$ when $t<0$, the Fourier transform of $r(t)$ becomes as:

$$R(\omega) = 1 / (1 + (\omega/A)i) \qquad (6)$$

To examine the properties of $R(\omega)$ in detail, we separate it into real part and imaginary part, which show an amplification and a phase lag, respectively. The amplitude spectrum becomes as:

$$|R| = 1/\sqrt{1 + (\alpha T_{1/2}/T)} \qquad (7)$$
$$(\alpha = 2\pi/\ln 0.5)$$

and the phase spectrum becomes as:

$$\theta = \tan^{-1}(\alpha T_{1/2}/T) \qquad (8)$$

where $T = 2\pi/\omega$. Eq. 7 and 8 show that both spectra are functions with respect to $(T_{1/2}/T)$, the ratio of the half fixing period to the wavelength of the field variation. Fig. 3 shows the two spectra. We also simulated the effect of the filter with respect to the function from experiment in which remanence acquisition terminates at the depth 250 cm. Both the amplification and the phase lag of the filter from experiment show almost the same change to those of exponential one, although small fluctuations occur in the curve of phase lag. If we adopt a linear function instead of an exponential, a more pronounced fluctuation, whose frequency is determined by the width of moment fixing zone, will grow up in both the amplification and the phase lag. Anyway the using of an exponential is appropriate for the approximation of the moment fixing function.

According to secular variations of the geomagnetic field from archeomagnetism (Hirooka, 1971; Kovacheva, 1980), there is no directional offset over 20° from a mean direction. Therefore, we can regard the change of declination and inclination approximately linear to the orthogonal axis. Then the amplitude attenuation and the phase lag shown in Fig.3 are applicable to the deformation of declination and inclination curves. As shown in Fig. 3, the large $(T_{1/2}/T)$ causes a large amplitude attenuation and a large phase lag in declination and inclination. If the $T_{1/2}$ is kept constant, the components of higher frequency are more deformed. On the other hand, the large $T_{1/2}$, which is equivalent to a small depositional rate, causes a large deformation. For instance when $T_{1/2}$= 500 yr, the directional change of T= 500 yr is deduced to 0.13 and its phase is delayed with 115 yr and that of T= 250 yr to 0.25 and with 53 yr. Thus a secular variation of the earth's field

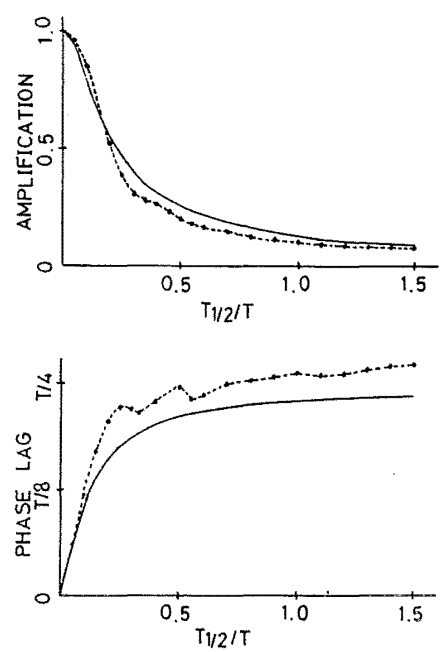

Fig.3 Amplification and phase spectra of the filter R. The true lines show the spectra of Eq.7 and 8. The dotted lines show the spectra on a function from experiment.

is recorded being modified variously by different filters.

5. Estimation of half fixing depth

Width of remanence acquisition zone is discussed on a depth axis (z) instead of time (t), since it is desirable for considering both magnetization mechanism and the exact effect of filtering. Then $T_{1/2}$ is replaced with a half fixing depth $Z_{1/2}$, at which a half of magnetic moments in a horizon is locked in. The width 95%-moments fixed is provided by 4.32 $Z_{1/2}$. We try to estimate the half fixing depths of natural sediments. A clear value for $Z_{1/2}$ is provided by the remanent intensity of deep sea sediments. It shows a progressive decrease prior to a polarity transition and an immediate recovery after that. The intensity drop shows a convex decrease and the following recovery a concave increase. These features are not only observed in natural deep-sea sediments (Opdyke et al., 1966; Harison & Somayajulu, 1966; Kobayashi et al., 1971) but also explained by some models (Løvlie, 1976; Niitsuma, 1977; Otofuji & Sasajima, 1981). The present model is applied to the magnetization data of the core KH 68-4-20 (Kobayashi et al., 1971). The remanent intensities and polarities determined from directions of remanence are shown in Fig.4.a. Intermediate directions of magnetization are not observed at the positions of polarity transition. Four successive polarity changes occur during the depth from 3.52 m to 5.5 m. The two reversals at 3.52-4.1 m and 4.75-5.5 m are paleontologically interpreted as the Kaena and the Mammoth events. Their ages determined from volcanic rocks (Labrecque et al, 1977) are shown in Fig.4.b. The intensity drop at the reversals, caused by only the cancellation of magnetic moments aligned in the opposite directions, is calculated using Eq.2 with a field expressed by the polarity change in Fig.4.b assuming that the depositional rate is constant at 7.6 mm/10^3yr. The calculations were carried out with respect to fore kinds of responces with $Z_{1/2}$ = 10, 20, 40, and 80 cm (Fig.4.c). The results represent that the shape of intensity pattern considerably changes with $Z_{1/2}$. The uppermost intensity peak in the three successive ones diminishes as $Z_{1/2}$ becomes large. The peak disappears completely when $Z_{1/2}$ reaches the width of the Kaena event. Then positions of polarity boundary are shifted downward depending on $Z_{1/2}$. The result of calculations reveals that a polarity transition is recorded being shifted downward by $Z_{1/2}$ and a small event shorter than $Z_{1/2}$ is not recorded in magnetization direction, although the trace is still remained in intensity. The intensity pattern with $Z_{1/2}$ of 20 cm seems to fit best the observed one. Thus the remanent intensity drop during a reversal can be explained by only the cancellation effect on the assumption that the field intensity is constant. According to some studies with volcanic rocks and intrusions, the intensity of the earth's field is decreased at a polarity transision. However, we can not know if the duration of the field intensity decrease is as long as those recorded in sediments, since the studies on polarity transition zone with igneous rocks can not be made on time axis. Width of a remanent intensity drop at a single reversal in sediments is usually less than 50 cm. No matter how fast a sediment is accumulated, the drop width in the sediment does not extend beyond this value. This fact suggests that the remanent intensity drop during a reversal in sediments is independent on the field intensity. If the intensity change consists of only the cancellation effect, a quite small $Z_{1/2}$ is enough to produce the intensity drop. Even the responce whose $Z_{1/2}$ is only 12 cm can produce the intensity drop more than 10 % over the width 30 cm. Many drops which extend over 10 cm or less were observed in densely measured cores of deep sea sediments (Sato, 1980). To make out an intensity drop of 10 cm-width, 2.5 cm is enough for the half fixing depth. Thus the small value 10 cm or less is generally appropriate for $Z_{1/2}$ of deep

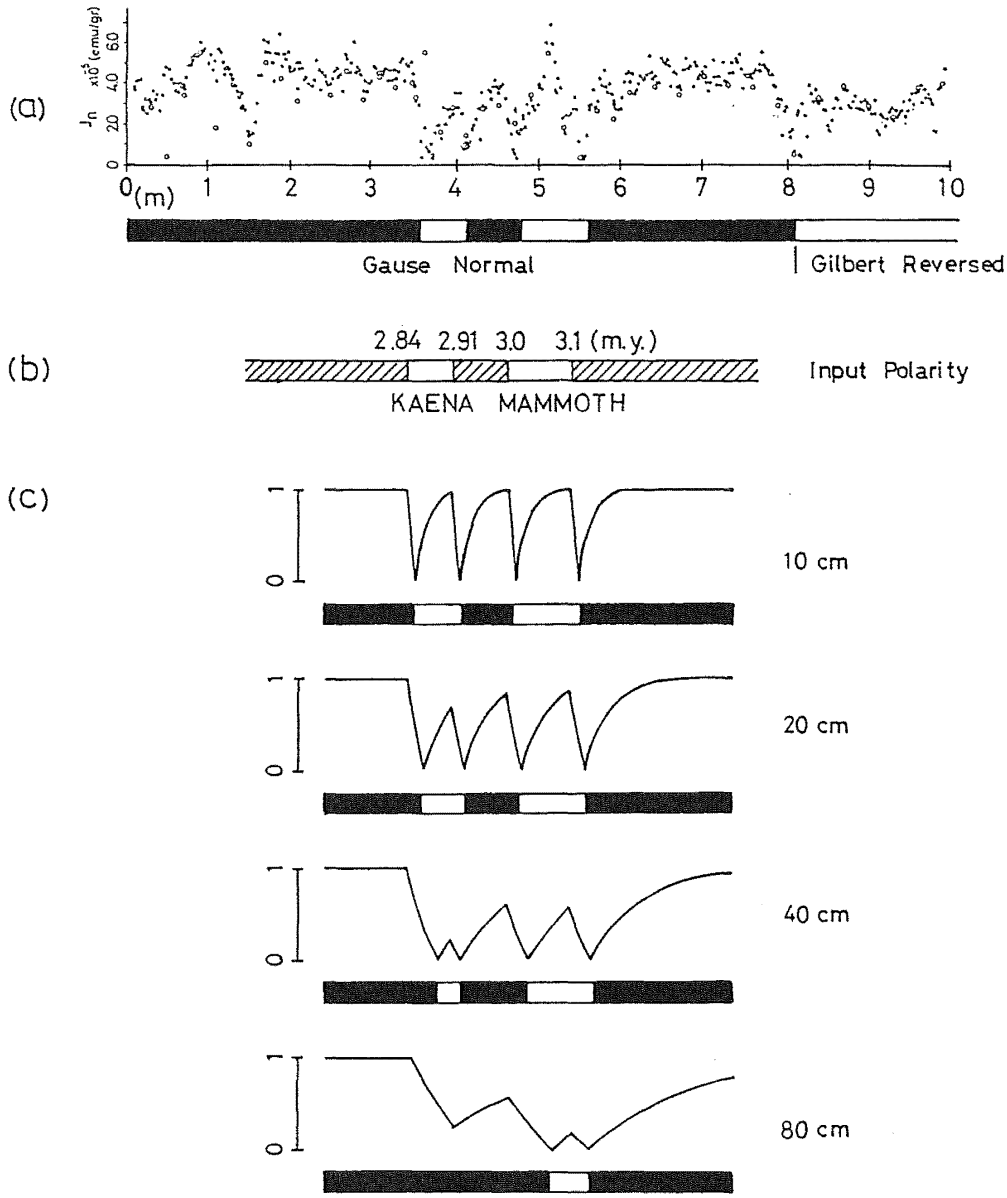

Fig.4 Intensity reduction due to cancellation in the polarity transition zone. (a) Magnetization intensities of deep sea sediment of the core KH-68-20 (after Kobayashi et al., 1971). (b) Polarity change of the input field. (c) Intensity patterns calculated with a field of the polarity change shown in (b). The right figure represents $Z_{1/2}$ used in the calculation of each curve.

sea sediments.

6. Discussion and conclusion

The model is characterized by proposing a moment fixing function. Although the function is provided by an exponential in the present study, it may take other forms. For example, the Dirac's δ function is possible to be taken if all magnetic particles are simultaneously fixed, or it may not show a monotonous decrease but any others like bimodal changes. But no experimental result which suggests these functions has been obtained. As discussed above, the change of the moment fixed in a horizon of a sediment column is controlled by a size distribution of magnetic and nonmagnetic grains, their shapes, magnetization intensities of them, properties of interstitial fluid, sedimentation rates, and intensity of geomagnetic field. All but the last two factors show physical properties of sediment. Assuming that the moment fixing can be expressed by an exponential function on every sediment, the half fixing depth $Z_{1/2}$ can be regarded as one of the physical properties of sediment. According to an experiment remagnetizing natural sediments in a laboratory, a sediment rich in sand shows a high possibility of remagnetization (Payne & Verosub, 1982). This fact suggests that the sand-rich sediment has a high value of $Z_{1/2}$. We can infer that a sediment, whose grain size distributes widely, would have a larger half fixing depth than an even-grained sediment. The value 10 cm or less has been estimated for $Z_{1/2}$ of deep sea sediments. We rather wish to know if the $Z_{1/2}$ of lake and shallow water sediments is as small as that of deep sea sediments. Some experiments with lake deposits have shown that few realignments of magnetic grains occur in a sediment redeposited. If the $Z_{1/2}$ is 2 cm, for example, the 82 % magnetic moment in a horizon is to be fixed at the depth 5 cm beneath the sediment/water interface. It would be difficult to detect the mechanism of PDRM in detail with these sediments. In Britain and Japan, the secular variations of geomagnetic field, which coincide with those from archeomagnetism, have been obtained from lake sediments and shallow water sediments (Creer et al., 1972 ; Hyodo & Yaskawa, 1980). These facts also indicate that $Z_{1/2}$ is small. Thus we can interpret by the small half fixing depth many observed data from lake and shallow water sediments, and many results of laboratory experiments with these sediments.

Let us consider a possibility to obtain a secular variation of geomagnetic field from sediments. The effect of the filter r(t) is described with depth axis in Fig.5. Amplification and phase lag of a secular variation of the earth's field, whose wavelength is expressed in centi-meter, are shown on several half fixing depths. When $Z_{1/2}$ is 40 cm, significant attenuation in amplitude and phase lag occur throughout the wavelength range more than 100 cm. The geomagnetic field

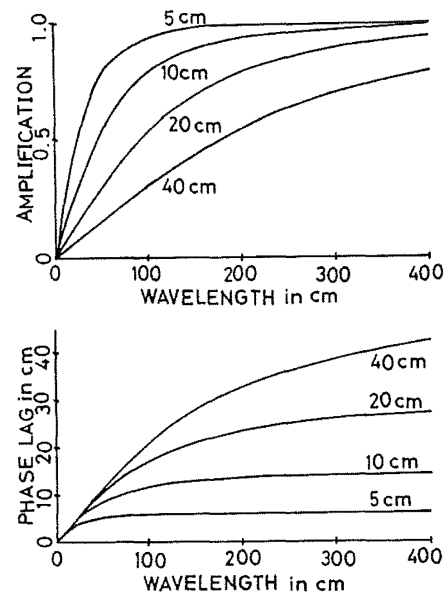

Fig.5 Amplification and phase lag due to the filter R.

direction appears to be recorded faithfully in a sediment of small $Z_{1/2}$. When we discuss the high-frequency component of the wavelength less than 50 cm, however, we should take the effect of the filter into consideration.

On the remanence preserved in sediments of large $Z_{1/2}$, some problems can be inferred. When a secular variation of geomagnetic field is recorded in sediment columns of different depositional rates, the recorded signals not only have different wavelengths but also undergo different filterings. These two sediments have distinct variations of magnetization, even if their half fixing depths are the same. This result may cause that no good coincidence exists in secular variation curves of the earth's field from various sediment cores of quite different depositional rates. Curves of declination and inclination, whose wavelengths of main spectra are extremely different from each other, are recorded with some difference in their phase lags. This matter provides us some warning in using the declination and inclination curves of remanence in sediments as a time scale. When depositional rates or half fixing depths vary with depth in a sediment column, it is quite difficult to reconstruct the original field variation from the remanence of the sediment.

In conclusion the paleomagnetic signals recorded in sediments are subjected to some deformations resulting from the effect of the filter r(z). For a precise paleomagnetic study on field variations, it is preferable to use homogeneous sediments with smaller half fixing depths, deposited at a high uniform rate of sedimentation.

References

Creer, K.M., D.L. Gross, and J.A. Lineback (1976) Geol. Soc. Amer. Bull., 87, 531.
Hamano, Y. (1980) Earth planet. Sci. Lett., 51, 221.
Harrison, C.G.A. and B.L.K. Somayajulu (1966) Nature, 212, 1193.
Hirooka, K. (1971) Mem. Fac. Sci. Kyoto Univ., 38, 167.
Hyodo, M. and K. Yaskawa (1980) J. Geomag. Geoelectr., 32, 581.
Irving, E. (1957) Phil. Trasns. Roy. Soc. Lond. A, 250, 100.
Irving, E. and A. Major (1964) Sedimentology, 3, 135.
Kent, D.V. (1973) Nature, 246, 32.
Kobayashi, K., K. Kitazawa, T. Kanaya and T. Sakai (1971) Deep-Sea Res., 18, 1045.
Kovacheva, M. (1980) J. R. astr. Soc., 61, 57.
LaBrecque, J.L., D.V. Kent and S.C. Cande (1977) Geology, 5, 330.
Løvlie, R. (1976) Earth Planet. Sci. Lett., 30, 209.
Lund, S.P., D. Bogdan, S. Levi, S.K. Banerjee and A. Long (1976) EOS Trans. Amer. Geophys. Un., 57, 910.
Niitsuma, N. (1977) Rock Magn. Paleogeophys., 4, 65.
Opdyke, N.D., B. Glass, D. Hays and J.H. Foster (1966) Science, 154, 349.
Otofuji, Y. and S. Sasajima (1981) Geophys. J. R. astr. Soc., 66, 241.
Payne, M.A. and K.L. Verosub (1982) Geophys. J. R. astr. Soc., 68, 625.
Sato, T. (1980) Phd Thesis, Osaka Univ.
Turner, G.M. and R. Thompson (1981) Geophys. J. R. astr. Soc., 65, 703
Yaskawa, K. (1974) Rock Magn. Paleogeophys., 2, 15.

(Submitted to J. Geomag. Geoelectr.)

K-Ar AGES OF VOLCANIC ROCKS OF DARUMA AND IDA VOLCANOES IN NORTHWESTERN IZU PENINSULA, CENTRAL JAPAN

Ichiro KANEOKA*, Eiichi KIKAWA** and Hajimu KINOSHITA**

* Geophysical Institute, Faculty of Science, University of Tokyo, Bunkyo-ku, Tokyo 113
** Department of Earth Sciences, Faculty of Science, Chiba University, Yayoicho 1-33, Chiba 260

Daruma and Ida volcanoes together with Tanaba volcano are regarded to represent the Quaternary volcanism in the northwestern part of the Izu Peninsula. Stratigraphically, Daruma volcano overlies Tanaba volcano, which is located to the south of the former. Although several investigators reported their geology (eg.) Kuno, 1938; Masuda, 1961; Sawamura, 1955; Shirao, 1981) and petrography (eg.) Kurasawa and Michino, 1976), no radiometric ages have been obtained. In the eastern part of the Izu Peninsula, there exist several Quaternary volcanoes such as Yugawara, Taga, Usami, Omuro and Amagi volcanoes. Based on some radiometric ages, their volcanism is estimated to have started at least 0.7 - 0.8 Ma ago (eg.) Kaneoka et al., 1970; Suzuki, 1970). Furthermore, Nanzaki volcano, located at the southernmost part of the Izu Peninsula, was revealed to have erupted about 0.4 Ma ago over the late Miocene rocks with the ages of about 7 - 8 Ma (Kaneoka et al., 1982). In order to compare the period of volcanism with these volcanoes, K-Ar ages were determined on six andesites of Daruma volcano and a basalt of Ida volcano.

Among volcanic rocks collected from Daruma and Ida volcanoes for paleomagnetic studies, six andesites of Daruma volcano and a basalt of Ida volcano were selected for K-Ar dating on the basis of their freshness and the distribution of sampling sites. In Daruma volcanic provinces, early and late lava flows are identified (Sawamura, 1955; Shirao, 1981). However, early lava flows are found to be mostly affected by alteration and unsuitable for K-Ar dating. Hence, all dated samples belong to the late lava flows, which are classified as olivine bearing two pyroxene andesites with porphyritic texture. Although olivine phenocrysts are slightly altered, these rocks do not show any other sign of secondary alteration. Hence, they are regarded to be suitable for K-Ar dating.

Among six samples of Daruma volcano dated, two samples show the normal NRM (natural remanent magnetization), but the other four the reversed NRM.

One sample of Ida volcano, collected at the west of Wakamatsuzaki, is an olivine bearing andesitic basalt, whose NRM has been revealed to be normal. This rock has a porphyritic texture. This sample is almost fresh and shows no sign of secondary products.

All samples were analysed as whole rocks. K was determined by flame photometry with the Li internal standard method. The amount of radiogenic ^{40}Ar was determined by the isotope dilution method with a ^{38}Ar tracer on a Reynolds type mass spectrometer.

The results indicate that the samples of Daruma volcanoes show K-Ar ages ranging from 0.59 to 0.83 Ma. The sample of Ida volcano shows a K-Ar age of 0.64 ± 0.05 Ma. Two samples of Daruma volcano show K-Ar ages of about 0.59 Ma. These three samples show NRM of normal polarity. Hence, they are regarded to have erupted in the Brunhes normal polarity chron in the magnetostratigraphic time scale. Four andesites of Daruma volcano with reversed NRM show older K-Ar ages which range from 0.72 to

0.83 Ma. Since the boundary between the Brunhes normal polarity chron and the Matuyama reversed polarity chron is regarded to be 0.73 Ma at present (Harland et al., 1982), all reversed samples of Daruma volcano seem to have erupted during the Matuyama reversed polarity chron.

These results suggest that at least some lava flows of Ida volcano are younger than those of Daruma volcano which might compose the main body of Daruma volcano. However, some samples of normal NRM of Daruma volcano show rather young K-Ar ages. If these ages correspond to the eruption of some new lava flows, they might have erupted from some different vents from those of older eruptions.

Although Shirao (1981) estimated the age of the late lava flows of Daruma volcano as rather young ages of around 0.18 - 0.30 Ma based on the geomagnetic stratigraphy, present results indicate that they should be older. We have not dated any early lava flows of Daruma volcano, because they are hydrothermally altered and not suitable for K-Ar dating. Since they also show reversed NRM, they probably erupted during Matuyama reversed polarity chron. Paleomagnetic studies indicate that volcanic rocks from Tanaba volcano also show reversed NRM. As introduced before, Daruma volcano overlies Tanaba volcano, but there seems no large age gap between them stratigraphically. Hecne, most volcanic rocks of Tanaba volcano probably erupted during Matuyama reversed polarity chron.

Of Quaternary volcanoes in the Izu Peninsula, volcanic rocks which show the reversed NRM have been found from Tanaba, Daruma, Usami and probably Jaishi volcanoes and other volcanoes show the volcanic rocks of only normal NRM (Kikawa et al., 1982; Kono, 1978; Koyama, 1982; Nagata et al., 1957; Shirao, 1981). Concerning the radiometric ages, K-Ar ages of 0.6 - 0.8 Ma are reported for Usami volcano (Kaneoka et al., 1970). A basanitoid of Nanzaki volcano was dated to be 0.43 ± 0.03 Ma by the K-Ar method (Kaneoka et al., 1982). For Yugawara volcano, fission track ages of 0.11 and 0.40 Ma were obtained on volcanic glasses (Suzuki, 1970).

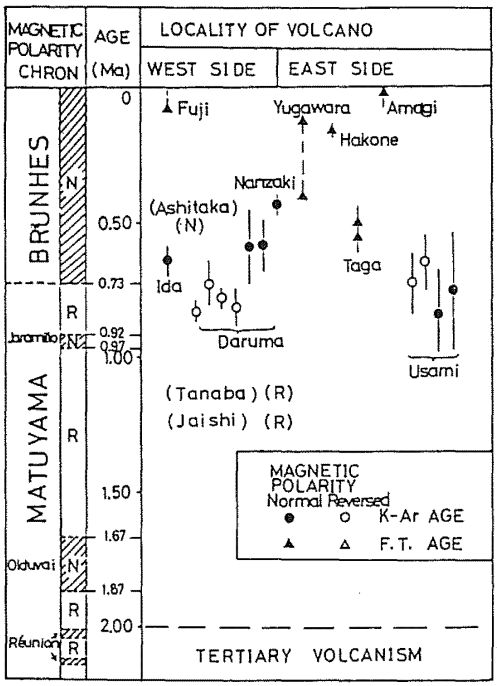

Fig. 1. Relation between the dated rocks and the magnetic polarity of NRM for Quaternary volcanoes in the Izu Peninsula.

The volcanoes in parentheses have not yet been dated radiometrically, but their relative ages are estimated stratigraphically. N and R indicate normal and reversed magnetic polarities, respectively.

For Taga volcano, fission track ages of about 0.5 Ma were also reported on volcanic glasses, whereas one volcanic glass of Amagi volcano was dated to be 0.01 Ma by the fission track method (Suzuki, 1970). These results are summarized in Fig. 1.

Based on these information, it is conjectured that most Quaternary volcanoes in the Izu Peninsula were formed less than 1 Ma ago. Of these volcanoes, Jaishi and Tanaba volcanoes were formed relatively earlier than the other volcanoes, but they might have erupted 1 - 1.5 Ma ago at most. At present, we have no radiometric age data on volcanism prior to these Quaternary volcanism except for two late Miocene samples from the Irōzaki area. In order to understand the tectonic history of the Izu Peninsula including the collision process against the Honshu Island (Matsuda, 1976), geochronological studies give among one of the most significant information. More systematic studies are required in this area.

References

Harland, W.B., A.V. Cox, P.G. Llewellyn, C.A.G. Pickton, A.G. Smith, and R. Walters (1982) A Geologic Time Scale (Cambridge Univ. Press) p. 131.

Kaneoka, I., S. Aramaki, and S. Tonouchi (1982) J. Geol. Soc. Japan, 88, 919.

Kaneoka, I., M. Ozima, and H. Kuno (1970) J. Geomag. Geoelectr., 22, 559.

Kikawa, E., T. Akimoto, H. Kinoshita, and T. Furuta (1982) Rock Mag. Paleogeophys., 9, 17.

Kono, M. (1968) J. Geomag. Geoelectr., 20, 353.

Koyama, M. (1982) Geosci. Repts. Shizuoka Univ., 7, 61.

Kuno, H. (1938) Bull. Earthq. Res. Inst., 16, 763.

Kurasawa, H. and K. Michino (1976) Bull Volcanol. Soc. Japan, 2nd Ser., 21, 11.

Masuda, C. (1961) Earth Science 'SHIZUHATA", 25, 31.

Matsuda, T. (1976) KAIYO KAGAKU (Ocean Science), 8, 21.

Nagata, T., S. Akimoto, S. Uyeda, Y. Shimizu, M. Ozima, K. Kobayashi, and H. Kuno (1957) J. Geomag. Geoelectr., 9, 23.

Sawamura, K. (1955) Text of geological map of Shuzenji, Japan. Scale 1 : 50000, Geol. Surv. of Japan.

Shirao, M. (1981) J. Geol. Soc. Japan, 87, 641.

Steiger, R.H. and E. Jäger (1977) Earth Planet. Sci. Lett., 36, 359.

Suzuki, M. (1970) J. Anthropol. Soc. Nippon, 78 (1), 50.

PALEOMAGNETIC EVIDENCE OF THE NORTHWARD DRIFT OF THE IZU PENINSULA, CENTRAL JAPAN

Kimio HIROOKA, Toru TAKAHASHI, Hideo SAKAI

Department of Earth Sciences, Faculty of Science, Toyama University
Gofuku, Toyama City 930

and

Tadashi NAKAJIMA

Geological Laboratory, Faculty of Education, Fukui University
Bunkyo 3-9-1, Fukui City 910

Introduction

The Izu Peninsula is located near a triple junction of the Pacific, the Philippine Sea and the Asian Plates. The peninsula is in the northern end of the Izu-Bonin Island Arc which is considered by many authors to have been migrated towards north and to have collided with the central Honshu (Sugimura, 1972; Kaizuka, 1975; Kobayashi and Isezaki, 1976; Matsuda, 1978). The estimated age of the collision is, however, different among the authors. Kobayashi and Isezaki suggested on the basis of the marine magnetic anomaly pattern of the Shikoku Basin that the collision took place before the middle Miocene at the latest. Whereas Matsuda (1978) inferred the timing of collision as in the early Quaternary from the morphological point of view. The temporal and spatial features of the migration and collision of the peninsula are a key to clarify the plate tectonic history of the western Pacific region.

We carried out the paleomagnetic study which would provide us the evidence of the paleolatitude and the rate of the northward migration of the peninsula.

Geological Setting of Sampling Sites

The greater part of the Izu Peninsula is covered with Neogene and Quaternary volcanics. Sedimentary strata bearing fossils are found only in very limited areas. A great many efforts have been exerted on geological studies of the peninsula since the end of the 19th century and many stratigraphic names were proposed by many geologists. Proposition of so many stratigraphic names, however, makes confusion in many cases of geological correlation. The standard stratigraphy is not easy to establish for the peninsula because of the structural complexity of volcanic materials and alteration of the older rocks caused by the succeeding volcanic activities. The Neogene system of the Izu Peninsula is generally divided into two groups: the Yugashima Group of Miocene and the Shirahama Group which is considered to be the late Miocene to Pliocene in age (Samejima, 1955). In the northeastern part of the peninsula, a stratigraphic succession mainly composed of pumice tuff, tuffaceous siltstone and pyroclastics is called the Umegi Formation or the Umenoki Tuff (Koyama and Niitsuma, 1980) which is correlative to the Shirahama Group in the southeastern part. The Yugashima Group in the northeastern part comprises the Okawabata Propylites, the Kadono Formation and the Shimoshiraiwa Formation from the lower to the upper, respectively (Kitamura et al., 1969). Tsuchi et al.(1974) and Samejima (1978) situated the Shimoshiraiwa Formation in the lowest part of the Shirahama Group. The lower part of the Yugashima Group in the western part is called the Nishina Formation (Moritani and Sawamura, 1965) which is

correlated to the Okawabata Propylites in the northeastern part of the peninsula.

The upper part of the Shirahama Group in the southeastern part is defined as the Harada Formation. In the lower part of the Group, there embed tuff breccia beds and a limestone layer bearing planktonic foraminifera called the Nashimoto Formation. Paleomagnetic sampling was carried out at 34 sites in 18 localities in the northeastern, western and southeastern parts of the peninsula, and paleomagnetic data were obtained from 19 sites in 11 localities. Geology and locations of the sampling sites are shown in Fig.1.

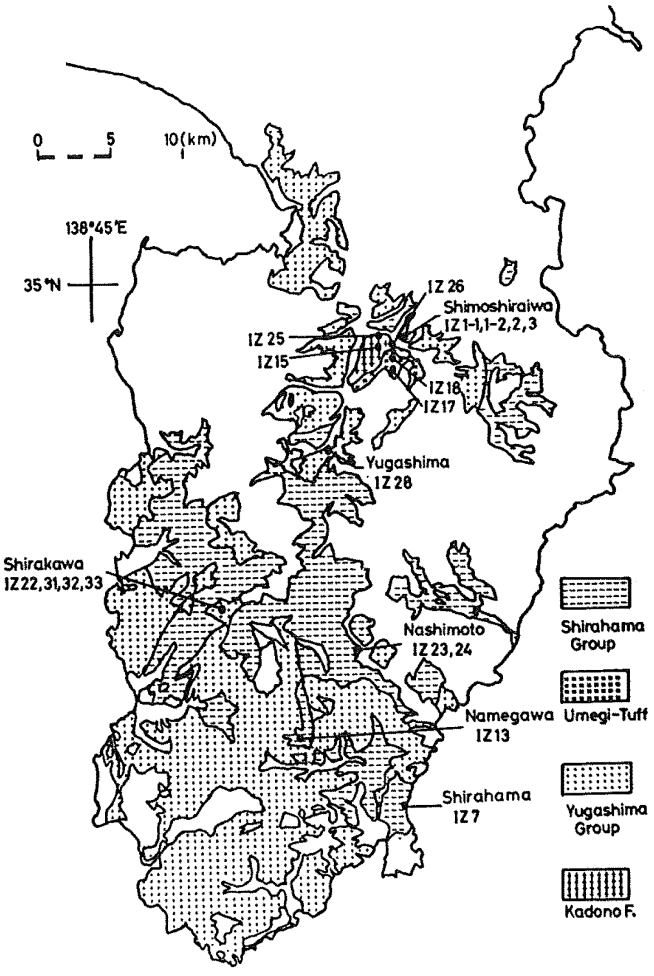

Fig.1. Geological map of the Izu Peninsula and sampling localities.

In the northeastern part of the peninsula, paleomagnetic samples were collected from one site (Site name; IZ 28) in the Okawabata Propylites, four sites (IZ 15, 25-1, 25-2 and 26) in the Kadono Formation and from four sites (IZ 1-1, 1-2, 3 and 4) in the Shimoshiraiwa Formation of the Yugashima Group. Samples were also obtained from two sites (IZ 17 and 18) in the Umegi Formation in the area. From four sites (IZ 22, 31, 32 and 33) in the Nishina Formation, samples were taken in the western part. Samplings were carried out from two sites (IZ 23 and 24) in the Nashimoto Limestone and from one site (IZ 13) in the Namegawa Formation and from one site (IZ 7) in the Harada Formation in the southeastern part.

By the planktonic foraminiferal analyses, the Shimoshiraiwa Formation is assigned to the Blow's horizon (Blow, 1979) of planktonic foraminiferal Zone N.14 (Saito, 1963; Ikebe and Chiji, 1971; Ibaraki, 1981) and the Nashimoto Limestone is of Zone N.17 (Ibaraki, 1981). Calcareous sandstone found near Namegawa and Shirahama both of which belong to the Harada Formation are of Zone N.19 (Ibaraki and Tsuchi, 1978). In Table 1 are summarized the stratigraphic divisions, the geological ages, and dips and strikes of bedding plane of sampling sites.

Results of Paleomagnetic Measurements

We collected ten hand samples at every site. From each sample, we obtained 2 or 3 specimens of cylindrical shape of 2.45cm diameter by coring. Magnetization of specimens was measured by a spinner magnetometer. Specimens of all the sites were submitted to both of the stepwise alternating field (A.F.) and thermal demagnetizing experiments. After the measurements of

Table 1. Stratigraphic names and ages of sampling localities.

Site NO.		Age (Ma)	Bedding*
IZ 1-1	Shimoshiraiwa Formation	10.4-11.6	N 13°W 29°E
IZ 1-2	Shimoshiraiwa Formation	10.4-11.6	N 13°W 29°E
IZ 2	Shimoshiraiwa Formation	10.4-11.6	N 2°E 32°E
IZ 3	Shimoshiraiwa Formation	10.4-11.6	N 6°W 40°E
IZ 7	Harada Formation	3.0-3.7	N 24°W 8°W
IZ 13	Namegawa Formation	3.7-5.1	N 36°W 7°W
IZ 15	Kadono Formation	Early Miocene	N 52°E 46°S
IZ 17	Umegi-Tuff	3-5	N 53°E 49°E
IZ 18	Umegi-Tuff	3-5	N 36°E 49°E
IZ 22	Nishina Formation	Early Miocene	N 76°W 28°N
IZ 23	Nashimoto Limestone	5.5-5.8	N 17°E 16°E
IZ 24	Nashimoto Limestone	5.5-5.8	N 44°E 24°E
IZ 25-1	Kadono Formation	Early Miocene	N 59°E 65°S
IZ 25-2	Kadono Formation	Early Miocene	N 59°E 65°S
IZ 26	Kadono Formation	Early Miocene	N 48°E 53°S
IZ 28	Okawabata Propylite	Early Miocene	N 28°W 46°E
IZ 31	Nishina Formation	Early Miocene	N 75°W 20°N
IZ 32	Nishina Formation	Early Miocene	N 74°W 30°N
IZ 33	Nishina Formation	Early Miocene	N 84°E 14°N

* strikes of bedding planes and declinations are the values referring to the geomagnetic north.

natural remanent magnetization (NRM) we chose two sets of 3 or 4 pilot specimens from every site and they were demagnetized thermally and by alternating field. Six steps of 50, 100, 150, 200, 250 and 300 Oe peak fields of A.F. demagnetization were applied on the pilot specimens to find out the optimum demagnetizing step when Fisher's precision parameter K (Fisher, 1953) became maximum. Additional 6 or 7 specimens were adopted from the remaining samples of the site and were demagnetized three times at the optimum and the neighbouring two steps. As the paleomagnetic data for the site, we accepted the results of the step at which the precision parameter K showed the greatest value.

We also applied the thermal demagnetization experiments of several steps, such as 100, 150, 200, 250, 300 and 400°C on the pilot specimens to see how the magnetic direction changed. In many cases, the magnetization changed to the similar direction which was observed in the A.F. demagnetization, so that we used the results of A.F.demagnetization as the paleomagnetic data in those cases. Change of magnetic direction and intensity of Site IZ 17 is shown as an example in Fig.2A. But specimens of some sites such as IZ 15 and 26 showed the magnetic direction change different way from that of A.F. demagnetized results (Fig.2B). In such cases we demagnetized additional specimens thermally to find the optimum step and adopted the results of the thermal demagnetization as the paleomagnetic data. The results of the paleomagnetic measurements obtained by the procedures mentioned above are tabulated in Table 2 and 3. Declination and inclination

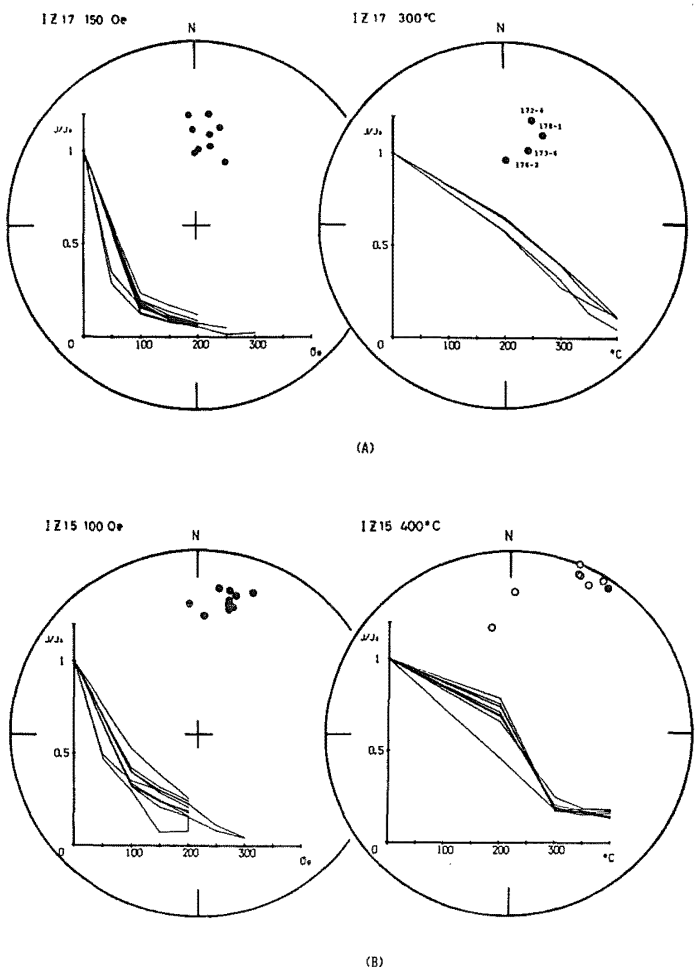

Fig.2. Examples of directional changes and normalized intensity decay curves of the remanence through A.F. and thermal demagnetizations.
A: Results of Site IZ 17; Similar directional change was observed in the both demagnetizing methods.
B: Results of Site IZ 15; Different directional change was observed in two demagnetizing methods.

in Table 2 are indicating *in situ* direction.

Since the strata of sampling sites are tilting as shown in Table 1, we applied bedding correction by making a bedding plane to the horizontal. Declination and inclination after correction are listed in Table 3. It is clear that declinations are greatly differing from location to location of the sampling sites. This fact may be explained by way of geotectonic deformation such as folding or rotation was different from each other for the respect location. Koyama (1982) demonstrated from the measurements of a single tuff layer of the northern part of the Izu Peninsula that the local transcurrent fault affected to paleomagnetic declination greatly.

Paleolatitudes of all the sites calculated from paleomagnetic inclinations and the mean paleolatitude for each geologic formation are also summarized in Table 3.

Northward Drift of the Izu Peninsula

The oldest formation so far sampled in the peninsula is the Nishina Formation whose age is the early Miocene. We get a very low mean paleolatitude of 14.5°N for the formation, while the mean paleolatitude of the youngest Harada Formation of the Pliocene age is 34.5°N which is almost the same as the present latitude of the peninsula.

Paleolatitudes of all the sites are plotted against their age in Fig.3. The age of the geologic formations is referred to the correlation of planktonic foraminiferal datum plane proposed by Tsuchi (1983).

It is obvious from Fig.3 that the Izu Peninsula which situated in the equatorial region of the latitude of 14.5°N in the early Miocene had been migrated towards the north until it reached to the present latitude at 3 to 5 Ma ago.

Difference of paleolatitudes between the Harada Formation (3-3.7 Ma)

Table 2. Paleomagnetic directions.

Site No.	Declination* (°E)	Inclination (°)	α_{95} (°)	k	O.D.F	No. of samples
IZ 1-1	5.9	50.8	7.45	66.7	100 Oe	7
IZ 1-2	2.8	54.1	13.51	17.8	100 Oe	8
IZ 2	-3.7	50.3	5.31	109.9	100 Oe	8
IZ 3	-7.0	47.5	10.12	30.9	100 Oe	8
IZ 7	-3.7	49.1	6.93	44.4	100 Oe	11
IZ 13	-3.0	56.6	5.59	85.7	100 Oe	10
IZ 15	19.9	-11.2	14.06	16.5	400°c	8
IZ 17	7.4	50.7	5.47	89.6	150 Oe	9
IZ 18	-15.2	48.2	9.81	28.5	200 Oe	9
IZ 22	-10.5	56.4	4.49	116.5	100 Oe	10
IZ 23	27.5	51.3	12.57	20.5	250 Oe	8
IZ 24	36.0	40.9	5.97	75.3	150 Oe	9
IZ 25-1	22.6	7.9	12.38	18.3	150 Oe	9
IZ 25-2	10.8	52.7	9.31	27.9	150 Oe	10
IZ 26	-10.0	43.6	6.70	69.4	350°c	8
IZ 28	8.4	61.5	9.56	26.5	150 Oe	10
IZ 31	-23.6	56.2	5.21	86.8	100 Oe	10
IZ 32	-84.2	19.7	2.71	318.2	100 Oe	10
IZ 33	31.4	29.5	10.18	32.9	300 Oe	9

* Declinations are the values referring to the geomagnetic north.

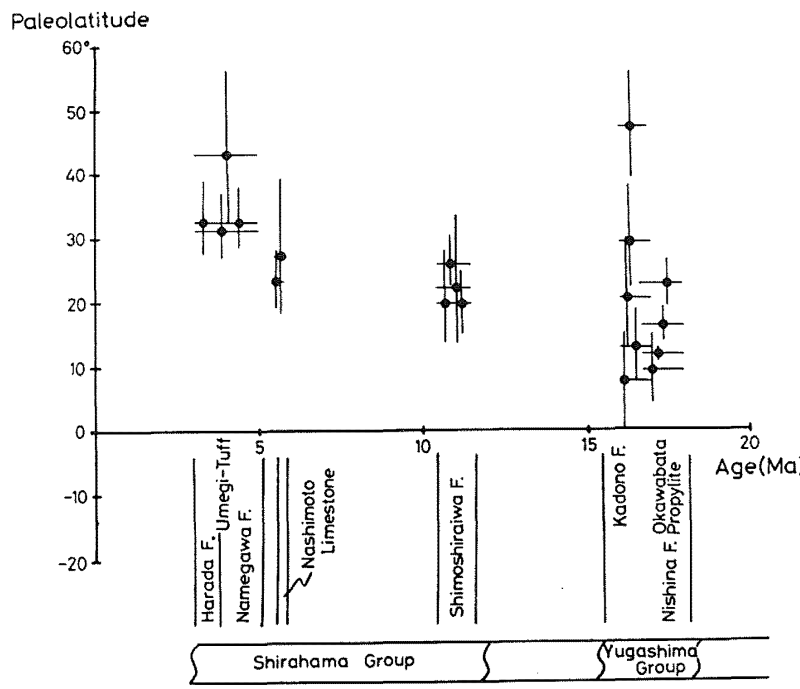

Fig.3. Paleolatitude versus time for the data from the Izu Peninsula.

Table 3. Paleomagnetic directions after bedding correction and paleolatitude.

Site No.	After Bedding Correction Declination (°E)	Inclination (°)	Mean Inclination (°)	Mean Paleolatitude (°)	Paleolatitude (°)
Harada,Namegawa Formation and Umegi-Tuff					
IZ 7	-19.3	51.4			32.1
IZ 13	-1.5	52.0			32.6
IZ 17	7.4	50.6	53.9 ±4.5	34.5 +4.7 -4.1	31.3
IZ 18	57.4	61.8			43.0
Nashimoto Limestone					
IZ 23	38.3	46.0			27.4
IZ 24	6.5	40.9	43.5 ±2.6	25.3 +2.1 -1.9	23.4
Shimoshiraiwa Formation					
IZ 1-1	23.4	35.3			19.5
IZ 1-2	23.8	39.1			22.1
IZ 2	24.1	43.5	38.4 ±3.3	21.6 +2.4 -2.3	25.4
IZ 3	30.6	35.5			19.6
Kadono Formation and Yugashima Group					
IZ 15	14.4	13.9			7.1
IZ 25-1	43.7	36.2			20.1
IZ 25-2	105.2	48.2	37.5 ±17.9	21.0 +14.1 -10.9	29.2
IZ 26	66.7	64.9			46.8
IZ 28	30.6	24.0			12.6
Okawabata Propylite and Nishina Formation					
IZ 22	-7.9	30.0			16.1
IZ 31	-18.1	39.2			22.2
IZ 32	-79.1	22.0	27.3 ±8.2	14.5 +5.1 -4.7	11.4
IZ 33	21.5	17.9			9.2

and the Nishina Formations (16.6-18 Ma) is about 20 degrees. The rate of the northward component of migration amounts to about 15 cm/year. This rate is much higher than the present estimated drifting rate of the Philippine Sea Plate. Kinoshita (1980) reported the paleolatitude change of the Daito Region from the paleomagnetic results of the Deep Sea Drilling Project Sites 445 and 446. Its mean rate of northward drift is 5 cm/year since the Eocene. Paleolatitudes of the Daito Region and the Izu Peninsula are plotted against their age in Fig.4. The paleolatitude of the Izu Peninsula and that of the Daito Region were almost the same in the Miocene. After that, the northward drifting of the Izu Peninsula was performed by a much higher rate as compared to the Daito Region.

Results of paleomagnetic study on Tertiary rocks in the Philippine Sea Plate were reported from Guam Island (Larson et al., 1975), and Bonin Islands (Kodama, 1981; Kodama et al., 1983). Paleomagnetic direction of the Eocene volcanics of the Bonin Islands showed very low inclination values of 3° to 10° and greatly deflected easterly declinations. Kodama et al. concluded that the islands have undergone a northward migration together with clockwise rotation of 30° to over 90°. The Bonin Island was situated very close to the equator in the Eocene when the Daito Region was located at the same latitude. Paleolatitude of Miocene rocks in the Guam Island is about 12.5° N

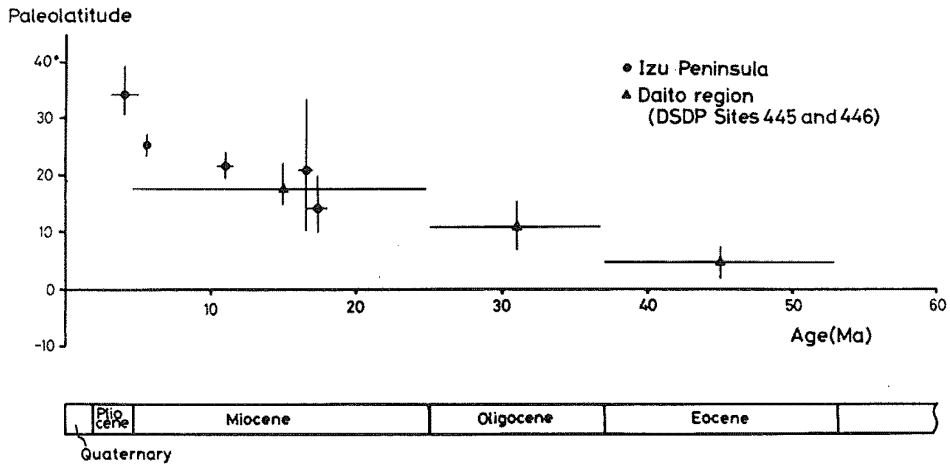

Fig.4. Paleolatitude versus time for the data from the Izu Peninsula and DSDP Sites 445 and 446 of the Daito Region (after Kinoshita, 1980). Data of the Izu Peninsula are the mean values for each geolocic formation.

which is very close to that of the early Miocene of the Izu Peninsula and also to that of the Daito Region of the Miocene.

Shir (1980) proposed from the skewness of magnetic anomaly patterns that the West Philippine Basin had migrated north for about 20-30° and had rotated clockwise as much as 50-70° since 35 to 40 Ma B.P. The agreement of paleolatitude of the Guam and the Bonin Islands, the Izu Peninsula and the Daito Region can be explained as follwing, by combining this northward drift and rotation of the West Philippine Basin, and spreading of the Shikoku and the Parece Vela Basins succeeded to the development of the West Philippine Basin.

First, the Daito Region and the Bonin Islands, and possibly the Guam Island and the Izu Peninsula basements, were located altogether close to the equator in the Eocene.

Then, by spreading and associated rotation of the West Philippine Basin, the Daito Region, the Izu Peninsula, the Bonin and the Guam Islands were transported to the north or to the northeast with a small clockwise rotation. In the Miocene time, the Shikoku and the Parece Vela Basins began to spread. If we could assume that the rotation of the West Philippine Basin was not completed in this period, the northward component of migration of the Izu Peninsula was greater than the Daito Region because the northward drifting component caused by the rotation was additional to the component originated from the spreading of the Shikoku Basin. Moreover, since the spreading rate of the Shikoku Basin was higher in the northern part than in the south as Kobayashi and Nakada (1978) proved, the northward drift of the Izu Peninsula became greater than that of the Bonin and Guam Islands which were migrated not to the north but to the east and rotated clockwisely by the eastward spreading of the Parece Vela Basin.

The abovementioned model concerning the development of the Philippine Sea Plate can explain not only the high northward migration rate of the Izu Peninsula but also the clockwise rotation of the Bonin and the Guam Islands. Although, we assumed a northward direction as the initial migration of the West Philippine Basin, our model is still valid in the case that the initial direction was northwestward as Seno and Maruyama (1983) proposed, as far as the clockwise rotation of the West Philippine Basin is allowed.

Finally, the Izu Peninsula reached the position to contact the Honshu

Island and collided with it at 3 to 5 Ma ago.

References

Blow, W.H. (1979) The Cainozoic Globigerinida, E.J. Brill, Leiden, Part 1, p.221.
Fisher, R.A. (1953) Roy. Astr. Soc. London, 217, A, 295.
Ibaraki, M. (1981) J. Geol. Soc. Japan, 87,417.
Ibaraki, M. and Tsuchi R. (1978) Rep. Fac. Sci. Shizuoka Univ., 12, 115.
Ikebe, N. and Chiji, M. (1971) J. Geosci. Osaka City Univ., 14, 19.
Kaizuka, S. (1975) Japanese J. Geol. Geogr., 45, 9.
Kinoshita, H. (1980) Initial Rep. Deep Sea Drill. Proj., 58, 765.
Kitamura, N., Takayanagi, Y., Masuda, K., Hayasaka, S., Mitsui, S., Sugawara, k. and Takahashi, K. (1969) Tohaku Univ. Inst. Geol. Pal., Contr., no.68, 19.
Kobayashi, K. and Isezaki, S. (1976) The Geophysics of the Pacific Basin and Its Margin (AGU), 235.
Kobayashi, K. and Nakada, M. (1978) J. Phys. Earth, 26, Suppl., S391.
Kodama, K. (1981) Bull. Earthqu. Res. Inst., 56, 347.
Kodama, K., Keating, B.H. and Helsley, C.E. (1983) Tectonophys., 95, 25.
Koyama, M. (1982) Geosci. Rep. Shizuoka Univ., no.7, 60.
Koyama, M. and Niitsuma, N. (1980) Geosci. Rep. Shizuoka Univ., no.5, 37.
Larson, E.E., Reynolds, R.L., Ozima, M., Aoki, Y., Kinoshita, H., Zashu, S., Kawai, N., Nakajima, T., Hirooka, K., Merill, R. and Levi, S. (1975) Geol. Soc. Amer. Bull., 86, 346.
Matsuda, T. (1978) J. Phys. Earth, 26, Suppl., S409.
Moritani, T. and Sawamura, K. (1965) Bull.Geol. Survey Japan, 16, 535.
Saito, T. (1963) Sci. rep. Tohoku Univ.,[2], 35, (2), 123.
Samejima, T. (1955) Chigaku Shizuhata, no.8, 15.
Samejima, T. (1978) Geology of Shizuoka, A Field Work (Shizuoka Education Press) 33.
Seno, T. and Maruyama, S. (1983) Tectonophys (in press).
Shih, T.C. (1980) The Tectonic and Geologic Evolution of Southeast Asian Seas and Island (AGU), 49.
Sugimura, A. (1972) Kagaku, 42, 192.
Tsuchi, R., Samejima, T., Iwahashi, T., Tokuyama, A., Ito, M., Kuroda, N., Fujiyoshi, O. and Ikegaya, S. (1974) Geological Map of 1/200,000 "Shizuoka Prefecture".

PALEOMAGNETIC EVIDENCE FOR NORTHWARD DRIFT AND LOCAL DEFORMATIONS OF THE MATSUZAKI AREA, IZU PENINSULA, JAPAN

Masato KOYAMA

Earthquake Research Institute, The University of Tokyo
Bunkyo-ku, Tokyo 113, Japan

1. Introduction

The Izu Peninsula is located on the northern edge of the Philippine Sea plate, and is thought to be colliding with the Honshu island (Sugimura,1972, Matsuda,1978,1982). The Peninsula has experienced with intense volcanic activities and crustal movements since at least the early Miocene. The author previously studied the geology of the Naka Izu area in the northeastern Izu Peninsula, and revealed the local tectonic rotation along a strike-slip fault using paleomagnetic data (Koyama,1981,1982).

The Nishina Group is thought to represent the oldest rocks in the Izu Peninsula (Moritani and Sawamura,1965) and is distributed in the area of the present study (Fig.1). Many active faults have been reported in and around this area (Hoshino et al.,1977,1978) such as the one moved at the time of the 1974 Izu Hanto Oki earthquake. The author has studied the stratigraphy and paleomagnetism in this area to reveal the crustal movements since the earliest stage of the geologic history in the Peninsula. Evidence for the local crustal deformations and the northward pre- late Miocene drift of the studied area are reported here. Lithologic and stratigraphic details of this area will be given in Koyama (1984).

2. Geology

The formations distributed in the studied area consist mainly of volcanics and are classified into following four groups: the Nishina, Yugashima, Shirahama, and Atami Groups, in ascending order (Fig.2, 3).

The Nishina Group consists mainly of basaltic volcanic breccia and lapilli tuff intercalated with pillow lavas in the lowermost part (Ishiki Basalts), with basaltic lavas, coarse and fine tuffs in the lower part (Yaenano Formation), with fine tuff and tuffaceous siltstone in the upper part (Deai Basalts), and with pumiceous tuff, fine tuff and basaltic lavas in the uppermost part (Neginohata Formation). The Nishina Group occupies the central part of the studied area. The total thickness of the group exceeds 4330m. The tuffaceous siltstone yields foraminifers. This group is thought to be the oldest group of the Izu Peninsula because of the uniqueness and uniformity of lithofacies.

The Yugashima Group is composed of an alternation of fine tuff, pumiceous tuff, and lapilli tuff in the lower part (Sakurata Formation and Shikura Formation), and an alternation of acid and basic pyroclastics and lavas in the upper part (Oosori Formation, Akebushi Volcanics, Funata Volcanics, Oogusu Andesite, and Minewa Tuff). This group is exposed widely in the studied area and its total thickness exceeds 3850m. The tuffaceous siltstone of the Sakurata Formation contains middle to late Miocene foraminifers.

The Shirahama Group consists mainly of acidic volcanic breccia intercalated with acidic lavas, pumiceous tuff, basic lavas and pyroclastics, fine tuff, calcareous sandstone, and limestone. This group

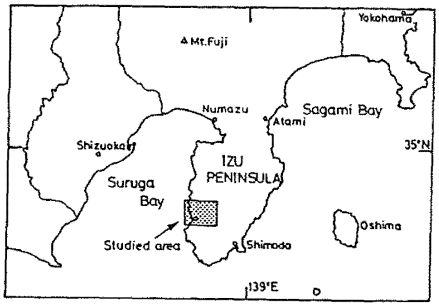

Fig.1. Index map showing the study area.

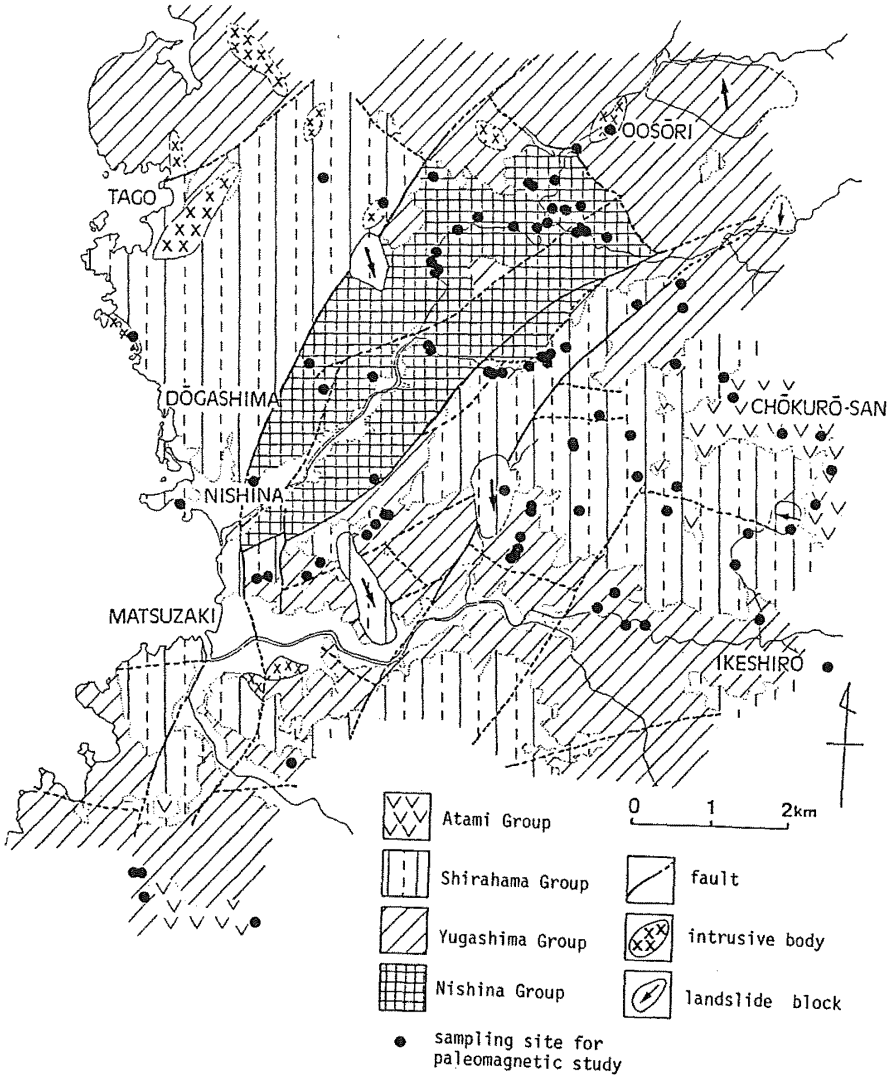

Fig.2. Simplified geologic map and sample localities for paleomagnetic study.

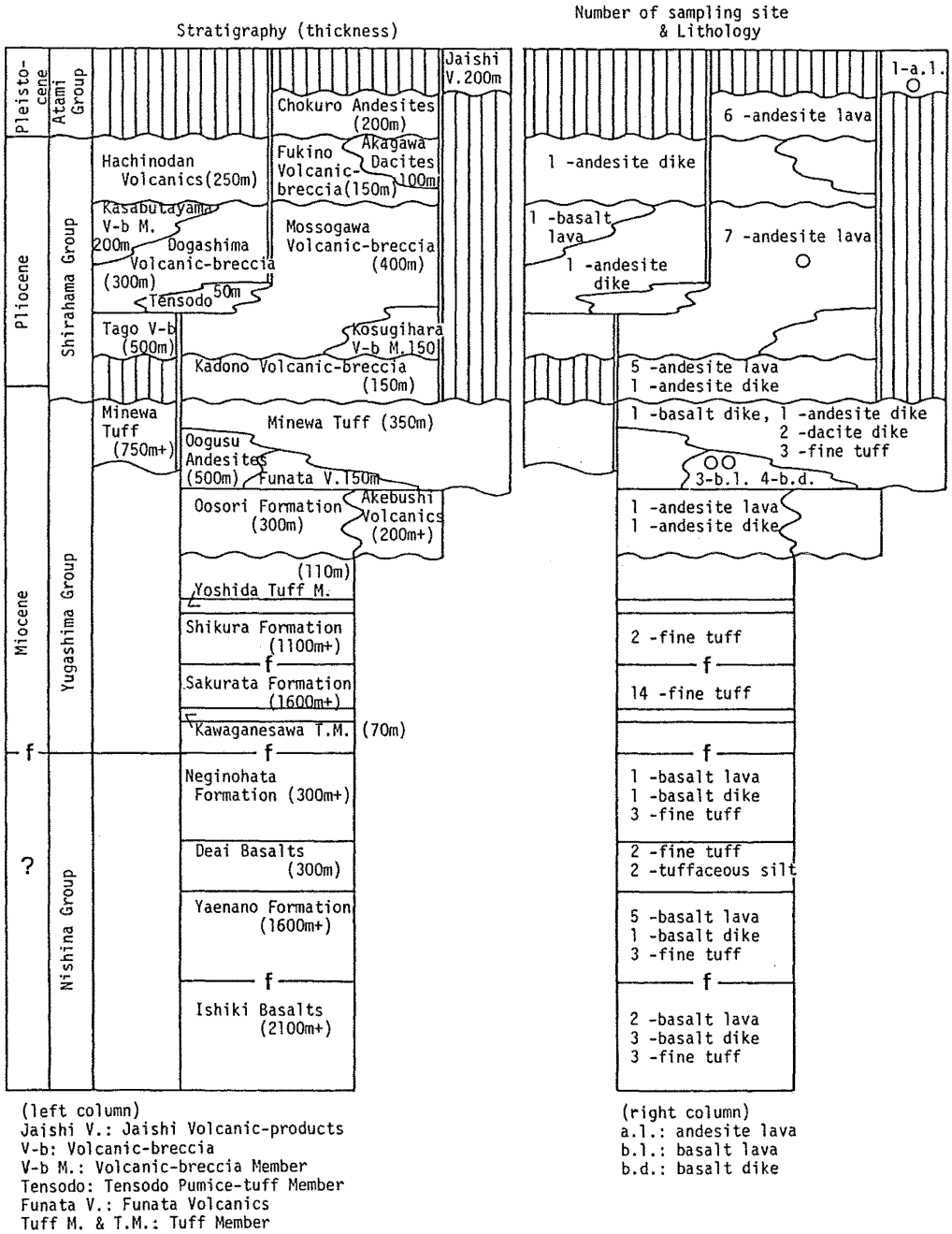

Fig.3. Schematic stratigraphic succession of the studied area (left column) and horizons and lithology of samples for paleomagnetic study (right column). The number in the right column indicates the number of sampling sites. o : sample with reversed polarity.

consists of following seven formations in ascending order: 1. Kadono Volcanic-breccia, 2. Mossogawa Volcanic-breccia, Tago Volcanic-breccia, and Dogashima Volcanic-breccia, 3. Hachinodan Volcanics, Fukino Volcanic-breccia, and Akagawa Dacites. This group is exposed widely in the studied area and its maximum total thickness is 1200m. The calcareous sandstones of the Kadono Volcanic-breccia and the Mossogawa Volcanic-breccia contain late Miocene to Pliocene larger and smaller foraminifers.

The Atami Group consists of andesitic lavas (Chokuro Andesites and Jaishi Volcanic-products). These rocks are all subaerial effusives and are distributed sporadically in the higher mountains of this area. The group has the maximum total thickness of 400m. Its age is estimated as the early Pleistocene on the basis of the existence of the preserved initial surface of effusives and magnetostratigraphy.

The relationships among these four groups are unconformable or fault-contacted. They lie almost horizontally in this area except in the middle to northeastern parts, where the Nishina Group and the lower part of the Yugashima Group show an oval semidome structure with dip of up to 80°.

There are two major faults, the Kadono and Matsuzaki-Shirakawa Faults. These faults run across the middle part of this area in a approximate NE-SW trend. There are remarkable differences in lithology and stratigraphy among the three blocks separated by these faults. The age of the lowermost formation and the base level of the Shirahama Group in each block become younger and lower respectively from northwest block to southeast one. The upper part of the Yugashima Group is exposed widely in the blocks on the northwestern side of the Matsuzaki-Shirakawa Fault and on the southeastern side of the Kadono Fault. In the block between these two faults the Shirahama Group directly covers the lower part of the Yugashima Group, and the upper part of the Yugashima Group is not exposed. The stratigraphy and lithofacies in the Shirahama Group is different from one block to another. These facts suggest that the Kadono and Matsuzaki-Shirakawa Faults have the large-scale strike-slip components of displacement. The last activity of these faults should have been later than the deposition of the Shirahama Group, namely in the late Miocene to Pliocene. These two faults were reported as active faults with left-lateral strike-slip component of displacement as indicated by the topography along the faults (Hoshino et al.,1977,1978).

3. Samples and Measurements

The samples for paleomagnetic measurements were collected at 81 sites from the four groups described above (Fig.2,3) and at 7 sites from dikes whose stratigraphic horizons are unknown. One hand sample was collected from each site except from three sites in the Nishina Group where three samples were collected. The hand-sampled blocks were cut into cubes with a side of 23mm. The remanent magnetization were measured on 1 to 4 cube specimens for one site with the Ring-core-type Flux-gate Spinner Magnetometer (Koyama anu Niitsuma, 1983). Alternatig field (AF) demagnetizations were carried out with the Current-regulated Three Axial

Alternating Field Demagnetizer (Koyama and Niitsuma, 1983). Stepwise AF demagnetizations were performed up to 35mT in a step of 5 mT on at least one specimen from each site.

4. Results

The intensities of natural remanent magnetization (NRM) of the samples range from 1.2×10^{-3} to 8.4×10^{0} A/m. As regards the volcanic rocks, their distribution of intensities of NRM is centered at the value of 1×10^{0} A/m, and range from 1.0×10^{-1} to 8.4×10^{0} A/m. The ratios of the NRM intensity to the intensity after 20mT AF demagnetization (J_{NRM}/J_{20mT}) range from 0.6 to 67 (1.0 to 20 for most of the samples). The group of smaller J_{NRM}/J_{20mT} ratio (0.6 to 3.0) consists mainly of samples from andesite lavas, and the group of larger one (3.0 to 66.7) consists mainly of samples from andesite dikes, basalt lavas and dikes, and dacite dikes. Particularly, the samples which have intensities of more than 1×10^{0} A/m after 20mT AF demagnetization have smaller J_{NRM}/J_{20mT} ratios (< 3.0), and stable components of remanent magnetization are dominant in these samples.

The NRM intensities of the samples of tuff and tuffaceous silt are distributed uniformly from 1.2×10^{-3} to 1.4×10^{0} A/m. The ratios J_{NRM}/J_{20mT} range from 0.65 to 13.2.

The NRM intensities of the samples of altered volcanic rock are two orders of magnitude smaller than the ones of volcanic rocks described above, and range from 5.4×10^{-3} to 3.6×10^{-2} A/m. The ratios J_{NRM}/J_{20mT} range from 1.0 to 6.6. Details about the changes of remanent magnetization vectors during stepwise AF demagnetization were described in Koyama and Niitsuma (1982).

The 39 samples which have to a certain extent reliable paleomagnetic vectors were selected by the following procedure :

1. During the stepwise AF demagnetization, the changes of the remanent magnetization directions of the most samples became less than 5° after 15 to 25 mT AF demagnetizations, and the converged directions were adopted as the stable remanent magnetization directions. As regards the samples which change the remanent magnetization directions more than 5° through all the demagnetization steps, the directions at the steps where they show the smallest changes from the previous steps, were adopted.
2. Out of the samples with stable remanent magnetizations selected by these procedures, the following (1)-(4) samples are further excluded from the present discussions because their remanent magnetizations are not thought to accurately represent the directions of geomagnetic field at the time when the sampled rock bodies were emplaced or deposited. (1) samples of which the data of bedding are unknown and therefore bedding corrections cannot be performed. (2) samples which have directions of remanent magnetization in agreement with the present geomagnetic field direction within the errors before bedding correction. (3) samples of altered volcanic rock described above. (4) samples whose α_{95}s of the measured directions are larger than about 20°.

5. Discussion and Conclusions

(a) Polarity -- Normal polarities are dominant in the selected 39 samples. The samples with reversed polarity are the following four samples : one from the Jaishi Volcanic-products, one from the Mossogawa Volcanic-breccia, and two from the Funata Volcanics (Fig.3).

(b) Inclination -- The inclinations from the Atami, Shirahama, Yugashima Groups agree with the present inclination within the errors, but the inclination from the Nishina Group (I= +24.2° ± 21.0°) is thought to be significantly smaller in comparison with the present value (Fig.4). If this observation is valid, then the Nishina Group might originally be deposited at the latitude lower than the present.

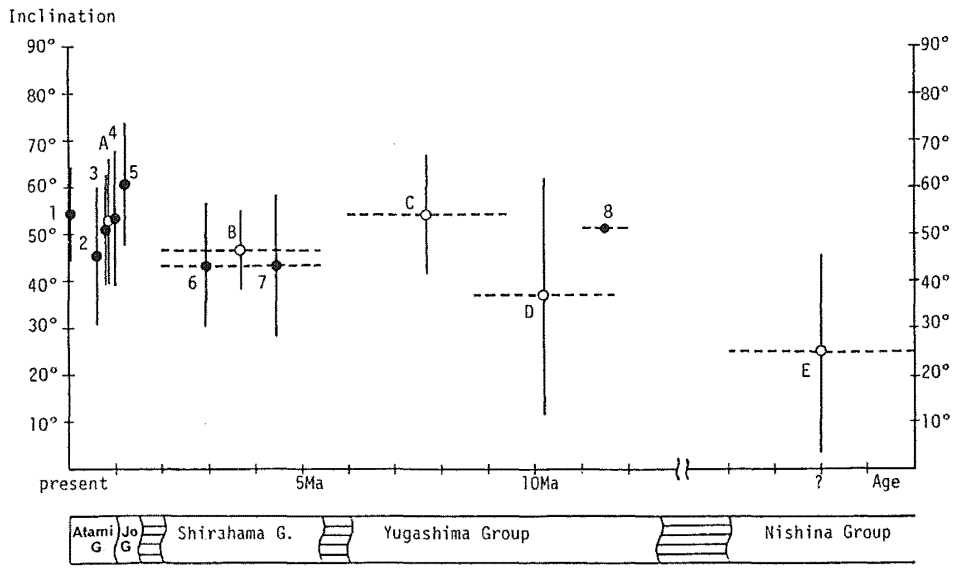

Fig.4. Relationship between the mean of absolute inclinations of remanent magnetization in each stratigraphic unit and its geologic age. Open circles correspond to the samples from the studied area, A: Atami Group (number of sampling sites N = 5), B: Shirahama Group (N= 8), C: upper part of the Yugashima Group (N= 9), D: lower part of the Yugashima Group (N= 10), E: Nishina Group (N= 7). Solid circles correspond to the samples from the northeastern Izu Peninsula (data 1 from Heki,1984, data 2-8 from Koyama,1981,1982), 1: Oomuroyama Volcanics (N= 22), 2: Tenshi Volcanic-products and upper part of the Usami Volcanic-products (N= 5), 3: lower part of the Usami Volcanic-products (N= 19), 4: Shimoonogawa Andesites (N= 7), 5: Yokoyama Siltstone (N= 5), 6: Umegi Formation (N= 5), 7: Mukai Tuff (N= 5), 8: Shimoshiraiwa Formation (N= 1). Each vertical error bar shows a standard deviation of inclination values of each unit. Horizontal error bars show the ages estimated by biostratigraphy, magnetostratigraphy, and radiometric age measurement. Details of the age estimation are given in Koyama (1982,1984). Paleomagnetic inclination (+54.5°) is expected from the present latitude of the Izu Peninsula and agrees well with the data 1 (+54.6°).

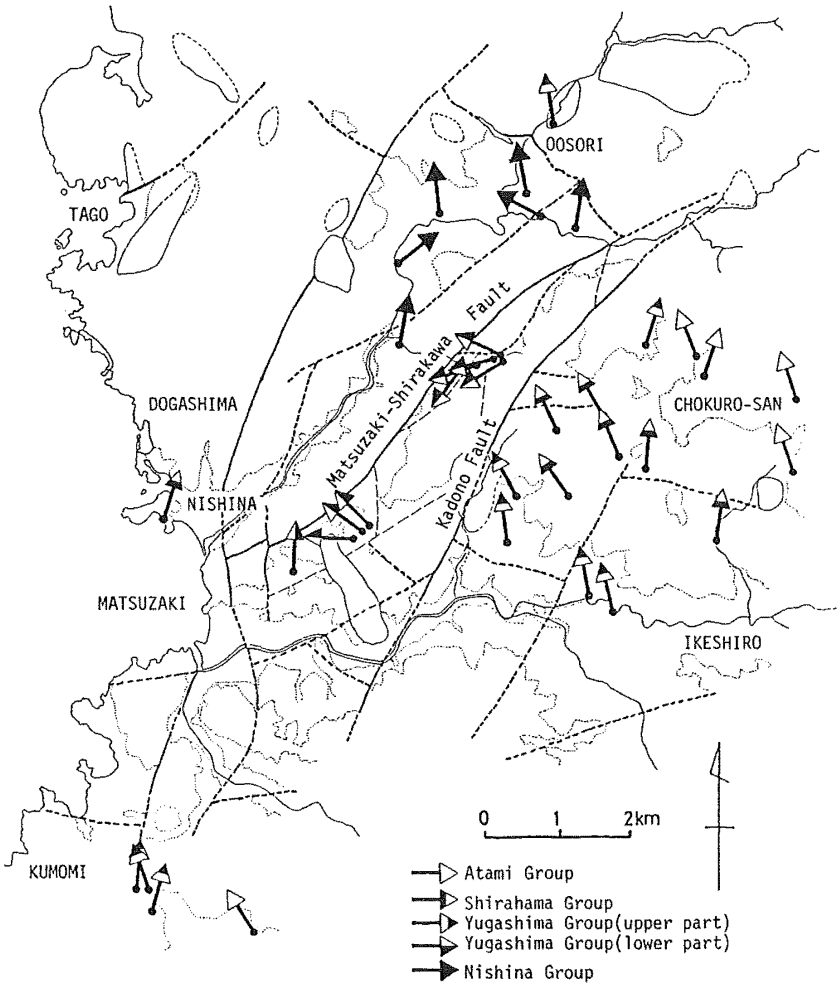

Fig.5. Map showing the direction of declination of remanent magnetization in each site and the localities of major faults. All the declinations are converted to normal directions for the sake of visual simplicity.

(c) Declination -- The directions of declination from the Atami, Shirahama, upper part of the Yugashima, and the Nishina Groups agree with the present north within the errors (Fig.5). That the directions of declination almost agree with the present north except for local deformations such as the ones described below suggests there was no rotation involving the whole study area, which can be detected as the change of declination of remanent magnetization. The directions of declination from the lower part of the Yugashima Group show the counterclockwise rotations from the present north by about 80° on the average. These samples were collected in the block between the Kadono and Matsuzaki-Shirakawa Faults. There is a possibility that paleomagnetic directions in a block between two left-lateral strike-slip faults undergo counterclockwise rotations caused by drags along the two faults (Fig.6). According to the geologic and topographic data, the Kadono and Matsuzaki-Shirakawa Faults are thought to have large-scale left-lateral strike-slip components of displacement (section 2 in this paper). Therefore, these horizontal counterclockwise rotations might be related with the drag rotations along the two faults. This estimation agrees with other available geologic data such as the changes of strike of bedding near the faults.

Fig.6. Schematic diagrams showing rotations of paleomagnetic vectors caused by (a) a drag along an left-lateral strike-slip fault (MacDonald,1980, Koyama,1981,1982), and (b) drags along approximately parallel two strike-slip faults (Beck et al.,1980, Jones et al.,1982).

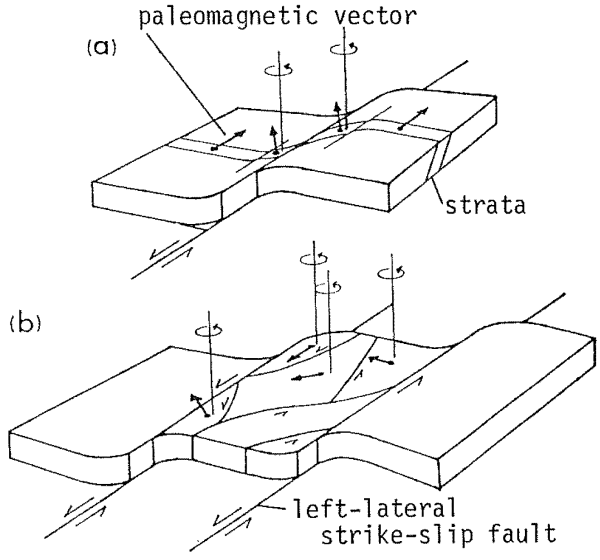

References

Beck, M. E. Jr (1980) J. Geophys. Res., 85, no.B12, 7115-7131.
Heki, K. (1984) in press in J. Geomag. Geoelectr.,36.
Hoshino, K. et al. (1977) Spec. Rept. Geol. Surv. Japan, no.6, 73-82.
Hoshino, K. et al. (1978) Tectonic Map 4, Geol. Surv. Japan.
Jones, D. J. et al. (1982) Scient. Am., 247, 50-64.
Koyama, M. (1981) Rock Mag. Paleogeophys. 8, 1-8.
Koyama, M. (1982) Geosci. Repts. Shizuoka Univ. 7, 61-85.
Koyama, M. (1984) in preparation.
Koyama, M. and N. Niitsuma (1982) Mem. Natn. Sci. Mus., no.15, 15-24.
Koyama, M. and N. Niitsuma (1983) Geosci. Repts. Shizuoka Univ. 8, 49-61.
MacDonald, W. D. (1980) J. Geophys. Res. 85, no.B7, 3659-3669.
Matsuda, T. (1978) J. Phys. Earth, 26, Suppl. S409-S421.
Matsuda, T. (1982) Mem. Natn. Sci. Mus. no.15, 9-13.
Moritani, T. and K. Sawamura (1965) Bull. Geol. Surv. Japan, 28, no.11, 1-14.
Sugimura, A. (1972) Kagaku (Science), 42, 192-202.

PALEOMAGNETISM OF TERTIARY IGNEOUS ROCKS FROM SAN'IN DISTRICT
- FURTHER EVIDENCE FOR ROTATIONAL MOTION OF SOUTHWEST JAPAN -

Yo-ichiro OTOFUJI* AND Takaaki MATSUDA**

*Department of Earth Sciences, Faculty of Sciences,
Kobe University, Kobe 657, Japan
**Department of Geology, Himeji Institute of Technology,
Himeji 671-22, Japan

INTRODUCTION

Previous paleomagnetic works indicated that Southwest Japan experienced clockwise rotational motion during the Cenozoic time (Sasajima et al., 1968; Kawai et al., 1971). A short sketch of the rotational motion in Tertiary was given by Otofuji and Matsuda (1983). Extensive paleomagnetic work combined with age determination documents the full process of rotation.

The work presented here is an attempt to determine the timing of rotation of Southwest Japan based on the more detaild paleomagnetic data. Our paleomagnetic approach is, at first, to measure the natural remanent magnetization (NRM) of rocks with age between 30 Ma and 35 Ma. These data shall provide the declination value which characterizes the rotational angle of Southwest Japan, because the main part of rotational motion occurred later than this period (Otofuji and Matsuda, 1983). The time interval of 5 Ma in this period is small enough to introduce the effect of apparent polar wander, because the swift motion of apparent polar wander ceased by 40 Ma (Irving, 1977; Harrison and Lindh, 1982). To estimate the timing of start of rotation, the declination value of 30 Ma to 35 Ma is compared with those of rocks younger than 30 Ma.

The reliable rotation angle about the vertical axis is obtained from the declination of rocks after tilting correction. The greatest source of error in inferring the declination value is the uncertainty in making

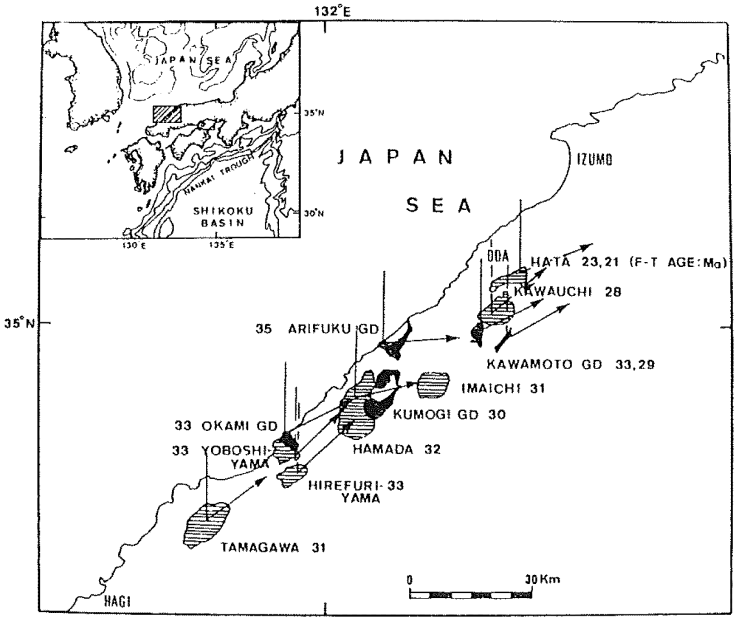

Fig. 1 Location of rock units where samples were collected. The shaded rock unit marks the volcanic production associated with caudlron formation and the solid rock unit the plutonic stock. Sampling localities are listed in Table 1. Arrows indicate the declinations of mean paleomagnetic directions obtained for the respective rock units. The age by fission-track dating technique (Matsuda, 1983) is assigned to each rock unit.

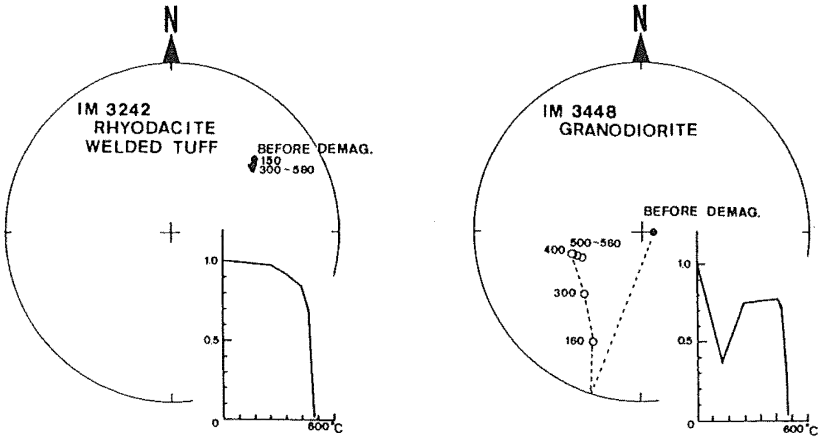

Fig. 2 Thermal demagnetization of magnetically stable sample from welded tuff in Yoboshiyama rock unit (IM 313) and a unstable one from Arifuku granodiorite (IM 323).

correction for tectonic deformation. The paleomagnetic work in this paper is forcused only on the following rocks; (1) they are evaluated to be subjected to little tectonic tilting based on the geological evidence or (2) tilting of these rocks are clearly observed. These rocks yield fairly reliable data after reducing the above uncertainty.

GEOLOGY AND SAMPLING

Extensive late Paleogene eruptives occurred in San'in district, Inner Zone of Southwest Japan. The volcanism were associated with the cauldron subsidences, and the volcanic products at each cauldron formed a rock unit which consisted of rhyodacitic to andesitic lavas and rhyodacitic to dacitic pyroclastics. Geological works have shown cauldron location and stratigraphy (Murakami, 1973; Matsuda and Oda, 1982; Masuda research group, 1982). Plutonic rocks intruded contemporaneously in this district. These volcanic and plutonic rocks have been dated by the fission-track dating technique (Matsuda, 1983); their ages range from 28 Ma to 35 Ma. Continued dacitic to andesitic volcanism produced younger volcanic unit (Hata Subgroup) whose age was obtained to be 21 Ma to 23 Ma by fission-track dating (Matsuda, 1983). These volcanic units and the plutonic rocks in this district were chosen for our work (Fig. 1).

Most samples were collected from the welded tuff in pyroclastic of each rock unit, because the welded tuff is very suitable for paleomagnetism; the reliable paleomagnetic direction could be obtained (Ellwood, 1982; Geissman, 1980) and the eutaxitic structure (lineation of stretched pumice and aligned phenocryst) is a good indicator of horizontal plane (Ross and Smith, 1961). Sampling was carried out from outcrops in which tilting was clearly observed through the eutaxitic structure of welded tuff, or sediment layers within or above andesite lavas. The outcrops with different tilting within a rock unit were prefered for sampling sites to ascertain the effect of the tilting correction. Samples were also collected from plutonic rocks which were estimated to have undergone little tilt. The sampling locations in each stock were widely spaced to cancel out the effect of tilting.

More than 400 samples were collected from seven volcanic units at 26 sites and from four plutonic rocks at 10 sites (Fig. 1). Sampling localities are listed in Table 1. Samples were taken by hand sampling; a magnetic compass was used for orientation. Each site typically comprised twelve independently oriented samples distributed over distances ranging up to 20 m.

Table 1. Summary of Paleomagnetic results

Rock unit	Age (Ma)	site	Locality	Demag		N	D	I	α_{95}	K
HATA										
Uppermost andesite lava		IM303	(132°30.9'; 35°06.3')	500-560°C	B	10	-109.1	-57.6	7.3	44.6
Upper rhyodacite welded tuff	21 ± 1	IM301	(132°30.6'; 35°05.6')	400°C	A	10	86.3	25.3	2.0	605.4
		IM302	(132°31.3'; 35°05.7')	400°C	A	12	61.9	56.1	1.9	532.5
		IM417	(132°31.0'; 35°05.3')	400°C	A	12	73.9	44.3	3.4	161.8
		IM418	(132°30.6'; 35°05.2')	400°C	A	12	46.8	36.7	3.0	206.2
Lower andesite lava	23	IM202*	(132°32.6'; 35°05.7')	550°C	B	9	-104.2	-64.1	6.1	72.3
KAWAUCHI (Sasahara Fm.)										
Dacite welded tuff	28	IM107*	(132°28.0'; 34°59.5')	400°C	A	10	52.4	15.9	3.6	185.6
		IM212*	(132°25.7'; 35°00.8')	500°C	A	11	83.5	21.6	5.8	63.2
		IM213*	(132°28.4'; 35°00.2')	500°C	A	12	42.0	30.9	1.8	552.1
		IM214*	(132°28.5'; 34°59.5')	500°C	A	11	35.6	35.1	3.6	164.1
		IM421	(132°27.4'; 34°58.7')	400°C	A	12	48.6	35.0	2.2	376.7
		IM422	(132°28.4'; 35°00.3')	400°C	A	12	43.6	47.3	3.6	147.9
IMAICHI										
Rhyodacite welded tuff	31 ± 2	IM321	(132°18.0'; 34°52.1')	400°C	B	11	130.6	38.5	2.5	322.3
		IM322	(132°15.8'; 34°52.6')	400°C	A	8	-104.6	33.3	6.2	79.8
HAMADA										
Rhyodacite welded tuff	32 ± 1	IM316	(132°07.5'; 34°52.0')	600-640°C	B	10	-108.9	-31.7	4.5	117.2
		IM317	(132°07.1'; 34°52.7')	500-540°C	A	13	98.6	43.2	2.1	378.0
		IM412	(132°06.9'; 34°52.6')	150°C	B	12	-134.9	-38.3	5.1	72.7
		IM413	(132°07.3'; 34°52.1')	400°C	A	13	83.8	33.2	4.3	93.9
		IM414	(132°07.2'; 34°51.7')	400°C	A	13	89.7	25.9	3.9	113.9
HIREFURIYAMA										
Rhyodacite welded tuff	33 ± 2	IM405	(131°56.7'; 34°41.2')	400°C	A	11	-117.3	-37.1	3.4	185.7
		IM406	(131°56.6'; 34°41.6')	400°C	A	11	-136.9	-32.1	3.4	180.7
Andesite lava		IM407	(131°52.7'; 34°40.7')	400°C	A	12	-149.4	-68.1	4.1	110.5
		IM408	(131°52.9'; 34°40.9')	500°C	B	12	-132.9	-43.9	3.3	169.1
YOBOSHIYAMA										
Rhyodacite welded tuff	33 ± 2	IM313	(131°55.0'; 34°44.0')	400°C	A	12	46.9	30.4	3.8	129.5
Andesite porphyrite		IM312	(131°55.5'; 34°43.3')	400-500°C	B	11	44.1	33.3	10.0	21.7
TAMAGAWA										
Dacite welded tuff	31 ± 1	IM404	(131°41.0'; 34°36.8')	500°C	B	5	-123.8	-60.1	6.6	134.0
OKAMI										
Granodiorite	33 ± 2	IM314	(131°54.4'; 34°46.3')	520-560°C	B	12	79.2	57.9	8.5	27.1
		IM410	(131°54.1'; 34°46.2')	500°C	B	9	71.2	63.5	7.3	51.1
		IM411	(131°54.0'; 34°45.3')	500°C	B	8	45.3	53.0	16.1	12.8
ARIFUKU										
Granodiorite	35 ± 2	IM323	(132°10.8'; 34°57.0')	520-540°C	B	10	-127.5	-55.4	6.3	60.0
		IM324	(132°09.1'; 34°58.1')	520-560°C	B	10	-118.6	-37.7	5.6	75.4
		IM415	(132°11.7'; 34°59.5')	300-500°C	B	11	-74.4	-44.1	9.9	22.2
		IM416	(132°14.0'; 35°00.2')	400-500°C	B	8	-69.0	-29.0	9.3	36.4

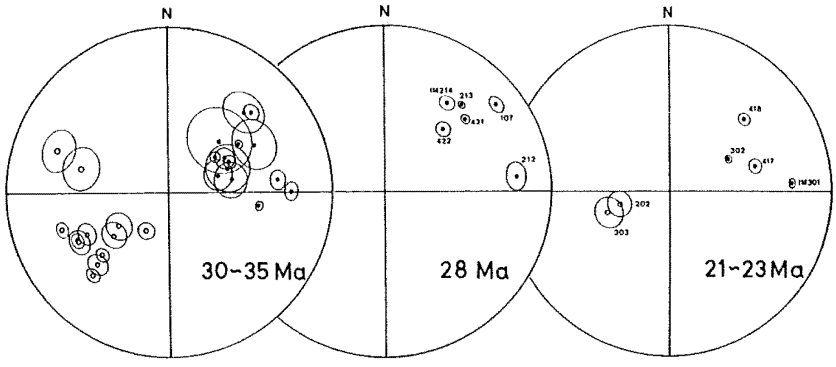

Fig. 3 Summary of site means directions with α_{95} confidence circles for three periods: 30 Ma-35 Ma, 28 Ma and 21 Ma-23 Ma. Projections are equal area, solid symbols on the lower hemisphere, open symbols on the upper hemisphere.

PALEOMAGNETISM

Individual specimens 25 mm in diameter and 25 mm long were prepared from samples in the laboratory. Schonstedt SSM-1A spinner magnetometer was used to measure the remanent magnetization of specimens. The stability of remanence was investigated through progressive demagnetization treatment by means of both thermal and alternating field methods. Three pilot specimens from each site were thermally demagetized in more than six steps. Specimens were heated in air in a noninductively wounded furnace enclosed in three cylindrical mu-metal in which the residual magnetic field was less than 10 nT. Demagnetization in alternating field up to 50 mT was carried out on one pilot specimen from each site with an magnetically shielded two-axis tumbler. Stability of remanence to thermal demagnetization for each site is given in Table 1. Magnetically stable site is defined as follows: Change in NRM directions of pilot specimens was less than 10 degrees during thermal demagnetizations. Typical results of thermally progressive demagnetization are shown in Fig. 2.

Results of demagnetization

One specimen from all independently oriented samples for each site were treated with thermal demagnetization to recognize the primary component, because in general thermal demagnetization technique successfully erased the secondary component which induced the unstable behaviour on specimens, rather than the AF demagnetization. The optimum demagnetization temperature to produce minimum dispersion was selected from three pilot specimens for magnetically stable sites. All samples in the other sites were progressively demagnetized to define the thermally stable end point magnetization. The range of demagnetization level to determine the charcteristic direction is listed in Table 1.

Table 1. All data except for those of granodiorite are after tilting correction. Data denoted by asterisk (*) are after Otofuji and Matsuda (1983). The ages are fission-track data after Matsuda (1983). Demag: the magnetic cleaning temperature and the behaviour of NRM direction during thermal demagnetization. A (stable): Change in NRM direction was less than 10 degrees during demagnetization; B: Change was more than 10 degrees. N is the number of samples in site mean computation, D is the site mean declination, I is the site mean inclination, and α_{95} and k are Fisher statistic parameter (Fisher, 1953).

[Granodiorite and andesite]

Internally consistent data were obtained after thermal demagnetization from these rocks, although their remanent magnetizations without any demagnetization treatment were highly scattered. The thermal demagnetization curves of granodiorite and andesite rocks showed Curie point of 580 °C (see Fig. 2), indicating that the stable portion of the remanent magnetization above 500 °C resided in the magnetite with little or no Ti content rather than hematite.

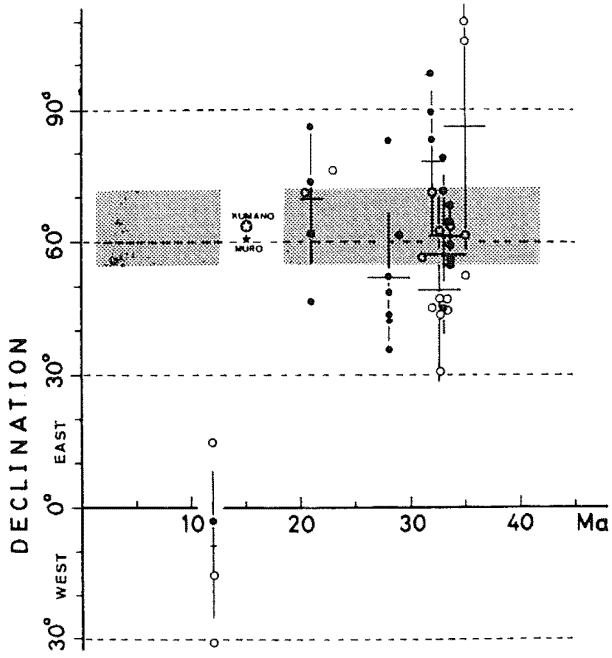

Fig. 4 Declination data of site means and rock unit means as a function of fission-track age. The declination error bars of rock unit means are the α_{95} values and age error bars are standard deviation of the average. Shaded declination zone is the declination with α_{95} value of mean direction of the period between 30 Ma and 35 Ma. This value characterizes the clockwise rotational motion of Southwest Japan. Closed circles show the data with normal polarity, open circles those with reversed polarity. The declination data of Muro and Kumano dacitic rocks are shown by stars.

[Welded tuff]

Almost all samples were found to be magnetically stable: They showed a single component in remanent magnetization (see Fig. 2). Magnetic phase with Curie temperature in the range between 580 °C and 680°C was identified in samples from four magnetically stable sites [IM321, IM 322, IM405, IM403] through thermal demagnetization curves. Since little change was observed in direction of remanent magnetization after demagnetization at above Curie temperature of magnetite, both magnetite and hematite phases probably recorded the paleomagnetic field with almost same direction.

Paleomagnetic data

Twenty eight sites survived the criterion: The acceptable site has at least five specimens cut from individually oriented samples: and a mean direction from the site has a mean circle of 95 % confidence less than 20°. The paleomagnetic data of the acceptable sites are listed in Table 1. Site mean directions were combined to obtain the mean directions of rock units listed in Table 2.

Paleomagnetic data are divided into three stages based on the fission-track ages; 30-35 Ma, 28 Ma and 21-23 Ma. Paleomagneic directions of each stage, combined with published data (Otofuji and Matsuda, 1983), are drawn in Fig. 3 and listed in Table 2. Paleomagnetic field direction

Table 2. Average paleomagnetic directions

Stage	Rock unit	N	$\bar{D}$(°)	$\bar{I}$(°)	α_{95}(°)	k	V.G.P.		∂p(°)	∂m(°)
[30-35 Ma]	Hamada	5	78.5	38.0	16.6	22.3				
	Hirefuriyama	4	49.1	46.6	21.2	19.8				
	Yoboshiyama	2	46.4	34.1	--	--				
	Tamagawa	1	56.9	61.6	--	--				
	Kawamoto(N)*	6	61.1	54.0	7.1	90.9				
	Kawamoto(R)*	1	64.2	44.9	--	--				
	Okami	3	64.8	60.5	16.5	56.9				
	Arifuku	4	86.3	46.3	28.1	11.7				
	mean	8	63.5	49.0	9.5	35.3	37.1°N	149.5°W	8.2	12.6
[28 Ma]	Kawauchi	6	52.2	33.5	15.3	20.2	41.1°N	130.2°W	9.9	17.4
[21-23 Ma]	Hata	6	69.9	49.5	14.5	22.2	32.2°N	152.7°W	12.8	19.3

Table 2. Directions are presented as the value at the representative point of Southwest Japan (134°E, 35°N). Data denoted by asterisk (*) are after Otofuji and Matsuda (1983). N is the number of sites, $\bar{D}$, $\bar{I}$ are mean declination and inclination, α_{95} and k are Fisher statistic parameter, and ∂p and ∂m are α_{95} semiaxes of oval of 95 % confidence.

in Table 2 is presented as the value at representative point (134°E, 35°N) of southwest Japan.

[30-35 Ma]

The five volcanic units and two plutonic stocks have preserved the record of paleomagnetism. The declination except for Imaichi rock unit lies insides a 46-86 degrees range which is concordant with the easterly declination previously reported from Southwest Japan (see Fig. 1).

The mean direction from plutons is compared with that from the other rock units: The latter is the value after tilting correction. Although the data from plutonic stocks have fairly deep inclination and easterly declination, the circles of 95 % confidence from plutonic and other rock units overlap (D=69.7°, I=51.9°, α_{95}=11.8° vs. D=57.9°, I=45.8°, α_{95} = 18.8°). This fact strongly suggest that the plutonic stocks have been subjected to little tectonic tilting and that they provide reliable paleomagnetic information. The reliability of the mean direction from eight rock units is also ascertained through the presence of normal and reversed polarity.

At sites of the Imaichi volcanic unit a partial field reversal was apparently recorded. These directions were excluded from the statistic computation for this stage.

[28Ma]

Two additional sites were measured for Sasahara tuff (Kawauchi cauldron) with age of 28Ma. These data confirm the strong easterly declination of this tuff (Otofuji and Matsuda, 1983).

[21-23Ma]

The Hata Subgroup has layers of welded tuff to which 21 Ma is assigned by fission-track dating. The magnetization of these tuffs showed normal polarity and easterly direction with about 60 degrees in declination. The tuff is stratigraphycally sandwiched by andesite lavas. Their NRM directions show a reversed polarity and antiparallel to that of tuff. The mean direction of the Hata Subgroup is therefore accepted to be an average direction of geomagnetic field over a long duration than the period of secular variation.

DISCUSSION

Amount of rotation

Sources of the error for paleomagnetism (tectonic tilting, geomagnetic secular variation, overprinting of secondary component upon primary magnetization) have been carefully eliminated through sampling and experimental procedure. The remaining error source to estimate the amount of rotation of southwest Japan is the effect of the apparent polar wander (APW). To minimize this effect , the following procedure is used. The expected paleofield direction at 30 Ma is calculated for the representative point of Southwest Japan (134°E, 35°N) from the APW path of Eurasia (Irving, 1977). And then its declination value is subtracted from that of the observed paleomagnetic direction. The observed data is Do= 63.5°, Io= 49.0°and uncertainty in declination (Δ Do = $\sin^{-1}(\sin\alpha_{95}/\cos I)$) is 14.6° , while the calculated paleofield direction is Dc= 9.7°, Ic= 58.9°and Dc = 6.6°. The rotation angle and its uncertainty are given by R=Dc-Do= 53.8°, $\Delta R = \sqrt{(\Delta Dc)^2 - (\Delta Do)^2} = 16.0°$. It is concluded that Southwest Japan has undergone a clockwise rotation through 54° since 30 Ma.

The fairly agreement between observed and calculated inclinations indicates that Southwest Japan has not been subjected to significant north-south translation.

Timing of rotation

Sixty degrees in declination characterize the clockwise rotation of Southwest Japan. A plot of declination of our study of southwest Japan versus age (Fig. 4) clearly shows that the characteristic declination has persisted until 21 Ma. Probably no clockwise rotation occurred until at least 21 Ma.

Some anomalous directions with about sixty degrees in declination have been reported from the Miocene rocks in Southwest Japan (Hirooka et al., 1967; Torii, 1979; Tagami, 1982). The dacite welded tuffs with age of 14-18 Ma collected at Muro (136.1°E, 34.5°N) have stable magnetization with 60.1° in declination and 66.1° in inclination (Torii, 1983), and the dacitic rocks with age of 15 Ma at Kumano (136.0°E, 34.0°N) show 63.9° in declination and 48.4° in inclination. The anomalous directions have been attributed to either the geomagnetic field reversal or the regional rotation of the blocks including these rock units. These declination values are quite consistent with the characteristic declination of Southwest Japan (see Fig. 4). Considering frequency and duration of geomagnetic field reversal, there is little chance that two independent rock units were produced in the period during field reversal and besides that they acquired the magnetization parallel to the characteristic direction of rotation of Southwest Japan during reversal. It is preferable to consider that these remanent directions reflect the tectonic rotation of Southwest Japan. These inference suggests a younger origin for rotational motion. The start of rotational motion of Southwest Japan is possibly younger than 15 Ma.

CONCLUSION AND IMPLICATION

It is concluded based on the paleomagnetism that: (1) Southwest Japan rotated clockwise 54° ± 16° during the past 30 m.y.; (2) The rotation took place suddenly later than 21 Ma; there remains a possibility that no rotational motion has begun until 15 Ma; (3) Taking into acount that rotational motion ceased at about 12 Ma (Otofuji and Matsuda, 1983), the rotation through about 55 degrees was completed within extremely short period of 3 m.y. to 9 m.y.

The geological evidence preserved on Southwest Japan appears to indicate the occurrence of the fast rotational motion of Soutwest Japan since 21 Ma (or 15 Ma). Andesitic to basaltic rocks of middle Miocene age in Southwest Japan forms the Setouchi Volcanic Belt which is arranged in a straight line nearly parallel to the Nankai Trough. Tatsumi (1982) summarized the characteristic of this belt as follows: (1) volcanic activity of this belt occurred within a very short time span of about 1 m.y. between 14 Ma and 13 Ma; and (2) this belt was generated by subduction of hot lithosphere. The rotation process proposed here affords both requirements for generation of this belt. Since the rotation of Southwest Japan was completed within a short time span just after Shikoku Basin had been created (24 or 25 Ma to 17and 15 Ma; (Kobayashi and Nakada, 1978; Shih, 1980), young and hot lithosphere of Shikoku Basin is expected to have been engulfed beneath the rotating Southwest Japan. The duration of subduction must have been short. This short duration in rotational motion provides a possible explanation for the short-lived volcanism.

REFERENCES

Ellwood, B.B. (1982) Earth Planet. Sci. Lett., 59, 303.
Fisher, R. (1953) Proc. R. Soc. London, Ser A, 217, 295.
Geissman, J.W. (1980) J. Geophys. Res., 85, 1487.
Harrison, C.G.A. and T. Lindh (1982) J. Geophys. Res., 87, 1903.
Hirooka, K. and N. Kawai (1967) Ann Progress Rep. Rock Mag. Res. Group Japan, 69.
Irving, E. (1977) Nature, 270, 304.
Kawai, N., T. Nakajima and K. Hirooka (1971) J. Geomag. Geoelectr., 23 267.
Kobayashi, K. and M. Nakada (1978) J. Phys. Earth, 26, suppl., S 391.
Masuda Research Group (1982) Jour. Geol. Soc. Japan, 88, 321.
Matsuda, T. (1983) Doctoral Thesis, Faculty of Sci. Kyoto University.
Matsuda, T. and M. Oda (1982) Jour. Geol. Soc. Japan, 88, 31.
Murakami, N. (1973) Mem. Geol. Soc. Japan, 9, 93.
Otofuji, Y. and T. Matsuda (1983) Earth Planet. Sci. Let., 62, 349.
Ross, C.S. and R.L. Smith (1961) U.S. Geol. Surv. Prof. Paper, 366, 1.
Sasajima, S., J. Nishida and M. Shimada (1968) Earth Planet. Sci. Lett. 5, 135.
Shih, T. (1980) Initial Rep. Deep Sea Drill. Proj., 58, 783.
Tagami, T. (1982) NOM, 9, 23.
Tatsumi, Y. (1982) Earth Planet. Sci. Lett., 60, 305.
Torii, M. (1979) Rock Mag. Paleogeophys., 6, 52.
Torii. M. (1983) Personal Communication.

(Submitted to Earth Planet. Sci. Lett.)

PALEOMAGNETIC EVIDENCE FOR RAPID CLOCKWISE ROTATION OF SOUTHWEST JAPAN AT MIDDLE MIOCENE TIME

Masayuki TORII

Department of Geology and Mineralogy, Kyoto University, Faculty of Science, Kyoto 606, Japan

Since the time of pioneer works of Kawai et al. (1961) and Sasajima et al. (1968), it is well known that most of Cretaceous and Paleogene rocks in Southwest Japan have paleomagnetic directions pointing east of the axial geocentric dipole field. These anomalous directions are widely accepted to indicate a clockwise rotation of Southwest Japan as a result of back-arc spreading of the Japan Sea. The timing of the opening of the Japan Sea is one of the key to understand the tectonic history for the Japanese Islands, and it has generally been postulated at some time prior to the late Tertiary on the basis of the paleomagnetic information (e.g. Uyeda and Miyashiro, 1974; Hilde et al., 1977; Ben-Avraham, 1978; Seno and Maruyama, 1983). Due to the recent progress of paleomagnetic study and radiometric age determination, it has become increasingly important to lead quantitative conclusion about the timing. Of special interest are the anomalous paleomagnetic directions which were recently obtained from Miocene rocks at three different localities in Southwest Japan (Tagami, 1982; Hayashida and Ito, 1983; Otofuji and Matsuda, 1983). These directions show affinity with those of Cretaceous and Paleogene rocks. The age of those rocks is estimated to rage from the early to middle Miocene (15 to 21 Ma).

In order to examine possible clockwise rotation in the Miocene, paleomagnetic study was carried out on sedimentary and volcanic rocks exclusive to middle Miocene strata in the Setouchi Province, Southwest Japan. Samples were collected in seven areas (179 sites), extending more than 500 Km along the Median Tectonic Line; namely Shidara, Muro, Mt. Nijo, northern Takamatsu, Tsuyama, Takanawa Peninsula and eastern Yamaguchi. Among those sites, 99 sites were recognized to show reliable paleomagnetic direction on the basis of tilting correction, thermal demagnetization experiments, statistical test, and so on. These paleomagnetic directions can be classified into two groups based on their declinations; one is showing almost parallel direction with the dipole field, and the other has clockwise deflected direction (Table 1 and Fig. 1). In addition to the present results, some previously reported paleomagnetic directions from middle Miocene rocks were combined to obtain more regional mean value respect to Southwest Japan such as the Kumano acidic rocks (Tagami, 1982) and the Ichishi Group (Hayashida and Ito, 1983). Finally, paleomagnetic directions of the middle Miocene can be arranged into two distinct groups: A and B (Table 1 and Fig. 1).

Group A is obtained from the Setouchi volcanic rocks, and the mean value is D=1.3°, I=49.5°(k=155). Mean radiometric age respect to the Group A is 13.3±1.5 Ma (N=17). Group B is obtained from the Setouchi Miocene series (mainly marine sediments) and some of the

TABLE 1 SUMMARY OF PALEOMAGNETIC MEAN DIRECTIONS OF THE MIDDLE MIOCENE ROCKS OF SOUTHWEST JAPAN

#	GELOGIC UNIT	DEC	INC	α_{95}	k	N	R	VLAT	VLON
group (a)									
1	Nansetsu Sg.	4.6	57.0	8.9	20.3	10	9.7031	85.5	-167.5
		(4.8	56.7)						
2	Nijo G.	-8.5	46.8	17.5	20.5	5	4.8002	80.3	6.2
		(-8.6	47.5)						
3	Shodo-shima G.	7.3	48.6	6.1	34.8	17	16.5408	82.1	-99.9
		(7.5	49.4)						
4	Takanawa Pen.	1.4	41.0	12.1	58.7	4	3.9489	79.5	-54.3
		(1.9	42.5)						
5	Yamaguchi area	3.5	55.8	12.6	96.9	3	2.9794	86.2	-179.8
		(3.4	57.0)						
6	Muro G.	60.6	66.1	3.7	76.0	21	20.7369	43.8	-170.3
		(60.9	65.5)						
group (b)									
7	Hokusetsu Sg.	48.0	50.0	14.0	44.0	4	3.9318	49.8	-140.2
		(47.4	48.0)						
8	Tonosho G.	42.2	60.3	11.1	69.6	4	3.9569	56.3	-160.3
		(42.6	61.1)						
9	Takakura F.	23.5	37.6	11.4	65.6	4	3.9542	65.0	-107.9
		(23.8	37.8)						
10	Ichishi G.	45.1	48.8	11.9	15.7	11	10.3634	51.8	-139.2
		(45.0	48.2)						
11	Kumano a.r.	57.5	49.7	20.6	37.0	3	2.9459	41.8	-147.0
		(57.9	49.8)						
Group A (1 - 5)		1.3	49.5	6.2	154.6	5	4.9741	85.2	-58.6
Group B (6 -11)		44.7	52.4	10.9	38.7	6	5.8707	53.2	-145.0

Mean direction in ( ) is field direction at the representative location of Southwest Japan (35°N, 135°E).

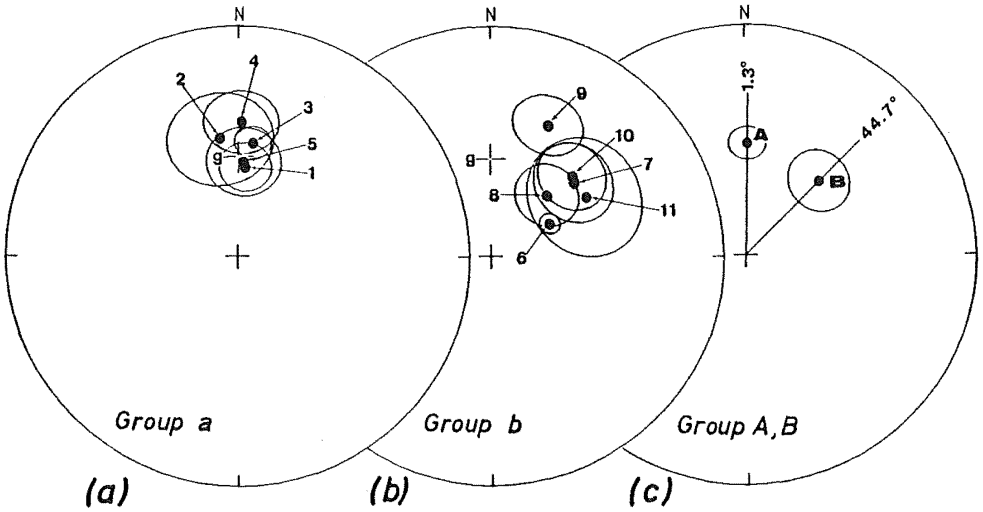

Fig. 1 Summary of paleomagnetic directions of Miocene rocks from Southwest Japan. (a) Directions from the Setouchi volcanic belt. (b) Directions from the Setouchi Miocene series, Kumano acidic rocks and Muro welded tuff. (c) Total mean directions of Group A and B. Numbers adjacent to symbols correspond to those appeared in Table 1.

overlying felsic igneous rocks (Kumano acidic rocks and Muro welded tuff). Mean paleomagnetic direction is D=44.7°, I=52.4° (k=39), showing considerable deflection from the dipole field. Mean radiometric age of the igneous rocks is 15.2±1.3 Ma (N=9) which is estimated to be significantly different from that of the Group A on the basis of the analysis of variance at 5% point.

The present results strongly suggest that Southwest Japan has undergone clockwise rotation through 45° within the period of emplacement of the Group A and B; namely from 15 to 13 Ma.

References:

Ben-Avraham,Z. (1978) Tectonophysics, **45**, 269.
Hayashida,A. and Y.Ito (1983) Earth Planet. Sci. Lett., (submitted).
Hilde,T.W.C., S.Uyeda and L.Kroenke (1977) Tectonophysics, **38**, 145.
Kawai,N., H.Ito and S.Kume (1961) Geophys. J. R. astr. Soc., **6**, 124.
Otofuji,Y. and T,Matsuda (1983) Earth Planet. Sci. Lett., (submitted).
Sasajima,S., J.Nishida and M.Shimada (1968) Earth Planet. Sci. Lett., **5**, 135.
Seno,T. and S.Maruyama (1983) Tectonophysics, (in press).
Tagami,T. (1982) NOM (News of Osaka Micropaleontologists), **9**, 23.
Uyeda,S. and A.Miyashiro (1974) Geol. Soc. Am. Bull., **85**, 1159.

(to be submitted to J. Geomag. Geoelectr.)

CHARACTERISTIC BACK-ARC SPREADING OF THE JAPAN SEA AND ITS RELEVANT PROBLEMS

Sadao SASAJIMA and Masayuki TORII

Department of Geology and Mineralogy, Kyoto University, Kyoto 606, Japan

Recent paleomagnetic study conducted by Otofuji and Matsuda (1983) has opened an important question on the latest Paleogene opening of the Japan Sea which was predicted by previous paleomagnetic results from Southwest Japan (e.g. Sasajima, 1981). One of their conclusions was that the major clockwise rotation of the Southwest Japan might have occurred during 28 - 12 Ma.

Soon after the publication, results of the paleomagnetic investigation by Hayashida and Ito (1983) on the Ichishi Group, one of middle Miocene series in Kinki district have restricted the initial timing of the predicted rotation of Southwest Japan as young as 16 Ma. Subsequently, Torii (1983) has completed a paleomagnetic study of the major part of Setouchi volcanic rocks and some felsic igneous members in the Outer Zone of Southwest Japan; the former builds about 500 Km long strip along the inner zone of the Median Tectonic Line. Paleomagnetic results of Torii (1983) were mostly obtained from radiometrically dated rocks distributed over the most part of Southwest Japan province, implying that the result is taken up as an actual representative of the whole landmass. It gives easterly rotation of 45°±18° during 15 Ma to 13 Ma.

All the authors reasoned that a remarkable rotation of the landmass is due to the back-arc spreading of the Japan Sea. This may be the first documented example that a certain back-arc spreading have been suggested by paleomagnetic techniques.

Some relevant problems to the subject are discussed. They are as follows:

1) Which one of two proposed models is preferable to account for this instance; the anchored slab (Chase,1978; Uyeda and Kanamori, 1979) and the retreating trench model (Molnar and Atwater, 1978).

2) Is an extensive arc volcanism synchronous with the back-arc igneous activities?

3) About the stress relation of the spreading to the Southwest Japan land block and reason for cessation of it.

1) The induced mantle convection hypotheses (e.g. Hsui and Toksoz, 1979; Ito et al., 1983) are most appropriate to account for the back-arc spreading of Japan Sea.

Recently, Seno and Maruyama (1983) have tried to establish the paleogeographic configuration of the Philippine Sea. They prefer the retreating-trench model rather than the anchored slab model by Uyeda and Kanamori (1979) through a case study on the evolutionary history of the Philippine Sea. In the case of back-arc spreading of the Japan Sea, it is very difficult to defend the anchored slab model, because of rapid-rate rotation of the Southwest Japan block. The rate of 20°/m.y. cannot alternatively ascribe to the counterwise rotational retreat of the Eurasian continent, and further we have so far had no paleomagnetic evidences proving any rotational retreat of the continent with the same negative rotation angle as the Southwest Japan did. For this reason we tend to support the retreating-trench mechanism for the spreading of

Japan Sea, although we cannot absolutely deny the other model.

Following the idea of Uyeda and Kanamori (1979), Ito et al. (1983) have tended to conclude that the back-arc spreading might have commenced at above the stagnation line of vortex by a retreating of the major landward plate away from the trench fixed. However, the initiation of the Japan Sea spreading is subsequent to the end of the spreading of Shikoku basin (Kobayashi and Sato, 1980), consequently it is probable that the pre-existed trench changed into a new transform fault, enabling the Shikoku basin plate to decouple, or partially decouple, from the proto-Japanese arc formed the eastern periphery of the Asian continental plate. Under such a condition the back-arc spreading may be accommodated by the overriding of the Southwest Japan microplate onto the Shikoku basin plate, and thereafter a new subduction of the latter may occur near the outermost front of the former.

It should be noted that the back-arc spreading could not occur solely due to the maximum tension stress expected in the bottom surface of the continental lithosphere (≃50 bar) without any additional tension tectonics, such as deep seated structural zone in the upper part of the lithosphere (Ito et al., 1983; Hsui and Toksöz, 1979). Based on their induced convection hypothesis for back-arc spreading Hsui and Toksoz (1981) maintained the retreating-trench model against the anchored slab model. The back-arc spreading of Japan Sea gives in fact a positive support to their argument.

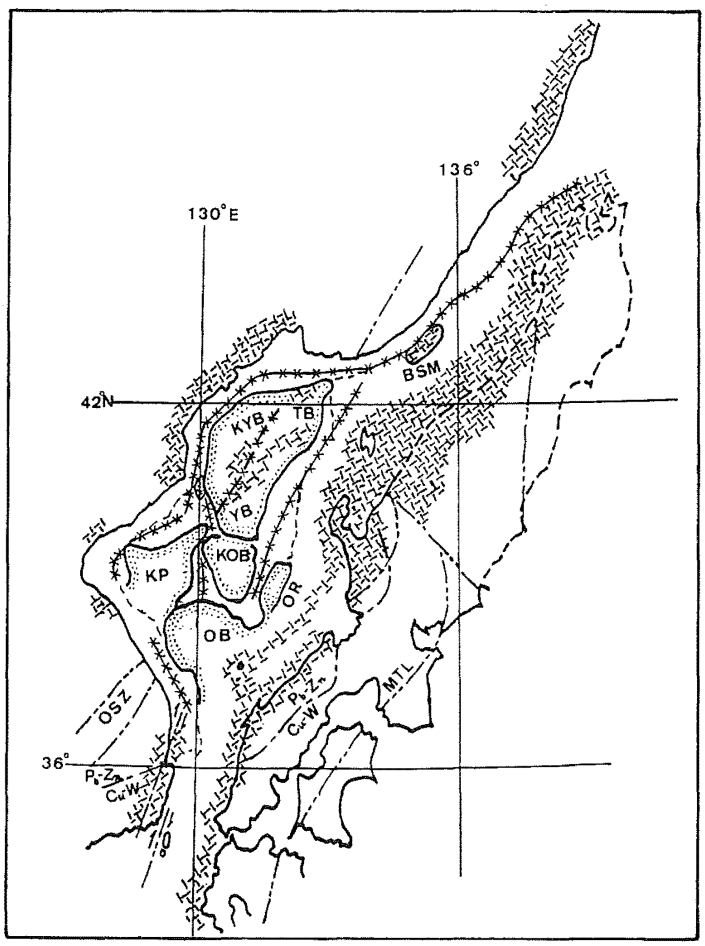

Fig. 1. Distribution map of Green Tuff volcanic products shown in the continental arc configuration of the Japanese islands: compiled after Shimazu (1982) and Inoue and Honza (1982).
Hatched area, solid line with crosses and chain line denote Green Tuff region, rifting system and main structural line, respectively.

2) Based on the recent reanalysis of the temporal relationship between back-arc spreading and arc volcanism in Philippine Sea (Sample and Karig,1982; Karig, 1983), Karig strongly suggested that pulses of spreading and volcanic activities are nearly synchronous opposing the previous views that back-arc spreading occurs or at least is initiated during relative minima in the intensity of arc volcanism. Thus it is of current importance to know whether the back-arc spreading is synchronized with the intensive arc volcanism.

Along the Japan Sea side of the Honshu island occurs so-called Green Tuff complex with the ages ranging from the late Oligocene to middle Miocene (Tanaka and Nozawa, 1977). We regard the Green Tuff volcanism as the representative arc volcanism closely associated with the back-arc spreading of the Japan Sea. From the distribution of Green Tuffs shown in the reconstruction map of Japanese islands arc before the opening of the Japan Sea (Fig. 1), outline of geologic setting of the circum Japan Sea region is seen. Green Tuff activity has been most comprehensively investigated in Northeast Japan, but in the San'in-Hokuriku province of Southwest Japan the strata are thin and igneous activity and structural deformation are not so strong compared with those of Northeast Japan. We thus prefer in this paper Northeast Japan at first to test exactly the above problem.

According to the Neogene chronostratigraphic correlation edited by Tsuchi (1981), the boundary between Nishikurosawa and younger Onnagawa Formation is defined within a period, 14.5 to 14.0 Ma (≃ Blow's N 10 - N 11). These formations are regarded as representing relatively later portion of Green Tuff activities. The extensive volcanic activities continued since the late Oligocene and declined sharply at the latest time of Nishikurosawa stage, during which time the intense mineralization of Kuroko deposits took place (Ishihara, 1974; Horikoshi, 1982). The age of Kuroko deposits is estimated at about 15 Ma by Horikoshi (1982). The Onnagawa Formation is characteristically composed mainly of siliceous shale, suggesting more or less deep-sea sedimentary environment during that stage. Bearing the opening period of Japan Sea, 15 - 13 Ma, in our mind together with the lithofacies changes appeared in these stages, it can be said conservatively that the violent arc-volcanism and back-arc activities were not in synchrony but in sequence. Namely, Green Tuff activities correspond to the latest stage of the continental arc volcanism and by the subsequent back-arc spreading the Japan island arc was renewed into the present state.

It is important that an unusually violent Miocene volcanism in Japanese island arc, Green Tuff activities, could have played indeed a vital role on, or triggered, the subsequent back-arc spreading. We wish to refer to the chemical and thermal studies by Bailey (1983) who has neatly summarized comparison of oceanic and continental rifts. It is pointed out tentatively that Green Tuff volcanism characterized by the bimodal type (basalt and dacite) magmatism (Konda, 1974) is a possible indication of the transitional phase from the continental into oceanic rifting stage. Beside this, taking into consideration the deposition period of Kuroko ores, it seems likely that they were produced just prior to or at the initial stage of the break-up of continental lithosphere. Concerning to this, it should be noted that metalliferous hydrothermal muds are often discovered in the crest of some mid-oceanic ridges (e.g. Edmond et al., 1982; Uyeda, 1983). A close causal relationship of both hydrothermal deposits seems to be a reflection of the common environment of passive plate margins, even though they are different from each other in size.

Very recently, Fujioka and Kitazato (1983) have presented an inter-

esting idea about a similarity in morpho-tectonic elements between Northeast Japan arc at the Nishikurosawa stage and the present Izu-Ogasawara arc. This is basically consistent with the present author's opinion excepting for the time setting. Our opinion is that the former appears to show the relic structure of a rifted margin in back-arc region (separated island arc) which is somewhat similar to the present Izu-Ogasawara arc being in an advanced phase from the former.

Contrasting to the spreading in Mariana basin, that of the Japan Sea clearly postdates to the violent arc-volcanism accompanied by an extensive tectonic movements. Nevertheless, it is of interest that the volcanicity in the former is estimated, in a parameter, to be larger than 15 $Km^3/m.y.$ for one Km segment of volcanic front (Sample and Karig, 1982) and it is nearly comparable to our calculation value for Nishikurosawa stage, 3 $Km^3/m.y.$, though it should be taken as a less estimation of the eruptive rate in the east Akita area of Northeast Japan (Ishihara, 1974). Finally, the above-mentioned discrepant timings of arc-volcanism between the two cases may be reconciled with their different situation, one belong to the continental arc and the other to the oceanic island arc.

3) It has been believed generally that rates of spreading in back-arc basins were rather sluggish in comparison with those of the mid-oceanic ridges. However, documented back-arc spreading all belonged to the oceanic or quasi-oceanic lithosphere and the quantitative nature of back-arc opening from continental lithosphere was first revealed from the Japan Sea, although a continental back-arc spreading was reported from the South China Sea with a slow spreading rate (Taylor and Hayes, 1983).

The spreading rate of the Japan Sea may be the biggest among those of back-arc basins so far known, and more or less comparable to the mid-oceanic ones. We have no plausible ideas to account for the matter, but it may partly relate to the possible occurrence of the transform fault along the proto-Nankai trough that was caused by the opening of Shikoku basin (30-17 Ma; Kobayashi and Sato, 1979).

The stress condition of the Japan Sea side in Southwest Japan seems to have changed its mode, even the data are not enough, from an extension to a compression state at about 15 Ma (Tsunakawa and Takeuchi, 1983). The change of he state may be better interpreted by the rifting of back-arc for the extension and during the spreading until its cessation for the compression of the region.

Hsui and Toksöz (1981) speculated the reason why the Japan Sea basin ceased its spreading in such way as we see at the present. They emphasized on a net contribution of increased compressive stress that was resulted from growing amount of the arc volcanoes, surpassed the tension stress due to the back-arc spreading. This might be wrong considering from our discussion mentioned above. We intend to propose that by the collision event of the Japanese landblock onto the proto-Izu island (ridge) and the Kyushu-Palau ridge much larger compression could have prevailed against the spreading force, resulting in the cessation of the spreading.

References:

Bailey,D.K. (1983) Tectonophysics, **94**, 585.
Chase,C. (1978) J. Geophys. Res., **83**, 5385.
Edmond,J.M., K.L.Von Damm, R.E.McDuff and C.I.Measures (1982) Nature, **297**, 187.

Fujioka,K. and H.Kitazato (1983) Gekkan Chikyu (The Earth, monthly), **5**, 447.
Hayashida,A. and Y.Ito (1983) Earth Planet. Sic. Lett., (submitted).
Horikoshi,E. (1983) Min. Geol. Spec. Issue, **11**, 183.
Hsui,A.T. and M.N.Toksöz (1979) Tectonophysics, **60**, 43.
Hsui,A.T. and M.N.Toksöz (1981) Tectonophysics, **74**, 89.
Inoue,E. and E.Honza (1982) Marine Geological Map Ser., **23**, Geol. Surv. Japan.
Ishihara,S (1974) Min. Geol. Spec. Issue, **6**, 235.
Ito,H., Y.Masuda and O.Kinoshita (1983) Bull. Univ. Osaka Pref., Ser. A, **32**, 47.
Karig,D.E. (1983) The Tectonic and Geologic Evolution of Southeast Asian Seas and Island, Part 2, Geophys. Monogr., **27**, (AGU, Washington D.C.) p. 318.
Kobayashi,K and N.Sato (1980) Developing Earth II, (Iwanami, Tokyo), p.125.
Konda,T. (1974) J. Geol. Soc. Japan, **80**, 81.
Molnar,P. and T.Atwater (1978) Earth Planet. Sci. Lett., **41**, 330.
Otofuji,Y. and T.Matsuda (1983) Earth Planet. Sci. Lett., **62**, 349.
Sample,J.C. and D.E.Karig (1982) J. Volcanol. Geotherm. Res., **13**, 73.
Sasajima,S. (1981) Paleoreconstruction of the Continents, Geody. Ser., **2**, (AGU, Washington D.C.), p. 115.
Seno,T. and S.Maruyama (1983) Tectonophysics, (in press).
Shimazu,M. (1982) Geology of the Japan Sea, (Tokai Univ. Press), p. 193.
Taylor,B. and D.E.Hayes (1983) The Tectonic and Geologic Evolution of Southeast Asian Seas and Island, Part 2, Geophys. Monogr., **27**, (AGU., Washington D.C.), p. 23.
Tanaka,K. and T.Nozawa (eds.) (1977) Geology and mineral resources of Japan, (Geol. Surv. Japan), p. 430.
Torii,M. (1983) this issue.
Tsuchi,R. (ed.) (1981) Fundamental data on Japanese Neogene bio- and chronostratigraphy, suppl., (Shizuoka Univ.), p. 124.
Tsunakawa,H. and A.Takeuchi (1983) Kagaku (Science, Tokyo), **53**, 624.
Uyeda,S. (1983) Min. Geol., Spec. Issue, **11**, 37.

CRETACEOUS REMAGNETIZATION OF THE PALEOZOIC ROCKS IN THE SOUTH KITAKAMI MOUNTAINS, N.E. HONSHU, JAPAN

Yoshiki FUJIWARA and Yukio MORINAGA

Department of Geology and Mineralogy, Hokkaido University
N10, W8, Sapporo 060

Recent pregress on a paleomagnetic research on a Paleozoic and Mesozoic rocks of the Japanese Islands in the last several years have greatly increased our knowledge concerned with accretion tectonics in the Circum Pacific Orogenic Belt.

In some previous papers (Minato and Fujiwara 1964,1965 Fujiwara 1968) a paleomagnitism of the Paleozoic rocks in the South Kitakami Mountains was studied. In order to get more detailed information concerning with change of pole positions as well as paleo-latitudes of Northern Japan, we undertook a paleomagnetic measurements of the Paleozoic and Mesozoic rocks developted in the South Kitakami Mountains.

Sampling and Measurements

The Kitakami Mountains is structually divided into two units; the South Kitakami Mountains and the North Kitakami Mountains. The boundary between these two units is called the Hayachine Tectonic Belt where it is defined by ultrabasic rocks of Cretaceous age. A total of 217 samples were collected from 63 sites on various localities in the South Kitakami Mountains. At least one specimen from each site was subjected to stepwise a.f. and thermal demagnetization. After each measurement, orthogonal projections of the magnetization vector (Zijderveld,1967) were plotted to isolate the secondary and characteristic directions.

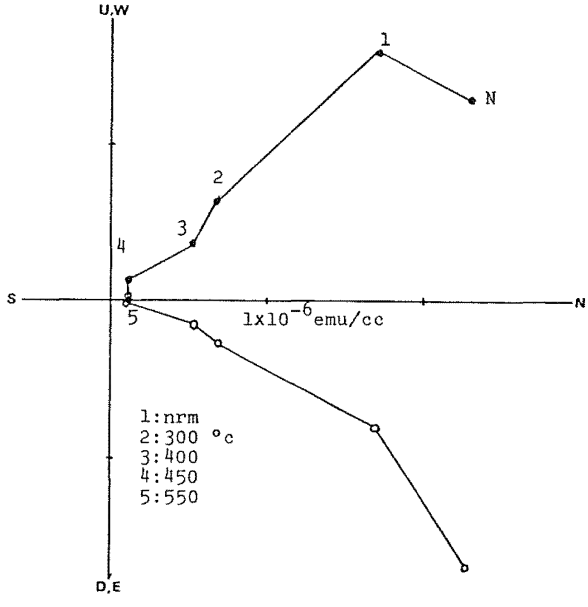

Fig.1. Orthogonal demagnetization projections of sample of Devonian sandstone.

The experimatal results suggest that most magnetization of the present Paleozoic rocks may represents a progressive overprinting of the high blocking temperature component. Fig.1 represents a very stable magnetization of the Devonian sandstone sample that persists up to highest temperatures of demagnetization. Fig.2a shows site mean directions inferred from lower Cretaceous volcanic rocks as well as plutonic rocks where are collected form various localities in the South Kitakami Mountains. These directions are more or less coincide with the results from the lower Cretaceous plutonic rocks collected from both South and North Kitakami Mountains reported by Ito et al. (1980).

Conclusions

The present our results strongly suggest that the magnetizations of these Paleozoic rocks probably remagnetization set during volcanism and plutonism occurred in lower Cretaceous age. Therefore, our former interpretation of Devonian and Carboniferous pole positions is retracted.

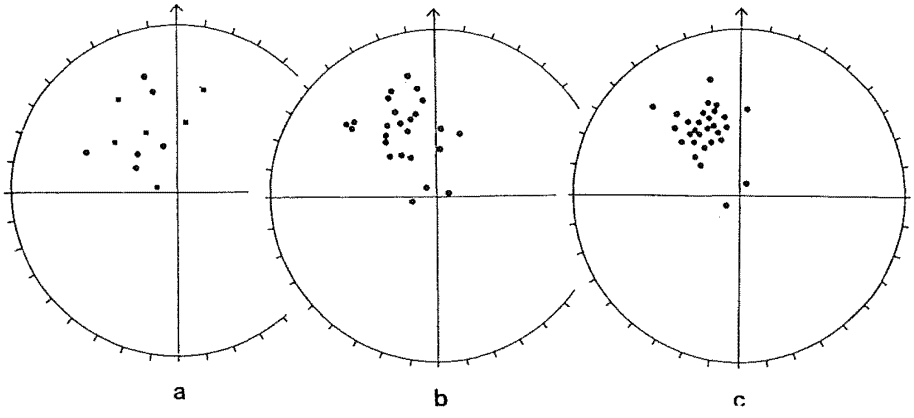

Fig.2. Projections of site mean directions; 2a: lower Cretaceous volcanic (square) and plutonic rocks (solid circle), 2b: Devonian rocks, 2c: Carbniferous rocks. The directions are plotted in the lower hemisphere of a Schmidt equal-area stereonet segment.

References

Fujiwara,Y. (1968) J. Fac. Sci. Hokkaido Univ. 14,2. 159-168
Ito, H.,Tokieda, K. and Notsu, Y.(1980) Rock mag. paleogeophys. 7, 113-117
Minato, M. and Fujiwara, Y.(1964) Compte Rendu 581-585
(1965) Earth Sci. 8, 21-22

Paleomagnetism of red cherts: A case study in the Inuyama area, Central Japan

Hidetoshi Shibuya and Sadao Sasajima

Department of Geology and Mineralogy, Faculty of Science, Kyoto University, Kyoto, 606, Japan

An attempt to extract and confirm the primary magnetization from red cherts was carried out. Cherts are very suitable material for paleomagnetic study. The advantages of cherts in paleomagnetic study are threefold; (1) recent progress in radiolarian biostratigraphy (e.g. Pessagno and Blome, 1980) make it possible to determine precise time of their deposition, (2) accurate tilting correction can be performed as their bedding plane is clearly defined, and (3) their slow depositional rate (e.g. Schlager and Schlager, 1974) enable us to detect records of geomagnetic polarity reversals, which improves reliability of paleomagnetic results.

In order to use cherts in paleomagnetic researches, we have to distinguish primary magnetization from secondary ones. Roy and Lapointe (1978) stated that rocks which have been formed millions or billions of years ago usually contain more than one component of magnetizations of different acquisition time. Moreover, as cherts usually appear in orogenic belts, they might suffer thermal and/or chemical alteration which influenced their magnetic properties. The purpose of the present study is to unravel the nature of the remanence of cherts, especially red cherts which seems to have stronger magnetization than the others.

Sampling was carried out in the Inuyama area, Central Japan (Fig. 1), which is situated in the southern part of Mino terrane. In the area, Yao et al. (1980) performed a detailed radiolarian biostratigraphic study. According to them, there exist middle Triassic to early Jurassic chert, middle Jurassic siliceous mudstone and late Jurassic(?) sandstone beds, piled up repeatedly with chaotic order (Fig. 1). These rocks are well exposed on the flanks of Kiso River, forming a syncline plunged to the west (Mizutani, 1964). The direction of bedding plane is, however, locally disturbed, since the chert beds occasionally form intraformational foldings. The bedding plane of the cherts is clearly observed and thickness of each bed generally ranges 2-5cm. Depositional rate of a chert sequence in the area was estimated as slow as 2.8 m/m.yr. (Yao, 1981 personal communication).

Samples for paleomagnetic study were collected by means of hand sampling. A few cylindrical specimens with length and diameter of about 24mm was prepared from each hand sample in the laboratory. Measurements of remanence were made mainly with a Schonstedt SSM-1A spinner magnetometer and partly with a SCT's Superconducting Rock Magnetometer. Thermal demagnetization was accomplished in a non-inductively wound electric furnace contained within three layered cylindrical mu-metal shield. The residual magnetic field in sample space of the furnace was maintained within 10 nT on cooling cycle. Progressive demagnetization was performed up to 660°C or 670°C, and measurements of remanence were taken in more than 10 steps. On the last step, remanence had become too weak for meaningful measurement or excessive build up of VRM, appeared after heating at higher temperature, prevented further remanence measurements.

At first, samples from site 3 and 4 in Fig. 1 were subjected to detailed demagnetization experiments. We already reported natural remanent magnetization (NRM) of cherts from these sites were stable and

showed no obvious directional change through progressive alternating field demagnetization procedure (Shibuya and Sasajima, 1980). The two sites were situated on a middle Triassic red chert body with a thickness of about 40m. These sites were chosen avoiding intra-formational foldings. The distance between the sites is about 50m. They seem to be on the same horizon, though a few faults introduce ambiguity to the stratigraphic correlation between them.

Progressive thermal demagnetization experiment revealed that NRM of the red chert is multicomponent. Fig. 2 shows a result of stepwise thermal demagnetization experiment of a pilot specimen from site 3 which is plotted on vector-demagnetization diagram (Zijderveld, 1967). As shown in the figure, magnetization of the pilot specimen consists of at least four components with blocking temperature (Tb) ranging about 25°C-100°C (A), 100°C-300°C (B), 300°C-610°C (C), and 560°C-660°C (D).

The most unstable component (A) had a direction close to the present geomagnetic field and was removed by a treatment less than 100°C. Component B with a reversal direction declining to the west was removed

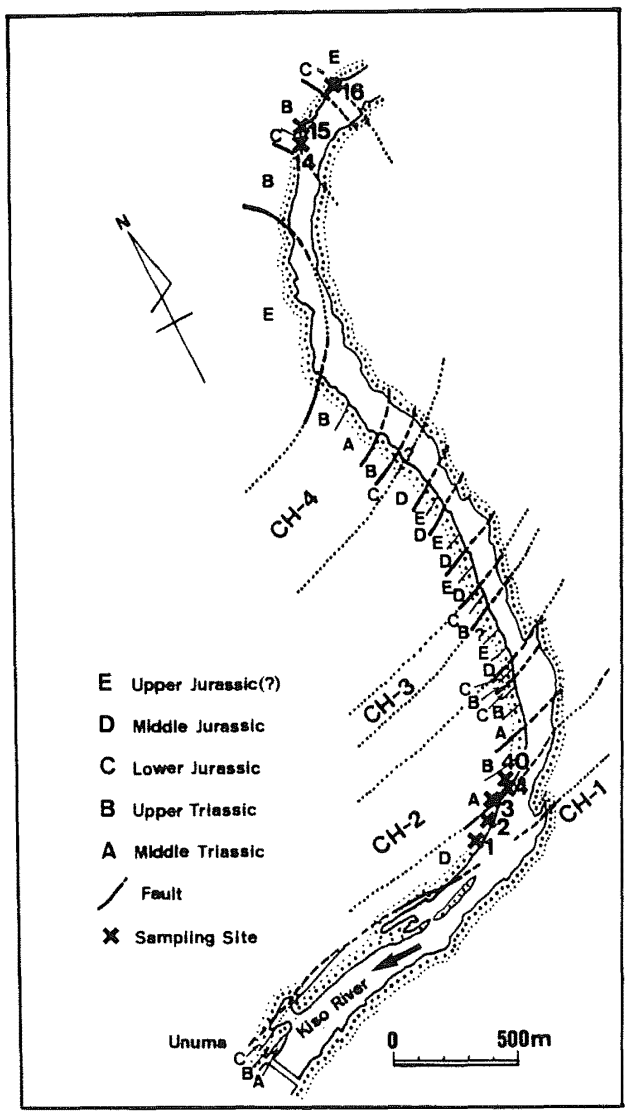

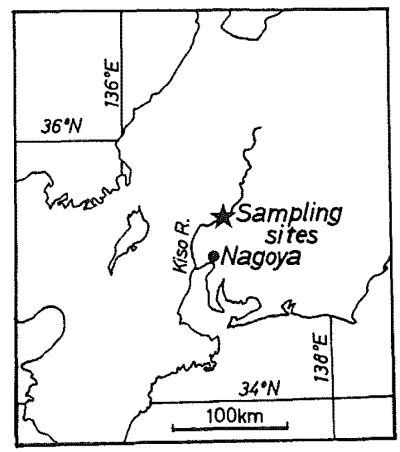

Fig. 1, Map showing sampling sites in Inuyama area. Base map and age classification were followed after Yao et al. (1980). CH-1 through 4 denote chert beds, and other beds are shales and sandstones.

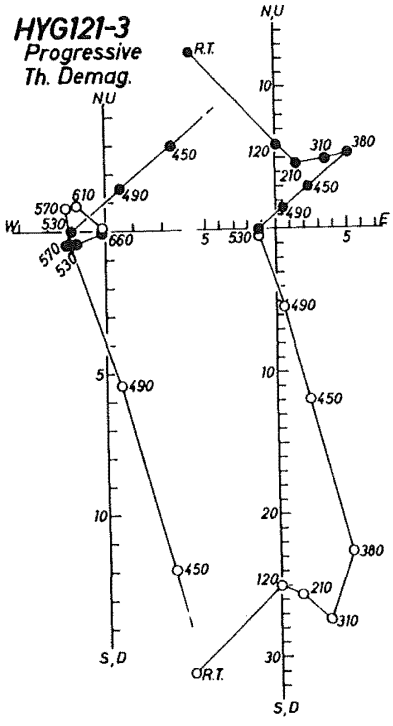

Fig. 2, Vector demagnetization diagram for a red chert specimen from site 3. Successive end point of magnetization vector during progressive thermal demagnetization are plotted in in situ coordinate. Left diagram is enlargement of the right, to illustrate high temperature part. Solid circles represent projection onto horizontal plane and open circles represent east-west vertical plane. Numerals denote demagnetization temperature. RT is room temperature.

over 100°C-300°C. After removal of these low Tb components, the dominant component (C) decayed linearly up to 560°C. However, it did not converge to the original point. This offset proves existence of the component D which survived at demagnetization temperature above 600°C. The same multiphase character of magnetization was observed in site 4. It is shown that magnetization of a pilot specimen from site 3 also consists of four components, which have similar directions and Tb-ranges corresponding to respective components of site 3.

The two components, A and B, can not be assigned to the primary magnetization because viscous partial thermoremanent magnetization (Chamalaun, 1964) should mask the primary magnetization in such a low blocking temperature (Pullaiah et al., 1975). Component A is probably VRM induced by the present field. Component B may be thermoremanent magnetization (TRM) or chemical remanent magnetization (CRM) which was acquired during uplift of the rock body in a certain reversed epoch. The westerly direction may indicate that the uplift occurred before the clockwise rotation of Southwest Japan in the Miocene (Otofuji and Matsuda, 1982). On the other hand, components C and D have so high blocking temperatures that either of them may be primary magnetization.

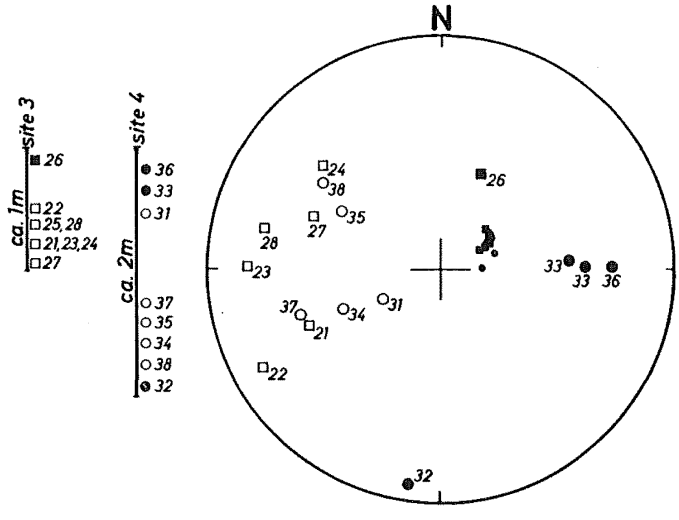

Fig. 3, Equal-area projection of directions of component C and D in situ (smaller and larger symbols, respectively). Squares and circles represent site 3 and 4. Open and closed symbols indicate upper and lower hemisphere. Diagram on the left shows relative stratigraphic position and polarity of each sample in the site.

Since the remanence decayed linearly from 380°C to 560°C on both site 3 and 4, we refer to the magnetization vector after a treatment at about 380°C subtracted by that at about 560°C as the characteristic vector of component C. On the other hand, the vector at about 610°C is accepted as the characteristic vector of component D. The directions of component C were very tightly clustered in both site 3 and 4, (Fig. 3) and the two site mean directions were included in the 95% confidence circles each other. The directions of component D of both sites were also overlapped to each other, and made two clusters antipodal to each other (Fig. 3), although they were considerably scattered because of their small intensity. For the sake of convenience, we refer to the down dip group of directions as normal polarity, and to the other as reversed polarity. As seen in the inset of Fig. 3, samples from the uppermost stratigraphic position of site 3 and 4 showed normal polarity and the other horizons showed reversed polarity except for an intermediately magnetized sample from the lowermost horizon of site 3 (HYG-132). Consequently, each sequence recorded one or two polarity reversal(s).

In order to understand the origin and significance of the remanent magnetization components of the cherts, magnetic minerals carrying them were identified through two experiments: coercivity spectrum analysis (Dunlop, 1972) and blocking temperature spectrum analysis. An isothermal remanent magnetization (IRM) of a red chert specimen from site 3 was measured in various direct field which was progressively increased up to 1.09 T. IRM acquisition curve for the cherts were characterized by a steep initial increase and a high saturation magnetic field (Fig. 4a). The former indicates presence of magnetite (or titanomagnetite) and the latter does that of hematite (Dunlop, 1972). An IRM magnetized in a direct field of 0.95 T was demagnetized thermally up to 680°C, and its remanence was measured at twelve steps. The result (Fig. 4b) indicates an evident discontinuity of the Tb spectrum at about 580°C. This enables us

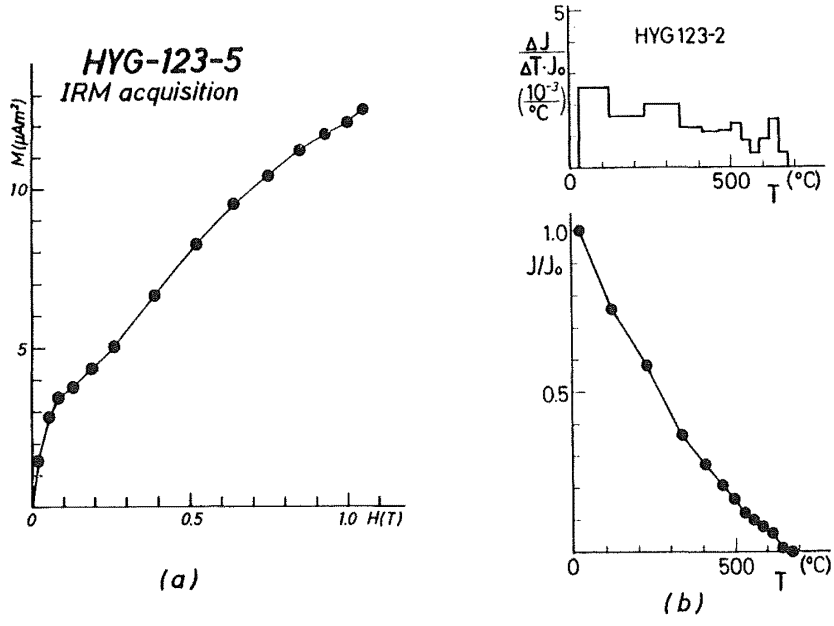

Fig. 4, Diagrams showing (a) acquisition of IRM, and (b) Tb spectrum produced by progressive thermal demagnetization of strong-field IRM (0.95 T) in Triassic red chert specimens from site 3.

to conclude that the red chert contains at least two magnetic minerals whose Curie temperatures, estimated as the highest Tb of each group of the spectrum, are about 560°C and 670°C, which are almost identical to those of magnetite (578°C) and hematite (675°C). The two experiments concerning to the properties of IRM of the cherts clearly show the presence of both magnetite and hematite (They may contain small amount of TiO_2). The Tb spectrums of component C and D of the NRM of the cherts well correspond to each magnetic mineral. The high Tb (550°C-670°C) of component D indicates that it is carried by hematite. Component C with Tb of 380°C-550°C is concluded to be carried by magnetite.

A folding test was performed to determine the order of aquisition of the two stable components (C and D). In the the chert body there exist many intra-formational foldings. One of them at a horizon 15m above site 4 was subjected to this study (site 40 in Fig. 1). The bed was so intensively deformed that both limbs form an angle as large as 120° deflection within a small distance of 70cm. The method of unfolding in this folding test was a rotation of northern limb around the folding axis until the bedding plane become identical to that of the southern limb. Magnetic directions of component C of site 40 were determined through thermal demagnetization at 450°C-580°C. They were well clustered within the site and also similar to those of regularly bedded sites (3 and 4) regardless of the folding (Fig. 5c). On applying the unfolding, component C from both limbs were clearly separated in two directions (Fig. 5d). By contrast, the directions of component D, which was the magnetization surviving after a treatment of 610°C, were different of each limb of the folding (Fig. 5a) and converged on applying the unfolding (Fig. 5b). This

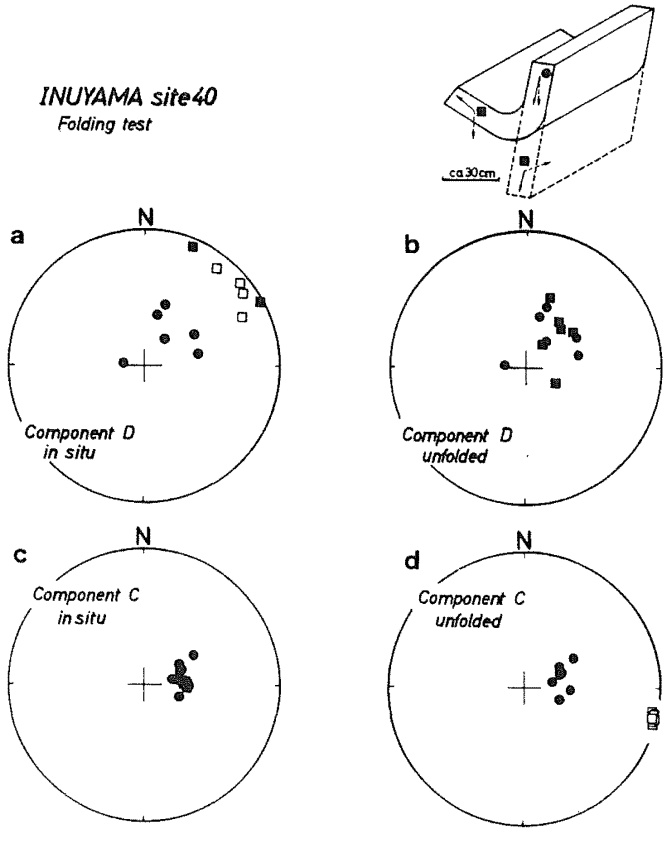

Fig. 5, Equal-area projections of directions of component C and D before and after unfolding the intra-formational folding. Squares and circles represent northern and southern limb of the folding. Open symbols indicate projections onto upper hemisphere and solid ones onto lower hemisphere. Unfolding was performed by a rotation of northern limb around the folding axis until the bedding plane become identical to the southern limb. Therefore, the circles situated in same position on both the diagrams and tilting is not corrected by unfolding procedure.

result clearly determines the order of the aquisition of the two components and the formation of the folding as follows; first, component D was acquired, secondly the intra-formational folding was formed, thirdly component C was acquired.

The acquisition of component D can be assumed to have occurred not simultaneously but sequentially because the red chert sequences have recorded a magnetic reversal. The component predates the intra-formational folding. These two facts suggest that the red chert acquired the magnetization of component D shortly after the deposition. It probably originated from a post-depositional remanent magnetization (p-DRM), or alternatively a CRM due to a diagenetic hematite growth very soon after the deposition, like a acquisition mechanism speculated on red pelagic lime stone from the Gubio section in Italy (Channell, 1982). In either case, the magnetization should have been acquired when the bedding plane was horizontal. This condition is very important to use a paleomagnetic result for tectonic discussion, because one can not perform bedding correction without confirming the condition. The magnetic directions of component D of site 3 and 4 corrected for bedding give a mean inclination of 11°. It indicates that the chert body was formed at equatorial area. (Inclination values presented in Shibuya and Sasajima (1981) should not be refered, because they are proved to be ones for secondary component.)

The two field tests, which prove the component carried by hematite is primary, can be commonly applied to other chert beds. Intra-formational foldings are very common in chert beds. On the other hand, very low depositional rate enable a sequence with a thickness of a few tens of meters to contain several number of magnetic reversals. They serve appropriate criteria to determine whether a component of remanence of certain red chert is primary or not.

References

Chamalaun, F. H. (1964) J. Geophys. Res., **69**, 4327.

Channell, J. E. T. (1982) Earth Planet. Sci. Lett., **58**, 189.

Dunlop, D. J. (1972) Geophys. J. R. astr. Soc., **27**, 37.

Mizutani, S. (1964) J. Earth Sci., Nagoya Univ., **12**, 17.

Otofuji, Y. and T. Matsuda (1983) Earth Planet. Sci. Lett., **62**, 349.

Pessagno, E. A. Jr. and C. D. Blome (1980) Micropaleontology, **26**, 225.

Pullaiah, G., E. Irving, K. L. Buchan and D. J. Dunlop (1975) Earth Planet. Sci. Lett., **28**, 133.

Roy J. L. and P. L. Lapointe (1978) Phys. Earth Planet. Inter., **16**, 20.

Schlager, W. and M. Schlager (1973) Sedimentology, **20**, 65.

Shibuya, H. and S. Sasajima (1980) Rock Mag. Paleogeophys., **7**, 121.

Yao, A., T. Matsuda and Y. Isozaki (1980) J. Geosci., Osaka City Univ. **23**, 135.

Zijderveld, J. D. A. (1967) Methods in Paleomagnetism, edited by D. W. Collinson, K. M. Creer, and S. K. Runcorn, p. 254, Elsevier, New York.

(submitted to J. Geophys. Res.)

GEOTECTONIC HISTORY OF THE JAPANESE ISLANDS INFERRED FROM PALEOMAGNETIC STUDIES

Kimio HIROOKA

Department of Earth Sciences, Faculty of Science, Toyama University

Gofuku, Toyama 930

Paleomagnetism has been acting an important role on the new developments of the earth sciences such as the hypotheses of continental drift and plete tectonics, and also plays the leading part on the current topics of the accretion tectonics. It seemed, therfore, noteworthy to review the paleomagnetic contributions to the geotectonic history of the Japanese Islands.

The bending of the Honshu Island proposed by Kawai et al.(1961, 1962) was the first study which described the geotectonic development of the Japanese Islands by the paleomagnetic results. They examined the paleomagneic direction of the pre-Neogene igneous and sedimentary rocks in the Honshu Island, and found that the declination in the northeastern part of the Honshu deflected towards the west while that in the southwestern part deviated to the east. The difference of the declination amounts to the order of 40° as is shown in Fig.1. On the contrary, the Neogene and the Quaternary volcanic rocks showed parallel directions in the both of northeast and southwest parts. They, therefore, concluded that the Honshu Island which was straight in its shape before Cenozoic was bent at about its central part and the northeastern Honshu was rotated counterclockwisely by an angle more than 40° relative to the southwestern Honshu.

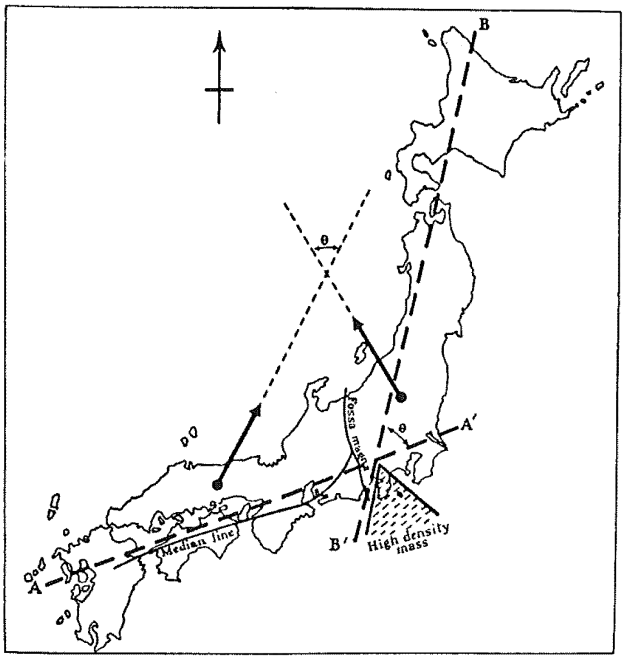

Fig. 1. Pre-Tertiary mean paleomagnetic declinations of the northeast and southwest parts of the Honshu Island (after Kawai et al., 1961).

Ten years later, Kawai et al.(1969, 1971) clarified the timing of the bending by the paleomagnetic measurement of granitic rocks whose radiometric ages were available. Paleomagnetic directions of the both of granitic and sedimentary rocks in the southwestern Honshu show a very good convergence throughout Mesozoic and Paleogene times. On the other hand, magnetic declinations of granitic rocks developed in the northeastern Honshu change from the westerly direction in the early Cretaceous to the easterly in the late Cretaceous as clearly seen in Fig.2. The main rotation occurred twice, one in a range extending from 120 to 115 Ma and then in a range from 100 to 85 Ma.

Shallow inclinations of the Paleozoic rocks were reported by Minato and Fujiwara(1964, 1965). The lower Carboniferous and the lower Permian rocks in the Kitakami Region, northeastern Honshu, show low paleolatitude values. Fujiwara continued the study on the upper Carboniferous in the Akiyoshi Province, southwest Honshu(Fujiwara, 1967) and summerized the paleolatitudes of the Paleozoic and Mesozoic in the Japanese Islands (Fujiwara, 1968). He pointed out that Japan had been situated in the lower latitude of 10° to 20°N during from the upper Carboniferous to the lower Cretaceous as shown in Fig.3.

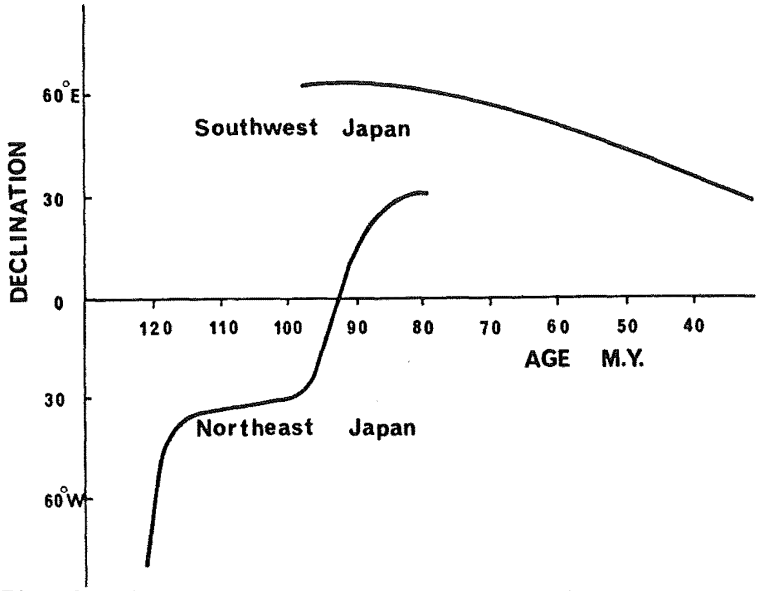

Fig. 2. Change in declination in Japan (after Kawai et al., 1971).

The Eurasian and the north American virtual geomagnetic poles of Cretaceous and Paleogene were located closer to Japan than present. So that the paleomagnetic inclination must be deeper than the present at that time. But the data obtained from the inner side of the southwestern Honshu do not show such deep inclinations. These results imply that the southwestern Honshu had been more south if we take the north American and Russian-Chinese virtual geomagnetic poles as the reference point(Sasajima and Shimada, 1966; Sasajima et al., 1968). Consequently, Sasajima and his colleagues proposed the northward drift of the Southwestern Japan in Paleogene. A clockwise rotation was undergone during the drift. The possible Paleogene position of the southwest Japan was estimated in the east of the present Taiwan Island as shown in Fig.4.

Yaskawa and Nakajima(1972) compared the Cretaceous paleomagnetic data of the southwest Japan with those of Korea. They came to the conclusion as shown in Fig.5, that the drifting of the southwest Japan was not northward but southward relative to the Korean Peninsula. By analysing all the Japanese paleomagnetic data so far reported, Yaskawa(1975) pointed out that the paleolatitude of the northeast Japan was lower than that of the southwest in Mesozoic time, if the bending took place and the northeast Japan rotated around a vertical axis as proposed by Kawai et al.(1971). The Honshu Island could not be a straight bar shape but would be divided into two parts. In order to connect the northeastern and southwestern parts, he proposed that the northeastern part tilted to the east with a horizontal axis of NNW-SSE direction, together with the counterclockwise rotation. Ito and Tokieda(1977) also proposed the tilting to account for the difference of paleomagnetic direction between the northeastern Honshu and the western Hokkaido (Fig.6).

Paleomagnetic data do not provide a unique solution in reconstructing the paleogeography. There are several factors such as drift, rotation, tilting and polar wondering which can be the cause of the magnetic direction change. It is very difficult in many cases to chose the proper causation when we try to reconstruct the paleogeography. The reconstructed position of land masses is depend upon what is emploied as the fixed reference

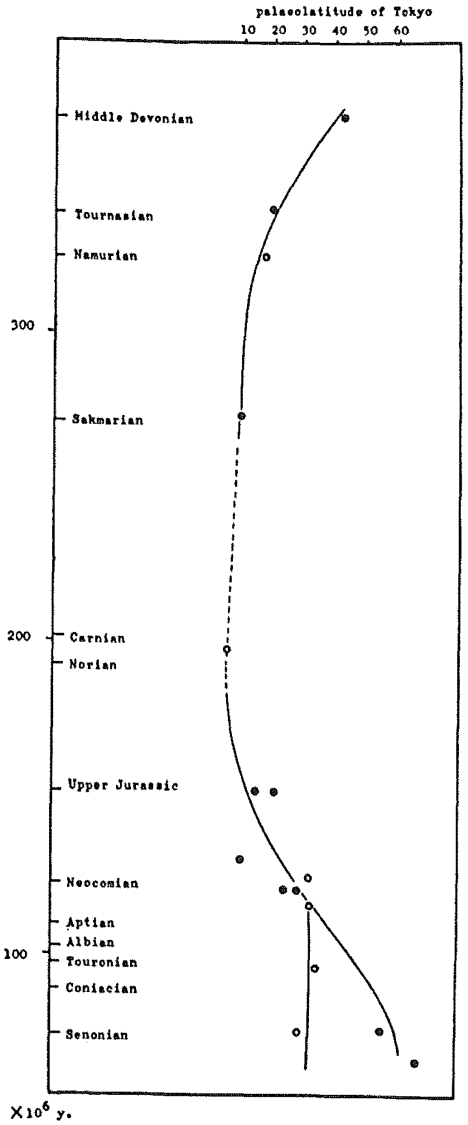

Fig. 3. Change of the paleolatitude of Tokyo through the Paleozoic and Mesozoic (after Fujiwara, 1968).

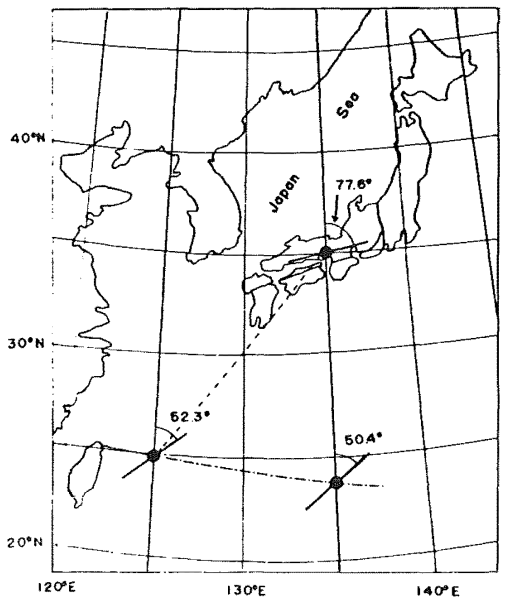

Fig. 4. A schematic view of supposed ancient situations of the southwest Japan (after Sasajima et al., 1968).

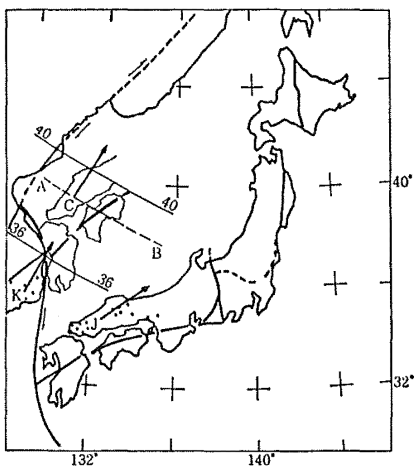

Fig. 5. Cretaceous paleoposition of the southwestJapan (after Yaskawa and Nakajima, 1972)

point.

Ito(1963) found a systematic declination change of Tertiary plutonic bodies cropping out along the east side of the fossa magna which is the major geotectonic line in central Japan as represented in Fig.7. It is clear that the direction of this geotectonic line and the declination are almost parallel. In the central part of the line near Lake Suwa where the direction of the fossa magna is in the northwest-southeast direction, the plutonic body has the westerly declination, while the declination deflect easterly in the northern part where the line curved to the north-northeast direction. He concluded this systematic declination change caused by the plutonic block rotation acompanied by the geotectonic movement which formed the present shape of the

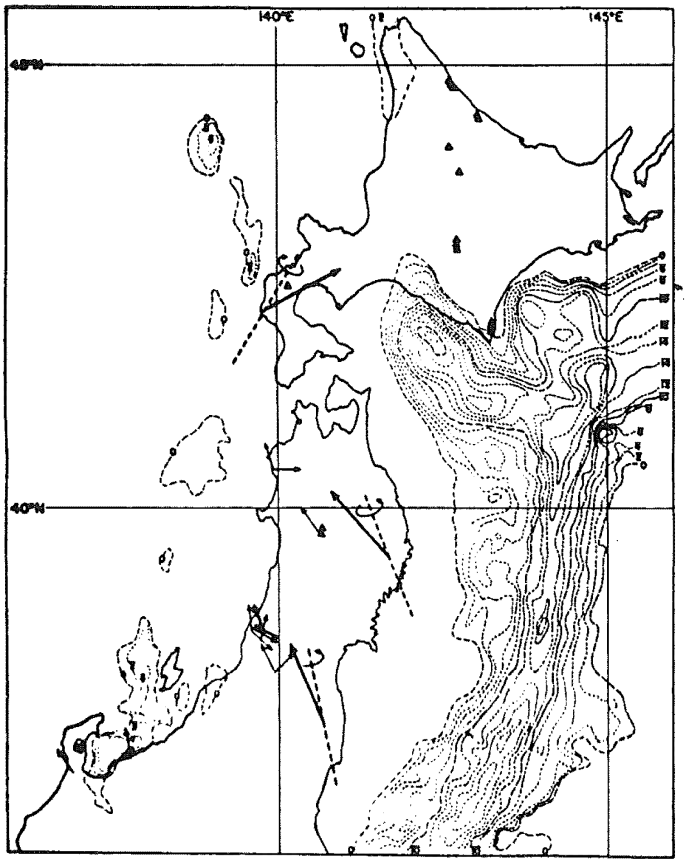

Fig. 6. Schematic tilting direction of the Kitakami Mountainland and the southwestern part of Hokkaido (after Ito and Tokieda, 1977).

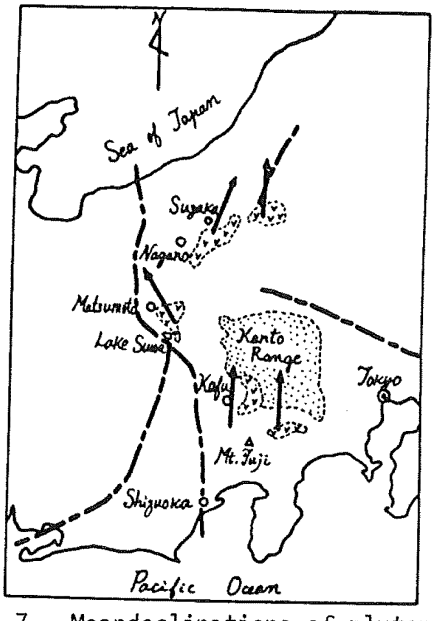

Fig. 7. Meandeclinations of plutonic bodies along the fossa magna (after Ito, 1963).

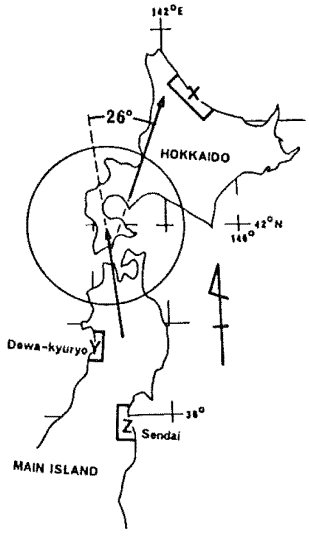

Fig. 8. Mean declination of Neogene and Quaternary volcanic rocks in the northeast Honshu and the west Hokkaido (after Kawai et al., 1972).

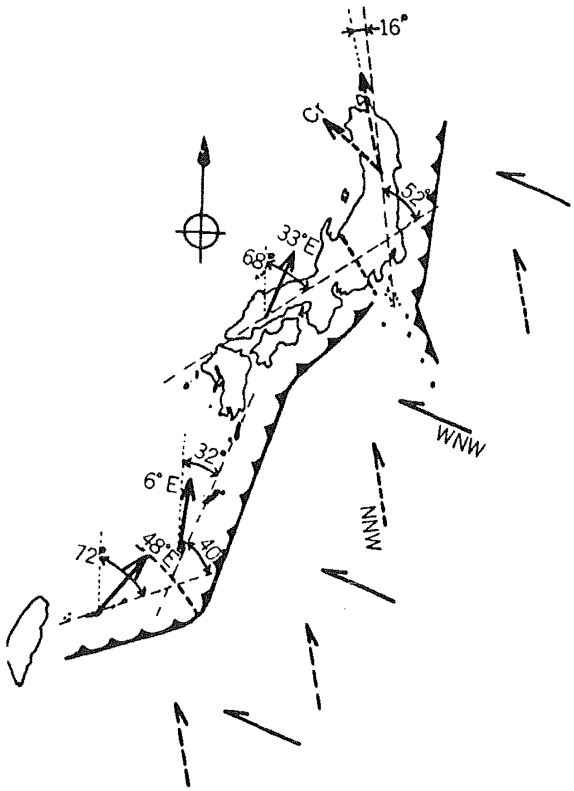

Fig. 9. Schematic tectonic map showing the relation between the Eocene paleomagnetic direction of sub-arcs and trenches (after Sasajima, 1977).

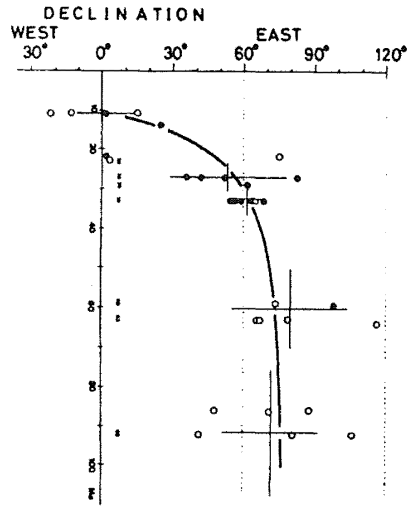

Fig. 10. Site mean declination data as a function of fission-track age together with representative mean direction for five periods (after Otofuji and Matsuda, 1983).

fossa magna.

A clock wise rotation of the southwestern Hokkaido relative to the northeastern Honshu was reported by Kawai et al.(1972). The rotation took place during or after Miocene. Similar rotations are assumed in Island Arcs of the Ryukyu (Sasajima, 1977) and the Mariana (Larson et al., 1975). A clockwise rotation of the southwestern sub-arc in the Ryukyu Arc occurred during Eocene through the earliest Miocene. The rotation of the Guam Island was initiated later than Miocene. Figs.8 and 9 show the relative rotation of the Hokkaido and the Ryukyu Islands.

Recently, Otofuji and Matsuda(1983) proposed that the southwestern Honshu rotated clockwisely by the angle of about 70° in Miocene from paleomagnetic measurements of igneous rocks in Shimane Prefecture, southwest Honshu. They obtained the declination greately deflected towards the east. On the basis of fission-track ages and paleomagneic declination, it is clarified that the motion of the clockwise rotation of 58 ± 4° took place later than 28 Ma and terminated around 12 Ma (Fig.10). They concluded that the rotational motion was associated with the opening of the Japan Sea Basin.

Such paleomagnetic studies on the local geotectonic rotation imply that the detectable geotectonic movements of the Japanese Islands have been continued until Miocene. Fig.11 is showing the paleomagnetic declinations of the southaest Asia summerized by Jarrard and Sasajima(1980). It is obvious that the declination of island arcs changes its direction as the axial direction of arcs changes. This fact suggests that the bow shape

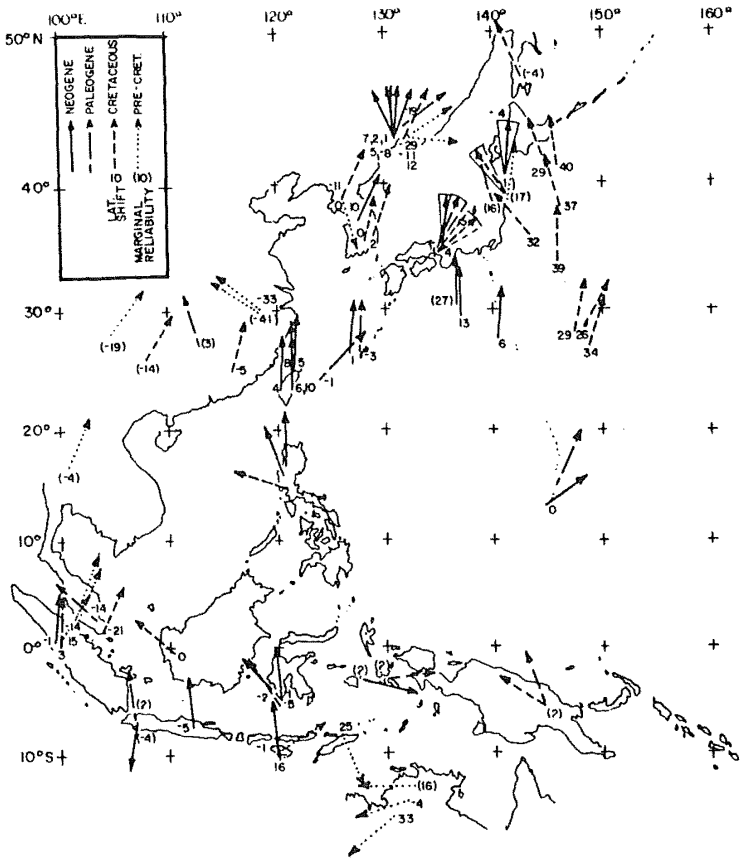

Fig. 11. Paleomagneitc results from Southeast Asia (after Jarrard and Sasajima, 1980).

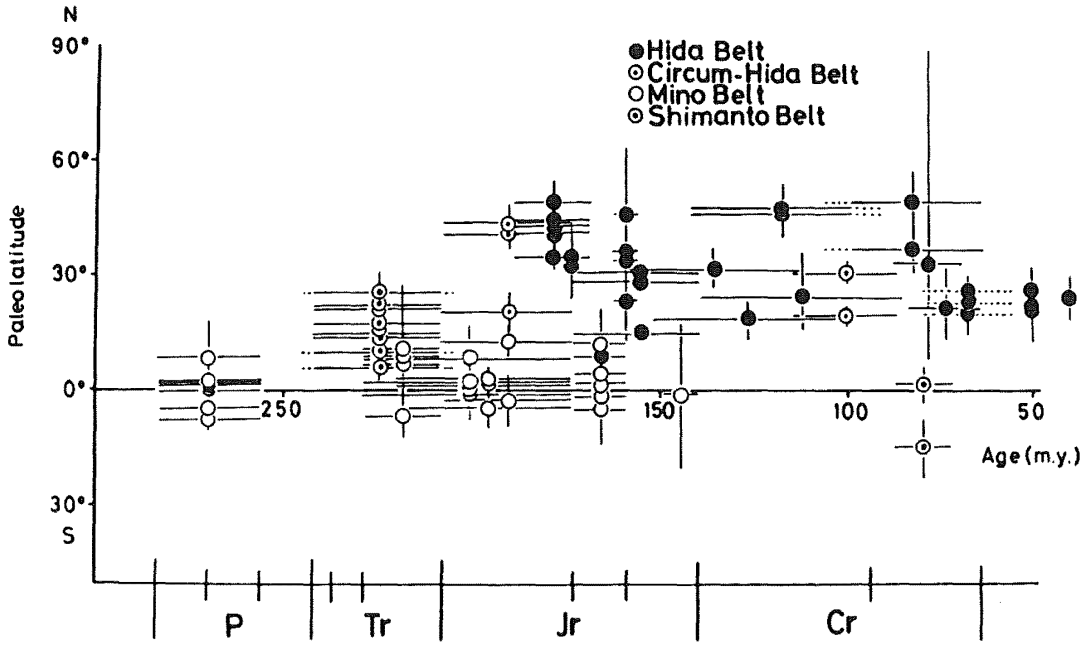

Fig. 12. Paleolatitude of the Hida, the Circum-Hida, and the Shimanto Belts in central Japan (after Hirooka et al., 1983b).

of all the arcs was formed after the rocks were magnetized.

The low paleolatitude of Paleozoic and Mesozoic times was confirmed by measurements of sediments and greenstones in the Mino Belt. Hattori and Hirooka(1977, 1979) carried out the paleomagnetic study on the Permian greenstones in the Mino Belt, central Japan. All of the results show very shallow inclinations. These rocks, therefore, considered to have been formed in the equatorial region. In the central part of Japan, Hirooka et al.(1983a, 1983b) studied the paleomagnetism of the Hida, the Circum-Hida, the Mino and the Shimanto Belts. Although the paleolatitude of the Hida Belt is almost the same as the present latitude since Jurassic, the rest of the belts show the paleolatitudes of the equatorial region as is clearly seen in Fig.12. From the figure, the following geotectonic history of the central Japan can be drawn. All of the geotectonic belts except the Hida Belt were formed in the equatorial region. Then the teranes of respective belts were migrated to the north until they collided with the Hida Belt, and finally accreted to it during Jurassic and Cretaceous.

References

Fujiwara, Y. (1967) J. Fac. Sci. Hokkaido Univ., Ser.IV, 13, 395.

Fujiwara, Y. (1968) J. Fac. Sci. Hokkaido Univ., Ser.IV, 14, 159.

Hattori, I. and K. Hirooka (1977) J. Japan Assoc. Min. Pet. Econ. Geol., 72, 340.

Hattori, I. and K. Hirooka (1979) Tectonophys., 57, 211.

Hirooka, K., T. Nakajima, H. Sakai, T. Date, K. Nittamach and I. Hattori (1983a)Accretion Tectonics in the Circum-Pacific Regions, ed. Hashimoto and Uyeda (TERAPUB, Tokyo) p.179.

Hirooka, K., S. Uchiyama, T. Date, H. Kanai, I. Hattori and T. Nakajima (1983b) Stanford Univ. Pub., Geol. Sci., Abstract vol. XVIII, (in press).

Ito, H. (1963) J. Geomag. Geoelectr., 15, 37.

Ito, H. and K. Tokieda (1977) Rock Mag. Pleogeophys., 4, 118.

Jarrard, R.D. and S. Sasajima (1980) The Tectonic and Geologic Evolution of Southeast Asian Seas and Islands, ed. Hayes (AGU, Washington) p.293.

Kawai, N., H. Ito and S. Kume (1961) Geophys. J. Roy. Astr. Soc., 6, 124.

Kawai, N., S. Kume and H. Ito (1962) J. Geomag. Geoelectr., 13, 150.

Kawai, N., K. Hirooka and T. Nakajima (1969) Palaeogeography, Palaeolimnol., Palaeoecol., 6, 277.

Kawai, N., T. Nakajima and K. Hirooka (1971) J. Geomag. Geoelectr., 23, 267.

Kawai, N., T. Nakajima, M. Torii, K. Hirooka, K. Yaskawa (1971) J. Geomag. Geoelectr., 23, 243.

Larson, E.E., R.L. Reynolds, M. Ozima, Y. Aoki, H. Kinoshita, S. Zasshu, N. Kawai, T. Nakajima, K. Hirooka, R. Merrill and S. Levi (1975) Geol. Soc. Amer. Bull., 86, 346.

Minato, M. and Y. Fujiwara (1964) Proc. Japan Acad., 40, 116.

Minato, M. and Y. Fujiwara (1965) Earth Science (Chikyu Kagaku), no.78, 21.

Otofuji, Y. and T. Matsuda (1983) Earth Planet. Sci. Lett., 62, 349.

Sasajima, S. (1977) Rock Mag. Paleogeophys., 4, 108.

Sasajima, S. and M. Shimada (1966) J. Geol. Soc. Japan, 72, 503 (in Japanese).

Sasajima, S., J. Nishida and M. Shimada (1968) Earth Planet. Sci. Lett., 5, 135.

Yaskawa, K. (1975) Geophys. J. Roy. Astr. Soc., 43, 835.

Yaskawa, K. and T. Nakajima (1972) Kagaku (Science), 42, 163 (in Japanese).

CLOCKWISE ROTATION OF SUMATRA IN QUATERNARY PERIOD

Takuo YOKOYAMA* and Agus DHARMA**

* Department of Earth Science, Doshisha University, Kyoto, Japan
** National Institute of Geology and Mineralogy, LIPI, Bandung, Indonesia

Introduction

Present situation of the Sumatra Island seems to indicate the clockwise rotation of about 40 degrees for Jawa. Ninkovich (1976) proposed a hypothesis that in the Late Cenozoic Sumatra rotated clockwise about 20 degrees and formed the present configuration. Moreover, Sasajima et al. (1980) said that after the Triassic until the Early Tertiary, Sumatra should have rotated clockwise by 62.4°. They said this conclusion contradicts Ninkovich's speculation.

In this work, the samples for paleomagnetic measurements were taken from Banten and Maling Ping Tuffs, and from andesite, basalt and welded tuff in Sibuk Island and South Sumatra (Fig. 1). This work is a part of the cooperative work between Kyoto University and LGPN, LIPI, Bandung and of the paper by Yokoyama et al. (1983). Based on these data, it may be clarified that Sumatra has been rotated about 10 degrees in last 2.0 my. and this movement continues up to recent.

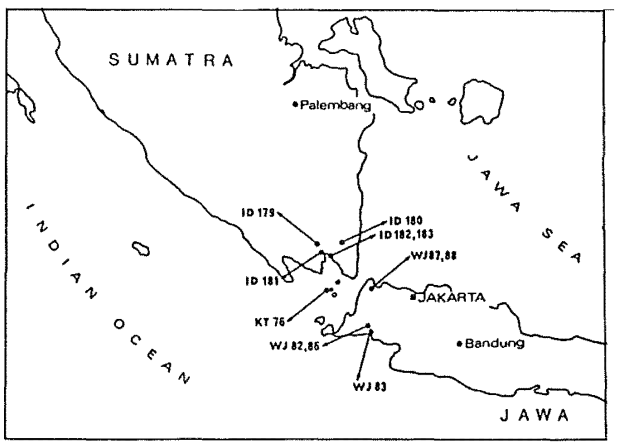

Fig.1 Sampling point

Paleomagnetism

The paleomagnetic samples were prepared into suitable specimens and mounted in cubic plastic boxes of 2 x 2 x 2 cm in the laboratory. The NRMs of specimens were measured by the Dijico spinner magnetometer in Doshisha University and the Schonstedt spinner magnetometer in Kyoto University. After the first measurement, a few pilot specimens were demagnetized in the alternation field with the peak fields of 50, 100, 150, 200, 250, 300, 400, and 500 Oe progressively. After that all specimens were demagnetized in the most suitable peak field, based on the intensity change of the pilot specimen. Some pilot samples were measured after 600 Oe damagnetization.

The changes of NRM direction through progressive demagnetizations are also shown in Fig. 2. Consequently, all specimens were demagnetized in a peak field of higher than 100 Oe, to avoid the influence of secondary soft component and to

obtain the reliable direction of NRMs.

In Jawa, as shown in Fig. 2 and Table 1, all specimens collected from Banten and Maling Ping Tuffs were normally magnetized, while samples obtained from old Quaternary Lava (WJ 83) were reversely magnetized. The specimens from Sibuk Island are normally magnetized. In Sumatra, all specimens from three sites are normally magnetized.

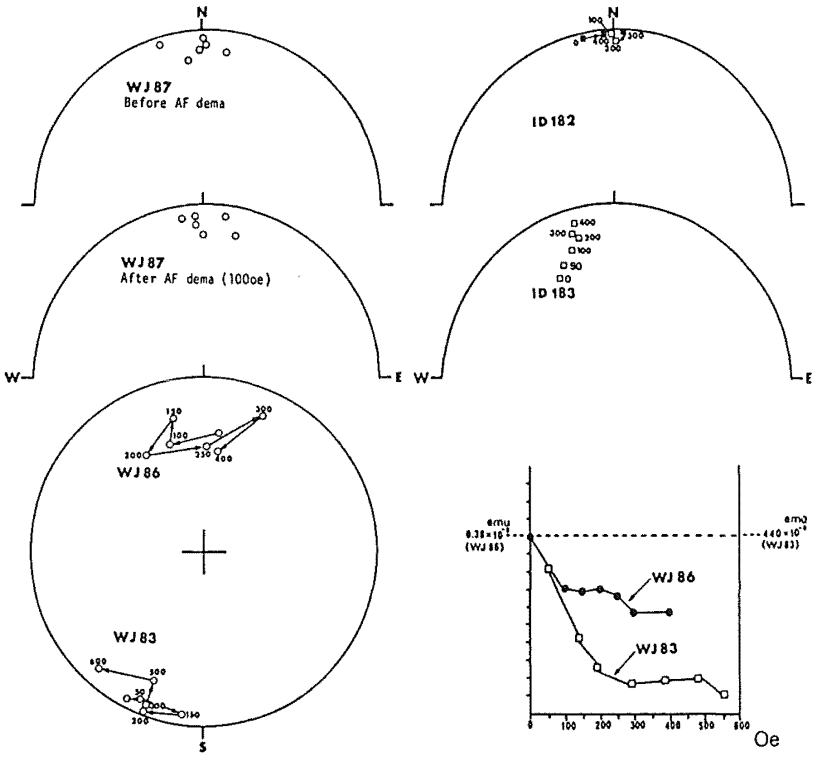

Fig.2 Result of stepwise AF-demagnetization of some pilot specimens

Discussion

(1) Geologic age

Banten and Maling Ping Tuffs in West Jawa: These beds surely belong to the Brunhes Normal Epoch in magnetostratigraphy, because of their normal polarities and fission-track age (0.1 ± 0.02 my. ; Nishimura et al., 1982). But as pointed out by Bemmelen (1970), these series are intercalated with some marine layers in a few horizons. As marine transgressions of glacial eustacy had been taken place generally at the interval of about 100 thousand years, the time range of these series may be rather long, about 0.3 - 0.4 my. Consequently, the geologic age of these series are late Pleistocene, not to be Pliocene in Bemmelen (1970).

Sukadana Basalt in Sumatra: Though the K-Ar age of this basalt in 0.80 my., the paleomagnetic polarity is normal (ID 180). It may belong to the early Brunhes Normal Epoch, that is 0.6 - 0.7 my. ago because this basalt layers are younger than the

Table 1. Results of Paleomagnetic Measurement

Site Number	Sample (material)	H(Oe)	Mean D(°)	Mean I(°)	N	K	α_{95}	VGP ϕ	VGP λ	Polarity
< West Jawa >										
WJ82	Ash flow (Maling Ping Tuff)	100	347.7	-33.5	2	252.6	15.7	73.9	332.9	N
WJ83	Lava	300	209.0	-4.5	3	80.3	13.8	-59.4	358.9	R
WJ86	Ash flow (Banten Tuff)	150	344.9	-27.2	4	8.6	18.2	73.7	350.0	N
WJ87	Pumice flow (Banten Tuff)	100	359.7	-10.7	6	84.8	7.3	89.3	84.3	N
WJ88	Pumice flow (Banten Tuff)	100	355.1	-14.3	3			85.0	0.9	N
< Sibuk Island >										
KT76	Lava	250	352.3	-8.4	4	102.6	13.2			N
< Sumatra >										
ID180	Basalt	200	9.8	-40.4	11		2.9	69.6	101.2	N
ID182	Ash flow (Lampong Tuff)	200	359.7	-2.7	3		11.1			N
ID183	Ash flow (Lampong Tuff)	100	340.1	-22.4	3		4.1			N

H: Demagnetizing field in Oersted. D: Declination(in degrees eastward). I: Inclination(in degrees downward). N: Specimen number. K and α_{95}: Precision parameter and radius of 95% confidence circle in degrees(Fisher, 1953). ϕ and λ: Latitude and longitude of virtual geomagnetic pole in degrees north and east, respectively. N and R in polarity column indicate paleomagnetic polarity of normal(N) and reverse(R) for each site.

Upper Palembang Beds (1.0 ± 0.22 my. ; Nishimura et al., 1982) in the stratigraphic investigation (Bemmelen, 1970).
Lampong Tuff: As the fission-track age of this tuff is obtained to be 1.0 ± 0.22 my. (Nishimura et al., 1982) and the polarity data are normal (Table 1), the Lampong Tuff may belong to the Jaramillo Event (0.95 ± 0.4 my.) in Matsuyama Reversed Epoch (0.73 - 2.43 my. by Mankinen and Darlymple, 1979).

(2) Neotectonics

For the purpose of discussion about the rotation of Sumatra and Jawa Islands in last 2.0 my., destribution of the declination value of the Quaternary Rocks was summrized in Fig. 3.

Data having the smaller value of α_{95} than 20.0 (from Hirooka et al. (1980), Yokoyama et al. (1980 a - c), Sasajima et al. (1980), Yokoyama & Dharma (1984), this work and our unpublished data) were selected to make this figure. As given in Fig. 3, the declination of specimens in Sumatra generally has eastward direction, while that in Jawa is westward direction. Although obtained data are not many for discussion, the declination value in Sumatra Island became larger to the older age, up to 2.0 my. ago. If the change of this declination value due to the rotation of Sumatra Island, these data maintain the hypothesis taht Sumatra Island has been rotating clockwise for Jawa Island from 2.0 my. ago to present.

Its angle speed of the clockwise rotation is between A and B line in Fig. 3 (0.5 - 1°/ 10 x 10^6 years). Of course, present data are not so many that this hypothesis must be checked by more measurements of paleomagnetism and age dating in future.

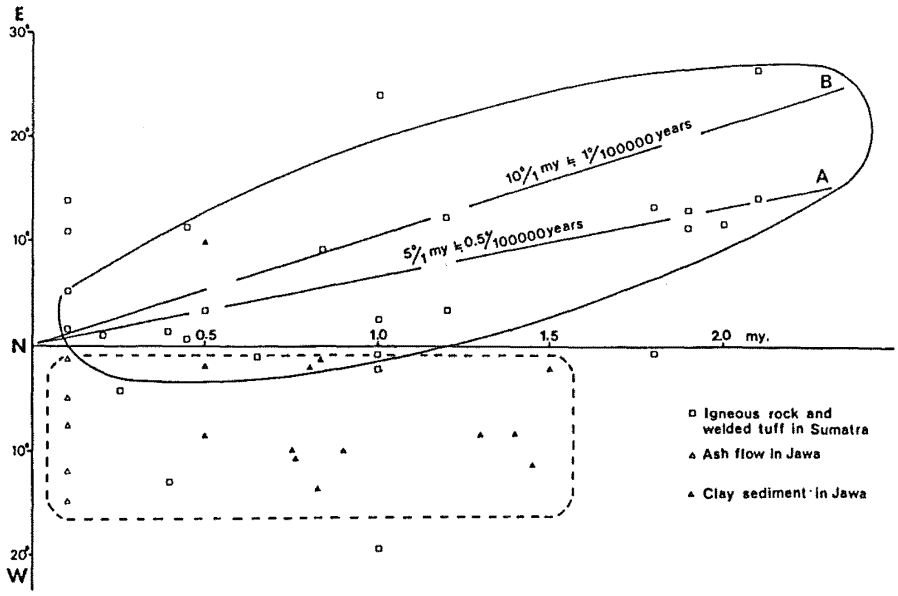

Fig.3 Relationship of declination values and their ages of Quaternary rocks around Sunda Strait

References

Bemmelen, R.W.V. (1970); The geology of Indonesia. 2nd ed., Governmental Printing Office, the Hague.

Hirooka, K., Otofuji, Y., Sasajima, S., Nishimura, S., Matsuda, Y., Thio, K.H., Dharma, A. and Hehuwat, F. (1980); Phys. Geol. Indonesian Island Arcs, 67-71.

Mankinen, E.A. and Dalrymple, G.B. (1979); Jour. Geophys. Res., 84, 615-626.

Ninkovich, D. (1976); Ear. Planet. Sci. Let., 29, 269-275.

Nishimura, S., Nishida, J., Ikeda, T. and Tamada, O. (1982); Tsukumo Earth Sci., 17, 64-77.

Sasajima, S., Nishimura, S., Hirooka, K., Otofuji, Y., Leeuwen, T.V. and Hehuwat, F. (1980); Phys. Geol. Indonesian Island Arcs, 13-22.

Yokoyama, T., Nishimura, S., Abe, E., Otofuji, Y., Ikeda, T., Suparka, S. and Dharma, A. (1980a); Phys. Geol. Indonesian Island Arcs, 122-143.

Yokoyama, T., Hantoro, W.S., Hadiwisastra, S., Matsuda, T. and Nishimura, S. (1980b); Riset. 1-7.

Yokoyama, T., Hadiwisastra, S., Hayashida, A. and Hantoro, W. (1980c); Phys. Geol. Indonesian Island Arcs, 88-96.

Yokoyama, T., Dharma, A., Hirooka, K. and Nishimura, S. (1983); Report in Sym. 100 year dev. Krakatau, Jakarta.

Yokoyama, T. and Dharma, A. (1984); United Nations ECAFE, CCOP. Tech. Bull., 14, in press.

PALEOMAGNETISM OF NEOGENE OCROS DIKE SWARM NEAR AYACUCHO, PERUVIAN ANDES

Kosuke HEKI[1], Yozo HAMANO[1], Masaru KONO[2] and Tadahide UI[3]

1.Geophysical Institute, University of Tokyo, Yayoi 2-11-16, Bunkyo-ku, Tokyo 113.
2.Department of Applied Physics, Tokyo Institute of Technology, Ookayama 2-12-1, Meguro-ku, Tokyo 152.
3.Department of Earth Sciences, Kobe University, Rokkodai-machi 1-1, Nada-ku, Kobe, Hyogo 657.

1) Introduction

Paleomagnetic studies on the rocks of the Peruvian Andes and the northernmost Chile have revealed post-Cretaceous oroclinal bending (Carey, 1955) of the Central Andes around an axis at the Peru-Chile border (Heki et al., 1983; Heki, 1983). It was also showed that Tertiary Ocros dike swarm shows about a half of the rotation angle of those of Mesozoic rocks. Recently, Hayashida et al. (in press) reported the counterclockwisely deflected declination of the Eocene red sediments of Salla Group in the Bolivian Altiplano and suggested the occurrence of the bending to be after the Eocene. Such Tertiary paleomagnetic studies will reveal the detailed chronology of the bending of the Central Andes. Here we report the full paleomagnetic description of Ocros dike swarm.

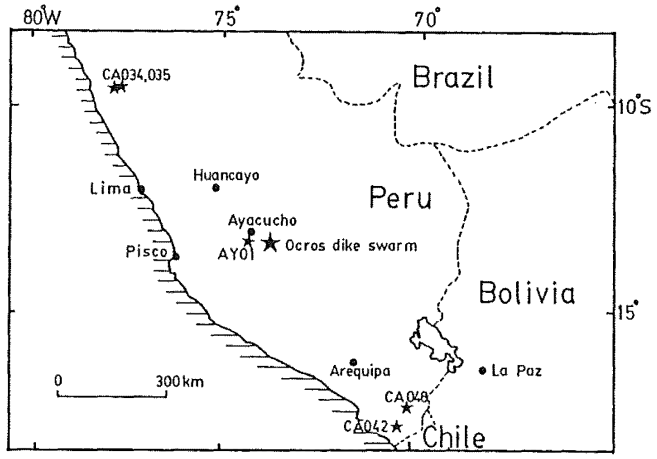

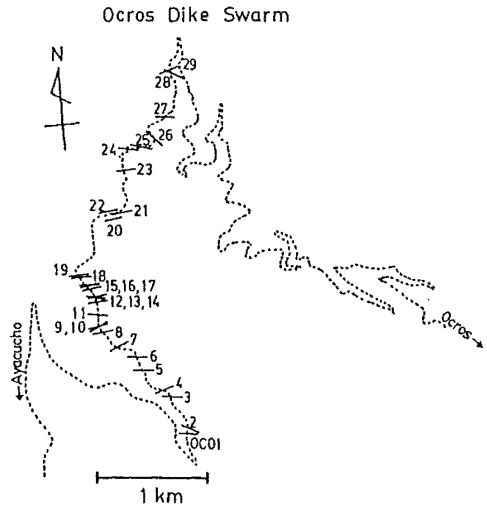

Fig.1 Sampling site of Ocros dike swarm. Direction of the bar indicates the strike of the dike.

2) Geology

Upper Cretaceous to Quaternary volcanic formations are widely distributed in Peru over the highland of the Cordillera Occidental (Western Cordillera). These formations are composed of lava flows, volcanic breccias, agglometes and tuffs and their compositions are mostly andesitic. These are divided into several stratigraphical groups from their degrees of the influences of the compressive pulses in the Andean orogeny. The youngest volcanic formations which were formed after the last compressive deformation (Quechuan orogeny; Bellido, 1979) is generically called Barosso Group. Plio-Pleistocene age is assigned to these volcanics but radiometric age determination studies often revealed that even the volcanic rocks whose ages were assumed to be Quaternary show the age of the Upper Miocene (Bellon and Lefèvre, 1976; Kaneoka and Guevara, 1983). This implies the importance of radiometric age determinations on these rocks.

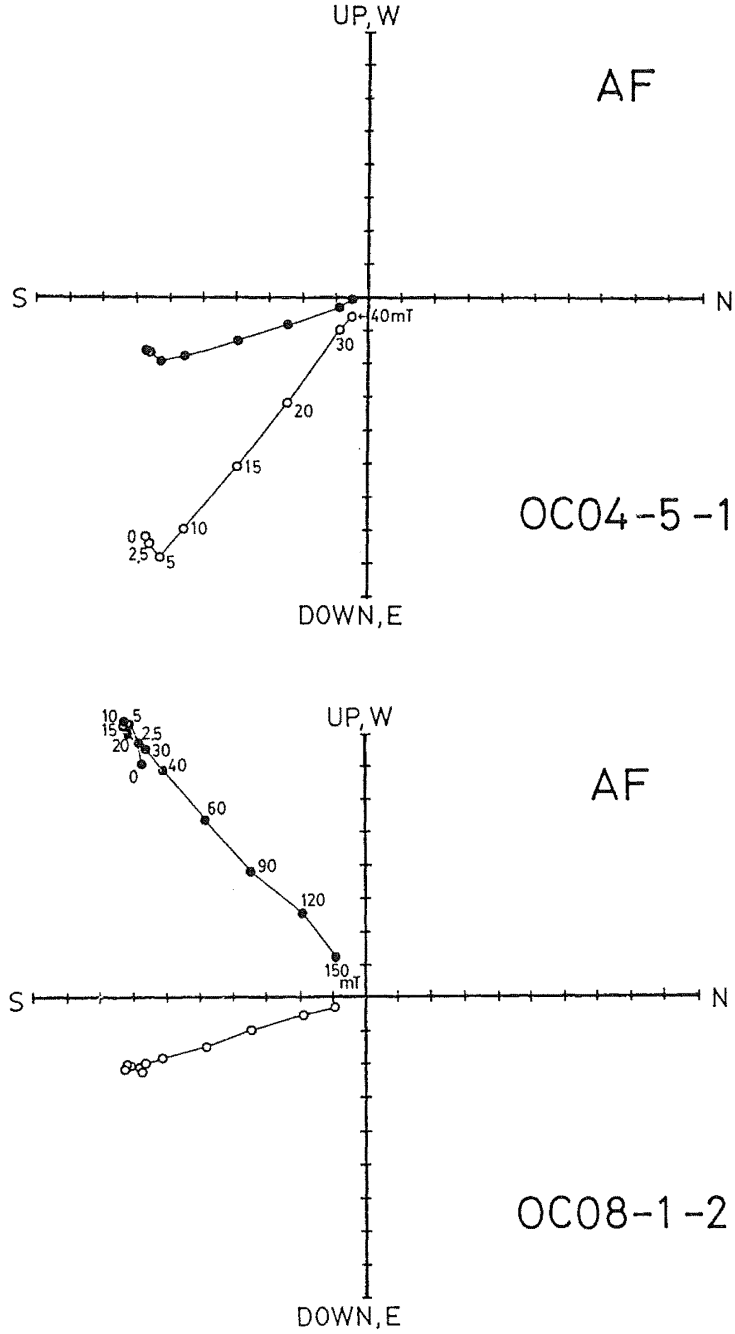

Fig.2 Zijderveld diagrams in AF demagnetization of the specimens of Ocros dike swarm. Open and solid symbols indicate projections onto vertical and horizontal planes respectively.

A dike swarm was found within a volcanic formation which is described as Barosso Group (Bellido, 1979) (Fig.1). The sampling route spans about 4km extending approximately north to south, along which we collected about two hundred oriented samples from 29 dikes intruding into alternation of lavas and pyroclastics (Fig.1, OC01-29). At several sites (OC03,05,06) lava flows adjacent to the dikes were also sampled. General trend of the dikes is N80°E which is consistent with present direction of maximum horizontal stress axis determined by focal mechanism solution of earthquakes in central and northern Peru (Stauder, 1975). Although Peruvian geologic map indicates Plio-Pleistocene age of the formation, our preliminary K-Ar dating suggested slightly older age, say Late Miocene (6-8Ma). Detailed geologic and petrologic descriptions are given in Ui et al. (1983).

3) Experimental Procedures

A Schonstedt spinner magnetometer in University of Tokyo was used for paleomagnetic measurements and alternating field (AF) demagnetization was carried out on each specimen stepwisely as far as most part of the original remanence was destroyed. NRM intensity ranged from 10^{-4} to 10^{-2} Am^2/kg. NRM directions are fairly stable against AF demagnetization and median destructive fields (MDF) in most cases were more than 20mT. In Fig.2 are shown demagnetization diagrams (Zijderveld, 1967) of typical specimens. Paleomagnetic field direction was determined as the gradient of the linear portion of the diagrams by least square fitting. Thermomagnetic analyses were performed on several specimens using an automatic Curie balance and approximately reversible Js-T curves were obtained with Curie temperatures mainly of magnetite (580°C). Initial susceptibility was measured using Bison AC bridge and natural Königsberger ratios (Qn ratio) were calculated to be ranging from 2 to more than 100. Susceptibility anisotropy measured by spinner magnetometer yielded no serious values as to affect the remanent magnetization directions.

4) Results and discussion

All paleomagnetic results are listed in Table 1 and illustrated with 95% confidence circles (Fisher, 1953) in Fig.3. We got four normal polarity dikes (OC12,15,16,17) and twenty-one reversed polarity dikes and lavas (OC01-07,13,14,18,22-29) which are almost antipodal and deviate counterclockwisely in its mean declination by about 15° from axial geocentric dipole field. Seven intermediate polarity dikes (OC08-11, 19-21) were also found. The angular standard deviation (ASD) was calculated using twenty-five normal and reversed polarity VGPs which are converted to a single polarity. The contribution of the within-site dispersion to the total ASD was corrected and the between-site ASD was isolated. The 95% confidence interval of the ASD was calculated from the table presented by Cox (1969). We got an ASD of 14.2° with the 95% confidence interval of 11.9°-17.7°. The ASD of Ocros dike swarm shows good agreement with global trend of Plio-Pleistocene ASD presented in McElhinny and Merrill(1975).

There are two groups in intermediate polarity dikes, that

Table 1. Paleomagnetic directional data of Ocros dike swarm.

Dike (lava)	N	Incl.** (°)	Decl.** (°)	R	k	α_{95} (°)	Pole Lat. (°N)	Pole Long. (°E)
OC01	4	3.9	176.5	3.9786	242	5.9	-78.0	88.9
OC02	6	0.8	-163.1	5.9209	63	8.5	-68.8	159.6
OC03	6	52.5	160.3	5.8739	40	10.8	-63.4	-34.9
OC03*	6	44.8	168.5	5.9649	142	5.6	-73.1	-36.0
OC04	5	42.4	179.3	4.8687	31	14.1	-78.8	-70.7
OC05	6	32.4	164.7	5.9578	118	6.2	-74.7	-1.8
OC05*	13	32.0	174.0	12.8808	101	4.2	-83.0	-18.6
OC06	6	24.7	170.2	5.8422	32	12.1	-80.5	17.6
OC06*	5	39.4	172.9	4.9244	53	10.6	-78.8	-37.9
OC07	6	17.5	164.4	5.9724	181	5.0	-74.1	30.6
OC08	5	17.2	-120.6	4.7201	14	20.9	-31.7	-161.8
OC09	6	13.1	-140.2	5.8151	27	13.1	-50.3	-169.7
OC10	6	9.5	-125.5	5.9375	80	7.5	-35.6	-167.7
OC11	6	8.8	-108.6	5.9755	204	4.7	-19.1	-163.9
OC12	6	-36.4	-32.5	5.9611	129	5.9	58.2	179.2
OC13	6	34.4	154.9	5.9335	75	7.8	-65.3	-0.1
OC14	6	34.6	167.7	5.9420	86	7.3	-76.9	-11.1
OC15	7	-34.6	-21.6	6.9315	88	6.5	68.5	178.0
OC16	6	-38.6	-30.7	5.9482	97	6.9	59.6	175.7
OC17	6	-41.6	-32.9	5.9043	52	9.4	57.2	172.5
OC18	7	38.4	-179.6	6.9192	74	7.1	-81.8	-76.6
OC19	4	-79.5	-37.0	3.8513	20	21.0	29.2	119.9
OC20	5	-75.4	-43.0	4.8872	36	13.0	32.3	127.9
OC21	6	-74.2	2.1	5.8976	49	9.7	42.9	104.6
OC22	6	31.2	150.5	5.9762	210	4.6	-61.3	5.4
OC23	6	43.8	176.1	5.9440	89	7.1	-77.2	-57.8
OC24	6	2.9	176.3	5.9655	145	5.6	-77.5	88.7
OC25	6	1.3	169.3	5.9709	172	5.1	-73.4	65.5
OC26	3	35.4	160.3	2.9963	545	5.3	-70.2	-4.7
OC27	5	41.9	168.1	4.9908	434	3.7	-74.4	-29.4
OC28	7	22.1	157.9	6.9487	117	5.6	-68.3	18.7
OC29	8	20.7	152.0	7.9520	146	4.6	-62.5	18.6

N:number of samples studied, R:length of resultant vector, k:precision parameter (Fisher, 1953), α_{95}:radius of 95% confidence circle.

**All directions are determined by least square fitting to the demagnetization diagram.

*lava flows (the others are dikes).

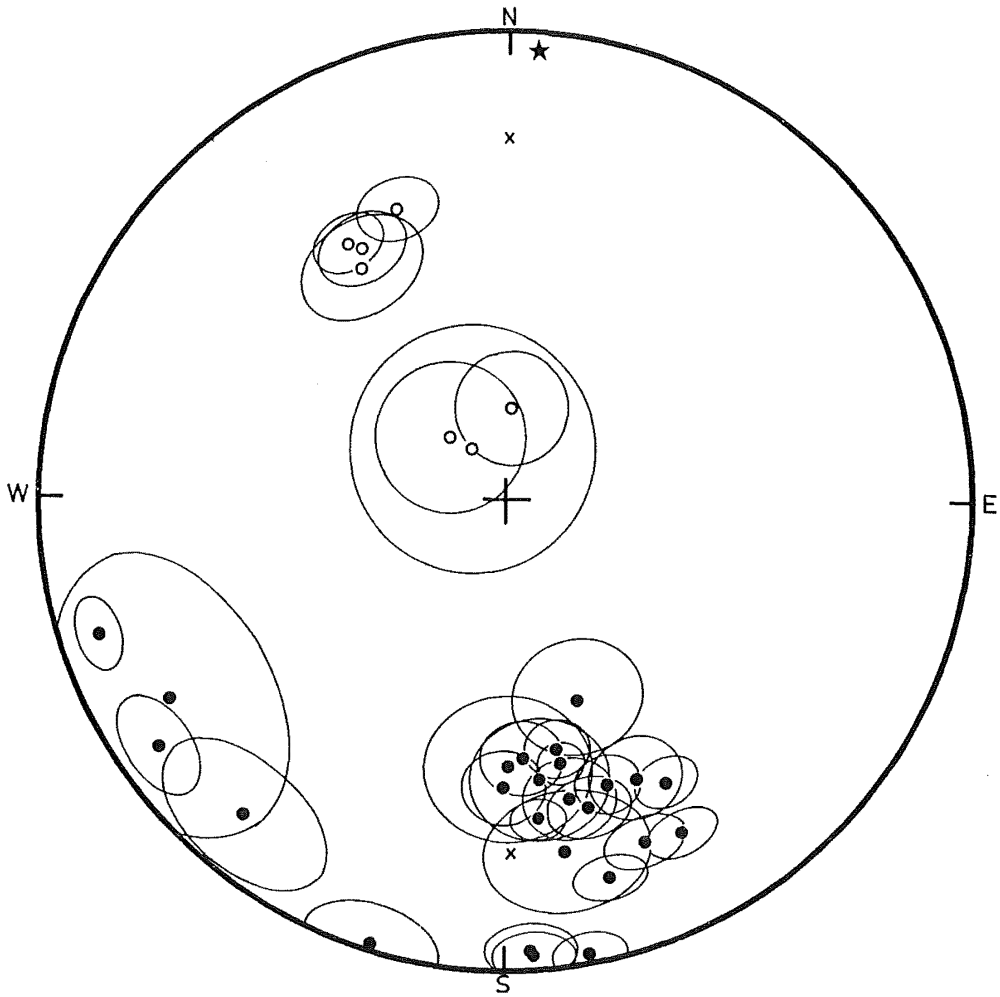

Fig.3 Equal area projection of dike-mean field directions of Ocros dike swarm. 95% confidence circles are also illustrated. Open and solid symbols denote negative and positive inclinations respectively. Star indicates present field direction and X indicates present axial dipole field.

is, almost horizontal and west-southwest seeking dikes (OC08,09,10,11) and almost vertical and upward seeking dikes (OC19,20,21). The former corresponds to VGP transition path to the west of the site about 90° apart and the latter corresponds to far-sided transition path. There are many short polarity events in Late Miocene time (e.g., La Brecque et al., 1977) and whether these two groups belong to a single polarity transition or represent multiple polarity transitions is unknown with present data only. It is, however, quite interesting that definite far-sided transitional VGPs were observed in southern hemisphere sites.

Dipole hypothesis predicts that geomagnetic field almost

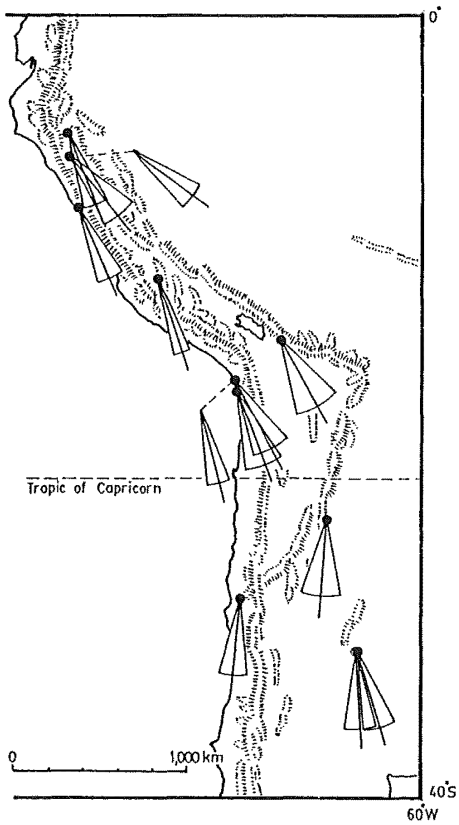

Fig.4 Rotations observed in the Central Andes after Heki (1983).

coincides with that of an axial and almost geocentric dipole when being averaged over a certain time range covering the whole periods of secular variation. Mean field direction obtained from Ocros dike swarm show about 15° of counterclockwise declination shift although paleosecular variation seems sufficient (ASD=14.1°) as to include the whole periods of secular variation. Paleomagnetic study of late Tertiary age in other area does not show a paleomagnetic pole significantly different from today's geographic pole (Creer and Valencio, 1969; Valencio et al., 1975) and this declination shift appears to be the results of the tectonic rotation of the region of Ocros dike swarm. It is also possible to explain it by assuming some undetected tilt. However, in order to convert axial dipole field direction to that of Ocros mean field, nearly 30° westward dip with a strike of N30°W is necessary. Observed contacts of Ocros dikes are almost vertical and so Plio-Pleistocene tilting up to 30° is quite unlikely.

It is more plausible to interpret that the large-area counterclockwise rotation is responsible for the declination shift. As already shown in Heki et al. (1983), paleomagnetic results suggest post-Cretaceous occurrence of oroclinal bending of the Central Andes (Fig.4). Paleomagnetic results of Ocros dike swarm give a strong constraint to the timing of the bending that about a half amount of the rotation still occurred after the time of the intrusion of Ocros dike swarm.

References

Bellido, B. E. (1979) Instituto Geologico Minero y Metalurgico Bol., 22, p55.

Bellon, H. and C. Lefèvre (1976) C. R. Acad. Sci., Ser. D., 283, 1.

Carey, S. W. (1955) Proc. R. Soc. Tasmania, 89, 255-288.

Cox, A. (1969) Geophys. J. R. astr. Soc., 18, 545-549.

Creer, K. M. and D. A. Valencio, (1969) Geophys. J. R. astr. Soc., 19, 113-146.

Fisher, R. A., (1953) Proc. R. Soc. London, Ser. A, 217, 295-306.
Hayashida, A., Y. Nogami, L. A. Rodrigo and A. Saavedra, in Kyoto University Overseas Research Report of New World Monkeys, Kyoto University Primate Reseach Institute, in press.
Heki, K. (1983) Doctoral thesis, Faculty of Science, University of Tokyo.
Heki, K., Y. Hamano and M. Kono (1983) Nature, 305, 514-516.
Kaneoka, I. and C. Guevara (1983) submitted to Geochem. J..
La Brecque, J. L., D. V. Kent and S. C. Cande, (1977) Geology, 5, 330-335.
McElhinny, M. W. and R. T. Merrill (1975) Rev. Geophys. Space Phys., 13, 687-701.
Stauder, W., (1975) J. Geophys. Res., 80, 1053-1064.
Ui, T., M. Kono, Y. Hamano and F. Monge (1983) submitted to J. Volcanol. Soc. Japan.
Valencio, D. A., J. F. Vilas and J. E. Mendia, (1975) An. Acad. brasil. Ciênc., 47(Suplem), 21-32.
Zijderveld, J. D. A., (1967) in Methods of Paleomagnetism, D. W. Collinson, K. M. Creer and S. K. Runcorn eds., 254-286, Elsevier, New York.

(Submitted to Geophysical Journal of R. Astron. Soc.)

PALEOMAGNETIC STUDY OF CRETACEOUS SEDIMENTARY AND VOLCANIC ROCKS IN NORTHERN CHILE

Kosuke HEKI[1], Yozo HAMANO[1] and Masaru KONO[2]

1.Geophysical Institute, University of Tokyo, Bunkyo-ku, Yayoi 2-11-16, Tokyo 113.
2.Department of Applied Physics, Tokyo Institute of Technology, Ookayama 2-12-1, Meguro-ku, Tokyo 152.

1)Introduction

The northernmost part of Chile, or the Arica region is an important area because it just corresponds to the zone of Arica-Santa Cruz deflection. In this article, we report Cretaceous paleomagnetic data of this region from red sandstone of Atajaña Formation and from one dike swarm (Arica dike swarm). Detailed interpretations are given in other papers (Heki et al., 1983; Heki, 1983).

2)Geology

Jurassic Arica Group is overlain unconformably by Neocomian Vilacollo Group, which consists of two supposedly synchronous formations: Atajaña Formation and Sausine Formation (Salas et al., 1966). Both units are composed of andesitic volcanics and continental clastic sediments and are overlain unconformably by Tertiary Azapa and Oxaya Formations.

Atajaña Formation crops out at the Cordillera de la Costa and consists of conglomerates, sandstone and andesite lava flows. It was first defined by Cecioni and Garcia (1960) for the rocks in Atajaña mountain in the department of Pisagua. In the Coastal Cordillera of Arica department, lithologically very similar rock sequences overlying Arica Group were found and suggested to correspond to Atajaña Formation by Salas et al. (1966).

Along Quebrada Vitor, some 30km south of the city of

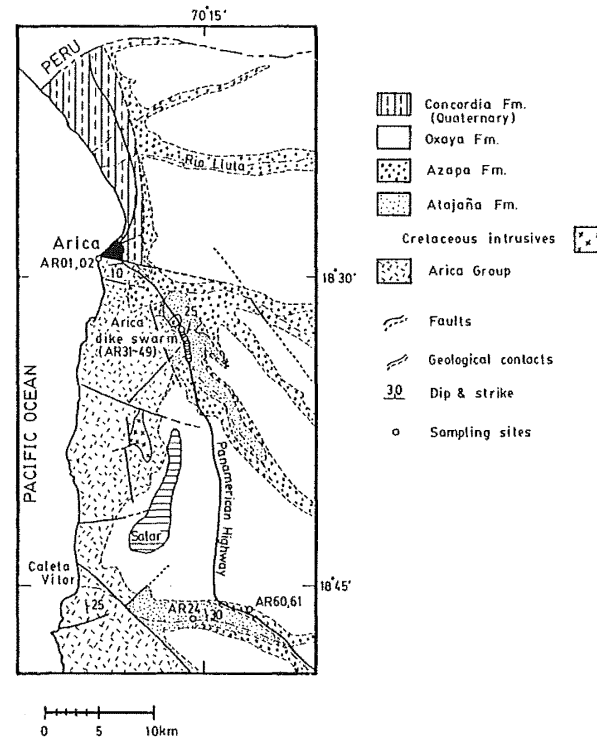

Fig.1 Geologic map (Salas et al., 1966) and sampling sites.

Arica, well stratified coase reddish violet sandstones crop out and are considered to correspond to the middle member of Atajaña Formation (Salas et al.,1966). 28 hand samples were taken from seven different horizons of very coarse to coarse grained sandstone layer in this exposure (AR24; 61, 51-54, 41-44, 31-35, 21-24, 11-14, 01-04, in ascending order). In Quebrada de la Higuera, some 10km southeast of the city of Arica, a basaltic and andesitic dike swarm was found in the red sandstone and tuff breccia layer of Atajaña Formation (named "Arica dike swarm"; Fig.1). Dikes trend generally east-west which is perpendicular to the general trend of dikes in Cuya dike swarm intruding into Jurassic strata (Heki et al., 1984) 50km south of Arica dike swarm. Thicknesses are typically 1-2m. Six hand samples were taken from each of 19 dikes (AR31-49) exposed along the Panamerican Highway. Country rocks have southward dip of about 15° with strike of N60°E. 6 paleomagnetic samples were also taken from the country rock (AR50) at the place far from the adjacent dikes. No thermal effects of dikes are considered to be present for AR50 samples.

2) Experimental procedure and paleomagnetic results

Red sandstone (AR24) Magnetic remanences of AR24 red sandstones were measured using a Schonstedt spinner magnetometer in University of Tokyo. Original NRM intensities are fairly uniform irrespective of their sampling horizons and are typically around 1×10^{-5} Am^2/kg. Alternating field (AF) demagntization performed up to 200mT only destroyed one fourth of the original intensity and was found to be ineffective. Instead of AF, stepwise thermal demagnetizations were performed on all specimens. Blocking temperatures were found to be distributed up to over 650°C suggesting the existence of hematite as the major carrior of the remanences (Fig.2). Magnetization directions showed little

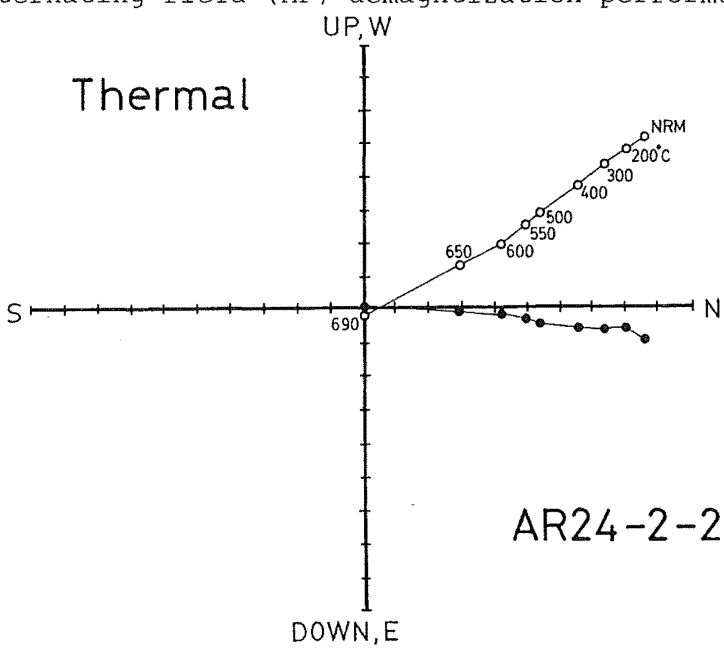

Fig.2 Zijderveld diagram in thermal demagnetization on AR24-2-2. Open and solid symbols denote projections onto vertical and horizontal planes respectively.

change after the demagnetization up to 600°C. As paleofield directions, those at 600°C step were adopted. Bedding corrections were made on these directions. All specimens showed normal polarity directions with the declination a little counterclockwisely deviated from north. No significant direction/intensity differences were detected among seven horizons. Paleomagnetic results are listed and illustrated in Table 1 and Fig.3 respectively.

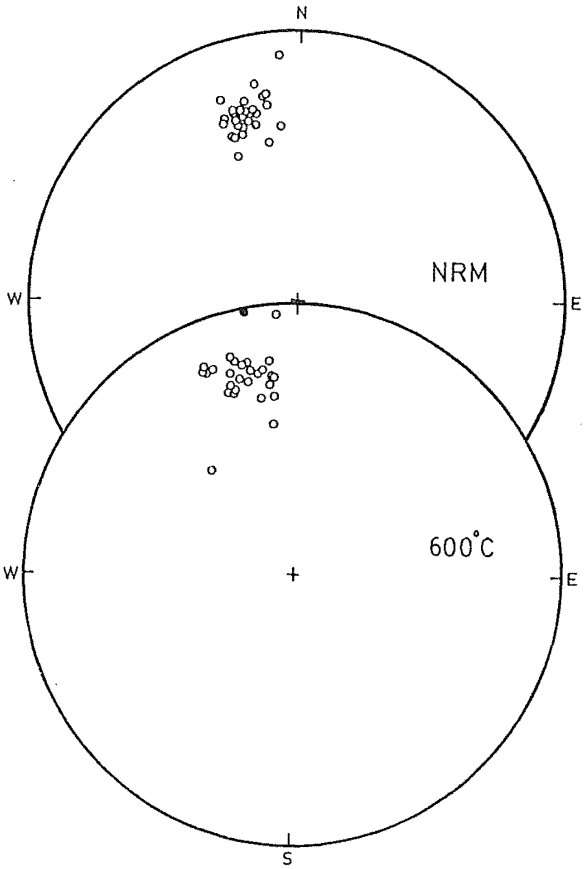

Fig.3 Lambert equal area projection of the field direction of AR24 at NRM step and 600°C step. Open and solid circles indicate negative and positive inclinations respectively.

Dikes (AR31-49) and their country rocks (AR50) Also a spinner magnetometer was used in these rocks. Dikes showed NRM intensities typically of the order of 10^{-5} Am^2/kg. Each dike specimen was stepwisely demagnetized in AF. MDFs were generally between 10 and 15mT. Several specimens were also thermally demagnetized. Zijderveld diagrams (Fig.4) of both kinds of demagnetization demonstrate that NRMs consist of stable single component with minor amount of secondary overprint. Paleofield directions were determined from the gradients of the linear portions of the demagnetization diagrams in principle. For several dikes (AR46, 49) which had large secondary magnetization and did not present sufficient length of linear portion, certain optimum demagnetization steps were selected by minimum dispersion criterion. No structural corrections were made on field directions because the intrusions are considered to be post-folding from the field observation of the attitude of dike contacts. All these directions showed normal polarities and also deviate by 10°-20° from north. Dike mean field directions are illustrated and listed in Fig.5 and Table 1 respectively.

For the host rocks (AR50), AF demagnetization up to 200mT reduced about a half of their original NRM intensities. Direction of remanent magnetization slightly changes its direction after AF demagnetization at 200mT. Stepwise thermal demagnetization was carried out on the specimens after AF demagnetization and showed

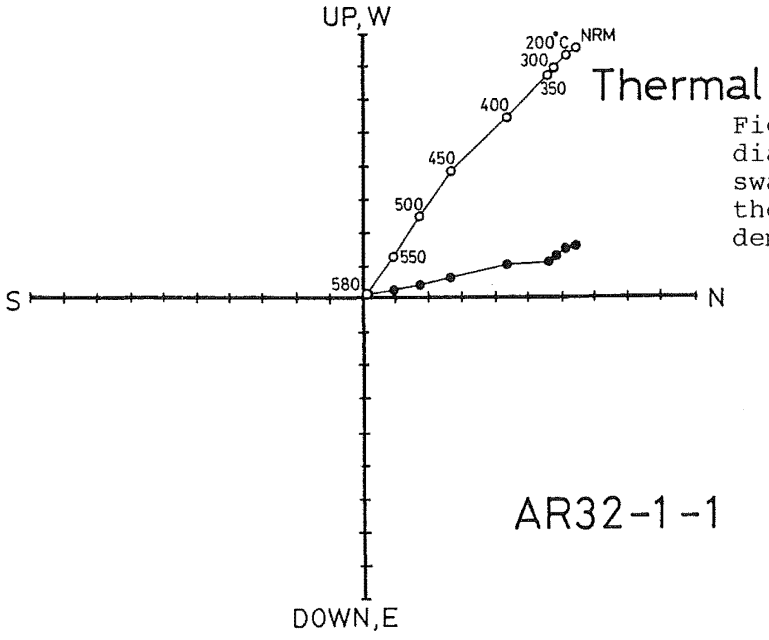

Fig.4 Zijderveld diagram of Arica dike swarm specimens in thermal and AF demagnetization.

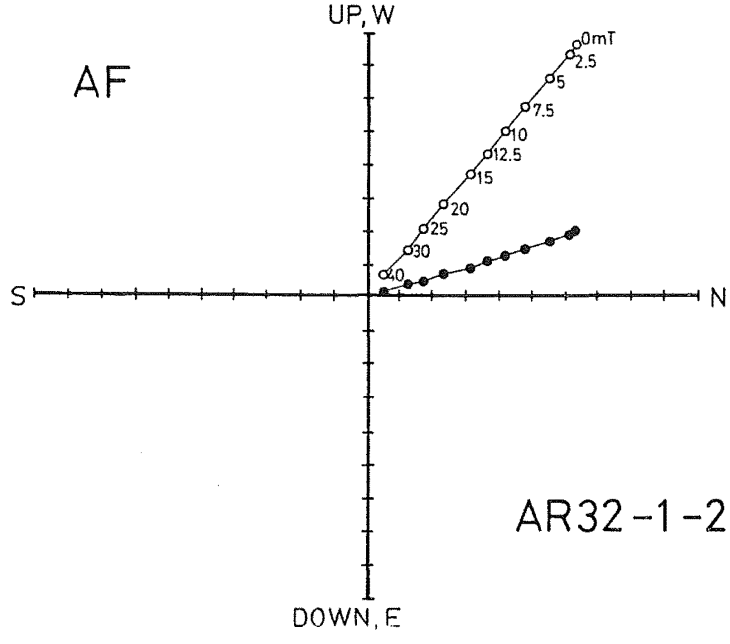

that upon further thermal treatment the direction of decreasing remanence remain steady, proving only one component was left after AF demagnetization. Field directions of AR50 after 200mT AF demagnetization were compared with that of AR24 red sandstone which was sampled in Quebrada Vitor some 20km south of AR50 and has a bedding plane different from AR50. Positive fold test

(Graham, 1949) shows these remanences are pre-folding (Fig. 6) and structural corrections are necessary on these directions.

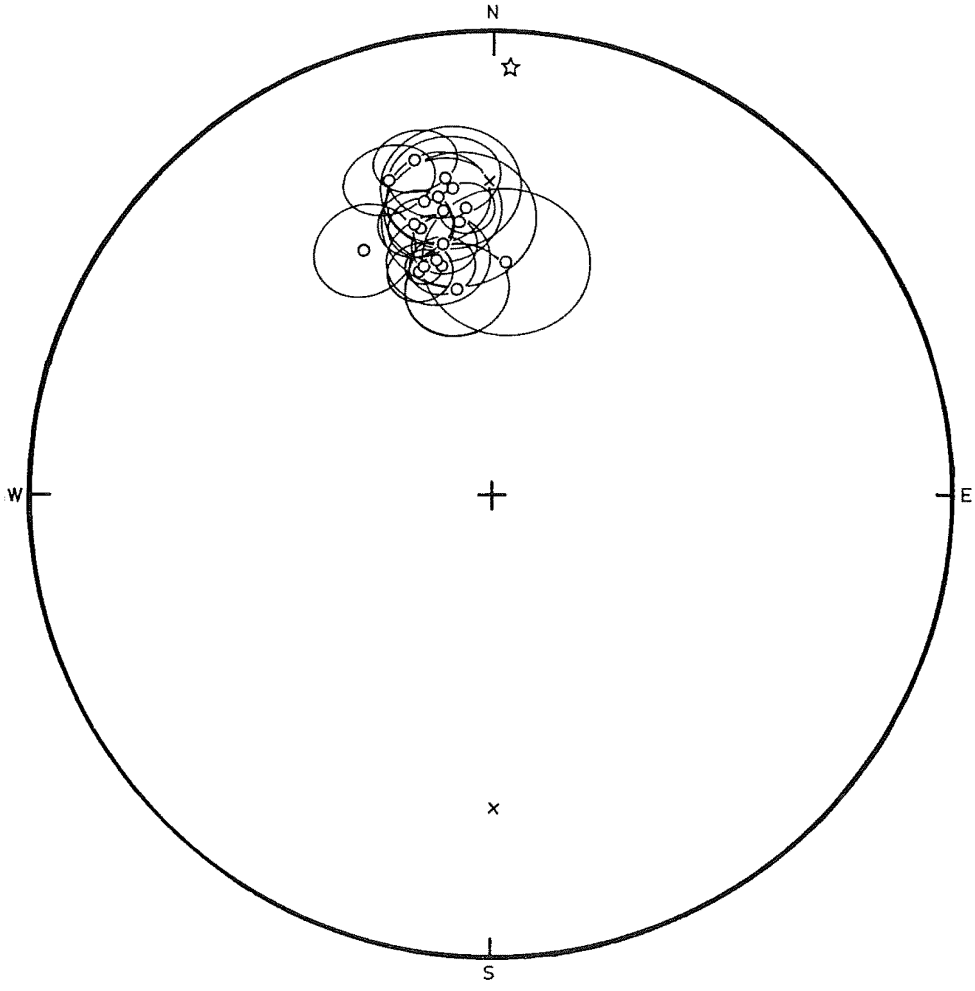

Fig.5 Lambert equal area projection of field direction obtained in Arica dike swarm (AR31-49). 95% confidence circles after Fisher (1953) are also illustrated. Star indicate present field direction in Arica region. X shows present axial dipole field direction. All inclinations are negative (upward).

3) Discussion

Paleofield directions of 28 specimens in AR24 were averaged and the pole corresponding to this mean direction was calculated. This pole is very similar to the Jurassic poles of this region in Heki et al. (1984).

VGPs of 19 dike mean field directions yielded the angular standard deviation (ASD) value of 7.2° with 95% confidence interval between 5.9° and 9.4°. This is considerably small in comparison with the value expected from Late Cenozoic global trend (McElhinny and Merrill, 1975). There are two possible

Table 1. Paleomagnetic directional data of Cretaceous rocks in northern Chile

Site	N	Incl. (°)	Decl. (°)	R	k	α_{95} (°)	Step (°C,mT)	Pole Lat. (°N)	Pole Long. (°E)
				(sedimentary rocks)					
AR24									
1-4	4	-27.3	-7.7	3.9859	213	6.3	650	81.5	-132.2
11-14	4	-21.7	-16.4	3.9827	173	7.0	600	72.5	-137.7
21-24	4	-23.2	-11.7	3.9094	33	16.2	600	77.0	-132.0
31-34	4	-25.5	-19.5	3.9775	133	8.0	600	70.6	-147.7
41-44	4	-24.9	-12.8	3.9633	82	10.2	600	76.5	-138.0
51-54	4	-25.5	-13.3	3.8266	17	22.7	600	76.2	-140.2
61-64	4	-30.0	-24.7	3.8876	27	18.1	600	66.3	-158.1
total	28	-25.6	-14.9	27.4089	46	4.1	600	74.7	-142.1
				(volcanic rocks)					
AR31	5	-39.0	-5.3	4.9825	228	5.1	LSF	84.0	164.1
AR32	7	-45.0	-11.6	6.9526	127	5.4	LSF	76.7	160.9
AR33	5	-36.1	-13.8	4.9709	138	6.5	LSF	76.9	191.2
AR34	5	-32.6	-8.8	4.9508	81	8.5	LSF	81.6	-155.8
AR35	6	-41.0	-15.4	5.9646	141	5.7	LSF	74.8	178.2
AR36	3	-48.1	-17.0	2.9986	1388	3.3	LSF	71.3	162.4
AR37	5	-38.7	-10.0	4.9448	73	10.0	LSF	80.1	179.0
AR38	6	-41.0	-28.1	5.9161	60	8.8	LSF	63.4	184.2
AR39	5	-30.4	-18.8	4.9646	113	7.2	LSF	71.9	-156.1
AR40	6	-53.5	-10.2	5.9216	64	8.5	LSF	72.1	138.2
AR41	6	-40.0	-16.1	5.9567	116	6.3	LSF	74.4	181.5
AR42	4	-41.4	-7.1	3.9355	47	13.6	LSF	81.6	160.4
AR43	6	-47.9	-13.6	5.9285	70	8.1	LSF	73.8	157.3
AR44	6	-48.9	-13.2	5.9658	146	5.6	LSF	73.6	154.2
AR45	5	-49.4	3.1	4.8797	33	13.5	LSF	78.0	96.7
AR46	6	-36.1	-10.5	5.9054	53	9.3	10	80.0	189.8
AR47	6	-48.8	-18.2	5.9690	161	5.3	LSF	70.1	162.4
AR48	6	-28.0	-13.4	5.9532	107	6.5	LSF	76.6	-146.2
AR49	5	-34.9	-7.7	4.9180	49	11.1	12.5	82.7	193.5
AR50	6	-30.9	-10.1	5.9811	265	4.1	LSF	80.2	-150.5
AR50	6	-27.9	-23.3	5.9873	395	3.4	200	67.4	-154.2

N:number of samples studied, R:length of the resultant vector, k:precision parameter, α_{95}:radius of 95% confidence circle, Step: optimum demagnetizing step (LSF means that field direction was determined by least square fitting to the linear portion of the demagnetization diagram).

Fig.6 Field direction of Atajaña formation in AR24 and AR50 before (small symbols) and after (large symbols) the bedding correction. 95% confidence circles are also illustrated for directions after the correction.

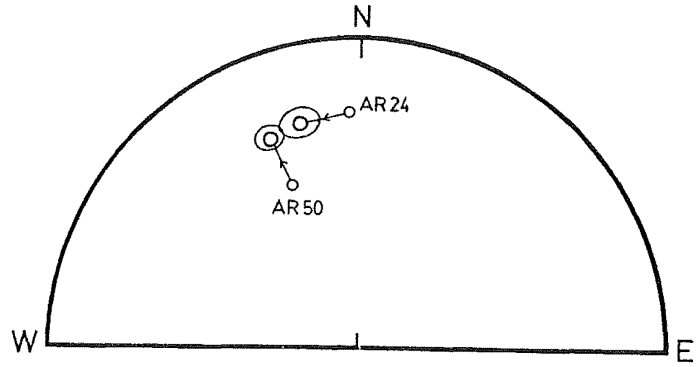

Table 2. Cretaceous poles in the northern Chile.

Rock unit	Locality Lat. (°S)	Locality Long. (°W)	Age	Pole Lat. (°S)	Pole Long. (°E)	dp (°)	dm (°)	A_{95} (°)
Atajaña Formation (AR24)	18.6	70.3	Kl	74.7	37.9	2.4	4.4	
Arica dike swarm (AR31-49)	18.6	70.3	K	77.2	352.4			3.3

Poles are converted to southern hemisphere poles. dp:radius of confidence oval measured in the direction from site toward pole, dm:radius of 95% confidence oval measured perpendicular to dp, A_{95}:radius of 95% confidence circle, K:Cretaceous, Kl:Lower Cretaceous.

Fig.7 Cretaceous paleomagnetic poles of Arica region (squares) and stable platform (stars) and their 95% confidence circles/ovals. Corresponding sites are illustrated as small open symbols in the map. After Heki (1983).

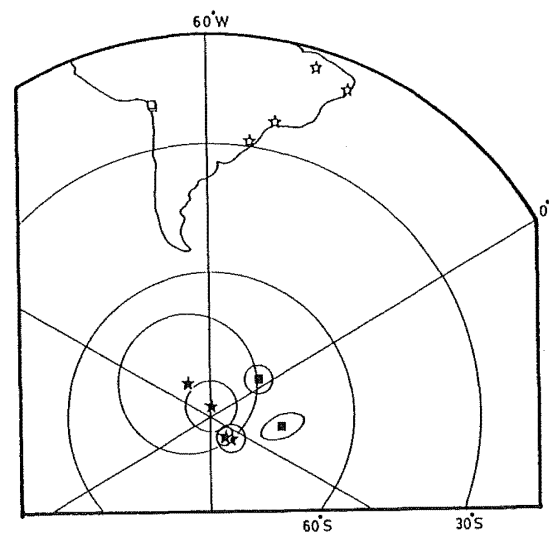

explanations: one that paleosecular variation is considerably smaller in the Cretaceous time than in Late Cenozoic time (Irving and Pullaiah, 1976) and another that these dike intrusions occurred in relatively short time length than the sufficient time span to contain the whole paleosecular variation periods. If the latter interpretation is correct, there might be small departure of their mean pole from true time-averaged pole. Cretaceous paleomagnetic poles of Arica region reported here are listed in Table 2 and are illustrated in Fig.7.

References

Cecioni, G. and F. Garcia (1960) Instituto de Investigaciones Geologicas, Chile, Boletin, 6, p28.

Graham, J. W.(1949) J. Geophys. Res., 54, 131-167.

Heki, K. (1983) Faculty of Science, University of Tokyo, Doctoral Thesis.

Heki, K., Y. Hamano and M. Kono (1983) Nature, 305, 514-516.

Heki, K., Y. Hamano, M. Kono, K. Nomura, N. Morikawa and H. Kinoshita (1984), Rock Mag. Paleogeophys., in this volume.

Irving, E. and G. Pullaiah (1976) Earth Sci. Rev., 12, 35-64.

McElhinny, M. W. and R. T. Merrill (1975) Rev. Geophys. Space Phys., 13, 687-701.

Salas, R., R. Kast, I. Montecinos and I. Salas (1966) Instituto de Investigaciones Geologicas, Chile, Boletin, 21, p113.

Zijderveld, J. D. A. (1967) in Methods of Paleomagnetism, edited by D. W. Collinson, K. M. Creer and S. K. Runcorn, pp254-286, Elsevier, New York.

(to be submitted to Journal of Geomagnetism and Geoelectricity)

PALEOMAGNETIC STUDY OF JURASSIC SEDIMENTARY AND VOLCANIC ROCKS IN NORTHERN CHILE

Kosuke HEKI[1], Yozo HAMANO[1], Masaru KONO[2],

Kazushige NOMURA[3], Naoaki MORIKAWA[3] and Hajimu KINOSHITA[3]

1. Geophysical Institute, University of Tokyo, Bunkyo-ku, Yayoi 2-11-16, Tokyo 113.
2. Department of Applied Physics, Tokyo Institute of Technology, Ookayama 2-12-1, Meguro-ku, Tokyo 152.
3. Department of Earth Sciences, Faculty of Science, Chiba University, Yayoi-cho 1-33, Chiba-city, Chiba 260.

1) Introduction

Palmer et al. (1980) reported that paleomagnetic results of Jurassic Camaraca Formation, Arica Group, northernmost Chile shows about 25° counterclockwise rotation with respect to the stable South American platform. Heki et al. (1983) and Heki (1983) showed that the rotation of the whole Peruvian block is responsible for this counterclockwise rotation. Here we report paleomagnetic description of our Jurassic results in Arica region. Our data consist of one dike swarm near Cuya and shale strata of Camaraca Formation in the city of Arica.

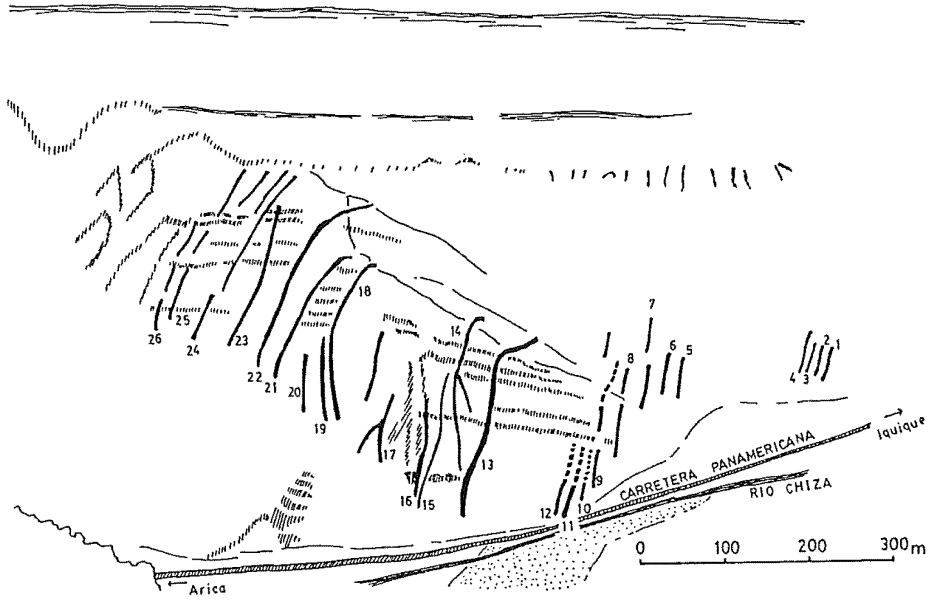

Fig.1 Sketch map of Cuya dike swarm intruding into sedimentary rocks of Jurassic Arica Group. Numbers attached to the dikes indicate serial number of dikes studied here.

2)Geology

The department of Arica covered by the geologic map of Salas et al. (1966) is mostly occupied by Mesozoic and Cenozoic sedimentary and volcanic rocks with the total thickness up to 8,000m. The oldest rock is Middle Jurassic Arica Group which consists of lower Camaraca Formation (upper Bajocian to Calovian) and upper Los Tarros Formation (Oxfordian). Camaraca Formation is made of dark color andesitic volcanics accompanied with some intercalations of marine sediments, and Los Tarros Formation is composed of the alternation of lutite, limestone, quartzite and minor amount of andesitic volcanic rocks. Arica Group is uncomformably overlain by Neocomian Atajaña Formation, Vilacollo Group.

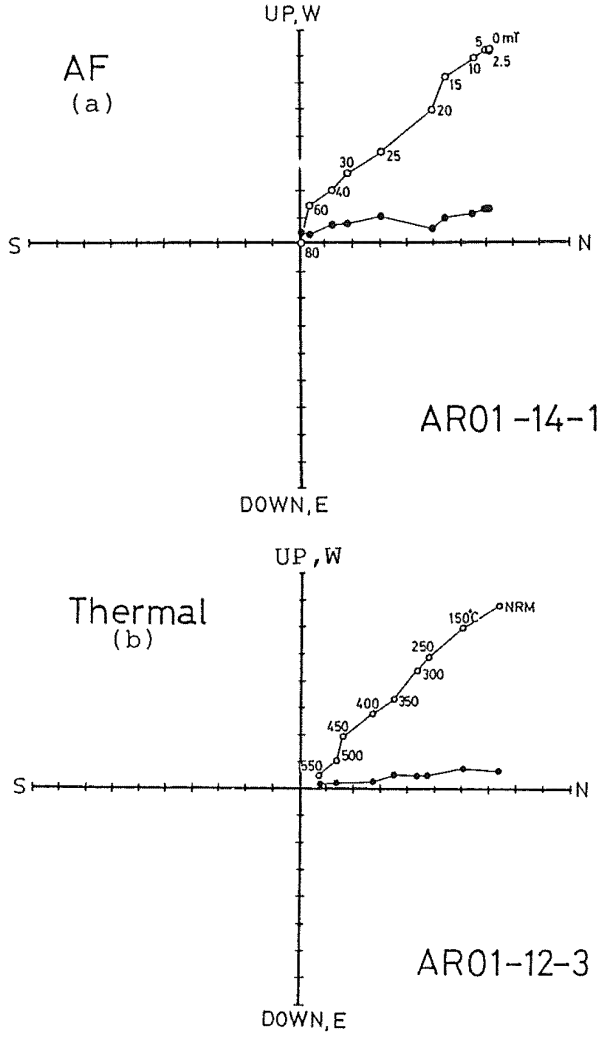

Fig.2 Zijderveld diagrams of progressive AF(a) and thermal(b) demagnetization. Open and solid symbols denote projections onto vertical and horizontal planes respectively.

Sedimentary paleomagnetic samples were taken from the shale layer exposed exposed at the northern face of the cliff called "Morro de Arica" which corresponds to the lower member of the Camaraca Formation. More than 20 samles were taken from four different horizons (AR01; 31-36, 11-15, 21-25, 41-47,51, in ascending order, for the locality, see Fig.1 of Heki et al. (1984, in this volume)). Their bedding plane dips by about 10° northward. The uppermost horizon (AR01;41-47, 51) is just under the boundary between these shale layers and overlying pillow lava layer. 10 samples were taken from this andesite pillow lava (AR02) for comparison. In this pillow lava, one sample was taken from the center of a pillow block. This pillow lava corresponds to the site "AR-1" in the table 1 of Palmer et al. (1980).

A dike swarm was found along the Panamerican Highway some

70km south of Arica, near the boundary between the departments of Arica and Pisagua (named "Cuya dike swarm"). Dikes range in their thicknesses from 0.5m to 7m and generally trend north-south. Most dikes are made of porphyritic andesite and the country rocks (Los Tarros Formation) are made of calcareous sandstone and limestone which dip northeastward by about 30°-50°. Their top is eroded and is horizontally overlain directly by Tertiary ignimbrite of Oxaya Formation. Generally six hand samples were taken from each of 26 dikes (CY01-26, Fig.1) and adjacent sedimentary rocks were also sampled at CY08 (CY08; 11-13, 21-23) and CY09 (CY09; 11-17, 21-27) with various distances from the contacts to carry out baked contact test.

3)Experimental procedure and paleomagnetic results

Shale and pillow lava (AR01,02) Natural remanent magnetization (NRM) intensities of samples of AR01 and AR02 are generally of the order of 10^{-5}-10^{-6} Am^2/kg and a Schonstedt spinner magnetometer was used for the measurement. Stepwise alternating field (AF) demagnetization was carried out for each specimen as far as the original remanence was mostly destroyed. Thermal demagnetization was also performed on several specimens to infer the blocking temperature distribution. Median destructive fields

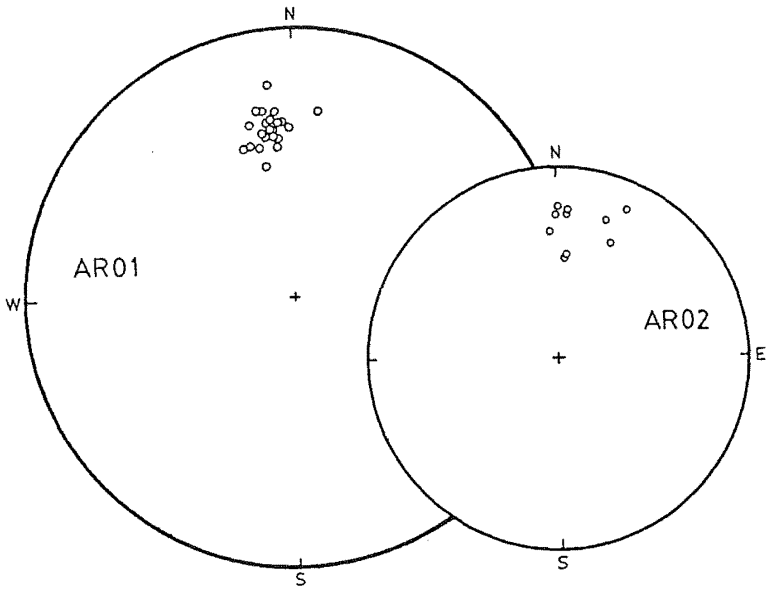

Fig.3 Equal area projection of the field directions of AR01 and AR02. All inclinations are negative (upward).

(MDFs) were usually between 20-25mT for AR01 and stable and single-component remanent magnetizations were suggested from demagnetization diagrams (Fig. 2a) of Zijderveld (1967). Thermal demagnetization (Fig.2b) showed that the blocking temperature is distributed from less then 150°C continuously up to about 550°C

and no blocking temperature higher than the Curie temperature of magnetite was observed suggesting the inexistence of hematite. Paleofield directions were determined by the least square fitting (LSF) to the linear portion of the diagram. Paleomagnetic field directions were obtained from 22 shale specimens in total. All specimens showed normal polarity magnetization with slight counterclockwise declination shift from north. Pillow lava samples (AR02) were also AF demagnetized and measured with a Schonstedt spinner magnetometer in the same way as AR01. Obtained field directions are not well grouped but show declination of about 10° which is significantly different from those of shales (Fig.3) suggesting that shale layers sampled here did not suffer any thermal effects from the overlying pillow lava. Structurally corrected paleomagnetic directions are listed in Table 1 and illustrated in Fig.3.

Dikes (CY01-27) and their country rocks (CY08,09) NRMs of the country rocks (limestones and calcareous sandstones) were measured using a cryogenic magnetometer in the National Institute of Polar Research and a Schonstedt spinner magnetometer in University of Tokyo. NRM intensities of these rocks have various values (vary in the order of two) in spite of their lithological similarities. NRM intensity is strongly dependent on the distance from the dike contact: NRM intensities of the order of 10^{-5} Am^2/kg at the baked part abruptly decrease at the distance of 50-100cm down to the order of 10^{-7} Am^2/kg indicating the diminishing of the thermal effects of the dikes (Fig.4). Baked part seems to have thermoremanent magnetization (TRM) acquired in times of the intrusions of CY08 and CY09 dikes and unbaked part seems to have pure detrital remanent magnetization (DRM) acquired

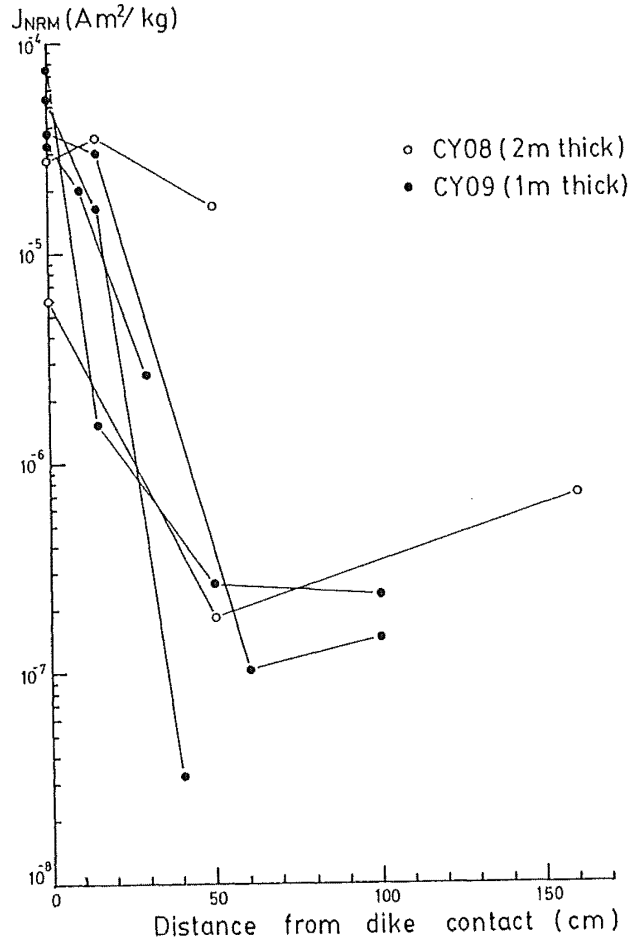

Fig.4 NRM intensity of country rocks versus distance from dike contact at CY08 and CY09.

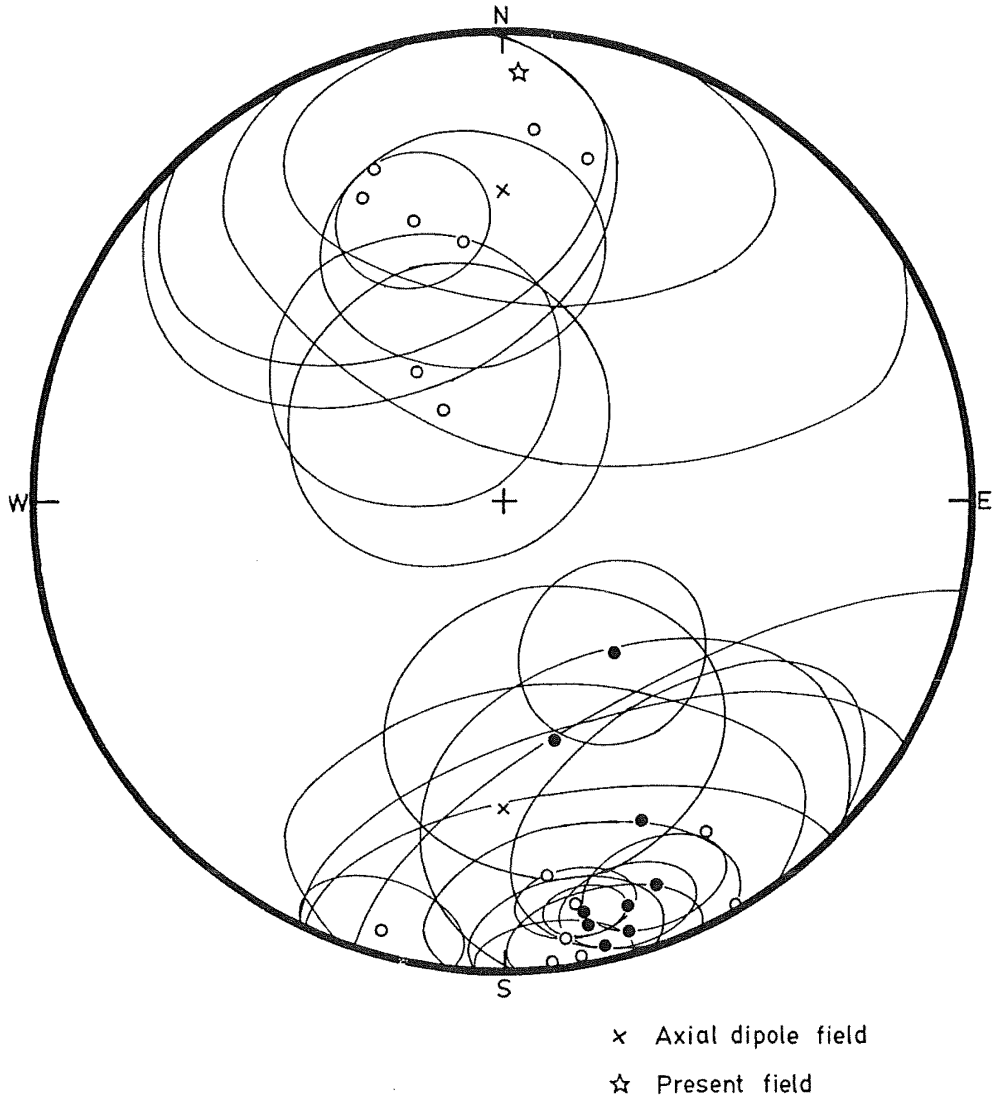

Fig.5 Equal area projection of dike-mean field directions of Cuya dike swarm. 95% confidence circles are also illustrated. Star indicates present field direction and X indicates present axial dipole field direction. Open and solid symbol denote negative (upward) and positive (downward) inclinations respectively.

in time of or soonly after the time of deposition of the country rocks. The existence of the unbaked part guarantees that this dike swarm did not suffer wide-region thermal remagnetization and that the TRMs of individual dikes are independent.

NRMs of the dike samples were measured using a Schonstedt spinner magnetometer in University of Tokyo as a bachelor thesis by Nomura and Morikawa (1983) and detailed paleomagnetic and rock magnetic descriptions are avialable in their thesis. NRM

intensities of dikes were small (typically $10^{-5}Am^2/kg$-$10^{-7}Am^2/kg$) in comparison with ordinary igneous rocks and are almost comparable with those of country rocks (CY08,09). On the other hand, initial susceptibilities are not so small making consequent natural Königsberger (Qn) ratios quite small (mostly less than unity). This may be due to some kind of alteration of magnetic minerals such as low temperature oxidation ubiquitously observed in microscopic analyses (Nomura and Morikawa, 1983). Js-T curves measured by a Curie balance often showed the existence of two phases: the lower one around 300-350°C and the higher one almost that of magnetite. About four fifths of the dikes showed irreversible Js-T characteristics suggesting the existence of low-temperature oxidation. Stepwise AF demagnetization was performed on each specimen. Several specimens showed stable magnetization direction in demagnetization process but for most specimens, remanent magnetization directions were too unstable to present linear portion in the Zijderveld diagrams. Hence, certain optimum demagnetizing step was determined by the objective criterion of minimum dispersion and remanent magnetization direction at that step were adopted. Several specimens were discarded due to their complete unstabilities against AF demagnetization. MDFs were widely distributed from 10mT to 80mT.

From 25 dikes, tolerably clustered paleofield directions were obtained as illustrated in Fig.5. Dike-mean field directions present bimodal and almost antipodal distribution, which are interpreted to represent normal and reversed polarities. Both distributions deviate a little counterclockwisely from present axial dipole field in their declinations. Bedding corrections were made on all these directions according to the structure of the country rocks. There are several dikes whose polarities appear to be intermediate (e.g., CY04) but it is not certain due to their large confidence angles (Fig.5). After all, all directions were classified into normal or reversed polarities by whether virtual geomagnetic poles (VGPs) are on the northern hemisphere or on the southern hemisphere and 8 normal and 17 reversed polarity directions were obtained. Paleomagnetic results are listed in Table 1.

4) Discussion

As for AR01 samples, because no external thermal effects were found in all four layers, paleofield directions of all 22 specimens were avgeraged irrespective of their horizons and the mean direction was obtained. The corresponding pole is thought to cancel out paleosecular variation and to be a paleomagnetic pole. 25 VGPs of Cuya dike swarm may include intermediate or transitional ones but all VGPs showed latitudes higher than 45° and were used for the calculation of the paleomagnetic pole. They were converted to southern hemisphere poles and the paleomagnetic pole was obtained by averaging them. Cuya dike swarm pole, AR01 pole and that derived by Palmer et al. (1980) on 33 lava flows of Camaraca Formation are listed in Table 2.

Arica region paleomagnetic poles were compared with Jurassic platform pole and are illustrated together in Fig. 6. Platform poles are roughly coincident with present geographic pole while

Table 1. Paleomagnetic directional data of Chilean Jurassic rocks

Site	N	Incl. (°)	Decl. (°)	R	k	α_{95} (°)	ODF (mT)	Pole Lat. (°N)	Pole Long. (°E)
				(sedimentary rocks)					
AR01									
11-15	4	-34.7	-0.9	3.9853	204	6.4	LSF	89.0	164.6
22-25	4	-40.3	-7.9	3.9860	215	6.3	LSF	81.4	167.1
31-36	6	-39.7	-9.3	5.9927	688	2.6	LSF	80.4	173.2
41-47, 51	8	-35.8	-10.5	7.9055	74	6.5	LSF	80.0	190.4
total	22	-37.6	-7.9	21.8261	121	2.8	LSF	82.1	179.4
AR02	10	-30.4	9.4	9.7351	34	8.4	LSF	80.8	7.7
				(volcanic rocks)					
CY01	4	8.6	168.6	3.8483	20	21.2	30	-71.4	71.6
CY02	4	-1.8	170.2	3.6321	8.2	34.3	40	-67.7	83.2
CY03	6	13.1	158.2	5.8864	44	10.2	30	-65.4	47.6
CY04	6	-71.5	-32.8	5.2570	6.7	27.9	5	45.6	135.4
CY05	4	-26.1	14.5	3.2212	3.9	54.2	0	75.1	0.7
CY06	5	-30.1	-24.6	4.2125	5.1	37.7	0	66.4	-156.7
CY07	6	-37.7	-17.5	5.8298	29	12.6	30	73.5	-166.9
CY08	5	46.8	167.8	4.5341	8.6	27.7	7.5	-75.8	-20.8
CY09	4	-18.3	148.4	3.7440	12	28.0	12.5	-47.7	59.6
CY10	4	-20.8	173.3	3.5543	6.7	38.3	20	-59.3	96.9
CY11	4	5.2	163.7	3.4694	5.7	42.5	15	-67.0	64.0
CY12	4	26.8	156.5	3.6616	8.9	32.7	10	-67.0	28.8
CY13	5	-14.1	169.8	4.9536	86	8.3	20	-61.8	88.0
CY14	6	11.8	168.9	5.9627	134	5.8	30	-72.9	69.1
CY15	4	-22.0	5.1	3.6096	7.7	35.5	0	80.8	-37.1
CY16	5	56.9	143.3	4.8273	23	16.2	10	-53.2	-17.8
CY17	4	-25.4	-21.0	3.6314	8.1	34.3	0	69.0	-147.2
CY18	4	-0.3	149.9	3.3317	4.5	49.0	30	-54.7	49.6
CY20	4	3.3	167.1	3.9439	53	12.7	20	-68.4	72.6
CY21	4	10.8	162.7	3.9673	92	9.7	20	-68.3	56.8
CY22	4	-0.6	173.9	3.9660	88	9.8	60	-69.6	92.1
CY23	5	-5.9	-164.4	4.9210	51	10.9	40	-63.1	146.2
CY24	3	-43.7	-8.3	2.9344	30	22.7	5	80.0	158.7
CY25	3	-63.4	-33.8	2.9188	25	25.4	10	52.0	149.6
CY26	3	-6.6	171.7	2.9786	93	12.8	5	-66.1	89.0
				--country rock--					
Baked (CY08)	2	23.3	164.0	1.9804	51	35.7	LSF	-73.1	42.1
Baked (CY09)	9	31.0	160.6	8.8730	63	6.5	LSF	-71.4	24.4
Unbaked part	5	3.8	161.6	4.7965	20	17.7	LSF	-65.0	61.5

N:number of samples studied, R:length of resultant vector, k:precision parameter (Fisher, 1953), α_{95}:radius of 95% confidence circle, ODF:optimum demagnetizing step (LSF means that the directions are determined by the LSF to the diagram).

those of Arica region listed in Table 2 show similar deviations as northern Chilean Cretaceous poles (Heki et al., 1984). Valencio et al. (1983) attributed the Camaraca Formation discordant pole (Palmer et al., 1980) not to the tectonic movements but to the hairpin motion of the South American paleomagnetic pole from the observation that the distribution of the VGPs contained in individual Jurassic paleomagnetic poles are not circular but are elongated toward the longitude of about 30°. However, Mesozoic paleomagnetic pole of the Arica region all deviate in a similar sense and the original interpretation of Palmer et al. (1980) of tectonic rotation appears more plausible.

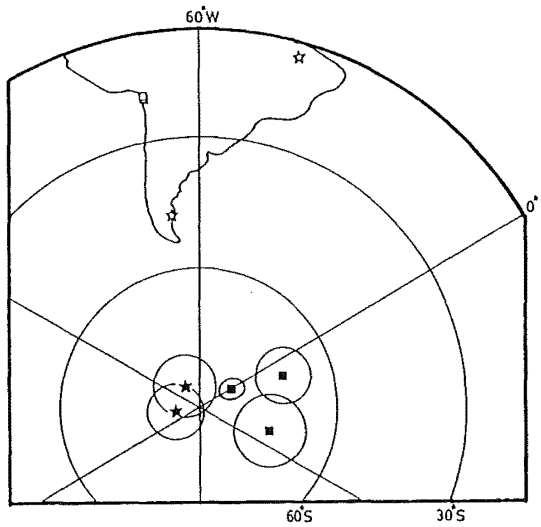

Fig.6 Paleomagnetic poles of Jurassic rock units in Arica region (squares) and stable platform (stars). After Heki (1983).

Table 2. Jurassic poles in the northern Chile.

Rock unit	Locality Lat. (°S)	Locality Long. (°W)	Age	Pole Lat. (°S)	Pole Long. (°E)	Pole dp (°)	Pole dm (°)	A_{95} (°)
Camaraca Fm. shale (AR01)	18.6	70.3	Jm	82.1	-0.6	1.9	3.3	
Camaraca Fm. lavas*	18.6	70.3	Jm	71	10			6
Cuya dike swarm (CY01-26)	19.2	70.2	J	74.1	49.1			7.8

dp:radius of confidence oval measured in the direction from site to pole, dm:radius of confidence oval measured perpendicular to dp, A_{95}:radius of 95% confidence circle, J:Jurassic, Jm:Middle Jurassic.

*Palmer et al. (1980)

References

Fisher, R. A., Proc. R. Soc., Ser. A, 217, 295-305.

Heki, K. (1983) Doctoral thesis, Faculty of Science, University of Tokyo.

Heki, K., Y. Hamano and M. Kono (1983) Nature, 305, 514-516.

Heki, K., Y. Hamano and M. Kono (1984) Rock Mag. Paleogeophys., in this volume.

Nomura, K. and N. Morikawa (1983) Bachelor thesis, Faculty of Science, Chiba University.

Palmer, H. C., A. Hayatsu and W. D. MacDonald (1980) Geophys. J. R. astr. Soc., 62, 155-172.

Salas, R., R. Kast, I. Montecinos and I. Salas (1966) Instituto de Investigaciones Geologicas, Chile, Boletin, 21, pl13.

Valencio, D. A., J. F. Vilas and I. G. Pacca (1983) Geophys. J. R. astr. Soc., 73, 135-151.

Zijderveld, J. D. A. (1967) in Methods of Paleomagnetism, edited by D. W. Collinson, K. M. Creer and S. K. Runcorn, 254-286, Elsevier, New York.

(to be submitted to Journal of Geomagnetism and Geoelectricity)

INCLINATION OF BASALT SAMPLES FROM DEEP SEA DRILLING PROJECT HOLES 597B AND 597C

Tadashi NISHITANI

Institute of Mining Geology, Mining College,
Akita University, Akita 010, Japan

Site 597 (18°48'S, 129°46'W) is located 2100 km east southeast of Tahiti on crust of late Oligocene age. It is situated 150 km northwest of the Austral fracture zone and is therefore on crust generated at the fossil Galapagos Rise, which now lies east of the East Pacific Rise (EPR) in the middle of the northern Nazca Plate (Fig.1). The crust at site 597 was generated at a spreading rate of about 6.5 cm/yr (Handschumacher, 1976), a rate similar to the present west flank accretion rate of about 7.0 cm/yr along the EPR between the Garret fracture zone at 13°S and the Easter mini-plate at 23°S (Rea, 1981). Seafloor depth is about 4150 m, unusually shallow for crust nearly 30 m.y. old. Such shallow depths are typical of the southeast Pacific between about 10°S and 35°S and from the EPR axis west at least to the Tuamoto and Austral Islands.

Recovery was 5.4 m of basalt at Hole 597B, and 48.5 m of basalt at Hole 597C. They are olivine-poor tholeiites to ferrobasalts containing plagioclase, clinopyroxene, magnetite, glass, and olivine. They are medium to fine grained, moderately vesicular (in Unit I) and fractured. Massive flows appear to comprise the entire sequence; only one small fragment, possible a pillow margin, with a glassy rim was recovered. Two units can be discerned within the basalt sequence. Unit I is 46 m thick and characterized by vesicular sub-spherulitic

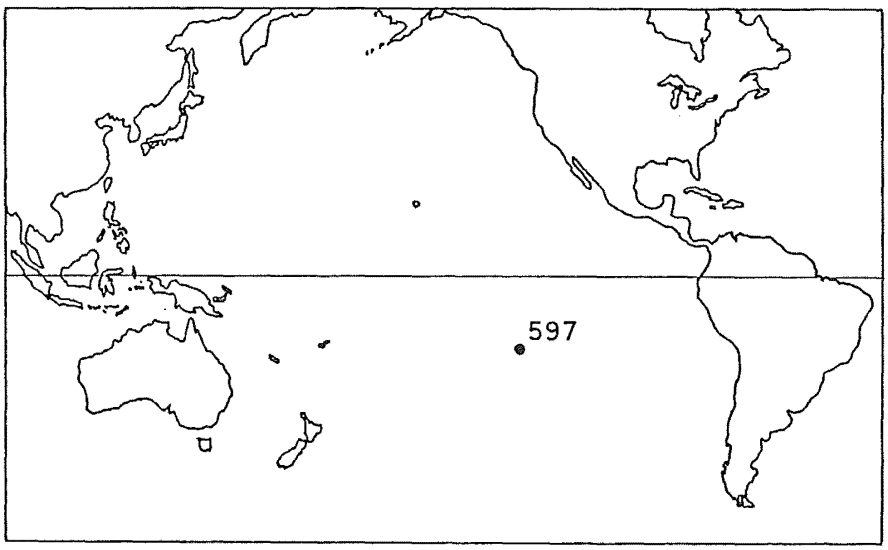

Fig.1 Location of Hole 597.

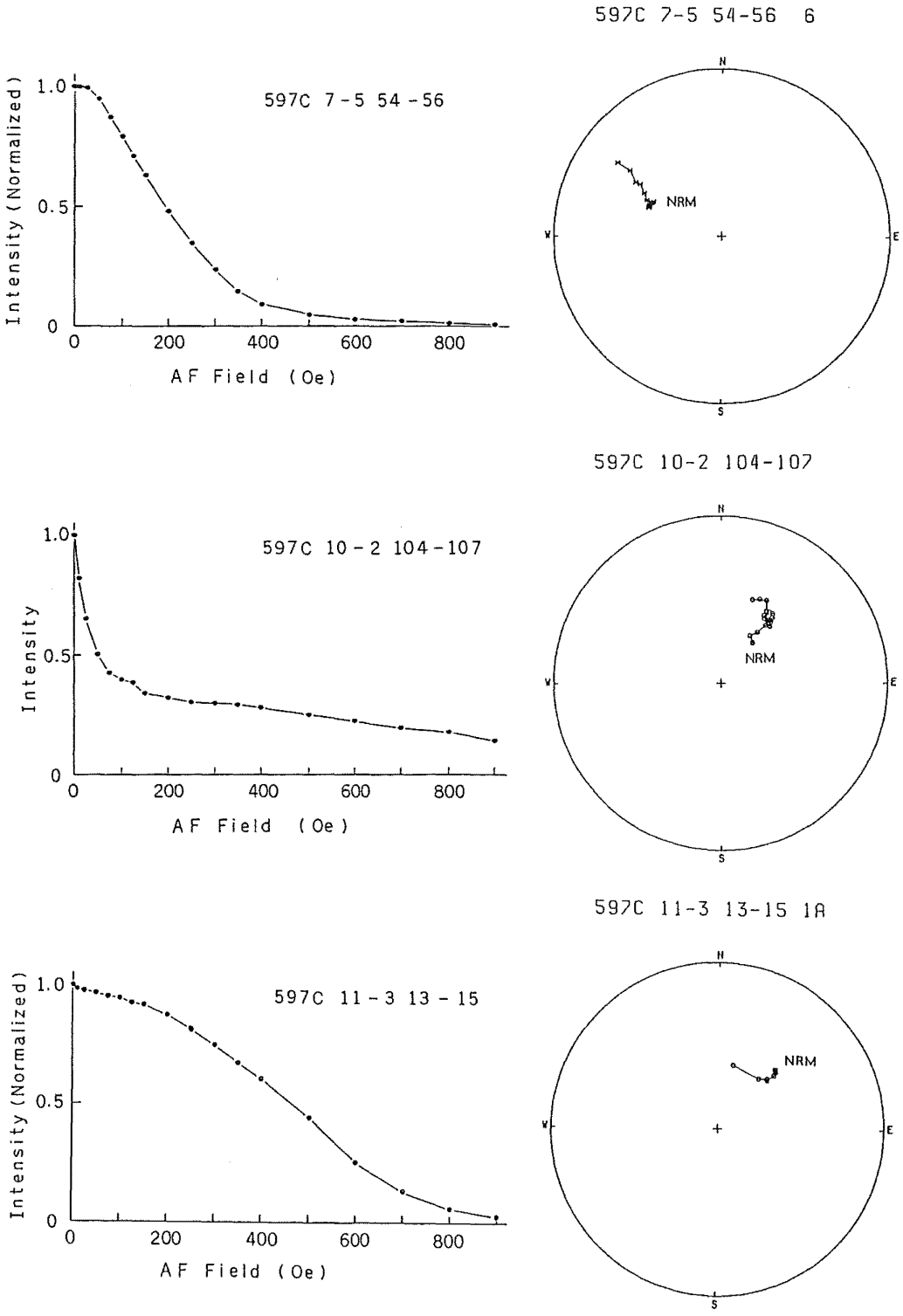

Fig.2 Some examples of AF demagnetization.

to intersertal texture and Unit II, 45 m thick, is dominated by intergranular and poikilophitic textures. Within both units olivine increases in abundance with depth. Several individual flow, defined by finer-grained flow boundaries, comprise each unit.

Eleven samples from Hole 597B and 58 samples from Hole 597C were measured for paleomagnetic studies. One or two oriented samples (2.54 cm in diameter) were taken from every section of each core. Natural remanent magnetization (NRM) was measured using Digico spinner magnetometer. The noise level of the magnetometer was less than 10^{-7} emu/cc. All measurements were performed under 128 spins to increase the signal to noise ratio.

Alternating field demagnetization was carried out. Some examples are shown in Fig.2. The range of MDFs is from 46 Oe to 195 Oe for 597B and from 35 Oe to 466 Oe for 597C. The mean values are 124 Oe (597B) and 136 Oe (597C). Low field susceptibility was measured with a susceptibility meter. Koenigsberger ratio (Q) was also obtained. At Holes 597B and 597C the earth's magnetic field was calculated to be 0.36 Oe. The Koenigsberger ratio is used as a measure of stability.

Fig.3 indicates results for Hole 597B. Intensities and inclinations for Hole 597C are shown in Fig.4 and the results of susceptibilities and Q ratios in Fig.5.

The average NRM intensity and susceptibility in 597B are 1.6 ± 1.0 x 10^{-3} emu/cc and 1.5 ± 1.2 x 10^{-3} emu/cc Oe, respectively. The average NRM intensity in 597C is 3.4 ± 2.0 x 10^{-3} emu/cc. There is a sudden increase in intensity in 597C 4-1 (13 m) which decreases slowly to the bottom of the hole with the exception of the sharp peaks found in 597C 7-2 (42 m), 597C 7-4 (46 m). A similar tendency can be seen in Q ratios.

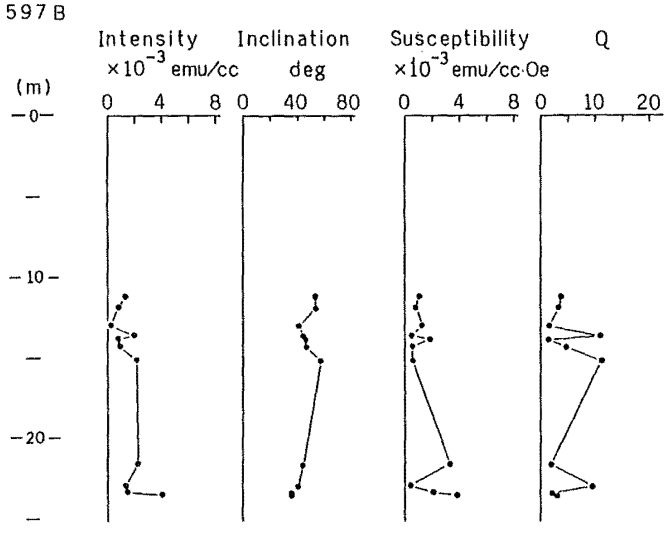

Fig.3 Intensities of NRM, inclinations after AF demagnetization, susceptibilities and Q ratios (H = 0.36 Oe) for Hole 597B.

Inclinations are calculated with respect to the horizontal plane, assuming that each core was drilled vertically, and are positive down. A positive inclination indicates reversed polarity at this latitude (18°48'S). All samples showed reversed polarity except for two points, (597C 7-4, 137-140 and 597C 7-5, 70-73). These two normal values are not peculiar, because susceptibility and Q ratios in the same sections do not show abnormal behavior. Some relationship may exist between the two normal values and the preceding high NRM intensity.

These studies show the basalts to be reversely magnetized and therefore probably from the reversed interval between anomalies 8 and 9. This would imply an age of 28.5 Ma for Site 597 (Harland et al., 1982), and age consistent with the nannofossil zonation of the basal sediments. Two magnetic reversals occur in the basalts of core 597C 7 (46-47 m), resulting in a brief period of normal polarity. The mean inclinations for 597B and 597C are 45.4 ± 7.1° and 45.0 ± 7.6° respectively. These values are greater than the calculated value of I = 34°, assuming a dipole field, expected at this site. Unusually high magnetic inclinations also characterize basalts from DSDP Sites 391 and 320 (Ade-Hall and Johnson, 1976), also on crust generated at the fossil Galapagos Rise. As yet there is no satisfactory explanation for these high inclinations.

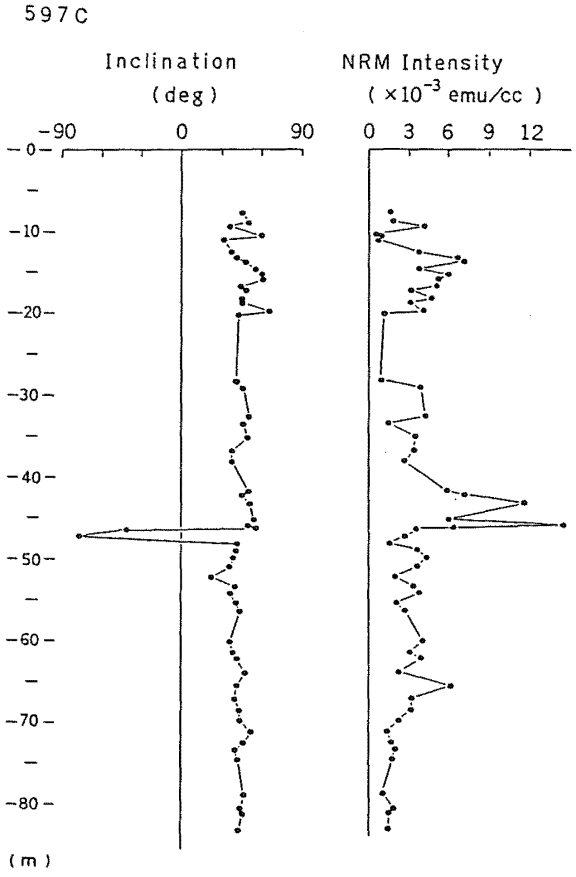

Fig.4 Inclinations after AF demagnetization and NRM intensities for Hole 597C.

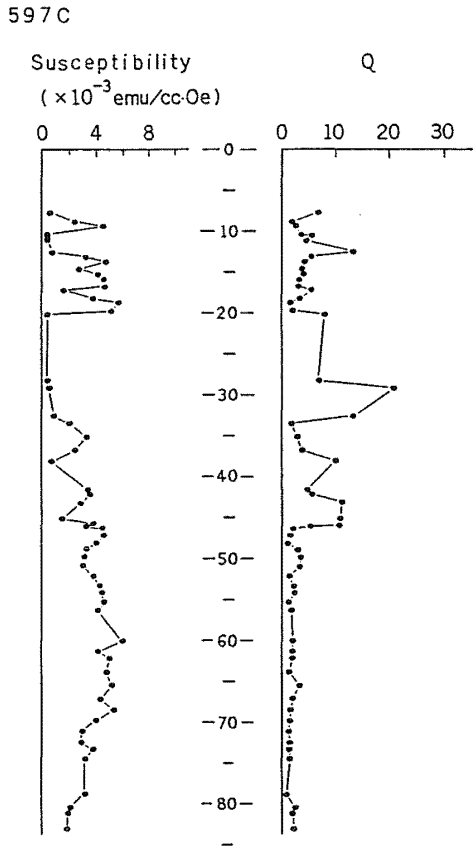

Fig.5 Susceptibilities and Q ratios (H = 0.36 Oe) for Hole 597C.

References

Ade-Hall, J. M. and H. P. Johnson (1976) Init. Repts. of Deep Sea Drilling Proj., 34, 513-532.
Handschumacher, D. W. (1976) The Geophysics of the Pacific Basin and its Margin. (Am. Geophys. Union, Washington), 177-202.
Harland, W. B., A. V. Cox, et al. (1982) A geologic time scale.
Rea, D. K. (1981) Geol. Soc. Am., 154, 27-62.

PROGRESS REPORT ON PALEO/ROCK MAGNETIC STUDY OF THE CENOZOIC ROCKS FROM THE WESTCENTRAL KYUSHU ISLAND, WEST JAPAN

Hiroshi MUNEOKA* and Haruo DOMEN**

*Ozuki Air Base, M.S.D.F., Shimonoseki 750-11, Japan
**Institute of Physical Sciences, Faculty of Education, Yamaguchi University, Yamaguchi 753, Japan

In the previous report (Domen and Muneoka 1982), the preliminary paleo/rock magnetic data on the Cenozoic rocks from the Amakusa district in the westcentral Kyushu Island, west Japan had been shown. Some more samples were collected afterwards from the same district and also its vicinity. On those samples thus obtained have been submitted to the paleo/rock magnetic study as well.

Fig. 1 is a map showing the sampling sites, some of the former ones inclusive.

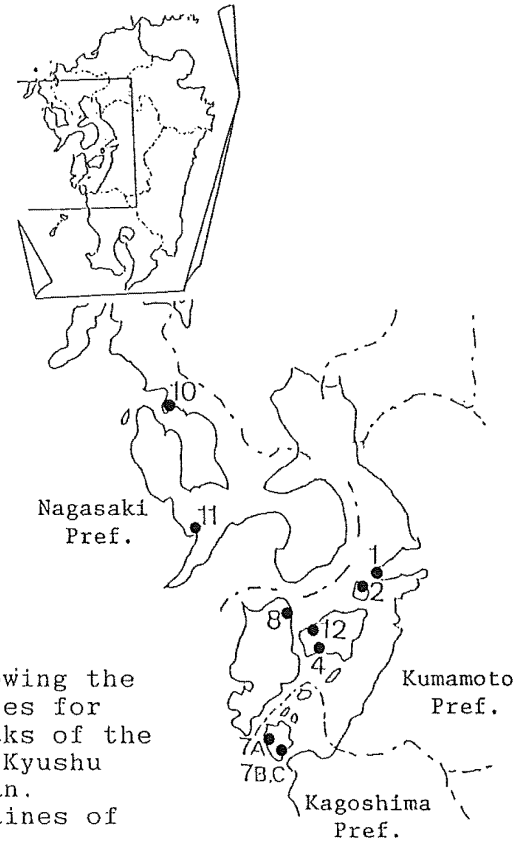

Fig. 1. Map showing the sampling sites for Cenozoic rocks of the westcentral Kyushu Island, Japan. Site 2 containes of 2-1 and 2-1.

Table 1. NRM direction and intensity of some Cenozoic rocks from the westcentral Kyushu Island, west Japan

	Sampling Site	Rock Type	Age	No. of samples	Mean Direction D(E)	Mean Direction I(D)	Mean Direction K	Mean Direction $\alpha_{95\%}$	$I \times 10^4$ emu/g
1.	Misumi-dake	Hornblende andesite	Pliocene	32	44.7°	25.7°	10	8.6°	2.1
2.	Tobi-dake(1)	Andesite agglomerate	Miocene	18	175.8	-55.3	47	5.1	39
2-1.	Shibao-yama	Andesite agglomerate	Miocene	10	150.9	-49.6	4	27.1	39
2-2.	Tobi-dake(2)	Andesite	Upper Miocene	13	6.4	48.4	6	18.7	18
4.	Miyata	Liparite	Lower Miocene	12	-36.8	-57.2	2	43.6	0.081
7A,B,C.	Naga-shima	Pyroxene andesite	Pliocen/ Miocene	19	172.3	-58.1	14	9.3	11
8.	Itsuwa-machi	Welded tuff	Pleistocene	18	3.8	41.4	15	9.2	0.52
9.	Kuchi-no-tsu	Basalt	Lower Pleistocene	15	-16.2	42.7	6	17.2	16
10.	Hayama	Basalt	Lower Pleistocene	8	-7.9	52.8	3	34.8	2.8
11.	Nagasaki	Hornblende andesite	Miocene ?	20	18.7	43.0	5	16.1	4.1
12.	Oshimago	Hornblende andesite	Lower Miocene	11	-86.6	-73.5	2	43.7	0.022

However the most of all samples obtained from the respective site had been magnetically cleaned by means of an AF demagnetizor (Domen 1982) and again the respective specimen has been submitted to the thermomagnetic analysis one by one, only the natural remanent magnetization: mean direction from the geomagnetic north at the respective site and mean intensity of the order of 10^{-4} in emu/g, obtained up to this time are shown in Table 1.

As has been seen, some reversed NRM are found in this district, say at the sites of 2, 2-1 and 7. And the NRM of those samples are rather stable against the alternative magnetic field agitation. Those geologic ages of the samples from sites 2, 2-1 and the site 7 are Miocene and Plio/Miocene respectively.

References

Domen, H. 1982, Bul. Fac. Educ., Yamaguchi University, 32(Pt. 2), 13-17.

Domen, H. and H. Muneoka 1982, Rock Magnetism and Paleogeophysics, 9, 36-40.

PRELIMINARY REPORT ON THE NATURAL REMANENT MAGNETIZATION OF CHICHI-SHIMA ROCKS OF BONIN ISLANDS, JAPAN

Haruo DOMEN and Hiroshi MUNEOKA

Institute of Physical Sciences, Faculty of Education,
Yamaguchi University, Yamaguchi 753, Japan

Recently, one (H.M.) of the present authors has collected some ten samples for the paleo/rock magnetic study from Chichi-Shima Island, Ogasawara; Bonin Islands, Japan.

The collected samples are the welded tuff and tuff breccia of Paleogene or Cretaceous (G.S.Japan 1971).

Few of these samples were submitted to the NRM measurement by means of an astatic magnetometer. Tentative data on the NRM thus obtained preliminary are as in Table 1.

However the directions of those NRM examined are rather scattered, both types of rocks show the reversed NRM.

Reference

Geological Survey of Japan 1971, Geological Map of Japan (1:2,000,000), 4th ed.

Table 1. NRM data of Chichi-Shima volcanics

Sample	Specimen No.	D(E)	I(D)	K	$\alpha_{95\%}$	I
welded tuff	32409	63.2°	35.5°			$1.9 \times 10^{-4} \frac{emu}{g}$
	324072	62.4	-76.7			8.6
	32407	-154.5	-54.5			8.1
	32405	-163.1	-15.7			1.1
	Mean	157.6°	-54.6°	1.4	widely scattered	4.9
tuff breccia	324071	-145.9°	-26.3°			8.3
	32413	137.2	-75.4			6.3
	32412	-168.7	-79.4			2.5
	32411	-169.6	-29.3			0.72
	32410	-161.6	-33.7			1.0
	32401	169.0	-36.1			1.2
	Mean	-169.9°	-48.2°	8.4	24.6°	3.4

A SHORT NOTE ON AN NRM DIRECTION OF CRETACEOUS SERPENTINITE FROM THE VICINITY OF UBE CITY, SOUTHCENTRAL YAMAGUCHI PREFECTURE, WEST JAPAN

Haruo DOMEN

Institute of Physical Sciences, Faculty of Education,
Yamaguchi University, Yamaguchi 753, Japan

Several outcrops of the Cretaceous serpentinite are distributed in the vicinity of Ube City, southcentral Yamaguchi Prefecture, west Japan, as has been shown in Fig. 1. in which the sampling sites for this preliminary survey are labaled as A and B.

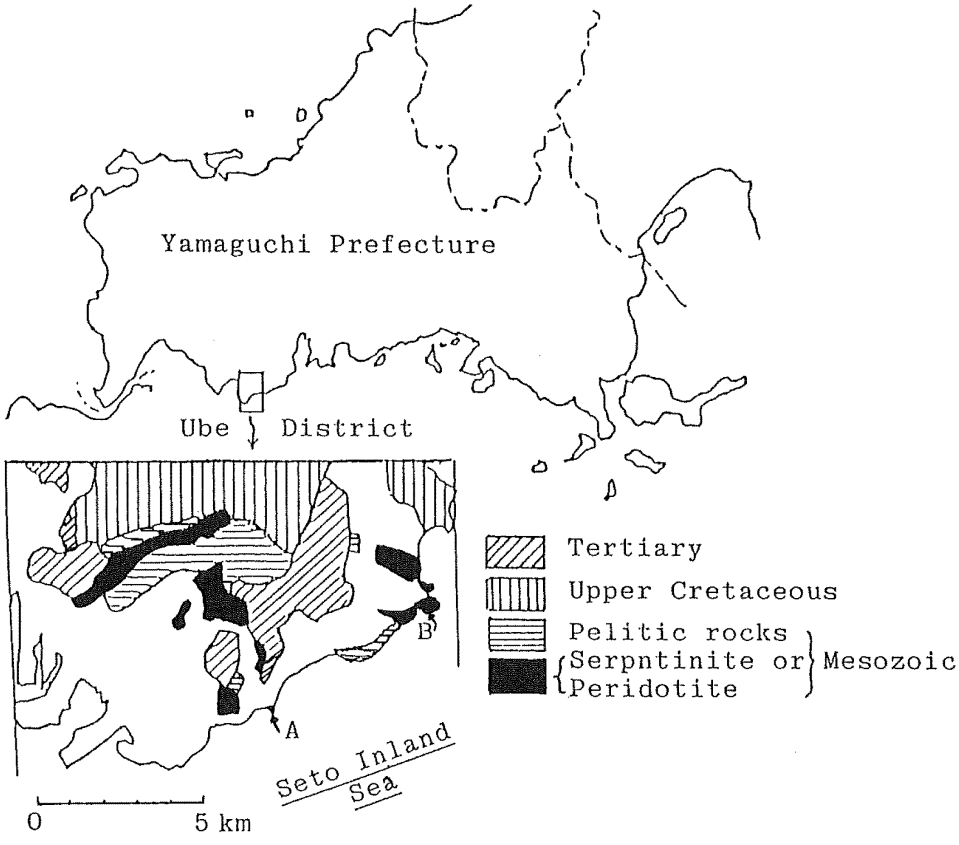

Fig. 1. A map showing two sampling sites for Ube district serpentinite. Rough geology is also shown (after Yamaguchi Geological Soc. 1975. Modefied by the present author).

The preliminary measurement on NRM directions of those samples had been carried out by means of an astatic magnetometer. Table 1 and 2 show the obtained NRM directions of test specimens from the site A and B respectively.

Table 1. NRM directions of each specimen of serpentinite from the site A.

	SAMPL N O	D(E)	I(D)
1	8212001	15.9°	44.6°
2	8212002	-25.0°	44.2°
3	8212003	-3.7°	41.4°
4	8212004	-25.8°	35.3°
5	8212005	20.1°	34.2°
6	8212007	22.2°	24.3°
7	8212009	50.8°	72.6°
8	8212010	15.4°	46.4°
9	8212012	-43.3°	41.5°
10	8212013	11.1°	58.0°
11	8212014	-60.8°	48.6°
12	8212015	-1.8°	49.9°
13	8212016	-119.0°	75.0°
14	8212017	28.2°	44.8°
15	8212019	-45.1°	66.7°
16	8212022	-9.8°	43.3°
17	8212023	11.7°	48.8°
18	8212025	-3.9°	30.1°
19	8212026	59.2°	37.2°
20	8212027	-7.3°	37.5°
21	8212028	12.5°	35.5°
22	8212029	3.2°	38.0°
23	8212030	-16.6°	61.1°
TOTAL	MEAN		
23		-0.1°	49.9°

P R E C I S I O N

K	ALFA 95%	DEL D	DEL I
11.4	9.4°	14.5°	9.4°
		DEL P	DEL M
		8.3°	12.5°

Both sampling sites; A and B are aparted by only several kilometers within this district as has been seen in Fig. 1. But the mean directions of those NRMs for the respective site are rather deviated each other.

Table 2. NRM directions of each specimen of serpentinite from the site B.

	SAMPL N O	D(E)	I(D)
1	580501	-10.0°	54.3°
2	580502	-42.3°	72.0°
3	580503	-4.2°	57.1°
4	580504	102.8°	14.6°
5	580505	97.0°	33.5°
6	580506	77.7°	37.7°
7	580507	61.1°	67.2°
8	580509	25.1°	60.2°
9	580511	31.4°	59.9°
10	580512	-65.8°	82.1°
11	580513	64.8°	66.0°
12	580514	61.1°	48.6°
13	580515	48.1°	64.4°
14	580516	78.0°	61.2°
15	580517	49.0°	83.7°
16	580519	30.8°	36.1°
17	580520	42.4°	29.2°
TOTAL	MEAN		
17		51.1°	60.9°

P R E C I S I O N

K	ALFA 95%	DEL D	DEL I
8.3	13.1°	27.0°	13.1°
		DEL P	DEL M
		15.4°	20.1°

Reference

Yamaguchi Geological Society 1975. Geological Map of Yamaguchi Prefecture, 1:200,000.

AUTHOR INDEX

(Continued to the next page)

AUTHOR INDEX (Continued)

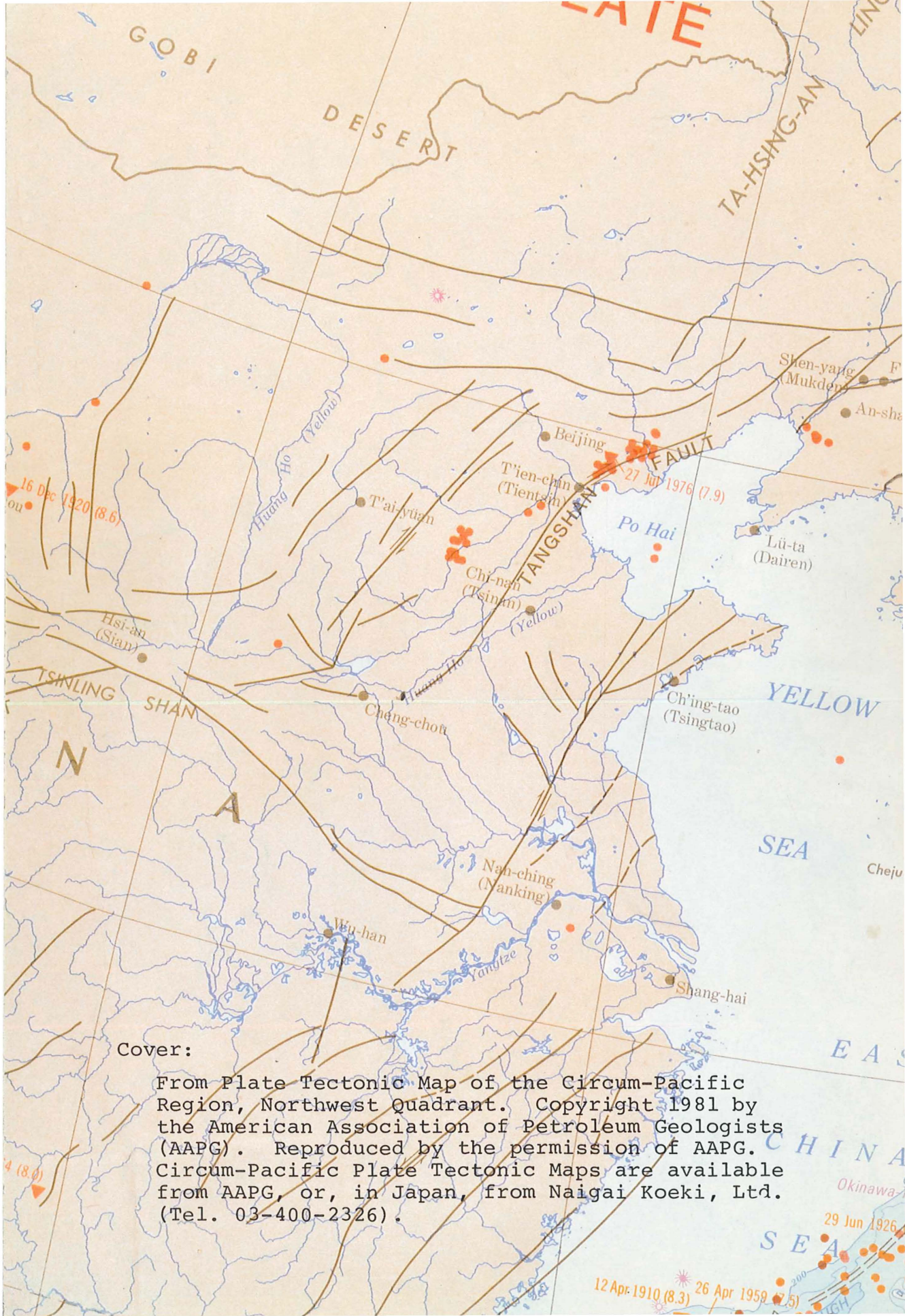

Cover:

From Plate Tectonic Map of the Circum-Pacific Region, Northwest Quadrant. Copyright 1981 by the American Association of Petroleum Geologists (AAPG). Reproduced by the permission of AAPG. Circum-Pacific Plate Tectonic Maps are available from AAPG, or, in Japan, from Naigai Koeki, Ltd. (Tel. 03-400-2326).